SPATIAL MAPPING OF FLOOD PRONE AREAS AND RISK ASSESSMENT OF CHALAKUDY RIVER BASIN USING HEC-HMS AND HEC-RAS MODELS

By

GUDIDHA GOPI

(2018-28-002)

Department of Irrigation and Drainage Engineering

KELAPPAJI COLLEGE OF AGRICULTURAL ENGINEERING AND TECHNOLOGY

TAVANUR, MALAPPURAM-679573

KERALA, INDIA

2021

SPATIAL MAPPING OF FLOOD PRONE AREAS AND RISK ASSESSMENT OF CHALAKUDY RIVER BASIN USING HEC-HMS AND HEC-RAS MODELS

By

GUDIDHA GOPI

(2018-28-002)

THESIS

Submitted in partial fulfilment of the requirements for the degree of

DOCTOR OF PHILOSOPHY

IN

AGRICULTURAL ENGINEERING

(Soil and Water Engineering)

Faculty of Agricultural Engineering &Technology

Kerala Agricultural University

Department of Irrigation and Drainage Engineering

KELAPPAJI COLLEGE OF AGRICULTURAL ENGINEERING AND TECHNOLOGY

TAVANUR, MALAPPURAM-679573

KERALA, INDIA

2021

DECLARATION

I, hereby declare that this thesis entitled **"SPATIAL MAPPING OF FLOOD PRONE AREAS AND RISK ASSESSMENT OF CHALAKUDY RIVER BASIN USING HEC-HMS AND HEC-RAS MODELS"** is a bonafide record of research work done by me during the course of research and the thesis has not previously formed the basis for the award to me of any degree, diploma, associateship, fellowship or other similar title, of any other University or Society.

G. Gopi

GUDIDHA GOPI

(2018-28-002)

Tavanur,

Date: 27-10-21

CERTIFICATE

Certified that this thesis entitled **"SPATIAL MAPPING OF FLOOD PRONE AND RISK ASSESSMENT OF CHALAKUDY RIVER BASIN USING HEC-HMS AND HEC-RAS MODELS"** is a record of research work done independently by **Mr. Gudidha Gopi (2018-28-002)** under my guidance and supervision and that it has not previously formed the basis for the award of any degree, diploma, fellowship or associateship to her.

Rema KP

Dr. Rema K.P

(Major Advisor, Advisory Committee)

Professor, Dept. of IDE

KCAET, Tavanur

Tavanur,

Date: 27-10-2021

CERTIFICATE

We the undersigned, members of the advisory committee of **Er. GUDIDHA GOPI (2018-28-002)**, a candidate for the degree of Doctor of Philosophy in Agricultural Engineering, majoring in Soil and Water Engineering, agree that the thesis entitled **'SPATIAL MAPPING OF FLOOD PRONE AREAS AND RISK ASSESSMENT OF CHALAKUDY RIVER BASIN USING HEC-HMS AND HEC-RAS MODELS'** may be submitted by **Er. Gudidha Gopi,** in partial fulfilment of the requirement for the degree.

Dr.Rema K.P.
(Chairman, Advisory Committee),
Professor& Head ,
Dept. of IDE ,
KCAET, Tavanur.

Dr.Sasikala D
(Member, Advisory Committee)
Professor,
Dept. of IDE,
KCAET, Tavanur.

Dr. Anu Varughese
(Member, Advisory Committee)
Assistant Professor,
Dept. of IDE,
KCAET, Tavanur.

Dr. Asha Joseph
(Member, Advisory Committee)
Professor,
Dept. of IDE,
KCAET, Tavanur.

Dr. E.K Kurien
(Member, Advisory Committee)
Professor & ADR(Engg),
KAU,Thrissur.

Dr. Sudheer Padikkal
(Member, Advisory Committee)
Consultant General Manager, KIIDC,
Govt of Kerala.

External Examiner
Professor & Head
Dept. of Soil & Water Engineering
Dr. NTR College of Agril. Engineering
BAPATLA - 522 101, A.P., India

ACKNOWLEDGEMENT

Successful accomplishment of this work would be incomplete without the words of encouragement and gestures of aid from several people. I take this opportunity to express my sincere gratitude to everyone who have supported me with their kind effort and perseverance.

I would firstly like to bow my head before ***The Almighty*** *for the loving and blissful showers of sustenance throughout journey of this venture. I also express my deep sense of gratitude to Kerala Agricultural University for financial and technical support for persuasion of my study and research work.*

It is with immense pleasure I reward this opportunity to express my gratefulness to my major advisor ***Dr. Rema K.P****, Professor& Head, Department of IDE, KCAET, Tavanur who constantly provide suggestions and honestly monitor the works. The sense of freedom and support provided by her generous mind, have set up my confidence level in every stage of research work.*

I am extremely indebted to ***Dr. Sathian,*** *Dean, KCAET, Faculty of Agricultural Engineering and Technology for the support offered while carrying out the project work. The data acquisition was made possible by his timely intervention of request letters.*

I engrave my profound gratitude to my advisory committee members, ***Dr. Sasikala, D.,*** *Professor, Department of Irrigation and Drainage Engineering, KCAET, Tavanur, for her help and encouragement during the whole period of the work and* ***Dr. Asha Joseph.,*** *Professor, Department of Irrigation and Drainage Engineering, K.C.A.E.T, Tavanur for her valuable advice and moral support. I would also like to convey special thanks to* ***Er. Sudher Padikkal.,*** *General Manager, Kerala Irrigation Infrastructure Development Corporation, Govt of Kerala for his valuable suggestions and evaluation of the project work.*

My special thanks and gratitude goes to ***Dr. Anu Varughese,*** *Assistant Professor, Department of Irrigation and Drainage Engineering, KCAET, Tavanur and a member of my advisory committee for being a really inspirational*

personality in learning modelling software. for her constant guidance and encouragement, untiring help and insightful consults throughout the period of the study.

I would like to express my gratitude to ***Dr. Kurien E.K.,*** *Professor and Head, ARS, Chalakudy and a member of my advisory committee for providing me the meteorological data which was prerequisite for the successful completion of my work.*

I am also grateful and thankful at the same time to all faculty members of the department and the staff members of KCAET for their support and encouragement. It also gives me immense pleasure in expressing out my sincere gratitude to all my friends at KCAET who had constantly encouraged and helped me by all possible means during the course of my project work.

I extend my sincere thanks and gratitude to my parents for their sacrifices, unceasing prayers and encouragement all throughout this work. It would have remained only a dream for the successful completion of this work and not a reality without their support.

Special thanks to ***Kerala Agricultural University*** *for giving me and opportunity and providing me a platform to study in this institute. It was indeed a wonderful and handful of experience to study in KCAET.*

Last but not least, I express my sincere gratitude to all those who have supported and helped me through their encouraging words and deeds and are directly or indirectly connected to my successful completion of work.

Gudidha Gopi

Dedicated to Agricultural Engineers

CONTENTS

LIST OF TABLES

LIST OF FIGURES

SYMBOLS AND ABBREVIATIONS

%	:	Percentage
<	:	Less than
>	:	Greater than
∑	:	Sum
≤	:	Less than or equal to
≥	:	Greater than or equal to
&	:	And
°C	:	Degree Celsius
CN	:	Curve Number
CWC	:	Central Water Commission
DEM	:	Digital Elevation Model
DFID	:	Department for International Development
DSS	:	Data Storage System
ERDAS	:	Earth Resources Data Analysis System
ET	:	Evapotranspiration
et al.	:	and others
Fig.	:	Figure
FPS	:	Foot–pound–second
Geo-HMS	:	Geospatial Hydrological Modelling System
GIS	:	Geographical Information System
h	:	hour
ha	:	Hectare
HEC	:	Hydrologic Engineering Centre
HMS	:	Hydrological Modelling System
HSG	:	Hydrologic soil group
Int.	:	International

IMD	:	Indian Meteorological Department
J.	:	Journal
km^2	:	Square kilometre
KSD	:	Kerala Sholayar Dam
Landsat	:	Land Satellite
m	:	Meter
mm	:	Millimeter
Mm^3	:	Million cubic meter
MCM	:	Million cubic meter
MSL	:	Mean sea level
NASA	:	National Aeronautics and Space Administration
No.	:	number
NSE	:	Nash Sutcliffe Efficiency
PBIAS	:	Percentage Bias
R^2	:	Coefficient of Correlation
RAS	:	River Analysis System
RCP	:	Representative Concentration Pathways
RMSE	:	Root Mean Square Error
RS	:	Remote Sensing
s	:	Second
Sci.	:	Science
SCS	:	Soil Conservation Service
SD	:	Standard Deviation
SI units	:	International System of units
Soc.	:	Society
SOI	:	Survey of India
SRTM	:	Shuttle Radar Topography Mission
RTMGL	:	Shuttle Radar Topography Mission Global

SSP	:	Statistical software package
SWAT	:	Soil and Water Assessment Tool
SWM	:	Stanford Watershed Model
TIN	:	Triangular Irregular Networks
TNAU	:	Tamil Nadu Agricultural University
UH	:	Unit Hydrograph
USGS	:	United States Geological Survey
viz.	:	Namely

INTRODUCTION

CHAPTER I
INTRODUCTION

Globally, floods are the most devastating natural disasters. It is reported that one sixth of the global population who are low income earners, live in the potential path of a 1- in -100 year return period flood according to the Department for International Development (DFID, 2012). In 2010 alone, 178 million people were affected by floods (Abhas *et al.*, 2012). Extreme precipitation and flooding are two hydro climatic events that draw a lot of attention in India every year during the monsoon season. Millions of people are affected by these natural calamities that often cause damage to infrastructure and agriculture in India. Extreme precipitation events have increased in the country during the last few decades, which are likely to increase further under the warming climate (Mukherjee *et al.*, 2018). In 2005, an extreme precipitation event in Mumbai affected over 25 million people and caused over 1000 deaths (Gupta and Nair, 2011). The 2013 extreme rainfall and flood event in Uttarakhand killed over 6000 people and caused the state more than $3.8 billion economic loss (Kumar, 2013). Furthermore, extreme precipitation in Chennai in November 2015 and Telangana in September, 2016 have resulted in more than $3 billion economic loss (Boyaj *et al*., 2018).

Kerala State, with a total area of 38,863 km^2, is located between the Arabian Sea in the West and the Western Ghats (Sahyadris) in the East. The state has an average annual precipitation of about 3000 mm which is contributed by the South-West and North-East monsoons. Kerala receives 90% of its rainfall and storms during the monsoon season which causes water to overflow in all rivers. The high intensity storms prevailing during the monsoon months result in heavy discharges in all the rivers. The continuous and heavy precipitation that occurs in the steep and undulating terrain finds its way into the main rivers through innumerable streams and water

courses. The year 1924 witnessed unprecedented and very heavy floods in almost all rivers of Kerala. Heavy losses to life and property had been reported. The heavy storm of 16-18, July 1924 was caused by the South-West monsoon that extended to the south of the peninsula on 15th July and caused rainfall in Malabar. Under its influence, heavy rainfall occurred in almost entire Kerala. The year 1961 also witnessed heavy floods and rise in the water levels of reservoirs. The monsoon season of 2018 witnessed consistent and excessive rainfall, resulting in a devastating flood disaster. It has received 42% more rain than usual at the start of the monsoon season. The first flood occurred at the end of July, 2018 as a result of significant rainfall that started in June and extended to July. Several parts of Kerala were hit by severe rains in the early days of August, 2018 and the various districts have received a total rainfall of around 1398 mm. The level of water in various reservoirs (35 out of 45) reached more than 90% of their full capacity as a result of the heavy rain, which forced the authorities to release the water from these reservoirs (Mishra *et al*., 2018). Another heavy rainstorm that hit Kerala towards the end of the second week of August and lasted until the third week had resulted in a major disaster and flood in various districts. According to the Indian Meteorological Department rainfall records, the calamity that occurred in 2018 as a result of heavy rainfall was similar to that of the cyclone that occurred in 1924. Kerala had never witnessed such a terrific disaster that resulted in the death of about 400 or more persons during the past 90 years.

The Chalakudy river basin in Kerala, one of the worst-affected river basins due to heavy rains and floods was selected for the present study. The Chalakudy river is the fifth largest river in Kerala. The river flows through two districts: Ernakulam in the south and Thrissur in the north. The basin has been the victim of many floods since the last few years and lot of damages to the basin had occurred including the loss of plantation, livestock, residential areas, and infrastructure such as buildings, roads, bridges and so on. Hundreds of people had to be evacuated from the region and spent several months in relief camps. Many people offered to help the people at relief

camps by distributing food, water, medicines and clothes. Chalakudy basin has encountered numerous critical situations such as repeated flood occurrences and dry seasons that has become an overwhelming element of this stream which is considered as the life saver of the area.

Flood is an overflow of river that submerges the land and as a result some of the water flows outside of the normal perimeter of the water body. Climate change, tsunamis, inadequate river management, cloud bursting and river silting are some of the major causes of flooding. Flooding frequently results in severe water pollution as well as epidemiological issues. Floods happen frequently, and as a consequence, this disastrous catastrophe has caused more damage than any other natural disaster. Ineffective flood warning systems, inadequately trained model users and inadequate use of hydro informatics technologies has contributed to the flood damage. Floods, are thus a source of concern in the field of hydrology, agriculture, civil engineering, and public health. As a result, for proper development, planning and design of water resources projects, a proper assessment of flood peak, occurrence and return period is essential. To design all the water resources projects in the preferred area, planners and engineers usually require reliable estimates of flood magnitude and frequency.

Today, researchers and practitioners utilize a wide variety of hydrological models. However, the applications of these models are highly dependent on the goals for which they are utilized. Some modelling approaches are purely research-oriented and attempt to better understand the hydrological processes in a real-world system while, others are designed as tools for simulation and prediction to support decision-making for proper flood risk management planning and operation. For instance, the real-time flood forecasting and warning system, currently operational in many countries, employs the results of rainfall-runoff modelling. These hydrological models have so far been used to estimate flood frequencies, give inputs for flood routing, and predict inundation. The end-results are widely used in climate and land use change impact assessments, as well as integrated watershed management.

Open water flood forecasts are typically prepared using a two-step procedure in which a hydrological model, such as the HEC-HMS model, is used to route the flood and generate expected flow hydrographs at the site of interest. The peak flow from this flood routing analysis is typically input for hydraulic model, such as the HEC-RAS model, to predict the corresponding flood levels expected along river reaches extending through populated areas along the flood plain. The HEC-HMS is a free and open-source software that allows to simulate base flow, interflow, and channel flow. HEC–I, the first version, which worked with MS-DOS, was continuously updated to HEC-HMS, which added more features and capabilities. Hydrologic Engineering Center – Hydrologic Modelling System is abbreviated as HEC-HMS. The hydrologic simulation software HEC-HMS is used to model rainfall-runoff processes in a dendritic watershed. The basin model, meteorological model, control parameters, time-series data and paired data are the basic components of the HEC-HMS. A watershed model is created by disintegrating the hydrologic cycle into manageable pieces and defining boundaries around the watershed of interest (USACE, 2000). Hydrographs produced by HEC-HMS model are used either directly or in conjunction with other tools for studies of water availability, urban drainage, flow forecasting, future urbanization impact, reservoir spillway design, flood damage reduction, floodplain regulation, and system operation (Scharffenberg and Harris, 2008). Several designers choose HEC-HMS because of its ease of use, handling, availability, superior technical advantage, and developer support. As a result, the HEC-HMS model was used in this study to simulate rainfall-runoff processes in the Chalakudy river basin in order to develop flood hydrographs.

To limit the loss of life and property due to floods, management plans and real-time monitoring and warning systems are essential. Monitoring and planning flood mitigation methods require a catchment-wide approach. Mitigating flood effects requires knowledge of flooding features and how certain characteristics propagate. Hydraulic models that can simulate flood events, depths, levels, velocity and timing

over a distributed model domain and time dimension can provide this information. HEC-RAS/HEC-GeoRAS is one of the most powerful models capable of simulating flooding features if sufficient high-quality input data is available. The availability of data with the required geographical and temporal resolution is essential in hydraulic flood simulation. There is no data available on river cross sections over the entire length for any river in Kerala The availability and quality of geometric data for river cross sections, is thus a significant limitation. A high-resolution DEM is required for such basic data generation. Digital Elevation Model (DEM) and/or its variants are utilized as input in hydraulic flood simulation for topographic data. For representing flood plain and river geometry, DEM is an important source of topographic data.

Flood managers require information about flooding characteristics and effects in order to make decisions on flood management techniques such as the construction of flood protection structures, the development of a flood emergency plan, and human settlement planning. With the development of new flood modelling technology such as hydraulic modelling (HEC-RAS) and GIS, it is now possible to model flood extent, depth, distribution, and other variables both in temporal and geographic dimensions. Previous flood studies in the Chalakudy basin, on the other hand, have ignored these applications. The assessment of flood risk areas in the basin for different return period storms would help the development of local level action plans for mitigation as well as for planning flood protection and rehabilitation measures. In the light of occurrence of extreme flood events in this basin in recent years and the lack of adequate reported research on flood prone area mapping and risk assessment to manage floods and related natural calamities, the present study was planned in the Chalakudy river basin of Kerala, with the following specific objectives:

1. Rainfall- Runoff modelling of Chalakudy river basin using HEC-HMS.
2. Development of geometric data of river channel using RAS Mapper
3. Hydraulic modelling using HEC-RAS to produce flood inundation maps for different scenarios.

4. Categorization of the vulnerable areas in the basin to aid future flood mitigation strategies.

CHAPTER II
REVIEW OF LITERATURE

Spatial mapping of flood prone areas and risk assessment of Chalakudy river basin in Kerala was done in this study. Hydrologic modelling was performed for developing flood hydrographs for the basin using HEC-HMS model and hydraulic modelling using HEC-RAS was done for developing flood prone area maps. Using interconnecting hydrological extensions like HEC-GeoHMS and HEC-GeoRAS, Arc-GIS was utilised to generate physical basin models for HEC-HMS and geometric river models for HEC-RAS. This chapter provides an insight to the past research done on the application of hydrologic and hydraulic models for flood prone area mapping in several flood affected areas of the world under the following sub headings.

2.1 ROLE OF REMOTE SENSING AND GIS IN HYDROLOGICAL MODELLING

Su *et al.* (1992) used RS and GIS functions for estimating the parameters for the distributed hydrological modelling. In one study, they used RS and GIS to integrate and develop some techniques. Satellite images, digital elevation models, and digitized thematic data were used to estimate the model parameters for the second study. Since this type of information offers a very high spatial resolution, it was necessary to add small area elements in the so-called hydrologically similar units (HSU) in the GIS. The most difficult problem caused by the large dimensions of the watersheds was dealing with the huge amount of data that results from the high spatial resolution. Therefore, the application of RS and GIS is essential for hydrological modelling. This coupling of RS and GIS allows to operate the model with future scenarios of a changed climate. With the help of these two softwares, the effects of hydrological processes can be analyzed.

Hoblit and Curtis (2001) analysed the software HEC-GeoHMS by the US Army corps of Engineers Hydrological Engineering Centre (HEC) which was used in

support of GIS software package for physically based hydrological model. They found that the recent development in spatial data analysis has made the Digital Elevation Model (DEM) easily downloadable and used this in HEC-GeoHMS package for watershed delineation. Also, HEC-GeoHMS and HEC-HMS were found to be effective software that could be used more accurately to create hydrological models for most of the watersheds in the United States.

Alemaw and Chaukra (2003) discussed the capability of GIS in handling large amounts of spatially detailed information derived from various sources such as remote sensing and ground surveys from a wide area. With the advent of increasing computing power and GIS techniques, physics-based hydrological modelling has become important in contemporary hydrology to assess the effects of human interference and / or climate change on hydrology and resources. river basins.

Seth *et al.* (2006) mentioned GIS to be advantageous software evolved for setting together and storing the voluminous data typically required for hydrological studies. Remote detecting and GIS together give fundamental data base to effective administration of water assets. The succinct view given by satellite remote detecting and investigation ability given by GIS offer an innovatively fitting strategy for considers in water assets.

Santillan *et al.* (2011) conducted a study to demonstrate the usefulness of multi temporal Landsat images in detecting land-cover change, recognizing regions for recovery and assessing restoration techniques for the administration of tropical watersheds in hydrologic displaying.

Singh *et al.* (2014) conducted large scale watershed analysis using GIS and remote sensing and stated that the The digital elevation model (DEM) can be a useful tool for determining terrain parameters such as bedrock type, infiltration capacity, and surface runoff, which has aided in a better understanding of landform status and processes, drainage management, and groundwater potential evolution for watershed planning and management.

Thakur *et al.* (2016) Investigated in the fields of groundwater hydrology, resource management, environmental monitoring and emergency response, collaboration and integration of Remote Sensing (RS), Geographic Information Systems (GIS) and Global Positioning Systems (GPS) are growing research areas. Advances in the disciplines of RS, GIS, GPS, and higher levels of computation, according to the study, aided in providing and handling a vast variety of data simultaneously in a short amount of time and at a low cost.

2.2 HYDROLOGIC MODELLING USING HEC-HMS

Abbott *et al*. (1996) reported that HEC-HMS model gives configurations that range from lumped to distributed type. For vast, aggregated regions of land, lumped models use composite parameters, whereas distributed models maintain parameters spatially varied. The configuration can be determined by the study's eventual goals and the information available. Over-parameterization and data restrictions are usually avoided with lumped models, although they may fail to adequately explain changing landscapes.

Fleming (2004) described the Hydrologic Engineering Center's Hydrologic Modelling System (HEC-HMS) program and its application in the watershed studies. With regard to the watershed point of approach, HMS has the possibility to function as a significant programme. It can simulate rainfall-runoff at any point within a watershed based on the watershed's physical parameters.

Clay *et al.* (2005) selected HEC-HMS model for rainfall-runoff simulation to evaluate the effectiveness of storm water detention basins in Valley Creek watershed. They used the model to assess the impact of alternative watershed management practises. The most effective method of reducing watershed peak flow rates was thought to be designing the watershed model according to runoff volume.

Hammouri and Naqa (2007) simulated the rainfall-runoff process to obtain the Intensity-Duration-Frequency (IDF) curves for 10 years and 50 years return periods, using HEC-HMS and GIS in a selected ungauged basin for the purpose of

groundwater artificial recharge. The total direct runoff volume and the peak discharge for 10 years return period and 50 years return period were estimated to be 151,000 m^3 and 5.43 m^3/s & 280,000 m^3 and 12.77 m^3/s, respectively. With a peak weighted root mean square error of less than 2%, the flow comparison graph for the calibrated model fits well with the observed runoff data.

Bakir and Xingnan (2008) used HEC-HMS for hydrological modelling. Using historical flood data from China's Wanjiabu watershed, the performance of HEC-HMS was compared to that of the Xinanjiang conceptual model. The findings of this study showed that HEC-HMS was more convenient for flood simulation, particularly in terms of parameter optimization. However, when compared to the Xinanjiang model, these are inaccurate. HEC-HMS is a sophisticated and versatile software that provides ample and accurate hydrological data to run various models within it. HMS may be used for calibration optimization and provides precipitation-runoff processing, loss models that can predict runoff volume, direct runoff, and hydrologic routing models.

Yener *et al*. (2008) conducted hourly simulation of event- based runoff scenarios to obtain IDF curves for sub-basins to obtain seasonal (spring, summer and fall) average values of the watershed using HEC-HMS model. They proposed that the runoff created by the frequency storm method could be used in future flood hazard and risk assessment studies to aid flood control.

Razi *et al.* (2010) developed the flood model by using HEC-HMS for the Johar river in Kotta Tinggi watershed. Different types of data were used to perform calibration and validation procedures. The model's performance was assessed, and the correlation coefficient was found to be close to one. R^2 was 0.905, and the percentage of incorrect values was 4%. They concluded that HEC-HMS might be used to estimate the Qpeak based on their findings.

Arekhi (2012) applied HEC-HMS model results for six events to compare the results of Green and Ampt, initial and constant loss rate and deficit and constant loss

methods for estimation of runoff losses. Percent error in peaks and volumes was considered as objective function for the selection criteria of the best method. The Initial and constant loss rate method had better results than Green and Ampt method. Deficit and constant loss rate method had less changes of simulated to observed discharges rather than Green and Ampt method. For objective functions, initial and constant loss rate method had less changes percent and it was selected as optimum method for simulation of surface runoff in the watershed with similar characteristics. Green and Ampt and constant loss rate methods were the next preferences in simulation methods based on this study.

Majidi and Shahedi (2012) performed simulation of rainfall-runoff process with rainfall events using HEC-HMS in Abnama watershed located in the South of Iran. The model validation with optimized lag time values showed 9.1% difference between the observed and simulated discharges and their coefficient of determination was 0.86. The results conveyed that the lag time was the sensitive parameter.

Sardoii *et al*. (2012) attempted in comparing different methods in HEC-HMS model, *i.e*., initial and constant, Green- Ampt, SCS curve number with regard to various error functions (percent error in peak, peak-weighted root mean square etc.) by taking into account of the obtained results of different storm events simulation. Considering objective functions, result indicated that Green and Ampt, SCS and 'initial and constant' method were placed as first to third in the order of preferences respectively. Therefore, Green- Ampt method was suggested as the suitable method that can be used in similar area and conditions.

Halwatura *et al.* (2013) made a study utilizing three unique ways to deal with calibration and validation of the HEC-HMS 3.4 model for Attanagalu Oya river catchment. The study used 20 years of daily precipitation data from five rainfall gauging stations scattered throughout the Attanagalu Oya basin, as well as monthly evaporation data and daily stream flow data from Dunamale from 2005 to 2010. GIS data layers containing information needed for stream flow simulation were created

with Arc-GIS 9.2 and then put into the HEC-HMS 3.4 model for Dunamale sub catchment calibration. The data used was daily stream flow data from 2005 to 2007. Three different strategies were used to calibrate the model.

Reshma *et al.* (2013) made a study for simulating runoff process utilizing HEC-HMS hydrological model in Walnut Gulch watershed situated in Arizona, USA. Green-Ampt, Clark's Unit hydrograph, and Kinematic wave routing were chosen to analyse infiltration, precipitation excess to runoff, and flood routing. Seven rainfall events were used to calibrate and validate the model. The calibration was done for four rainfall events (July 20 2007, August 28 2008, August 23 2009 and July 29 2011) and validation for three rainfall events (August 4 2009. September 13 2009 and August 28 2010). From the outcome of the model it was perceived that HEC-HMS model has performed satisfactorily for runoff simulation of different rainfall events. From the simulated results of calibrated events they concluded that the volume of runoff has been simulated within the variation of 60% except for the event July 29, 2011 where the variation was 93%. For validation, the variation was found to be -27% except for the event of August 28, 2010. Time to peak has been simulated within the variation of 33% for calibration period while for validation a variation of -3% was observed.

Choudhari *et al.* (2014) utilized HMS model for their study to simulate rainfall-runoff process in Balijore Nala watershed of Odisha, India. SCS curve number, SCS unit hydrograph, Exponential recession, and Muskingum routing methods were chosen to determine runoff volume, peak runoff rate, base stream flow, and stream routing procedures. Rainfall-runoff simulations were performed using data from 24 irregular rainstorm events over four years (2010–2013). The model was calibrated using 12 events, and the model was validated using the remaining 12 events. The value of mean absolute relative error (MARE) obtained were 0.20 and 0.25 while root mean square error (RMSE) between the simulated and observed information were 0.28 mm and 2.30 m^3/s for depth of runoff and peak discharge.

After optimization of the parameters were done, the error decreased to 0.10, 0.12, 0.75 mm and 0.09 m^3/sec in succession. The simulated model with improved parameters was utilized for validating the model.

Hilbert (2015) made a study utilizing hydrological model and GIS in Kuantan watershed to develop a relationship between rainfall-runoff and to analyze the use of HEC-HMS model in runoff forecasting and assessing the precision of altered SCS-CN in tropical areas. HEC-HMS model was utilized to simulate the occurrence of storm event that happens in the watershed for which calibration and validation of the model was done. The transform method used in the model was the SCS Unit Hydrograph, the loss method was SCS-CN, and the flood routing method was lag time. The simulation was completed based on two different storm events, the first in December 2006 and the second in January 2012. The initial abstraction ratio estimations used were 0.2 and 0.05, and the results were analysed using both values of the ratio. Values of the simulated results over the actual values of runoff were used to estimate the Nash-Sutcliffe Efficiency (NSE).The NSE value for the model when calibrated ranged from 0.7 to 0.9. The use of two distinct equations to figure the lag time gave slight changes in the outcome as the utilization of Kirpich equation gives a superior result in contrast to the utilization of SCS curve number equation for the forecasting of peak discharge.

Narasayya (2015) used a GIS based hydrological model to conduct the stream flow estimation. The SCS-CN loss strategy delivers larger stream flow volumes than the initial and continuous loss methods from both Muskingum and Lag routing systems, according to the statistical results and graphs. Using the SCS-CN loss approach, it is possible to estimate ultimate peak flows and maximum stream flows in Muskingum and Lag routing schemes. The study's final conclusions suggest that better spatial resolution DEM and temporal resolution satellite imageries can also be used to estimate stream flow volume.

Pampaniya *et al.* (2015) used HEC-HMS 5.0 hydrologic model for simulating runoff in the Hadaf stream watershed, Gujarat, India. Two elevation datasets (DEM) of the Hadaf Basin were used *i.e.,* SRTM 90m DEM and ASTER DEM 30m which were further processed to generate HEC-HMS model input files by applying HEC-GeoHMS extension tool of ArcGIS 10. Land use maps for three different years i.e. 2008, 2012 and 2013 were prepared which was obtained by utilizing remote sensing satellite images. Two transformation methods were used to simulate runoff for the calibration and validation of the HEC-HMS model as well as the evaluation of several unit hydrographs *i.e*., SCS UH (approach-1) and the Clark UH (approach-2). In rainfall-runoff simulation, it was found that the Clark technique outperforms the SCS-UH transformation approach in terms of peak runoff and runoff volume. The study concluded that the enhancement of the parameters altogether improved the model.

Praveen *et al.* (2015) performed lumped continuous hydrological modelling using HEC-HMS accounted loss with the help of Green-Ampt method. The SCS unit hydrograph and Snyder unit hydrograph approaches were used to estimate runoff. The FAO Penman-Monteith method was used to determine the reference ET. The Nash-Sutcliffe coefficient values were greater than 0.8, and the correlation coefficient was greater than 0.9.

Rathod *et al.* (2015) made an investigation to compute runoff for various precipitation events in three sub basins of Tapi river in India. Continuous lumped hydrological model was produced for the study area utilizing HEC-HMS 3.5. For calculating the losses Green-Ampt strategy was utilized. For better runoff estimation SCS unit hydrograph and Snyder Unit hydrograph techniques were compared and best appropriate strategy for the study region was picked up for the last simulation. The FAO Penman-Monteith approach was used to calculate the reference evapotranspiration. Sensitivity analysis was carried out on the model's numerous parameters, with the most sensitive ones being improved and the parameters being

used for calibrating and verifying the model. The aim of their examination was to fit the peak flow discharge and amplify the Nash-Sutcliffe efficiency. The Nash-Sutcliffe efficiency for the three sub basins was more than 0.8, according to the final figures. For the three sub basins, the correlation coefficient between observed and simulated discharges was more than 0.9. Their research found that the HEC-HMS model may be used to estimate runoff for the Tapi River using reasonable estimates.

Sampath *et al.* (2015) developed HEC-HMS 3.0.1 model for Deduru Oya River. Soil moisture accounting loss method for five layer of soil, The HEC-HMS model's Clark unit hydrograph (transformation method) and base flow (recession method) were used for hydrological modelling. The results depicted by giving input data of long-term daily rainfall, land use and soil showed a great accuracy of the model with Nash Sutcliffe efficiencies of 0.80.

Demetrio *et al*. (2016) conducted a study in Mesima Torrent, Southern Italy to identify the best infiltration method in HEC-HMS out of SCS-CN, Green-Ampt and 'Initial and Constant' methods. Because of the presence of small and intermittent water courses that were frequently subjected to high-magnitude flash floods and erosive events in the study area, evaluation of runoff prediction by known infiltration methods in semi-arid torrents was particularly relevant. In order to estimate runoff volume and peak flow, HEC-HMS infiltration methods were used. Following the calibration of the curve numbers, it was understood that the SCS-CN method accurately predicted runoff volume. The 'Initial and Constant' method, on the other hand, provided a superior estimate of peak flow. Except for the Green-Ampt approach, which had low reliability, calibrated hydrographs were fairly close to findings for both SCS-CN and 'Initial and Constant' methods.

Ismael *et al.* (2017) assessed the hydrological processes of Ruiru reservoir catchment to compute its runoff using HEC-HMS 4.1 hydrologic model (with Soil moisture Accounting Algorithm). WMS 10.1 (Watershed Modelling Surface) was utilized as an interface to delineate the watershed and produce some input parameters.

The SMA parameters were computed in WMS utilizing land use and soil type information. Daily precipitation and monthly evapotranspiration for 5 years (2011-2015) were utilized for the meteorological information sources. The outcomes demonstrated an absolute volume of runoff 202,860,900 m^3 during the five years of the simulation. The peak discharge was seen as79.6 m^3/s and the average daily inflow during the five years was seen as 1.28 m^3/s. The model evaluation revealed that the model's efficiency was 0.74 and 0.72 for calibration and validation, respectively, indicating that the simulation results were good.

Adnan and Atkinson (2018) investigated the impacts of changes in precipitation and land use on hydrological responses such as peak discharge and runoff volume in the Kelantan river basin in Malaysia.. Because of land use changes, upstream gauge had differences in runoff volume and peak discharge compared to climate-related fluctuations, according to simulation results from HEC-HMS hydrologic modelling. Downstream catchments, on the other hand, were far more affected by precipitation fluctuations. According to the research, the downstream catchment in the Kelantan monsoonal catchment will be more prone to flooding.

Koneti *et al.* (2018) made an investigation utilizing the HEC-HMS model and remote sensing-GIS procedures for detecting the spatial and qualitative changes in the precipitation overflow that had occurred because of the LULC changes from 1985–2014 in the Godavari river basin. The LULC changes in the Godavari basin were studied for the years 1985, 1995, 2005, and 2014.The findings uncover an expansion of developed land, an abatement of shrub land and an increase in water bodies for the period 1985-2014. The study obtained a 92 percent general classification accuracy and a 0.9 general Kappa co-efficient. The hydrology of the Godavari basin was simulated using the HEC-HMS model. The analysis done was essentially focused on the effect of LULC changes on the stream flow design. To examine the progressions that have happened as a result of changes in LULC, the surface runoff was simulated for the year 2014. On September 9, 2014, the observed and simulated peak stream

flow were the same, at 56,780 m^3/s. Linear regression was utilized for validating the model to relate the observed and simulated stream flow information at the gauging station of the Badrachalam outlet for the Godavari river basin and a relationship co-efficient of 0.83 was obtained. The hydrological modelling that was done utilizing the HEC-HMS model has drawn out significant effect of LULC on rainfall-runoff at the Pranhita sub-basin scale demonstrating the model's capacity to effectively reflect the entirety of the ecological and scene factors. The investigation's findings revealed that remote sensing, GIS, and the hydrological model (HEC-HMS) may all be used to effectively illustrate hydrological concerns in a stream basin.

Paudel *et al.* (2019) simulated the flow of Marshyangdi river basin situated in Nepal. Furthermore, the assessment and investigation of discharges for each sub basins of Marshyangdi basin was done in their study. The HEC-HMS model was utilized to calibrate (from 2003-2007) and validate (from 2008-2012) the Marshyangdi basin. The discharge value at the catchment's outlet was the model's major output. At last, the output was compared with the observed discharge at selected gauging stations of the basin. During the calibration and validation period, the model's performance was examined for the river basin. The results were satisfactory and acceptable in terms of runoff modelling. The SCS curve number technique, SCS unit hydrograph strategy, constant monthly technique and Muskingum routing technique were utilized as the loss method, direct runoff transformation, base flow and routing methods respectively. As a result of their research, they discovered that the HEC-HMS model can accurately predict the upper Marshyangdi river basin for improved evaluation and hydrological response. Result shows both NSE and R^2 value to be 0.778 for calibration period and 0.842 for validation period which indicates the model has well simulated the daily stream flow at the outlet of the river basin.

Tassew *et al.* (2019) simulated the surface runoff utilizing the Hydrologic Modeling *i.e.*, HEC-HMS for the Gilgel Abay Catchment (1609 km^2) located in

Ethiopia. Delineation of the basin was done utilizing 30m×30m DEM of the Lake Tana Basin. Precipitation data was used to generate the meteorological model within the HEC-HMS model and the period and time step of the simulation run were defined by the control specifications. The SCS-CN, SCS-UH, and Muskingum methods were used to account for losses, runoff estimation, and flood routing. Six extreme daily time series occurrences were used in the rainfall-runoff simulation. The calibration of the model was carried out with an optimization method and sensitivity analysis. The after effects of the sensitivity analysis indicated that the curve number was a very sensitive factor. Furthermore, the model's results were validated, indicating a significant difference in peak flow (Relative error in peak, REP = 1.49 percent) and total volume (Relative error in volume, REV = 2.38 percent). The model fit perfectly for hydrological simulations in the Gilgel Abay Catchment, according to the observed and simulated hydrographs, model execution (Nash Sutcliffe Efficiency = 0.884), and their co-relation (R^2 = 0.925).

Sudheer *et al.* (2019) studied on the role of dams on the floods of August 2018 in Periyar river basin, Kerala. This study presents the results and analysis of a modelling exercise that used HEC-HMS to simulate and analyse the function of dams and reservoir activities during the August 2018 floods. The results suggest that releases from the PRB's major reservoirs played a smaller impact in the flood damage. Reservoir operations, according to the analysis, could not have prevented the flooding because only 16-21 % peak attenuation could be achieved by emptying the reservoir ahead of time, and the majority of runoff contributing to the flooding came from intermediate catchments with no reservoirs to control. It should be highlighted that the probability of such EREs in August in PRB is extremely low (0.6 %), therefore any planned activity would have been ineffective in preventing flooding.

Parvathy and Thomas (2021) made a study on impact of urbanization on flooding in Chalakudy river. The Chalakudy river basin was entirely flooded during Kerala's devastating floods in 2018. Due to agricultural development, deforestation,

increased urbanisation, and other factors, this area has witnessed significant environmental changes during the 1990's. These facts add to the necessity for a hydrologic and land use/land cover (LULC) change investigation to determine the causes, impacts, and solutions for reducing flood damage. A Geographic Information System (Arc-GIS) and a hydrological model have been used to achieve this goal (HEC-HMS). The authors show that land use patterns have changed dramatically over the last few decades, with the most notable change being a 1003.9 percent rise in built-up area. In this study area, the rise in flood peak of the deadly Kerala Flood 2018 is found to be roughly 22% due to this land use change/urbanization.

2.3 CALIBRATION AND VALIDATION OF HEC-HMS MODEL

Legesse *et al.* (2003) used HEC-HMS 3.5 hydrologic model HMS by using soil moisture accounting algorithm-SMA for the calibration and validation of the upper Blue Nile river basin. The Nash-Sutcliff (E) and Coefficient of determination (R2) were used to assess the model's performance. For model parameter calibration and validation, twenty-one flood occurrences were chosen. The HEC-HMS model can simulate the response of the Dong-wan watershed using the satisfactory results, indicating that the runoff in the catchment rainfall

Alaghamand *et al.* (2011) Using HEC-HMS 3.1.0, researchers evaluated multiple sets of calibrated and validated data for the Sungai Kayu Ara river basin in Malaysia. Lumpur which was located in the west part of the Kuala in Malaysia. The calibrated parameters in this study were imperviousness, lag time and peaking coefficient. To choose best set of values among them, the average, median, and mode were determined. R^2 values for average median and mode were 0.8922, 0.8954, and 0.8678, respectively, according to the results. It can be concluded that the calibration data set average and median parameter values were more accurate and reliable than the validation data set mode parameter values.

Ali *et al.* (2011) To evaluate the effects of land use changes in the Lai Nullah basin, researchers employed the HEC- HMS (rainfall runoff model). The model was

calibrated and verified for the five storm occurrences, with good consistency between the simulated and observed unit hydrographs ranging from 76 to 98 % of Nash - Sutcliffe model efficiency at the basin's outlet. Based on the Islamabad Master Plan and growth pattern, a future land use scenario was projected. The master plan for land use in the future was expected to increase runoff by 51.6 to 100 % and peak discharge by 45.4% to 83.3%, resulting in an increase in total flow. The findings were useful for land use planning and management, and the approaches utilised can be used to future land use impact studies.

Abood *et al.* (2012) used the hydrological model (HEC-HMS) to assess the Kenyir and Berang catchments' performance in simulating rainfall-runoff using two alternative infiltration methods for determining infiltration parameters (abstraction losses, rainfall). The SCS Curve Number method and the Green and Ampt method are two of these methods. The coefficient of determination (R^2), the mean square error (MSE) and the mean absolute percentage error (MAPE) were the statistical analytic functions they used. They've also used HEC- HMS to ensure simulation accuracy. The simulation errors output by the SCS Curve Number technique were 6.5% and 8.2%, respectively. for the Berang and Kenyir catchments, and also 9.13% and 11.11% for the Green and Ampt method errors.

Asadi *et al.* (2013) used HEC-HMS for the rainfall runoff process in small sub basin Delibajak and Kabkian basin in combination with HEC-GEOHMS. With the simultaneous SCS curve number approach of rainfall - runoff modelling, the model was regarded to be carefully calibrated. The historical data review was validated using the sub-basin. The maximum proportion of flow and volume mistakes are within acceptable limits, and the flood events and dealing with all of the locations for computing the coefficients were over 0.9. Between the two basins, hydrologic factors such as curve number and start abstraction were also compared.

Majidi and Shahedi (2013) analysed surface run-off simulation in Abnama watershed with Green-Ampt method and Soil Conservation Service (SCS) methods

using HEC-HMS hydrological model. The HEC- HMS model had been calibrated and validated for hydrograph and related hyetograph had been used for four events after the input parameters to determine the methods for selecting the appropriate method for two different managed using the HEC- HMS model had been calibrated and validated for hydrograph and related hyetograph had been used for four events after the input parameters to determine the methods for selecting the appropriate method for two different. The Green Ampt method's model calibration and validation findings were less than the SCS system's to estimate the difference in lower peak discharge and time to peak. Green Ampt comparison technique based on SCS results has been confirmed to correlate with more than SCS method, as well as their values and the correlation between simulated and observed hydrographs. It may be stated that the Green-Ampt approach of simulation was more precise than the SCS method.

Kabiri (2014) had investigated that the assessment of the SCS CN loss method to evaluate the performance of the SCS CN loss method in Klan-g watershed. They found that the SCS-CN loss technique may be employed for the Klan-g watershed due to strong agreement between observed and simulated in HEC-HMS. In terms of fit, the findings showed that a modified CN with an initial abstraction ratio of 0.5 is better than 0.2. As a consequence, in the Klan-g watershed, CN0.05 may be used to mimic runoff using the SCS technique.

Yao *et al.* (2014) utilising the hydrologic modelling system to examine the influence of underlying surface change on catchment hydrological response. For model parameter calibration and validation, twenty-one flood occurrences were used. The HEC-HMS model was used to simulate the response of the Dong-wan watershed using the satisfactory results, showing that the runoff in the catchment rainfall

Supe *et al.* (2015) used to simulate continuous rainfall-runoff modelling by HEC-HMS model for Wan river basin, Akola, Maharashtra. The relationship between rainfall and runoff was modelled using the soil-moisture accounting approach (SMA). The calibrated model parameters for Groundwater 1, Groundwater 2, GW1

coefficient, and GW2 coefficient were 72, 10, 387, and 1010, respectively. In terms of RMSE, R^2NS and CRM (0.12 m^3/s, 0.93, and -0.02), the model looked excellent.

Waikhom and Manoj (2015) used HEC-HMS model HEC-HMS in order to simulate the stream flow continuous soil moisture accounting (SMA) algorithm in in Vamsadhara river basin, India. The catchment was split into smaller sub-watersheds, yielding a catchment with a diverse terrain, land use, land cover, and soil. During the calibration period, statistical and visual evaluations of the model yielded results ranging from good to very good, with a coefficient of determination R^2 = 0.71, N.S.E = 0.701, percentage error in volume = 2.64 %, percentage error in peak PEP=0.21 percent, and index of agreement d=0.94. With R^2 =0.78, N.S.E=0.762, percentage error in volume = 12.33 %, PEP = -15.2 %, and d= 0.93, the validation period performance evaluation ranges from good to very good. The sensitivity analysis of parameters was performed by ranking the parameters after checking the percentage difference in simulated runoff volume. Finally, the SMA method in the HEC-HMS conceptual model was shown to produce acceptable results and could be used for long-term rainfall-runoff modelling.

Skhakhfa and Ouerdachi (2016) indicated that in order to establish a validation procedure in HEC-HMS, the general consistency of simulated outcomes was required. For calibration and validation, different sets of parameters (CN, SCS Lag, and Muskingum K) were used in the study. When evapotranspiration was not a factor, flood modelling was limited to short durations. The developed flood model's performance was evaluated, and it was found that the correlation coefficient R^2 was close to 1, which was an optimum result.

Abdessamed *et al.* (2018) conducted hydrological modelling in semi-arid region of AinSefra, Algeria, using HEC-HMS. To compute the loss rate and unit hydrograph, the frequency storm and SCS-CN methods were chosen. After calibration and validation, the N.S.E was 0.95, suggesting a reasonable result for rainfall-runoff model simulation.

2.4 COMPARISON OF HEC-HMS WITH OTHER MODELS

The HEC-HMS model was found to be a very basic conceptual model that has been successfully applied by numerous hydrologic modellers across the world and is useful for simulating precipitation-runoff and routing processes in both natural and controlled environments. In comparison to the Revitalised Flood Hydrograph (ReFH),it was shown to be a good model for peak flow modelling because of the semi-distributed modelling concept as acclaimed by Sai *et al.,* (2017).

Akbarpour (2004) carried out simulations of the rainfall-runoff process by using ANN and HEC-HMS model. Daily rainfall and runoff data from 1991 to 2000 were used to calibrate and validate the HEC-HMS model. The research found that predicting flood flows in ungauged catchments using a calibrated HEC-HMS model for a basin was more successful.

Abed *et al*. (2005) developed the simulation using the Spatial Water Budget Model (SWBM) and HEC-HMS Model. Using reservoir inflow data, the models were calibrated and validated. With R^2 values of 0.90 and 0.85 for calibration and 0.75 and 0.80 for validation, both models produced satisfactory results. They compared the results of both models and ran a sensitivity analysis on the HEC-HMS parameters. Watershed characteristics such as imperviousness, curve number, and base flow, in additional to the other parameters on the list, was found to have a significant impact on output. They reached the conclusion that the HEC-HMS developed better results.

Hu *et al.* (2006) applied input data in two models: distributed snow process model (DSPM) and HEC-HMS for gridded snowmelt. The impacts of flooding caused by snowmelt and rain, snowmelt alone, and rainfall alone were all studied. It was hypothesised that combining the DSPM and HEC-HMS models may replicate the snowmelt/rainfall-runoff process through model calibration and validation.

Verma *et al.* (2009) discussed rainfall runoff modelling using HEC-HMS and WEPP hydrologic models, with the support of remote sensing and GIS techniques. During the calibration and validation periods, the HEC-HMS model outperformed the

WEPP model, with reduced root mean square error (RMSE) and standard deviation ratio (SDR) and greater Nash-Sutcliffe efficiency (NSE), percent deviation (D_v), and coefficient of determination (R^2).

Joo *et al.* (2013) tested the Revitalized Flood Hydrograph (ReFH) and HEC-HMS rainfall runoff model for two Korean catchments. The impacts of flooding caused by snowmelt and rain, snowmelt alone, and rainfall alone were all studied. Through model calibration and validation, it was suggested that merging the DSPM and HEC-HMS models may simulate the snowmelt/rainfall-runoff process.

2.5. FLOOD FREQUENCY ANALYSIS USING HEC-SSP

Several statistical distributions have been used in studies to quantify the likelihood and intensity of floods, but none of them have gained widespread acceptance.

George and Gary (2000) performed detailed investigation on flood-frequency prediction methods for unregulated, ungauged rivers and streams of Tennessee, U.S.A. The optimal method for determining flood-peak estimates suited for design purposes at gauged sites was to combine the log-Pearson Type III station estimates as outlined in Bulletin 17B of the Interagency Advisory Committee on Water Data (1982). As a result, flood frequency at each of the gauging sites included in this study was calculated by fitting peak streamflow data to the log-Pearson Type III distribution using supplementary history data for each station.

Kristi and Tatiana (2010) performed hydrologic analysis of the Sana'a Basin in the capital of Yemen using HEC-SSP software. There were very few historical flood records, few historical rainfall records, non-standard hydrologic input data, poorly understood local hydrology, and considerable changes in land use due to rapid urbanisation. Flood danger regions were easily identified for extreme storm occurrences based on the findings of the hydrologic study and subsequent hydraulic modelling, which aided natural disaster risk assessment.

The concept of flood frequency analysis is the assessment of how frequently a specific flood event will occur. Prior to estimate, stream flow data analysis was critical in determining the probability distribution of floods (Ahmad et al., 2011). Flood frequency information was useful for building structures in or near the river that may be flooded, as well as flood structures that would guard against predicted incidents (Izinyon and Igbinoba, 2011). This assures the catchment area's safety and cost-effective hydrologic design.

Fisherman (2015) performed a volume frequency analysis of the river Sava Dolinka, Slovenia using HEC-SSP software to understand the containment of flood flows with different durations and the influence on flow downstream of the barrier in reservoir HPP Moste. The necessary containment volume of the reservoir for a given maximum inflow volume and operational installed flow of the reservoir was found in the study.

Wai (2015) conducted a study using four commonly used probability distribution functions *viz.,* Gumbel Extreme Value Type I, Log-Normal, Log-Pearson Type III and Pearson Type III distribution. Flood frequency analysis was carried out using historical discharge data on three rivers: the Kelantan, Perak, and Pahang rivers. The parameters of all distribution functions were estimated using method of moments. Two goodness-of fit test: chi-square test and Kolmogorov-Smirnov test were used to study how well the distribution fits with the historical data for return periods of 5, 10, 25, 50, 75 and 100. Three software namely “Easy fit”, “HEC-SSP” and “Microsoft Excel” were used to assist computing data, cross checking the results and fitting the distribution functions. Goodness-of-fit test for all the distributions was found satisfactory in every software.

Arturo (2018) conducted a study of historical and measured flood events in the Papaloapan river basin of Mexico. The HEC-SSP software was used to determine peak discharges for a certain return time in each hydrometric station using the Log Pearson type III probability distribution. The logistic regression model correctly

predicted 92 % of the flood events. The final result was such that, when discharge was higher than the 50-year return period river discharge of 11,869 m^3/s, it was a catastrophic event. On the other hand, if it was higher than the 20-year return period river discharge of 9,711 m^3/s, it was an extraordinary flood.

Joan *et al.* (2019) conducted the Hydrologic Frequency Analysis (HFA) using the rational equation and Flow Duration Curve (FDC) for the actual and simulated streamflow data. HFA was conducted using HEC-SSP, in which Log Pearson III distribution was best fitted with both actual and simulated data.

Mike and Matthew (2019) evaluated the performance of 700 dams and 15,000 miles of levees throughout the United States, by risk assessments through hydrologic hazard curves and HEC-SSP software. They developed a "hydrologic hazard curve" to assess the hydrologic risk of dams and levees. For a wide variety of peak flows, flow durations, and stages, this gave flood magnitudes and probability.

2.6 HYDRAULIC MODELLING USING HEC-RAS

Christopher (1999) presented a simple method for enabling two- and three-dimensional floodplain mapping and analysis in the ArcView Geographic Information System by processing output data from the HEC-RAS hydraulic model. A stretch of Waller Creek in Austin, Texas was studied using this approach. A planar floodplain perspective was created using digital orthophotos as a basis map. Using HEC-RAS cross-sectional coordinate data and a digital elevation model of the research region, a digital terrain model was created. A stretch of Waller Creek in Austin, Texas, was studied using this approach. As a foundation map, digital orthophotos were used to construct a planar floodplain viewpoint. Using HEC-RAS cross-sectional coordinate data and a digital elevation model of the research region, a digital terrain model was created.

Evans *et al. (*2004) GIS applications in flood risk mapping include anything from storing and managing hydrological data to creating flood inundation and hazard maps to aid flood risk management, according to the report. GIS was used to

manipulate and process various forms and types of spatial data for the strategic flood risk assessment, which was coupled with 1D and 2D flood modelling techniques. TUFLOW was used to carry out the flood modelling procedure. Among the results of their efforts are flood risk/hazard maps and evaluations for the study area. They also created a two-dimensional simulation scenario as part of their research. Flood modelling in the study area surroundings was also part of their research. It covered the area where the project's drainage network data (a key data requirement for the modelling phase) was collected. The flood modelling method was carried out using the HEC modelling software (HEC-HMS and HEC-RAS). Other types of data, such as precipitation data and information on the elevation of buildings, were input in the production of a two-dimensional representation of the flood modelling results (flood inundation map) and a three-dimensional representation of the study area, respectively, in addition to the key data requirements such as the drainage network, LIDAR (DEM), and land use data.

Knebl *et al.* (2005) developed a framework for regional scale flood modelling that integrated NEXRAD rainfall, GIS and a hydrological model for the purpose of flood management. For the San Antonio river basin in the United States, the HEC-HMS model was used to convert precipitation surplus to overland flow and channel runoff. Based on HEC-HMS-derived hydrographs, a hydraulic model (HEC-RAS) was able to model the unsteady state flow through the river channel network and produce floodplain polygons that were comparable to satellite images.

Salajegheh *et al. (*2009) conducted a study on floodplain mapping using HEC-RAS and GIS in semi-arid regions of Iran. This study connects HECRAS hydraulic modelling with ArcView GIS spatial presentation and floodplain data analysis. This study shows how to use ArcView to handle the output of the HEC-RAS hydraulic model, allowing for two- and three-dimensional floodplain mapping and analysis. The study was place on a stretch of the Polasjan river basin on Iran's central plateau. The resulting surface model portrays the general topography accurately and provides

extra information in the stream channel. The findings of the study show that GIS may be used to map and analyse floodplains.

Prafulkumar *et al.* (2011) developed flood prone areas using HEC-RAS model and also the accuracy of calibrated model was verified for the floods of the year 2006. The roughness coefficient of the channel Manning's n values for the river were calculated using HEC-RAS flood simulations for the years 1998 and 2003, and compared to images of river sections taken during a field visit to the lower Tapi River. For the Kakrapar gauging station, there was a good agreement between the simulated and observed stages.

Hakim *et al.* (2012) conducted one dimensional steady flow analysis using HEC-RAS model for river Jhelum, Jammu and Kashmir. Based on peak flood data, the HEC-RAS model was used to forecast anticipated flood levels. For the 50-year and longer return periods, the model's output suggests an overflow at the river's maximum locations. The left bank of the river was found to be more vulnerable to flooding than the right bank, emphasising the necessity for river channel engineering features such as dykes and levees.

Sardoii *et al*. (2012) attempted in comparing different methods in HEC-HMS model, *i.e*., initial and constant, Green- Ampt, SCS curve number with regard to various error functions (percent error in peak, peak-weighted root mean square etc.) by taking into account of the obtained results of different storm events simulation. In terms of objective functions, the results showed that Green and Ampt, SCS and the ‘initial and constant' method were ranked first, second, and third, respectively. As a result, the Green-Ampt method was recommended as a suitable method for application in similar areas and conditions.

Khaleghi *et al.* (2015) used GIS to create flood zone maps and integrated them with hydraulic and hydrological models in a research. Flooding in the Lighvan basin wreaked havoc on gardens, agriculture, and residential areas. Land use changes in prior years were also major contributors to these effects. Flood prone areas with

different return times were generated using GIS and the HEC-RAS model along a 16-kilometer length of the Lighvan Chai River, and land use changes during a 10-year period (2000-2010) were extracted using satellite data. The ratio of flooded area by 25-year return period to flooded area by 200-year return period is nearer to 67 percent, according to flood zoning results. According to the report, floods that last 25 years or less account for approximately 67% of total flooding. Dense pasture, barren land, and irrigated farming are decreasing, while residential areas, weak pasture, and rain fed farming are increasing, according to the land use change analysis.

Nareth *et al*. (2015) made a study on floodplain management and mapping of Nam Phong river basin, Thailand using HEC-RAS and GIS. A approach that included a hydraulic simulation model, HEC-RAS, and GIS analysis was utilised to delineate flood extents and depths inside the Nam Phong river in northeast Thailand. It is necessary to simulate advanced hydraulic behaviour of the river in a more simple fashion for the purposes of maintaining and executing all river training activities. The flood extents and depths inside the Nam Phong river in northeast Thailand were delineated using an approach that included a hydraulic simulation model, HEC-RAS, and GIS analysis. For the objectives of maintaining and executing all river training activities, it was essential to simulate complicated hydraulic behaviour of the river in a more basic way. The important flooding locations along the river were identified using a grid layer of flood depths. The findings revealed that combining hydraulic simulation with GIS analysis might be beneficial for a variety of floodplain management and mapping applications, as well as offering alternative scenarios for river training and flood mitigation design.

Serede *et al.* (2015) studied on hydraulic analysis of irrigation canals using HEC-RAS Model was conducted in Mwea irrigation scheme, Kenya. The HEC-RAS model was used to predict canal capacity potential and was tested for error estimation. Thiba main canal reach in Mwea Irrigation Scheme (MIS) was chosen, which is around 100 km^2 north of Nairobi City. Because MIS is a model programme

in the country, it has a built-in contribution to food security and sector growth. Using two sets of observed discharges, gate openings, and water levels, the HEC-RAS model was chosen, calibrated, and validated. To evaluate the model's performance, statistical and graphical methodologies were applied. Finally, the model was utilised to calculate the major canal reach's potential capacity. According to the findings, raising the hydraulic resistance of Link Canal II (LCII) from 0.022 to 0.027 reduced the anticipated maximum capacity by 10.97 percent. Increasing the roughness coefficient from 0.015 to 0.016 resulted in an 11.61 percent drop in predicted maximum capacity for the Thiba Main Canal (TMC). As a result, flow rates in Link canal II and TMC were only 9.9 m^3/s and 5.7 m^3/s, respectively.

Alfredo *et al.* (2016) performed research on urban flood risks as a result of river flooding, as well as the necessity for hazard maps and the identification of possible flood zones. The goal of this project was to talk about developing a system for hazard mapping of river floods on a municipal scale, as well as mapping flood-prone regions. The study area is the municipality of Ipojuca in the state of Pernambuco, which covers 527.11 km^2 and has a population of 80,637 people. The first method employs the HEC-HMS and HEC-RAS models for hydrologic-hydraulic modelling of the lower course of the Ipojuca river. The hydraulic model used the streamflow estimated in the rainfall-runoff model as input to replicate the water surface profile in the river. This allows for the calculation of water depth and flow velocity, both of which are required for the definition of hazard indicators.

Vahdettin Demir *et al.* (2016) studied flood hazard mapping by geographic information system and hydraulic model for the Mert river. Their article describes in detail the procedure followed for preparing flood hazard maps using ARC-GIS, HEC-RAS & HEC- Geo RAS. The authors completed the study for the Mert river basin in Samsun, Turkey, in response to the flood of 2012. The authors suggested that when predicting flood profiles for certain return periods, always use a flood model in conjunction with GIS. There are three stages to the overall procedure. First, a 1:1000

scale digital elevation model was created using Arc-GIS and then a flood risk map was created. The second stage involves modelling and analysis, which includes the use of HEC-GeoRAS for datum creation and the provision of hydrologic data for 10, 25, 50 and 100 years of floods. The software was also given the manning's value based on land use and land cover pattern at this stage. Concrete, brush wood, and woodland river banks had Manning's roughness values of 0.022, 0.026, and 0.045, respectively, whereas river base had a roughness coefficient of 0.03. The third and final stage was comparison to previous pictures and creating water surface profiles.

Olayinka and Hudson (2017) conducted a study to use remote sensing, HEC (Hydrological Engineering Centre) modelling packages including HEC-HMS and HEC-RAS, and GIS software (Arc-GIS 10.1). for the flood modelling and mapping of the adjoining areas of the Lagos Island and Eti-Osa Local Government Areas (LGAs) which are a part of Lagos state, Nigeria. The flood model output shows a range of flood depths as well as their extent in the study area. Buildings (structures) with the highest risk (within the flood area indicated by the model result) are mainly used for residential and commercial uses, with total percentage coverage of 72.34%. These results suggest that residents' lives, as well as commercial activities, are in grave risk, and that this will have a significant negative impact on residents' social well-being.

Sandhyarekha and Shivapur (2017) studied on flood plain mapping of river Krishna using HEC-RAS model at Kudachi and Ugar villages of Belagavi district, Karnataka. The main aims of this project were to determine the flooded area cover during the worst flood occurrences along the Krishna river and to create a floodplain map of the area. The Krishna basin's watershed area had been successfully modelled, and a map showing flooded areas along a section of the Krishna basin had been produced. The flooded area spatial distribution was clearly depicted on the floodplain map. High water depths typically flow along the main channel and gradually expand to the floodplains. Along the Krishna river, the total flooded area for the 100-year

return period rainfall was around 300 acres near Kudachi and 116 acres near Ugar village. Thus, integration of geospatial processes and hydraulic modelling can produce inundation flood map with good accuracy.

Sunilkumar and Vargheese (2017) made a study on the occurrence of high intensity rainfall for some continuous days that resulte in flooding in most parts of Kerala. The research location was the Mangalam river basin, which is prone to severe flash floods during periods of heavy rainfall. The catchment's flood hydrograph was created using the Hydrologic Engineering Centre's Hydrologic Modelling System (HEC-HMS) software's time distribution coefficient method, and the flood inundated area was modelled using the Hydrologic Engineering Centre's River Analysis System (HEC-RAS) software, with inundation maps created in GIS. One of the goals was to figure out the maximum flood that might happen in the research region. The greatest discharge recorded inside the basin was 524.1 m^3/s. This calculation aids in the design of a civil structure in the research field.

Prabeer (2018) made a study on flood management in Mahanadi Basin using HEC-RAS and Gumbel's Extreme Value Distribution. Because this flood is regarded the most major and happens under shifting climatic circumstances, the research was conducted utilizing 25-year return period floods (45067 cumecs). According to the findings of the research, raising the embankment in the left bank from a minimum of 0.11 m to a maximum of 10.63 m should be done in 23 of the 36 cross sections. Heightening of the right bank embankment, ranging from 0.09 m to a maximum of 9.94 m, is also necessary. This can significantly reduce the Mahanadi river system's flood risk.

Ali and Jaber (2018) did flood inundation area mapping at Wadi Attarat Um Al Ghurdan Oil Shale mining concession area. Using the HEC-RAS model, GIS for spatial data processing, and HEC-GeoRAS for interface between HEC-RAS and GIS, the flooded regions along the major Wadi of Al-Ghadaf catchment area have been mapped based on flow rates for different return periods. The research area's regions

along the major wadi were flooded for 5, 10, 25, 50 and 100 years. Inundation maps show the spatial extent of potential flooding in various situations and can be depicted statistically or subjectively. Flood inundation models were generated using Arc-GIS for return periods of 25, 50 and 100 years. The major findings of the study revealed that the water level in some waterlogged areas reaches 5.0 m. along the wadi. As a result, flood hazard control, particularly in low-lying flood-prone areas, can be undertaken to limit the detrimental effects of floods.

Tunas *et al. (*2019) Integrated TIN data into the HEC-RAS Hydrodynamic Model to conduct flood routing for assessing river capacity and predicting variables that cause floods for the Lantikadigo river in Central Sulawesi, Indonesia as a model. This river floods almost every year, with different degrees of inundation. Integrating data is a method of creating geometric data that is then fed into the HEC-RAS Model in a GIS context. Because input geometry data is done through the import data facility, data integration improves the efficiency of simulation time when compared to manually input geometry data. The highest water level and during 1-year return period exceeded the river bank elevation on both the left and right sides of the entire segment, according to the findings of this study. At the Lantikadigo Watershed's outlet, the hydrograph's maximum flow for a one-year return period is 55.3m^3/s. The average channel capacity is much lower than the peak discharge, indicating that the average channel capacity is significantly lower than the peak discharge. Flooding in the Lantikadigo river is mostly caused by morphological changes in river geometry, according to modelling results.

Avanti *et al.* (2020) made a study on flood modeling and flood forecasting of Mutha river using HEC-RAS. This helps in the decision-making process for flood mitigation and disaster relief efforts in the area. The city of Pune in Maharashtra endures flooding and damage during the monsoon season. Several river crossings are submerged during this time, resulting in communication failure and inundation of the city and the surrounding area. The depth of the water, velocity, and height of the

water surface are all calculated using this model throughout the time. The relevance of 2D flood modelling was underlined in the study because it assists in the creation of management strategies for dealing with anticipated future disasters through the implementation of flood risk reduction approaches.

Selman and Fevzi (2020) did floodplain analysis between Diyarbakır-Silvan Highway and historical Ten-Eyed Bridge. The road under examination includes a historic bridge, as well as lush agricultural lands, buildings, and hospitals on the Dicle University campus, the UNESCO-listed Hevsel Gardens, and some residential neighbourhoods. The study's objective was to analyse flood zones and produce a flood hazard map that might anticipate dangerous spots along this important route. One of the goals of the study was to safeguard the Tigris River Rehabilitation Project. The AutoCAD Civil 3D programme was used to digitise the 1/1000 maps in the study area, and cross sections were created using the region's digital elevation models. The hydraulic characteristics of the flood bed and the water surface profiles of the Q25, Q50, Q100, and Q500 flood recurring and one-dimensional floodplain analysis of the Tigris river were determined using the HEC-RAS software.

Sathya and Santosh (2021) worked on preparing a flood inundation map for a stretch of the river Cauvery for different return periods. Hydraulic modelling was done using the HEC-RAS software. To create a flood inundation map, GIS was utilized to process spatial data, and HEC-GeoRAS was used to interface HEC-RAS and GIS. The inundation map created shows the entire submergence of the surrounding regions along the chosen stretch, emphasising the necessity for a proper flood warning system and flood protection measures along the stretch. These, along with proper land use management and afforestation, can greatly decrease the harmful consequences of flooding, particularly in low-lying regions. The study's findings will help departments and agencies in establishing river basin flood management plans.

CHAPTER III

MATERIALS AND METHODS

This chapter gives a detailed description of the study area, model generated and collected data, flood modelling in HEC-HMS, flood frequency analysis using HEC-SSP and the stepwise procedures for the integration of HEC-HMS and HEC-RAS models with GIS to develop a regional model for flood inundation mapping and risk assessment of Chalakudy river basin. The theoretical consideration of various model components and the different methods applied to carry out the research are also explained briefly in this chapter.

3.1 STUDY AREA

The study area was Chalakudy river basin in Kerala. Chalakudy river is the fifth longest river in Kerala and drains through Palakkad, Thrissur and Ernakulam districts. This was one of the worst affected basins in the Kerala floods of 2018 and most of its basin area was severely affected. The basin lies between 10° 05’ to 10° 35’ North Latitude and 76° 15’ to 76° 55’ East Longitude. The river originates from Anamalai hills of the Western Ghat mountain ranges and flows through the Northern part of Periyar river after draining through varied physiographic and geologic terrains of Tamil Nadu and Kerala states. The river basin is bounded by the Karuvannur sub–basin in the North and Periyar sub-basin in the South. The shape of the basin is roughly triangular with its base along the East, having a length-width proportion of 3:1. The basin receives an average rainfall of about 3000 mm. The total length of the river is about 130 km and the catchment area is about 1,704 km^2. Out of the total catchment area, about 300 km^2 lies in Tamil Nadu and nearly 1400 km^2 lies in Kerala state. There is a river gauging station at Arangali at the downstream, monitored by the Central Water Commission (CWC), India.

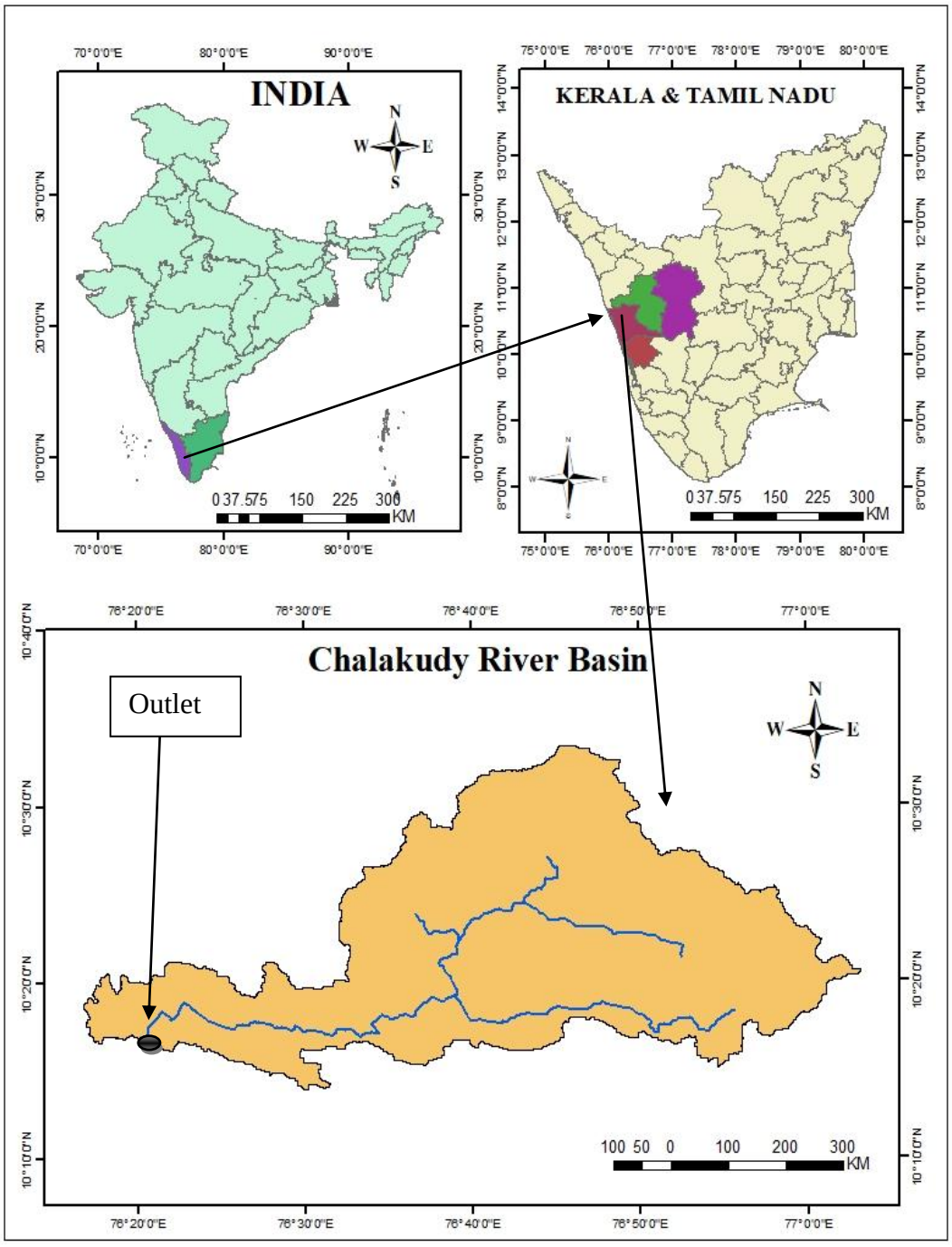

Fig. 3.1 Study area and location map of Chalakudy river basin

3.2 METEOROLOGICAL AND PHYSIOGRAPHIC INFORMATION OF THE BASIN

3.2.1 Physiography

Chalakudy river is formed by the confluence of four major tributaries namely Sholayar, Parambikulam, Kuriarkutty and Karapara.

3.2.1.1 *Sholayar river*

The Sholayar river originates in Tamil Nadu's Coimbatore area. It runs for 44.8 km before turning north and joining the Parambikulam river 1.6 km before Orukumbankutty, at an elevation of 464 m above mean sea level (MSL). At the southern end of the Nelliampathy plateau, the Sholayar river enters Kerala.

3.2.1.2 *Parambikulam river*

The Parambikulam river originates in Tamil Nadu's Coimbatore district. It runs North of the Sholayar river and enters Kuriarkutty at 536 m above sea level.

3.2.1.3 *Kuriarkutty river*

Kuriarkutty river flows from Kerala's Anamalai highlands and enters the Parambikulam river in Kuriarkutty.

3.2.1.4 *Karapara river*

The Karapara river originates in the Nelliyampathy hills of Kerala's Palakkad district. It runs west and then south west till it reaches Orukumbankutty, 455 metres above sea level, where it joins the main river. The Chalakudy river flows from the point where the Karapara river meets the main river and reaches the plains after a few kilometres.

3.2.2 Dams in the basin

The six dams in the basin are Poringalkuthu, Sholayar, Upper Sholayar (in Tamil Nadu), Parambikulam, Peruvaripallam, and Thunakadavu. (In the Indira Gandhi Wild Life Sanctuary in Tamil Nadu, there are a few minor dams in the basin). Details of the dams are given below.

Table 3.1 Details of dams in Chalakudy river basin

Sl. No.	Name of the dam	Year of commissioning	Purpose	Storage MCM
1	Poringalkuthu	1957	Electricity generation	32
2	Thunakadavu	1965	Diversion	15.77
3	Kerala Sholayar	1966	Electricity generation	153.49
4	Parambikulam	1967	Diversion	504.66
5	Peruarippallam	1971	Diversion	17.56
6	TN Sholayar	1971	Electricity generation & diversion	152.7

3.2.2.1 *Poringalkuthu dam*

Poringalkuthu dam is constructed across the Chalakudy river to divert flow to Poringalkuthu hydroelectric project (48 MW). The project is located in Thrissur district of Kerala State. The dam is located at latitude, 10° 18’ 45” N and longitude 76° 38’ 10” E.

Table 3.2 Salient features of Poringalkuthu dam

Catchment area (km^2)	752.20
Average runoff (M.Cu.m)	538.01
Design flood (Cu.m/sec)	2265.35
Type of dam	Masonry gravity
Full reservoir level (m)	423.97
Number of generating units	4

2.2.2 *Kerala Sholayar dam*

This project is situated at Ambalappara in Mukundapuram taluk of Thrissur district at 10° 77’ North latitude and 76° 45’ East longitude. Three dams were constructed to create Sholayar reservoir as part of the Sholayar hydroelectric project

(54 MW). Sholayar main, Flanking and Saddle dams are the three dams. The reservoir spillway arrangement is provided by Flanking Dam. These dams are built across the Sholayar stream and its tributaries. The river Sholayar is a main tributary of the Chalakudy. The reservoir's water is diverted to the power station via a tunnel/penstock system. Sholayar brook carries the spill water to the Chalakudy river. Poringalkuthu reservoir receives runoff from the power plant.

Table 3.3 Salient features of Sholayar dam

Catchment area (km^2)	186.48
Average Runoff (M.Cu m)	396.43
Design flood (Cu.m/sec)	1710.33
Type of dam	Masonary gravity
Full reservoir level (m)	811.68
Number of generating units	3
Installed capacity(MW)	54.0

3.2.2.3 *Tamil Nadu Sholayar dam*

This dam is situated within the Coimbatore district of Tamil Nadu. Storage capacity is 153 MCM. Inflow from 121 sq.kms area and diverted waters from Upper and Lower Nirar reaches the dam.

3.2.2.4 *Parambikulam dam*

The storage capacity is 17820 Mcft (504 MCM).The dam gets inflow from own catchment (228sq.km) & from powerhouse (no1) and flood release from TNS.

3.2.2.5 *Thunakadavu*

The full reservoir level of Thunakadavu dam is 539.49 m MSL.

3.2.3 Rainfall

The annual average precipitation over the basin is about 3,300 mm, varying from 3,700 mm in the uphill area to 2,900 mm in the downstream area (Maya, 2005). The rainfall in the area increases from west to east. About 68.2% of the total rainfall

is received from the month of June to September (South- West monsoon). A portion (17.5%) of total rainfall occurs from October-February (North East monsoon), 13% of total rainfall from March to May and the remaining rainfall during the month of January to February. Daily rainfall data collected from five rain gauge stations along with other meteorological data like maximum and minimum temperature, relative humidity, sunshine hours, wind speed *etc.*, collected from ARS, Chalakudy and IMD, Pune were used in the study. There are no stations in the river's middle and downstream sections, as well as to the west of Chalakudy. With the data provided, it is impossible to get an accurate picture of the rainfall in the basin. More rain gauge stations, evenly distributed over the basin, are required for a better understanding. Daily stream flow data at CWC gauging station, Arangali, located near the outlet of the basin has been collected from Cauvery & Southern Rivers Circle, CWC, Bangalore, for the study period.

The daily rainfall data collected from ARS Chalakudy and IMD, Pune for the years 1997-2017 was used for determining the average monthly rainfall values and the results are shown in section 4. The table 3.4 shows the GPS locations of the rain gauge stations. The rainfall and flow data collected are given in appendix I and II.

Table 3.4 GPS location of the rain gauge stations

Sl. No.	**Gauging station**	**Latitude**	**Longitude**
1	Thunacadavu	$10^{o}20'\ 03''N$	$76^{o}\ 46'\ 54''E$
2	Chalakudy	$10^{o}\ 18'46''N$	$76^{o}\ 20'\ 30''E$
3	Peruvaripallam	$10^{o}\ 27'\ 00''N$	$76^{0}\ 46'10''E$
4	Parambikulam	$10^{o}\ 23'18''N$	$76^{o}\ 46'\ 07''E$
5	Kerala Sholayar Dam (KSD)	$10^{o}\ 17'55''N$	$76^{o}46'\ 49''E$

3.2.4 Climate

The Chalakudy basin has a humid tropical climate, with summers lasting from March to May and rainy seasons lasting from June to September. In the higher slope ranges, a wet climatic condition dominates. The relative humidity was higher

during the monsoon period in the region. Highest wind speed is recorded during May (10.9 km/h) (Maya. 2005). Throughout the year, the temperature in the basin is quite stable. During the month of March, the maximum temperature varies between 25.7°C to 35.1°C. The data on climatic variables were collected from ARS Chalakudy over a 27-year period (1990-2017). Appendices III, IV, V and VI gives the meteorological data of the study location.

3.2.5 Soil

The basin soils are divided into six categories. They are called 'lateritic soil,' 'riverine alluvium,' 'seaside alluvium,' 'hydromorphic saline,' 'earthy coloured hydromorphic,' and 'timberland topsoil,' respectively. Lateritic soils are the most common type of soils found in the midland district. The earthy-coloured hydromorphic soil can be found in the valley base of the midland's undulating geology. Timberland soil was rich in organic matter and covers a large portion of the upland. Along the waterway channels and their tributaries, there is riverine alluvium. The soil data for the Kerala region was collected from the Department of Soil Survey and Soil Conservation, Govt. of Kerala, Thiruvananthapuram and the soil data for the Tamil Nadu region was collected from the Dept. of Remote sensing and GIS, TNAU, Coimbatore, because the Chalakudy river basin spans in both Kerala and Tamil Nadu.

3.2.6 Land Use Land Cover (LULC)

Kerala soils are categorised as Laterite, Coastal alluvium, Riverine alluvium, and Kuttanad alluvium based on their morphological characteristics and physiochemical qualities. The Thrissur district is mostly made up of agricultural land, including both irrigated and rainfed regions. Paddy is cultivated in the valleys and lowlying areas, coconut plantation is practiced in the elevated areas. Ernakulam district is separated into three categories based on land use: arable, forest, and waste areas. The eastern half is primarily forested, with rubber and cashew crops thrown in for good measure. Around 80% of the area is suitable for farming, while the remaining 10% is used for planting and reserve forest (Maya, 2005). The forest land,

which is distributed over the central section of the country, is adjacent to the arable land.

3.3 DIGITAL DATABASE USED

3.3.1 DEM

It is a three-dimensional representation of a terrain's surface created using data on the elevation of the ground surface in relation to any reference datum. DEM is a computerised representation of geography and terrain that is frequently employed in hydrologic and geologic examinations, hazard checking and monitoring, natural resource study, and other applications. The basin was delineated and basin characteristics such as elevation, slope, slope length, flow direction, and drainage features were determined using a The Shuttle Radar Topography Mission (SRTM) DEM of 30 m resolution downloaded from USGS earth explorer.

3.3.2 Satellite Image

Sentinel satellite imagery for the year 2020 were downloaded from the USGS earth explorer to generate the LULC map. Sentinel images were downloaded because they allow for the simultaneous collection of high-resolution multispectral data of the earth's surface. The imagery for the month of April, 2020 was selected for the study in order to make sure that the image was cloud-free.

3.4 DETAILS OF VARIOUS SOFTWARE AND EXTENSION TOOLS USED

3.4.1 Geographical Information System (GIS)

Geographic information system (GIS) is used to capture, store, manage, and present a wide range of spatial data. GIS enables hydrologists to coordinate different information from various sources with equal geographical reference into an acceptable framework because of its remarkable potential for spatial information research. HEC-GeoHMS, an ArcGIS extension tool, was used to represent the physical surface by identifying sinks, determining stream flow direction and accumulation, and creating stream networks (Islam, 2015).

3.4.2 ERDAS Imagine

ERDAS Imagine is an image processing software developed by Intergraph in the United States that allows users to handle geospatial, vector data, and other imagery. It can also handle hyper spectral imaging and LiDAR data from various sensors, as well as provide a 3D virtual module (Virtual GIS). The LULC map was prepared using the ERDAS Imagine 2014 software, available in the Geo spatial laboratory, KCAET, Tavanur and the method adopted was unsupervised classification.

3.4.3 HEC-GeoHMS (Geospatial Hydrologic Modelling Extension)

HEC-GeoHMS is an ArcGIS extension tool that is designed to handle geospatial data to create input documents for the HEC-HMS. One can analyse the results and outline the sub-basin to produce the hydrologic inputs using the Graphical User Interface (GUI), which consists of a collection of menus and tools. Soil map, DEM, land use data, precipitation, and other data are included in the GIS database. HEC-GeoHMS uses the DEM to establish the basin outline and set up various HEC-HMS inputs.

The HEC-GeoHMS extension tool was utilized to delineate the basin using DEM in this study. Using the tool 'Gage Theissen polygon,' the basin average precipitation was computed by Theissen polygon method. By integrating both the land use map and soil map polygons, the ‘Generate CN grid' tool was used to generate the Curve Number (CN).

3.4.4 HEC-HMS model

The Hydrologic Engineering Centre of the US Army Corps of Engineers developed the Hydrologic Modeling System HEC-HMS. This is a more advanced version of the US Army Corps of Engineers' HEC-1 model, which was developed in 1968. HEC-HMS has been widely used in hydrology since then to model the rainfall-runoff process, flood forecasting system design, estimating the effects of land-use changes and runoff simulations in ungauged basins (Halwatura and Najim 2013). A

basin model and a meteorological model are the two main models of the HEC-HMS model. HEC-GeoHMS generates a number of files that can be used directly by the HEC-HMS model. The "meteorological model document," "background shape files," "basin model file," and "recorded project" are among these documents. All of the hydrologic parameters that will be included in the model run should be evaluated and manually put into the HEC-HMS basin model. After all of the model segments have been completed, the user can conduct a simulation to calibrate the model and optimise the parameters involved.

3.4.5 HEC-SSP Software

The statistical functions were computed using HEC-SSP software, which consists of public domain executable code and documentation developed by the Hydrologic Engineering Centre for the US Army Corps of Engineers with US Federal Government resources. This software can be downloaded from the HEC website (www.hec.usace.army.mil). The user can use this software to do statistical analyses on hydrologic data. Flood flow frequency analysis based on Bulletin 17B, "Guidelines for determining flood flow frequency" (1982), a generalised frequency analysis on not only flow data but also other hydrologic data, a volume frequency analysis on high and low flows, a duration analysis, and correlation analysis are all possible with the current version of HEC-SSP.

3.4.6 RAS Mapper

HEC-RAS Mapper is an interface that can be used from the main HEC-RAS software and provides input data as cross sectional data of river for the HEC-RAS, simulation results, and other relevant geospatial data to help users develop river hydraulic models more effectively.

3.4.7 HEC-RAS model

The Hydrologic Engineering Centre of the US Army Corps of Engineers developed HEC-RAS, a hydrodynamic model. The hydraulic model is capable of both one-dimensional and two-dimensional hydraulic simulation. It can do one-

dimensional (1D), two-dimensional (2D), or combination 1D and 2D hydraulic computations for a whole network of natural and man-made channels. HEC-RAS was used to predict the movement of the runoff water over the surface. Results of the hydrological model created (rainfall runoff volume) was used by HEC-RAS to analyse the way the water moves on the study area and the places where it concentrates, creating inundation problems.

3.5 MODELLING OF FLOODS

Awareness of flood and the study of its behaviour require sufficient data about the basin hydrologic condition and river discharge. Achieving this goal is not possible in seasonal rivers and regions where no steady flow occurs. With the advancement of new techniques for flood modelling these days, it is possible to model the flood extent, depth, distribution etc. in the temporal and spatial dimensions. Past flood studies in the area however ignores these applications. Hence use of hydrologic models for simulation of rainfall-runoff processes and hydraulic models for analysis of the runoff flow in the river and its distribution is necessary.

In the course of determining flood inundation areas in this study, two modelling components namely the hydrologic model and the hydraulic model were used. HEC provides two platforms, HMS and RAS, over which each of these were conducted. Because of the simplicity of parameterization of geographical data available for the study area, HEC modelling packages were selected in this study. These packages have been used by various people in mapping inundation extents and have been proved efficient in flood modelling. The models are well-suited to GIS applications, ensuring that the platforms interact in a fast and efficient manner throughout the modelling process. The modelling software are especially well suited to the study area since they have show superior practical usage in modelling river basins using elevation and land cover data throughout time.

3.5.1 HEC-HMS Hydrologic modelling

The hydrological simulation modelling was performed using HEC-HMS, which is a semi-distributed hydrologic model with the ability to perform continuous as well as event based simulations in dendritic watershed systems. The catchment is built in HEC-HMS by disintegrating the components of the hydrological cycle into manageable pieces, such as precipitation, initial abstraction, evapotranspiration, infiltration, surface runoff and base flow. Sub-basin, reach, junction, reservoir, diversion, source and sink are some of the features used in this model to define the physical description of the watershed. Runoff is calculated in a step-by-step manner, starting with canopy storage and progressing through surface or depression storage, infiltration, and transformation into a base flow/surface flow hydrograph. The flow hydrograph is the model's output and it uses rainfall as well as other regionally distributed watershed features like land use/land cover and soil as inputs (Scharffenberg *et al.,* 2008).

Different components included in the HEC-HMS are listed below.

- *Basin Models:* Basin models include the physical basin area, as well as hydrologic components (sub basins, junctions, reaches, and reservoirs) and the catchment's drainage network.
- *Meteorological Models:* In a meteorological model, information about meteorological components such as temperature, precipitation evapotranspiration, sunlight, humidity and snowmelt is defined. Each meteorological component can be defined in a variety of ways with HEC-HMS.
- *Control Specification:* The start and end dates and times of the simulation, as well as the computing time step, are specified in the control specification.
- *Time series Data:* This section provides real-time series data for all of the meteorological elements defined in the meteorological model. In addition to the meteorological elements stated above, discharge data can be provided for calibration and simulation of the constructed model. It can be supplied to the

software manually or in the form of HEC-DSS, the Hydrologic Engineering Center Data Storage System.

- *Paired Data:* As coupled data, meteorological data in tabular/graphical format is provided. (Scharffenberg, 2008)

Data required for hydrologic modelling using (HEC-HMS) are:

i. Digital Elevation Model (DEM).
ii. Land use
iii. Soil map and
iv. Meteorological data

3.5.1.1 *Digital Elevation Model (DEM)*

Digital topography is one of the most useful types of geospatial data. A DEM is used to derive topography features such as slope and drainage direction. Watershed boundaries, channel slope and other features are traditionally defined by contours of equal elevation in a landscape model. In this study, the basin was delineated and basin properties such as elevation, slope, slope length, flow direction, and drainage features were determined using a SRTM DEM of 30 m resolution downloaded from USGS earth explorer.

3.5.1.2 *Preparation of Land use land cover map*

ERDAS Imagine 2014 software, which is available in the Geo Spatial lab of KCAET, Tavanur, was used to create the land use land cover map. The USGS Earth Explorer website (http://earthexplorer.usgs.gov/) has provided 30m spatial resolution Cloud Free Sentinel satellite data (geocoded using UTM projection, spheroid, and datum WGS 1984, Zone 43 North). Unsupervised classification was the method used in this study. The Unsupervised option from the Classification menu was selected. After that, the Sentinel image for the year 2020 was selected as the input file and the output file was given a name. A 40-class initial classification with 100 iterations was created. The Isodata classification method was selected by default. This algorithm finds 16 data clusters in the image, calculates the mean for each picture channel and

then assigns each pixel to one of the clusters using the minimum distance to mean rule. It is not necessary to establish a signature file or adjust the convergence threshold. The number of classes was initially set to forty, and pixels from the same class category were merged into a single class using the recode menu. To develop eight LULC classes, each merged class was renamed and iterations were performed using the same process. In this study, the land use classes taken were eight *viz.*, water body, forest/other vegetation, urban area, barren land, tea, paddy, oil palm and coffee/cardamom. The top region is made up of arid ground, forested areas and water bodies. Forest plantations cover about 10% of the forest area, degraded forest covers 12%, deciduous forest covers 8%, and semi-evergreen forest covers 5%. (Maya, K. 2005). The upland area is covered by 40% agricultural land, the majority of which is planted with a mix of agricultural and horticultural crops. Wasteland covers about 10% of the upland region, with the rest of the area being covered by water bodies. Paddy fields and urban communities dominate in the basin lower regions.

Ground truthing and data collection were done before identifying the different classes within the study region. Cross-checking the basin region using ‘Google Earth Pro' for identifying the different classes was also done. After the classification of each pixel was completed, every class ought to be inspected and a name assigned to it.

3.5.1.3 ***Preparation of Soil map***

The soil data collected for the Kerala region from the Department of Soil Survey and Soil Conservation, Govt. of Kerala, Thiruvananthapuram, and for the Tamil Nadu region from the Dept. of Remote sensing and GIS, TNAU, Coimbatore, were used in this study. Soil map contain the areal extent of different soil classes prevailing in the area, morphological description of the soil and its properties. Model requires soil hydrology groups for generation of curve number grid map. The hydrological soil group and soil characteristics were assigned to the soil type which aids in the modelling process. Soils of Chalakudy river basin fall within 6 broad

categories. They are: 1) Lateritic soil 2) Hydromorphic saline soil 3) Brown hydromorphic soil 4) Riverine alluvium 5) Coastal alluvium and 6) Forest loam.

3.5.1.4 ***Preparation of CN grid map***

The loss module in the HEC-HMS model requires CN. It was created using HEC-GeoHMS and the prepared LULC and soil maps. In addition, the CN value was optimized in HEC-HMS during calibration at a later stage. The steps to obtain a Curve Number grid for the catchment area involved the following procedure:

- Vectorization of LULC and HSG maps.
- Table or vector union operation performed to develop polygons through unique combination of both the maps in Arc-GIS software.
- CN value generation from unique polygons by query operation in Arc-GIS and thereby, created a CN grid map.
- CN value determination for each sub-basin from the attribute table.

3.5.1.5 ***Metrological data***

The climate in the research region is tropical humid, with summer months from March to May and rainy months from June to September. The average annual rainfall in the region is 3000 mm. The South-West monsoon is responsible for 83 of the 133 wet days. Throughout the year, the temperature in the area is nearly constant. However, the highest temperature was recorded in March and the lowest in December. The average monthly rainfall data calculated from the daily data collected (ARS, Chalakudy and IMD, Pune) is shown below in Table 3.5.

Table 3.5 Average monthly rainfall (mm) at different gauge locations for the period 1997-2017

Month	**Thunacadavu**	**Chalakudy**	**Peruvaripallam**	**Parambikulam**	**KSD**
Jan	1.00	5.00	1.57	0.90	2.69
Feb	11.71	14.86	11.86	11.03	17.76
March	41.29	26.53	46.48	75.45	64.00
April	72.81	87.24	78.90	139.87	114.05

May	97.43	233.69	101.62	157.89	219.49
June	285.33	661.4	295.48	501.13	788.13
July	384.33	629.24	391.90	643.81	909.40
August	274.24	444.89	289.90	428.62	660.83
Sept	213.67	386.18	227.67	324.14	488.00
Oct	216.48	348.98	232.38	325.15	370.75
Nov	125.29	178.07	144.52	121.62	122.35
Dec	33.57	29.51	39.09	30.13	18.56

3.5.1.6 ***Flow data***

The hydrological model is calibrated using daily discharge data. Only one discharge gauging station (CWC gauging station, Arangali) is available for measuring daily discharge data in the Chalakduy river basin. For the study period, daily stream flow data at this station was received from Cauvery & Southern Rivers Circle, CWC, Bengaluru is shown below in Table 3.6.

Table 3.6 Average Stream flow recorded at Arangali gauging station for the period1997-2017.

Year	**Average flow (Cumec)**	**Year**	**Average flow (Cumec)**
1997	45.7	2008	42.53
1998	78.27	2009	55.91
1999	67.86	2010	51.94
2000	36.84	2011	64.94
2001	43.63	2012	29.47
2002	42.86	2013	82.39
2003	48.33	2014	65.83
2004	60.09	2015	49.92
2005	64.66	2016	31.62
2006	54.36	2017	42.94
2007	101.85		

The highest average stream flow (101.85 cumecs) at the outlet was recorded in the year 2007 followed by the year 2013 (82.39 cumecs) while the least was found to be in the year 2012 (29.47 cumecs).

3.5.1.7 *Determination of average precipitation by Thiessen polygon method*

When there are multiple observation stations over a catchment region, the Thiessen Polygon approach is the most commonly used area-based weighting method in hydrometeorology for determining average rainfall. After graphically connecting the rain gauge stations to produce a network of triangles, a perpendicular bisector line was drawn. The watershed was divided into many polygons, with each component representing a fraction of the total area of that polygon. The weighted average of the data based on the size of each polygon was determined depending on the proximity of the station to the watershed region. Measurements that cover a significant percentage of the polygons are given greater weight than measurements that cover a small percentage of the polygons. Calculation of weighted average rainfall all over the catchment was obtained by the formula:

$$\overline{P} = \frac{P_1A_1 + P_2A_2 + P_3A_3 + \cdots + P_nA_n}{A_1 + A_2 + A_3 + \cdots + A_n} = \sum_{i=1}^{n} P_i \frac{A_i}{A}$$

Where, $\frac{A_i}{A}$ is called the weightage factor, $P_1, P_2, P_3, \ldots P_n$ are the rainfall values and $A_1, A_2, A_3, \ldots A_n$ are the area of respective Thiessen polygons.

3.6 HYDROLOGICAL MODEL DEVELOPMENT

Rainfall-Runoff modelling was carried out with the help of HEC-HMS and HEC-GeoHMS a hydrological extension in Arc-GIS. An overview of the rainfall runoff model is shown with the help of a schematic diagram below in Fig.3.2.

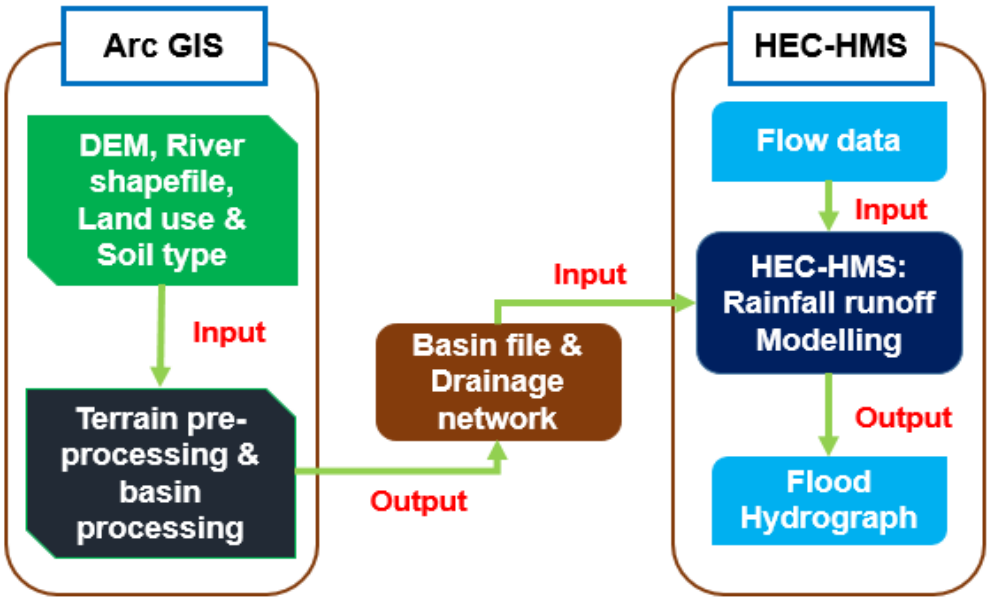

Fig. 3.2 Flow chart of Rainfall-Runoff modelling using HEC-HMS

The methodology used for carrying out rainfall runoff modelling can be described by categorizing it into three sections, as follows:

i. Creating basin model

ii. Developing hydrological parameters

iii. Hydrological modelling

3.6.1 Creating basin model

A new empty map is produced after opening Arc Map. The context menu with accessible tools displays when you right-click on the menu bar, and the HEC-GeoHMS tool is checked to add the toolbar to the map project. The HEC-GeoHMS toolbar has been added to Arc Map. The Spatial Analyst extension has to be activated, by clicking Customize->Extensions and then the box next to Spatial Analyst is checked.

3.6.1.1 *DEM reconditioning*

The function requires input in the form of a raw DEM and a linear feature class (such as the river network), both of which must exist in the map document. On

the Arc Hydro toolbar, select Terrain Pre-processing->DEM Manipulation->DEM Reconditioning.

3.6.1.2 *Fill sinks*

The 'Fill Sinks' function fills a grid of sinks. If higher-elevation cells surround a cell in the model, the water becomes trapped in that cell and cannot flow. To solve these issues, the 'Fill sink' function adjusts the elevation values.

On the Arc-Hydro Toolbar, Terrain Pre-processing->Data Manipulation->Fill Sinks was performed.

3.6.1.3 *Flow direction grid*

The flow direction for a given grid is computed. The directions of the steepest descent from each cell are indicated by the values in the flow direction grid cells. On the Arc-Hydro Toolbar, select Terrain Pre-processing->Flow Direction.

3.6.1.4 *Flow accumulation grid*

This function computes the flow accumulation grid for each cell in the input grid, which is made up of the accumulated number of cells upstream of that cell.

3.6.1.5 *Stream definition grid*

Select Terrain Pre-processing -> Stream Definition from the Arc-Hydro toolbar. Fac is the input to the Flow Accumulation Grid. The Stream Grid called Str is the result (default).

The geomorphologic river network attributes are consistent with objective methods for selecting the stream delineation threshold to create the highest resolution network. The threshold area was set to 25 km^2 in this study.

3.6.1.6 *Stream segmentation grid*

This function generates a grid of stream segments, each of which has its own unique ID. In this situation, a segment can be either a head segment or a segment between two segment junctions. The cells in a segment all have the same grid code.

On the Arc-Hydro toolbar, Select Terrain Pre-processing -> Stream Segmentation.

We can see how each link has its own value at this stage. The map document was then saved.

3.6.1.7 *Catchment grid delineation*

This function generates a grid with a grid code (value) for each cell denoting the catchment to which the cell belongs. The value is the same as the value carried by the stream segment draining that area, as defined in the stream segment link grid.

Select Terrain Pre-processing -> Catchment Grid Delineation from the Arc Hydro toolbar. Confirm that Fdr and Lnk are the inputs to the Flow Direction Grid and Link Grid, respectively.

3.6.1.8 *Catchment polygon processing*

There are three functions. The raster data obtained is converted to vector format using Drainage Line Processing, Adjoint Catchment Processing, and Drainage Point Processing. All of the rasters that have been made so far have been saved in a folder (Layers). Within the geo-database linked with the map document, the vector data will be saved in a feature dataset called Layers.

Select Terrain Pre-processing -> Catchment Polygon Processing from the Arc-Hydro toolbar. The process of converting a catchment grid into a catchment polygon feature is known as catchment polygon processing.

3.6.1.9 *Drainage line*

This function creates a drainage line feature class from the provided Stream Link grid. The identification of the catchment in which the drainage feature class is located is carried by each line in the drainage feature class.

On the Arc Hydro toolbar, select Terrain Pre-processing -> Drainage Line Processing.

3.6.1.10 *Adjoint catchment*

From the Catchment feature class, this function generates the aggregated upstream catchments.

Select Terrain Pre-processing -> Adjoint Catchment Processing from the Arc Hydro toolbar. Ascertain that the Drainage Line and Catchment inputs are, in fact, Drainage Line and Catchment. Catchment is the default name for the output (Adjoint Catchment).

3.6.1.11 *Drainage point*

The drainage points connected with the catchments may be generated using this function. Select Terrain Pre-processing -> Drainage Point Processing from the Arc Hydro toolbar. Verify your inputs. Drainage Point is the default name for the outflow (Drainage Point). The point feature class "Drainage point" is added to the map when this procedure is completed successfully.

3.6.1.12 *HEC-GeoHMS project setup*

The HEC-GEOHMS project setup menu includes options for identifying the watershed outlet and delineating the HEC-HMS project's watershed. Because numerous HMS basin models can be created from the same geographic data, these models are divided into two feature classes: Project Point and Project Area.

Dataset Setup: On the HEC-Geo HMS Main View toolbar, go to HMS Project Setup -> Data Management. In the Data Management box, confirm/define the relevant map layers.

Click Project Setup->Start New Project to start a new HMS project. Confirm the project area and point. Project Point and Project Area feature classes will be created as a result of this. Provide the following information in the next window.

Finally, for Project data location, we may pick the outside Main View Geo database and navigate to our working directory where Chalakudyriver.mxd is located, and write any metadata if necessary. On the notification about the project's successful creation, click OK. The table of contents in Arc Maps has been updated to include new feature classes Project Area and Project Point. These feature classes are stored in the same Chalakudy.gdb geodatabase.

Next, zoom in to the Arangali's downstream portion to determine the watershed outflow.

Select the Add project Points tool on the HEC-GEOHMS toolbar, and then click on the downstream outlet area of Arangali to define the outlet point.

Then click OK to accept the default point name and description (Outlet). This will add a point to the Project Point feature class for the watershed outflow. After that, the map document was saved.

3.6.2 Developing hydrological parameters

In HEC-GeoHMS, the hydrologic parameters menu offers tools for estimating and assigning a number of watershed and stream parameters for use in HMS. SCS curve number, Time of concentration, channel routing coefficients and other parameters are among them. The techniques can be specified in the HMS. This tool will be used for the transform method (rainfall to runoff) and routing (channel routing).

Select HMS processes->Select Hydrologic parameters from the drop-down menu. The Subbasin and River feature classes were confirmed, and then the OK button was hit. The Loss method (collecting surplus rainfall from total rainfall), the Transform method (converting excess rainwater to direct runoff), the Base flow type (Recession technique), and the Route method (Muskingum) were chosen (channel routing).

Table 3.7 Methods selected for HMS

HMS Processes	Method
Loss	SCS Curve Number Method
Transform	SCS Unit Hydrograph
Base-flow	Recession
Routing	Muskingum

3.6.2.1 *CN Lag*

The lag time for the transform method based on the CN grid was estimated using this function. Land use and soil cover layers were used to create the CN grid in Arc-GIS. CN values adopted for Chalakudy river basin according to different land uses are given in Table 3.8.

Table 3.8 CN values adopted for different land use classes (USDA, 1984)

Description	**Curve Number for Hydrologic Soil Group**			
	A	**B**	**C**	**D**
Barren Land	71	80	85	88
Urban land	77	85	90	92
Coffee/Cardamom	68	75	85	89
Tea/ Oil palm	67	75	85	89
Water body	100	100	100	100
Paddy	67	78	85	89
Forest/other vegetation	30	58	71	78

The hydrological process of converting rainfall to runoff is represented in HEC-HMS by four processes: loss, transform base flow, and routing. The next section explains these procedures:

3.6.2.2 *Loss method*

This model calculates the catchment's runoff volume by subtracting interception, surface storage, and infiltration, evaporation, and transpiration losses from the precipitation at each time step. The losses can be calculated in five different ways using HEC-HMS (Mihalik *et al.*, 2008). There are eleven techniques inbuilt in the software for converting excess rainfall into surface overflow shown in table. 3.8. Some methods are meant mainly for event based simulation while some methods are meant for long period continuous simulation. Nonetheless, all the methods are based on mass conservation. The “SCS Curve Number Loss” method was chosen for this

study since the parameters required for the SCS CN method were available. This method uses the CN to estimate incremental losses.

The equation for runoff computation by SCS Curve Number method is given by,

$$Q = \frac{((P-0.2S)^2}{(P+0.8S)} \quad \text{For } P > I_a$$

$$Q = 0 \quad \text{For } P < I_a$$

$$S = \frac{25400}{CN} - 254$$

Where, Q = Volume of runoff (mm)

P = Rainfall volume (mm)

I_a = Initial abstraction (mm)

S = Maximum potential retention (mm)

CN = Curve number

3.6.2.3 *Transform method*

SCS UH model is a predominant, dimensionless, single-peaked unit hydrograph. This dimensionless unit hydrograph expresses the unit hydrograph discharge (U_t) as the ratio to the unit hydrograph peak discharge (U_p) for any time t, in the fraction of time T_p which is the time of unit hydrograph peak. Researchers suggest that the following relation between unit hydrograph peak (U_p) and time of unit hydrograph peak (T_p) as:

$$U_p = C\frac{A}{T_P} \qquad \text{……..1)}$$

Where A denotes the watershed area and C denotes the conversion constant (2.08 in SI and 484 in FPS). The duration of the unit of excess precipitation is related to the time of peak or rise in the following way:

$$T_p = \frac{\Delta t}{2} + t_{lag} \qquad \text{……2)}$$

Where, Δt is the excess precipitation duration that serves as the computational interval in HEC-HMS model, lag ‘ t’ is the basin lag time which is defined as difference in time between the centre of mass of rainfall excess and the peak of the

unit hydrograph. When the lag time is specified, equation 1) and equation 2) can be solved successively to find the time of UH peak and the UH peak in HEC-HMS respectively. It is also interesting that lag time t_{lag} is the only input for this method in the model. With U_p and T_p parameters known, by their multiplication, the UH can be found from this method and that is included in HEC-HMS model.

3.6.2.4 ***Base flow method***

Base flow in HMS indicates subsurface flow in the catchment. Interflow and flow in a groundwater aquifer make up base flow. In the case of a small rainfall event, the contribution of base flow is negligible, therefore it can be neglected. In the case of a long rainfall event, the base-flow contributes to the hydrograph recession limb and has a considerable impact on flood volume. For calculating base flow, HEC-HMS provides two options: Recession and Constant monthly. An exponential decay function of a defined starting base flow is used in the recession technique. The user just provides a constant monthly base flow number for each month in the constant monthly approach. Zero base flow is also an option, and base flow may typically be ignored in basic hydrologic models over short time periods or in heavily urbanised basins with waterways.

In this study, Recession method was used for base flow computation. According to Recession method, basin flow is calculated by:

$$Q_t = Q_o R^t$$

Where, Q_0 = Initial base flow at time t = 0, Q_t = Threshold flow at time t, and R = Exponential decay constant.

Inbuilt software Initial base flow (Q_o), recession constant (R), threshold flow (Q_t) is calculated based on the observed flow hydrograph, which is affected by the source of base flow. (USACE –HEC, 2008).

3.6.2.5 ***Routing method***

Flood routing is a method of estimating the flow hydrograph at a catchment's downstream point using sound information about the hydrograph upstream. It's a

method for estimating how a flood wave's magnitude and frequency change as it goes down the watershed, compared to the inflow point. The slope and length of the channel, as well as channel roughness, channel geometry, downstream control, and initial flow condition, all influence flood routing along the watershed (Rahman *et al.,* 2015). Hydrologic modelling is based on the continuity equation, whereas hydraulic modelling is based on the Saint-Venant equations, which are a combination of continuity and momentum equations. The HEC-HMS model has six hydrologic routing techniques namely: “Kinematic wave”, “Lag”, “Modified Puls”, “Muskingum”, “Muskimgum-Cunge” and “Straddle stagger”. “Muskingum” method was selected for the routing and for the loss/gain option, the “Constant” method was selected. "K" value represents the time required to pass through the reach, and the value provided in the editor box was calibrated. The weighting factor is represented by the "X" number, which typically varies from 0.0 to 0.5 (Barry and Bajracharya, 1995). Maximum attenuation occurs when the "X" value equals "0," but no attenuation occurs when the "X" value equals "0.5." Since the number of sub reaches within the basin was three, the number of sub reaches selected for this study was three.

Two equations are used to derive the Muskingum channel routing method (Linsley *et al.,* 1982). The first is the continuity equation or conservation of mass as shown below:

$$\frac{I_1 + I_2}{2}\Delta T - \frac{O_1 + O_2}{2}\Delta T = S_1 - S_2$$

Where I_1 and $I_2$are inflow discharges at time 1 and time 2, O_1 and $O_2$are outflow discharges at time 1 and time 2, ΔT is the time difference, S_1 and S_2 are values of reach storage at time 1 and time 2.The second equation is a relationship of storage, inflow, and outflow of the reach as indicated below:

$$S = K[XI + (1 - X)O]$$

Where S is the reach storage, I is the inflow discharge, O is the outflow discharge, K is the storage constant or proportionality coefficient. Values of K and X in Muskingum method was determined in HEC-HMS for channel routing. These parameters are fitted in the model while calibrating the observed hydrograph.

6.3 Developing HEC-HMS model files

In this step, model files such as background map file, basin model file and meteorological model file required for HEC-HMS were generated. All of the physical characteristics of reaches and sub-basins were first transformed to a user-defined unit system. The SI system was utilised in both situations in this example. The basin map was then updated with HMS basin schematics and legends. HMS basin diagrams contained HMS nodes that represented sub-basins and junctions, as well as HMS connections that depicted rivers. HMS nodes indicating sub-basins and junctions were substituted with HMS legend by adding HMS legend. Further, coordinates were added to the features in HMS nodes and HMS links.

Background-map files acquired from basin files were produced and exported to HMS using HEC-GeoHMS. For the meteorological model file for the basin, the gauge weight technique was selected. In Arc-GIS, a Thiessen polygon was constructed for the available precipitation stations within or on the periphery of the basin region in order to use this approach.

Finally, the Control Specifications menu defined the time-related information for a simulation, such as the start and finish dates, as well as the computation time interval. The calibration, simulation, and verification time stages for the HEC-HMS model for the catchment were separated into distinct time steps.

3.7 OPTIMIZATION OF THE MODEL

This process involves the utilization of observed flow for optimizing the performance of the model automatically by parameters estimation. At the end of the model, many objective functions are provided to evaluate the “goodness of fit” between the simulated and observed flow. The parameters can be adjusted manually

or automatically through the software's optimization menu. A "Basin model," a "Meteorological model," and time series data are all included in each optimization experiment. The time interval was set to "1 Day," with a tolerance level of 0.01 and a maximum of 150 iterations. The starting date and time as well as the ending date and time were mentioned in the trial watershed explorer window. The parameters to be optimized were added under the trial menu which was done by right clicking the "Trial" menu and choosing the "Add parameters" menu. For optimizing the parameters, the elements *viz.*, reach and sub basins were chosen and the parameters of each element which are to be optimized were selected specifically, its initial as well as the minimum and maximum values were mentioned in the window explorer. The results of the optimization run can be displayed in the form of an objective function summary. This displays the volume and peak flow values with percentage differences, a comparison of the observed and simulated flow hydrographs, and optimised parameter tables with units, initial values, and final optimised values for each parameter.

The minimum and maximum parameter values in simulation of rainfall-runoff models and the range of feasible and acceptable parameters is limited. The assumed maximum and minimum range of parameter values is shown in Table 3.9. Optimization options in HEC-HMS include methods such as simplex method, univariate and Markov Chain Monte Carlo method, in which simplex technique was adopted for optimization of parameters in this study.

Table 3.9 Range of Calibrated parameters

Model	**Parameter**	**Minimum value**	**Maximum value**
SCS UH	Lag time	0.1 hr	500 hr
SCS loss	Initial abstraction	0 mm	500 mm
	Curve number	1	100
Muskingum routing	K	0.1 hr	150 hr
	X	0	0.5
	Number of steps	1	100

3.8 CALIBRATION OF THE MODEL

In the calibration process, all the parameters were manually adjusted to get the best fit between the model simulated and observed values obtained for the basin .It was primarily done to reduce the differences between observed and simulated model values, as well as to get the optimal set of parameters for calibrating and validating the model (Cheng *et al.* 2002). The primary goal of calibration is to approve the model, which is essentially an alignment technique. This is to ensure that the calibration procedure carefully analyzes all variables that may have an impact on the model results. After the model has been executed by adjusting the parameters, the model approval is done through quantitative and qualitative testing, which includes comparison of observed and simulated values as well as statistical analysis such as "Nash-Sutcliffe efficiency" and "Correlation-coefficient. Calibration of the model consists of a “Basin model” which includes the methods for each sub basin, “Meteorological model” where the meteorological data are entered and “Control specifications” which includes the starting and ending date and time. The output of the calibration run is a summary table with the hydrologic elements, drainage area, peak discharge, time of peak and volume. Calibration can be done on event basis and also on the basis of long term simulations (HEC-HMS 4.7.1 users manual 2021). In this study event-based simulations using daily available rainfall and discharge data from the year 2005 to 2007 were used for model calibration.

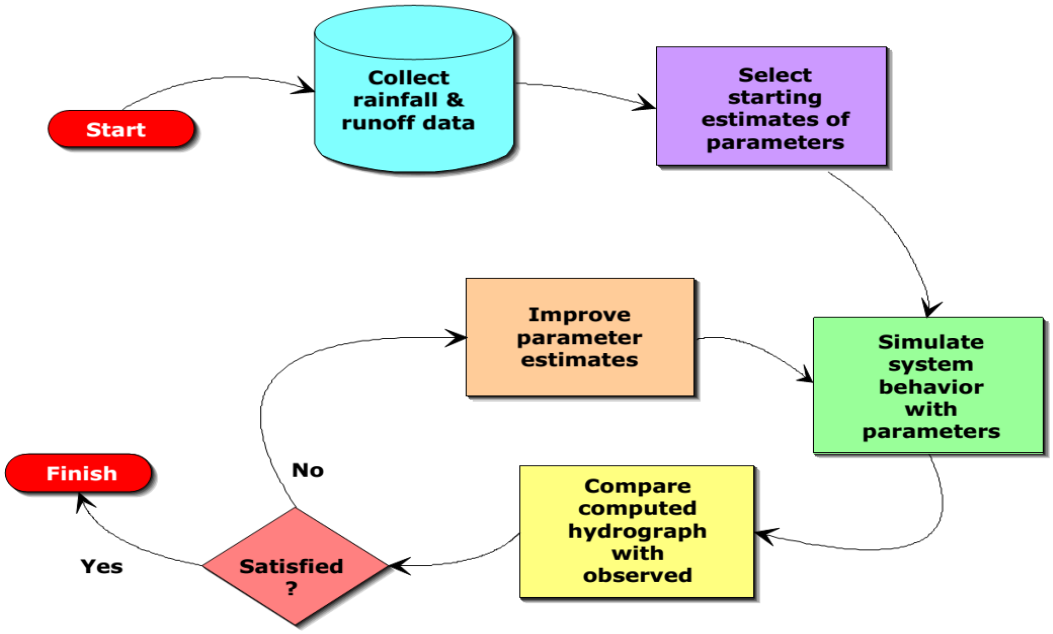

Fig. 3.3 Schematic model calibration procedure

3.9 VALIDATION OF THE MODEL

Once the parameters were optimized, the validation of the model was done. All the optimized parameters obtained during the calibration period were used as the input parameters for the validation period. The validation of the model was done for two years from 2009-2010. The same procedure as that of the calibration was followed for validating the model. Validation of the model consists of a “Basin model”, “Meteorological model” and “Control specifications”. Graphs, summary tables, and statistical analyses have been used to present the results. The obtained NSE and correlation coefficient values indicate the model's satisfactory performance.

3.10 MODEL PERFORMANCE EVALUATION

Model performance was evaluated during calibration and validation on the basis of the following performance indicators:

1) ***Nash Sutcliffe efficiency (NSE)***

$$NSE = 1 - \frac{\sum_{i=1}^{n}(O_i - P_i)^2}{\sum_{i=1}^{n}(O_i - \overline{O_i})} \times 100$$

Where, P_i represents predicted runoff, O_i represents observed runoff and $\overline{O_i}$ represents mean of observed runoff. The value of Nash–Sutcliffe efficiency varies between 0 and 1. Closer value to 1 indicates better model performance.

2) ***Percent bias (PBIAS)***

$$PBIAS = \frac{P_p - O_p}{O_p} \times 100$$

Where, O_p and P_p are the peak value of observed and predicted runoff, respectively.

3) ***Root mean Square error-standard deviation Ratio (RSR)***

$$RSR = \sqrt{\frac{1}{n}\sum_{i=1}^{n}(O_i - P_i)^2}$$

Where, O_i and P_i are the peak value of observed and predicted runoff RSR is always greater than 0 and closer the values to 1, it indicates better the model performance.

Performance ratings of NSE, PBIAS and RSR to be obtained for the HEC-HMS model calibration as reported by Rossi *et al*., 2008 is shown in Table 3.10.

Table 3.10 General performance ratings for statistical performance indicators

S. No	Criteria	Value	Rating
1	**NSE**	>0.65	Very good
	NSE	0.54-0.65	Adequate
	NSE	≥0.50	Satisfactory
2	**PBIAS**	≤±20%	Good
	PBIAS	±20% to±40%	Satisfactory

	PBIAS	≥±40%	Unsatisfactory
3	**RSR**	0.00≤RSR≤0.50	Very good
	RSR	0.50<RSR≤0.60	Good
	RSR	0.60<RSR≤0.70	Satisfactory
	RSR	RSR>0.70	Unsatisfactory

NSE=Nash-Sutcliffe efficiency value

PBIAS= Percent bias

RSR=Root mean square error-standard deviation ratio

3.10 RAINFALL FREQUENCY ANALYSIS USING HEC-SSP

Frequency analysis for determining the precipitation depth was performed using HEC-SSP. In this study, frequency analysis was conducted using the annual maximum daily precipitation of agro-met data for 1990-2019 in HEC-SSP software, using the plotting position method. There are different options within HEC-SSP for computing plotting positions *viz.*, Weibull, Median, Hazen, Hirsch/Stedinger and user entered constants. In this study, the Weibull plotting position was adopted. It was then fitted with the Log Pearson Type III distribution.

Finally, the design precipitation values obtained from the Log Pearson Type-III plots were used to determine the rainfall intensities for the 10, 20, 50, 100, 200 and 500 year return period over 24 hours rainfall duration.

3.11 FLOOD FREQUENCY ANALYSIS

Planners and engineers usually require reliable estimates of the magnitude and frequency of floods to design all the water resources projects in the preferred area. One of the most common ways for determining the relationship between the magnitude of a flood event and the frequency with which that event is exceeded is flood frequency analysis (Chow, 1951). Fitting a probability model to a sample of yearly flood maxima observed during a period of observation for a catchment is also included.

For flood frequency analysis, frequency distributions such as Gumbel Extreme Value distribution, Log Pearson Type III distribution, (Pickands, 1975), Log Normal, distribution are commonly used. (Rahman *et al.,* 2015). The software HEC-SSP generally used to perform flood flow frequency analysis was used in this study.

Flood frequency analysis can be done to determine the flood peak values for different return periods using two methods such as

1) Frequency storm method in HEC-HMS
2) Flood frequency analysis using HEC-SSP

3.11.1 Frequency storm method using HEC-HMS

The input from HEC-GeoHMS and using some edition from the calibrated HEC-HMS parameters, the model was simulated for rainfall intensities of 10, 20, 50, 100, 200 and 500 year return periods. Flood peak values for different return periods were determined with HEC-HMS model using frequency storm method.

The depths accumulated over twenty four (24) hours duration as a function of the 10, 20, 50, 100, 200 and 500 years return period of the storm events was determined using equation (1) shown (Butler & Davies, 2004). The duration for all the storm precipitation was chosen as 24 hours (one day).

$$d = i_{24} \times t \qquad (1)$$

Where d = Rainfall depth (mm) for duration time (t)

i_{24} = 24 hour rainfall intensity (mm/hr)

t = Rainfall duration time (h)

Finally, the HEC-HMS model result was compared with the frequency analysis results of HEC-SSP software. The methods applied in this study are selected based on their efficiency and simplicity. But the primary criterion is their correlation with the simulated flow data of the Chalakudy river.

3.11.2 Flood Frequency Analysis using HEC-SSP

Daily stream flow data at CWC gauging station, Arangali, located near the outlet of the basin has been collected from Cauvery and Southern Rivers Circle, CWC, Bengaluru, for the study period of 28 years (1990-2018). The data was used as the basic input data for flood frequency analysis. The annual maximum discharge was extracted from the daily discharge data. The monthly average discharges of Arangali gauging station is given in Appendix II.

HEC-SSP software that encompasses executable code and documentation that is available in public domain, was used to compute the statistical functions. First, using the plotting position method, the hydrologic data was used to determine the return period. It was then fitted with distributions such as the Gumbel, Log Pearson Type III and Log Normal distributions.

The goal of frequency analysis is to predict how often specific values of a variable hydrologic phenomenon will occur and to analyze the accuracy of the variable's prediction (Drissia *et al.,* 2019). The General Frequency Analysis component was used to conduct frequency analysis on hydrologic data. Annual maximum stream flow was the type of data used in this study.

3.11.2.1 General frequency analysis editor

The user can use the general frequency analysis editor to perform frequency analyses on hydrologic data using a variety of methodologies. Flow and precipitation are the data that can be considered in this study. The discharge data could be manually entered or imported from a HEC-DSS file, a USGS website, or an Excel spreadsheet. In this study, it was manually inputted. The Data Importer is where you may import, input, and examine data. To use the data importer, go to the Data menu and choose 'New' from the drop-down menu. A data importer will appear.

3.11.2.1.1 *Plotting positions*

Plotting positions were used for plotting the input discharge data set on a probability scale accompanied by the computed frequency curve and confidence

limits. There are different options within HEC-SSP for computing plotting positions *viz.*, Weibull, Median, Hazen, Hirsch/Stedinger and user entered constants. In this study, the Weibull plotting position method was adopted. The selection of plotting position option varies from one frequency analysis to another according to the need of user. Generalized plotting position equation used for the study is as follows:

$$P = \frac{(m - A)}{(N + 1 - A - B)}$$

Where, m is the rank of largest flood values and is equal to one, N is the number of flood peaks in the data set, A and B are the coefficients dependent on which equation is used (Weibull A and B=0; Median A and B = 0.3, Hazen A and B=0.5 and Hirsch/Stedinger A and B=0).

In a word, plotting positions are estimations of the chance of each data point exceeding its limit. Different methodologies are used to calculate the probability of the highest and lowest points in a given data set. However, it is believed that the method chosen for plotting positions has no effect on the curve calculated.

By arranging the data in decreasing order of magnitude, the operation for plotting position was started. The plotting-position formula, as mentioned above in the equation with coefficients A and B supplied conferred to the Weibull technique, was used to determine the probability P of each event being equalled to or exceeded (plotting position). Return period (also called the recurrence interval or frequency) T is defined by the equation (Haan, 1977):

$$T = \frac{1}{P}$$

Q versus T in a semi logarithmic graph was then plotted, which yielded probability distribution. The most common challenge in frequency analysis is predicting severe flood occurrences. Specific extreme value distributions were assumed to address this problem, and the appropriate statistical parameters were calculated from the given data. As a result, it was possible to estimate the flood magnitude for a particular return period. Most frequency distribution functions useful

in hydrologic research, according to Subramanya (2008) and Chow (1951), may be represented using the following generic equation of hydrologic frequency:

$$x_T = \overline{x} + K\sigma$$

Where x_T =Value of variate x of a random hydrologic series with a return period T, $\overline{x}$ = Mean of the variate, σ = Standard deviation of the variate and K = Frequency factor, which depends on the return period and assumed frequency distribution.

The tab of general frequency analysis editor opens a window, which provided an interface for selecting Weibull plotting position for the selected distribution functions.

Log- Pearson Type III distribution, Gumbel distribution and Log Normal distribution were then selected from the General Frequency Analysis Editor option. Interface to choose distribution functions.

3.11.2.1.2 ***Distribution fitting***

It is the process of selecting a probability model for an unknown population and simulating that model with a representative sample of the population. Despite the fact that uncertainty will always be a part of the inference due to a small sample size, the model allows for inferences about the population even when all of its properties are unknown. Better inferences about population attributes will arise from selecting an appropriate model for the population. There are several distributions available totally in the software, including the combination with and without using log transform. Flood frequency analysis was performed in this study by fitting the data to the Gumbel, Log Pearson Type III and Log Normal distributions.

3.11.2.1.2.1 ***Log –Pearson Type-III distribution***

Log-Pearson type-III distribution is a statistical technique for fitting frequency distribution to predict the design flood for a river basin. The frequency curve depicted could be used to calculate the probabilities of floods of varying sizes and quantities. The values for events with return periods well beyond the observed flood events can be extrapolated, making the distribution more reliable and helpful. This is the

standard technique for fitting the frequency distribution of floods used by federal agencies in the United States. This frequency distribution informs you the likely values of discharges to expect in the river at various recurrence intervals based on the current historical record. This is useful when developing constructions near or in rivers to avoid flooding or the worst-case scenario. As a result, it is common practise to conduct a flood frequency study utilising data from the instantaneous peak discharge. However, the maximum values of mean daily discharge data can be used to fit the Log-Pearson Type III distribution. If x is the variety of a random hydrologic series, then the series Z value is calculated as:

$$Z = \log x$$

$$X_T = antilog(Z_T)$$

For this Z series, for any recurrence interval T,

$$Z_T = Z + K_Z \sigma_Z$$

Where K_Z represents the frequency factor which is a function of recurrence interval T.

σ_Z Represents standard deviation of Z variate sample and it is calculated by the formula $\sqrt{\frac{\sum(z-\bar{x})^2}{N-1}}$

Coefficient of skew $C_s$of z variate is computed by the following equation:

$$C_s = \frac{N\sum(z-\bar{z})^2}{(N-1)(N-2)(\sigma_Z)^3}$$

The log-Pearson type-III distribution has been widely employed in hydrologic frequency analysis. The following equations were used to compute the probability density function (PDF) and cumulative distribution function (CDF) of the Log-Pearson type-III distribution:

$$f(x) = \frac{1}{x|\beta|\tau(\alpha)}\left(\frac{\ln(x)-y}{\beta}\right)^{\alpha-1} e^{-\frac{\ln(x)-y}{\beta}}$$

$$F(x) = \frac{\tau \frac{\ln(x)-\gamma}{\beta}(\alpha)}{\tau(\alpha)}$$

Where, α, β and γ are shape, scale and location parameters, respectively.

3.11.2.1.2.2 *Gumbel distribution*

The Gumbel distribution is the most extensively utilised probability distribution function for predicting flood peaks (Zelenhasic, 1970). This method has been adopted for flood frequency analysis due to the following reasons: The peak discharge data are homogeneous and independent, therefore lack long term trends. The second reason is because the river is unregulated, therefore it is unaffected by reservoir operations, diversions, or urbanisation. The third reason is that discharge data is of high quality and covers a lengthy period of time (more than 30 years) (Mujere, 2011). As per the Gumbel distribution fitting technique, following equations were used to predict the flood peaks at different return periods T, based on an annual series of flood (Sarma, 1999):

$$x_T = \overline{x} + K\sigma_{n-1}$$

Where, σ_{n-1} denotes standard deviation of the sample of size N, computed using the equation:

$$N = \sqrt{\frac{\sum(x-\overline{x})^2}{N-1}}$$

K is the frequency factor, computed by the equation $\frac{y_T - \overline{y_n}}{S_n}$

y_T is reduced variate corresponding to a recurrence interval T, obtained by the equation $-\left[\ln.\ln\frac{T}{T-1}\right]$

$\overline{y_n}$ and $S_n$is the reduced mean and standard deviation respectively, which is a function of sample size N (Subramanya, 2008).

The Gumbel distribution can be used to model the maximum and minimum values (extreme values) of a random variable set. The graph for the Gumbel

maximum probability distribution function is presented in Fig. 3.4 in general. The following equations were used to compute the Gumbel distribution's probability density function (PDF) and cumulative distribution function (CDF):

$$f(x) = \frac{1}{\sigma} e^{\left(-\frac{x-\mu}{\sigma} - e^{\left(-\frac{x-\mu}{\sigma}\right)}\right)}$$

$$F(x) = e^{\left(-e^{\left(-\frac{x-\mu}{\sigma}\right)}\right)}$$

Where σ and μ are the scale and location parameters, respectively.

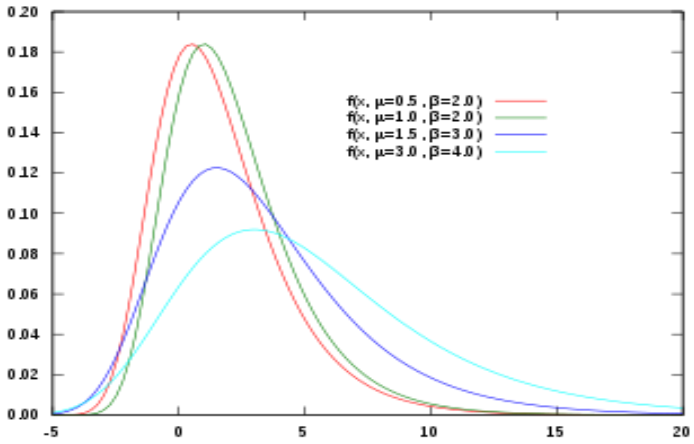

Fig. 3.4 Plot of Gumbel max probability distribution function

3.11.2.1.2.3 *Log Normal distribution*

The most important continuous probability distribution in the entire field of statistics is the normal distribution. The Log-Normal Distribution is a two-parameter positively skewed distribution that explains random variables using Normal distribution logarithms. The parameters and are the location and scale parameters of a Normal-distributed logarithm logb(x), not of a Log-Normal distributed random variable. If the PDF of X is skewed, it's not normally distributed. If the PDF of Y = log (X) is normally distributed, then X is said to be log normally distributed.

$$f(x) = \frac{1}{x\sigma\sqrt{2\pi}} \exp\left(-\frac{(y-\mu_y)^2}{2\sigma_y^2}\right) \qquad x > 0, \text{ and } y = \log x$$

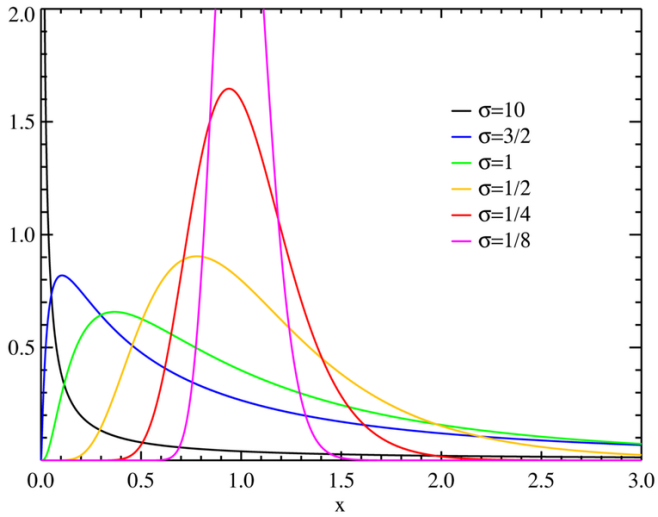

Fig. 3.5 Plot of Log Normal max probability distribution function

3.11.2.2 Test for Goodness of Fit

These tests are meant to notify the user if there are large deviations in the data away from the selected and calibrated probability model. The results of goodness of fit tests can be compared to determine which probability distribution to use for the basin. When one or more distributions are valid for the data being modelled, the tests mentioned below were employed to test the goodness of fit. Assuming $(x_1, x_2, \ldots, x_n)$ as the samples from population *X*, hypothesis is created such that; H_0 : F(x) = F_0 (x), where F_0 (x) is the probability distribution function with the parameters estimated from the sample data for checking the goodness of fit for any population (Zeng *et al.*, 2015). The quality of fit was assessed using the Chi-Square and Kolmogorov-Smirnov tests. The following hypothesis H_0 and H_1 were used in this study: H0: the selected distribution fits the discharge events well, and H_1: the selected distribution does not match the discharge events well.

3.11.2.2.1 *Chi-Square Test*

Chi-Squared Test also known as Pearson's Chi-Squared Test is a parametric test for goodness of fit. The test works by dividing the sample data into discrete classes or bins and estimating the observed proportion of the data in each bin vs. the expected proportion of the data based on the model. Finally, as a result of its

computational technique, this software generates a test statistic. In practise, if the proportions differ by a significant amount, the null hypothesis derived from the suggested model is rejected. The chi square test gets its name from the Chi-Squared Distribution, which governs the distribution of proportion differences. A Chi-Squared Distribution with (k – 1) degrees of freedom can be used to calculate the critical value for rejection, where k is the number of bins utilised in the test. Among statistical functions, The Chi-Square (C-S) test is a simple and straightforward hypothesis test that is linked to overall fit. The methodology is as follows (Zhang and Luo, 2000):

1) Choosing k-1 numbers as follows: $-\infty < t_1 < t_2 < \ldots < t_{k-1} < +\infty$, $k \approx 1.87(n-1)^{(0.4)}$, and the number axis is divided into k interval sections, $(-\infty, t_1]$, $(t_1, t_2]$, …, $(t_{k-2}, t_{k-1}]$, $(t_{k-1}, +\infty]$.

2) Counting the number of samples that fall into the interval, i=1, 2,..., k, and then computing the probability of a population that follows an alternative probability density function fallen into the i^{th} interval:

$$p_1 = P(X \leq t_1) = F_0(t_1)$$

$$p_2 = P(t_1 < X \leq t_2) = F_0(t_2) - F_0(t_1)$$

$$\ldots\ldots\ldots\ldots\ldots$$

$$p_{k-1} = P(t_{k-2} < X \leq t_{k-1}) = F_0(t_{k-1}) - F_0(t_{k-2})$$

$$p_k = P(t_{k-1} < X) = 1 - F_0(t_{k-1})$$

Constructing a statistics:

$$\chi^2 = \sum_{i=1}^{k} \frac{(n_i - np_i)^2}{np_i}$$

which obeys Chi-square distribution with the degree of freedom m, m=k-1, or m=k-1-r when there are r independent parameters of $F_0(x)$ need to be estimated by samples. Examining the level of significance α, if $p\ (\chi^2 \geq \chi^2_{1-\alpha}) \geq \alpha$, then accept the hypothesis H_0, otherwise reject the hypothesis. In this study, level of significance α was taken as 5% and degrees of freedom as 33.

3.11.2.2.2 *Kolmogorov-Smirnov Test*

The K-S Test is a nonparametric method for determining if two continuous probability distributions are equal. When sample data is approximated with an empirical distribution, the empirical distribution and an alternative model for the data can be compared to see if they are similar. The biggest difference in cumulative distribution function between the proposed model for the data and the empirical distribution of the data is determined by the test. The algorithm will return a test statistic that is the outcome of the computing method previously indicated. In practise, if the difference is significant enough based on the sample size, the null hypothesis that the data are from the suggested model is rejected.

The largest disparity between the observed and predicted distribution is computed by the test. Melo et al., 2009; Wang and Wang, 2010) explain the procedure as follows:

a) Sorting the samples X (x_1,x_2, …, x_n) in ascending order, and storing it to a new vector X ′ (x'_1 ,x'_2 , …, x'_n)

b) Calculating the empirical distribution function:

$$F_n(x') = \begin{cases} 0, x' < x'_1 \\ \frac{k}{n}, \ x'_k \le x' < x'_{k+1} \\ 1, x' \ge x'_n \end{cases}$$

c) K-S statistics $D^{(n)}$ is calculated as:

$$D^{(n)} = max_{x'_i \le x' < x'_n} |F_n(x') - F_0(x')|$$

$$= max_{1 \le i < n} \| \frac{i}{n} - F_0(x'_i) \| \frac{i-1}{n} - F_0(x'_i) \|$$

d) Considering the significance level α, if p ($D^{(n)} \ge D^{(n)}(1-\alpha)$) ≥ α, then accept the hypothesis H_0, otherwise reject the hypothesis. In this study, level of significance α was taken as 5%.

3.12 HYDRAULIC MODELING

HEC-RAS is an integrated system of software designed for interactive use in a multitasking, multi-user network environment. A graphical user interface (GUI), distinct hydraulic analysis components, data storage and administration capabilities, visuals and reporting tools are all part of the system (USACE, 2002). The HEC-2 river hydraulics package, which was a one-dimensional, steady-flow water surface profiles programme, has been superseded by the HECRAS software. In July of 1995, the first version of HEC-RAS was released. Since then, numerous versions of this software package have been produced, including versions 1.1; 1.2; 2.0; 2.1; 2.2; 3.0; 3.1; 4.0; 4.1; 5.0; 5.0.1; 5.0.3; 5.0.4; 5.0.5; 5.0.5; 5.0.6; and 5.0.7, which was released in March of 2018. HEC-RAS is a computer programme that analyzes one-dimensional hydraulics for a network of natural and man-made channels in one dimension. In its current version, HEC-RAS offers steady and unsteady flow water surface profile computations, sediment transport modelling, and water quality simulation.

The HEC-RAS and HEC-GeoRAS, an Arc-GIS extension, can be used to do a hydraulic analysis of the river system. The approaches utilised in completing one-dimensional flow calculations within HEC-RAS are described in the following paragraphs.

3.12.1 Steady flow water surface profiles

HEC-RAS can currently calculate one-dimensional water surface profiles for steady, gradually varying flow in natural or constructed channels. It is possible to determine water surface profiles in the subcritical, supercritical and mixed flow regimes. Some of the topics covered in this section include basic profile calculations, cross section subdivision for conveyance calculations, composite Manning's n for the main channel, velocity weighting coefficient alpha, friction loss evaluation, contraction and expansion losses, computational procedure, critical depth determination, applications of the momentum equation, and the steady flow model's

limitations.

3.12.1.1 *Equations for water surface profile calculations*

By solving the Energy equation iteratively, the conventional step technique is utilised to create water surface profiles from one cross section to the next. The Energy equation is written as follows:

$$Z_2 + Y_2 + \alpha_2 V_2^2/2g = Z1 + Y1 + \alpha_1 V_1^2/2g + h_e.$$

Where, Z_1, Z_2 = Elevation of the main channel inverts

Y_1, Y_2 = Depth of water at cross sections

V_1, V_2 = Average velocities (total discharge/ total flow area)

a_1,a_2 = Velocity weighting coefficients

g = Gravitational acceleration,

h_e = Energy head loss

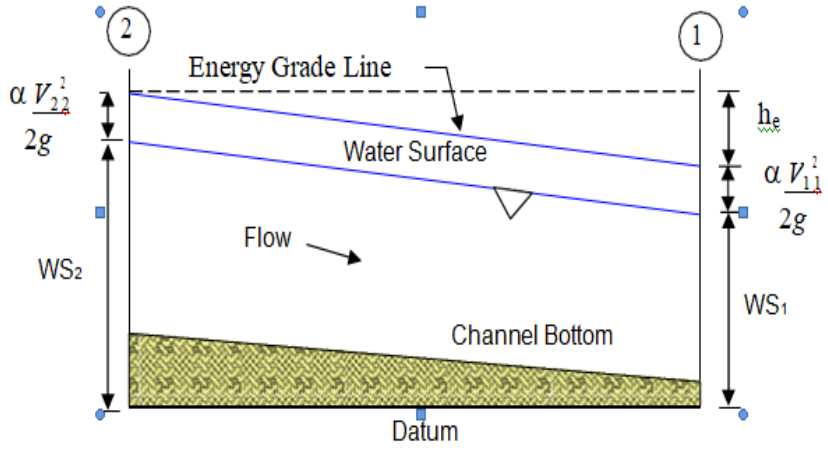

Fig. 3.6 Representation of terms in energy equation

3.12.1.2 *Friction losses*

The energy loss term "h_e" is composed of friction loss h_f and form loss h_o.

Only contraction and expansion losses are considered in the geometric form loss term.

$$h_e = h_f + h_o$$

The river is divided into strips with similar hydraulic properties in the flow direction to simulate the transverse distribution of flow. Each cross section is divided into subsections, which are subdivided into smaller sections. Friction loss is calculated as shown below:

$$h_f = \left(\frac{Q}{K^1}\right)^2$$

$$\text{Where, } K^1 = \sum_{j=1}^{J}\left[\frac{1.49}{n_j}\right]\frac{\frac{(A_2 + A_1)}{2}\left[\frac{R_2 + R_1}{2}\right]_j^{1/2}}{L_j^{1/2}}$$

A_1, A_2 = Downstream and upstream area, respectively of the cross sectional flow normal to the flow direction(m^2)

J = Total number of subsections

L_j = Length of the j^{th} strip between subsections(m)

n = Manning's roughness coefficient

Q = Water discharge(m^3/s)

R_1, R_2 = Downstream and upstream hydraulic radius(m)

3.12.1.3 ***Other losses***

Energy losses due to contractions and expansions are computed by the following equation:

$$h_0 = C_L \left| \frac{\alpha_2 V_2^2}{2g} - \frac{\alpha_1 V_1^2}{2g} \right|$$

C_L stands for contraction and expansion loss coefficient. The flow is contracting if the quantity in the absolute value notation is negative, and C_L is the contraction coefficient; the flow is growing if the quantity in the absolute value notation is positive, and C_L is the expansion coefficient.

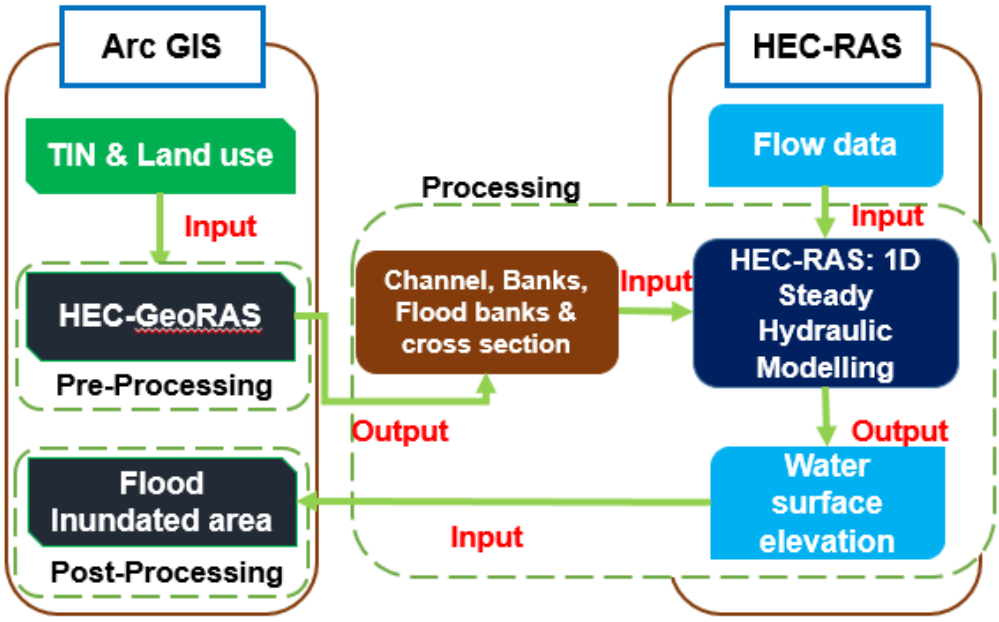

Fig. 3.7 Flow chart of modelling approach for flood inundation mapping

3.12.2 Data for hydraulic modelling: HEC-RAS

Data required for Hydraulic modelling (HEC-RAS) are:

i. Digital Elevation Model (DEM)

ii. Land use

iii. Flow data

3.12.2.1 *Digital Elevation Model (DEM)*

The hydraulic analysis of a river system requires the use of a digital terrain model. Because all cross-sectional data will be extracted from it, the DEM must be of high resolution with a continuous surface and should represent the river's bottom and adjacent flood plains.

3.12.2.2 *Land use*

Manning's roughness coefficient represents the resistance to flow in the channels and floodplains. The average bed slope at the boundary condition site is frequently utilized as a friction estimate. Surface roughness, vegetation, channel irregularities, degree of meander, obstacles, and channel size and form are all variables that influence the Manning's n-value. To calculate the energy losses due to friction, Manning's n values must be applied to both the channel and overbank flow regions. Manning's n values for various land use categories were utilized in this study. the incline. Table 3.11 lists the land use descriptions and their corresponding Manning's n values.

Table 3.11 Manning's n values

Land use type	Manning's n value
Paddy	0.06
Coffee/Cardamom	0.06
Tea/ Oil palm	0.06
Barren land	0.04
Water bodies	0.035
Forest/other vegetation	0.15
Urban land	0.12

(HEC-RAS 5.0.7 Hydraulic reference manual)

3.12.2.3 *Flow data*

Flood peak values determined from HEC-HMS for 10, 20, 50, 100, 200 and 500-year return period's data is used for hydraulic modelling of Chalakudy river basin.

3.13 FLOOD INUNDATION MAPPING IN HEC-RAS

For performing hydraulic analysis, the methodology is divided into three parts which are as follows:

- Pre-processing: Developing geometry of river in RAS Mapper,
- Processing: Performing hydraulic computation in HEC-RAS
- Post-processing: Processing RAS results in Arc-GIS

3.13.1 Pre-Processing of geometry data of river in RAS Mapper

Geometric layers such as stream centrelines, bank lines, flow route centrelines, and cross section cut lines were created using RAS Mapper based on the DEM and aerial photos of the study area. Polylines were used to produce the stream centerline, bank lines, flow path centrelines and cross-section cut lines. RAS Mapper automatically generated cross-sectional cut lines at regular intervals, which were then manually refined based on their necessity. All of the layers were required to generate characteristics such as name, length, topology, elevation, and location in order to be identified as they were imported into HEC-RAS. Further, according to land use land cover classes, the values for Manning's coefficient were entered on all the cross-sections.

3.13.1.1 *RAS Mapper application*

Geometric data establishes the connectivity of the river system. It is composed of cross-sectional cut lines, junction, river, reaches, cross-sectional bank station, the flow path, downstream reach lengths between two cross-sections for the left overbank, main channel, and right over bank. These data were obtained using RAS Mapper software that allows you to create a river schematic and extract different properties from an existing Digital Elevation Model (DEM). Topographic data is a

critical input in hydraulic modeling. In this study, the DEM data for the study area (30m resolution) was used. Thereafter, the grid file was brought into RAS Mapper to create a terrain of the study area after geo referencing. When using RAS Mapper for flood analysis, geo referencing the grid file is critical since it enables for the viewing of water surface elevation and velocity on a map. The geometric data was created using the terrain file.

3.13.1.2 *RAS themes creation*

The RAS themes are generally, the file data in RAS Mapper used to develop geometric data. For this study, they are essentially line themes:

3.13.1.3 *Stream centre line*

The centre lines were drawn from upstream (North) to downstream (South) in the direction of the flow (South). During the development of the centre line, the DEM was superimposed over google satellite images for accuracy.

3.13.1.4 *Main channel banks*

For the centre line, the main canal banks, left bank and right bank, were specified. The centerlines are drawn from upstream to downstream, looking in the direction of the flow. The banks allow the main canals to be separated from the over banks.

3.13.1.5 *Flow path center lines*

The hydraulic flow path in the left overbank, main channel, and right over bank has been identified. The floodplain area is determined by the length of the flow channel. The reach lengths between two consecutive cross-sections are determined once again using the flow routes.

3.13.1.6 *Cross-Sectional cut lines*

The cross-section cut lines have been defined to represent the location, position, and expanse of the cross-sections. To conform with the RAS Mapper user manual guide lines, the cross-section cut lines were drawn from left to right, looking downstream and perpendicular to the stream centerline (River). There are 119 cross-

sections in all. While the cut lines show the cross-sections' planar location, the station elevation data was extracted from the terrain along the cut line.

3.13.2 Performing hydraulic computation in HEC-RAS

All of the geometric data were imported into HEC-RAS, and the data quality was checked. The flood analysis was carried out using a 1D steady flow simulation in a subcritical flow regime. The HEC-HMS model was used to determine flood values for 10, 20, 50, 100, 200 and 500 return periods, as indicated in Section 3.11. These flood values were utilised as input for steady flow data along with appropriate boundary conditions. Because the chosen flow regime was subcritical, the river boundary condition was only defined at the downstream end. The normal depth, which is the slope of the riverbed, was used to define it. The software predefined the boundary conditions at the intersection. The simulation output was the water level for all of the flood levels. The river water level can be seen in cross-sections and longitudinal sections. Water surfaces for 10, 20, 50,100, 200 and 500-year flood and river centreline were exported back to Arc-GIS. The file exported from HEC-RAS to Arc-GIS was in spatial data format (SDF).

3.13.3 Post-processing of RAS results in Arc-GIS

The SDF file exported from HEC-RAS was first converted to XML, the format which Arc-GIS can read. This step involved mapping the flood-inundated areas, depths, and inundation velocity. To begin, a new set of layers was created before processing the HEC-RAS results, and the terrain model (DEM) developed in the pre-processing step was specified for executing the floodplain delineation. The rasterization cell size for the output DEM was also determined in this stage. After that, the HEC-RAS outputs were transformed to XML before being loaded into Arc-GIS. While doing so, Arc-Map was used to construct stream centerlines, cross-section cut lines, bank points, velocity points, and a bounding polygon. The software creates separate boundary polygons, the geographic limit for floods, based on the water surface height at cross-section cut lines for different year floods. Finally, water

surface generation and raster floodplain delineation were accomplished in two phases to finish flood mapping. The altitude of the water surface in each cross-section was utilised to generate DEM for water surface for 10, 20, 50, 100, 200 and 500-year floods. The floodplain was delineated using the water surface DEMs obtained in the previous phase and the terrain model DEM. As a result, the floodplain borders and depths were determined. Polygons were used to depict flood inundation zones for various flood values, while DEMs were used to indicate their depths (raster format).

3.14 CADASTRAL LEVEL RISK ASSESSMENT OF CHALAKUDY RIVER BASIN

This was done by superimposing of Cadastral level map of Chalakudy river basin with flooded area polygons obtained from HEC-RAS output for different return periods. Classifying the flood inundated areas into three categories such as high, medium and less inundated was done. Based on the water surface profiles such as depth, velocity and elevation, Cadastral level risky areas were classified into three categories such as high, medium and low.

3.15. FLOOD VULNERABILITY ANALYSIS

The flood vulnerability is influenced by the land use characteristics of the areas under the influence of flood. That is, a flood with the same likelihood of exceeding the threshold will have various levels of vulnerability depending on the land use characteristics and damage potential. As a result, the vulnerability study entails determining the land use regions that might be impacted by a flood with a specific return duration. For each of the flood occurrences being simulated, vulnerability maps were created by clipping the land use themes of the floodplains with the flood area polygons. As a binary model, this represents the vulnerability element of the flood risk in a certain location in terms of the presence or absence of floods during a specific return time. The land use areas under the influence of each of flooding events were reclassified for the calculation of the total vulnerable areas. Based on the results of risk assessment and vulnerability analysis, the flood prone

areas of Chalakudy river basin for different return period flood events were identified and mapped.

CHAPTER IV
RESULTS AND DISCUSSION

The present study was intended to analyze the flood frequency and to perform the hydrological and hydraulic modelling for Chalakudy river basin using the data on climatological and terrain characteristics of the basin. The flood frequency analysis was carried out using HEC-SSP tool and the hydrological and hydraulic modelling was conducted using HEC-HMS and HEC-RAS models. The various results obtained from the study are explained and discussed in this chapter under the following subheadings.

4.1 INPUT DATA COLLECTED

4.1.1 Digital Elevation Model (DEM)

As topographical factors influence the hydrological modelling, selecting the appropriate DEM is crucial. DEM identifies the drainage related features such as ridges, valley bottoms, channel networks and surface drainage patterns and quantifies the sub basin and channel characteristics like size, length and slope. The accuracy of DEM depends on its quality and resolution and the processing algorithms that extracts the DEM data. DEM of 30 m resolution downloaded from the USGS earth explorer is shown below in Fig. 4.1.

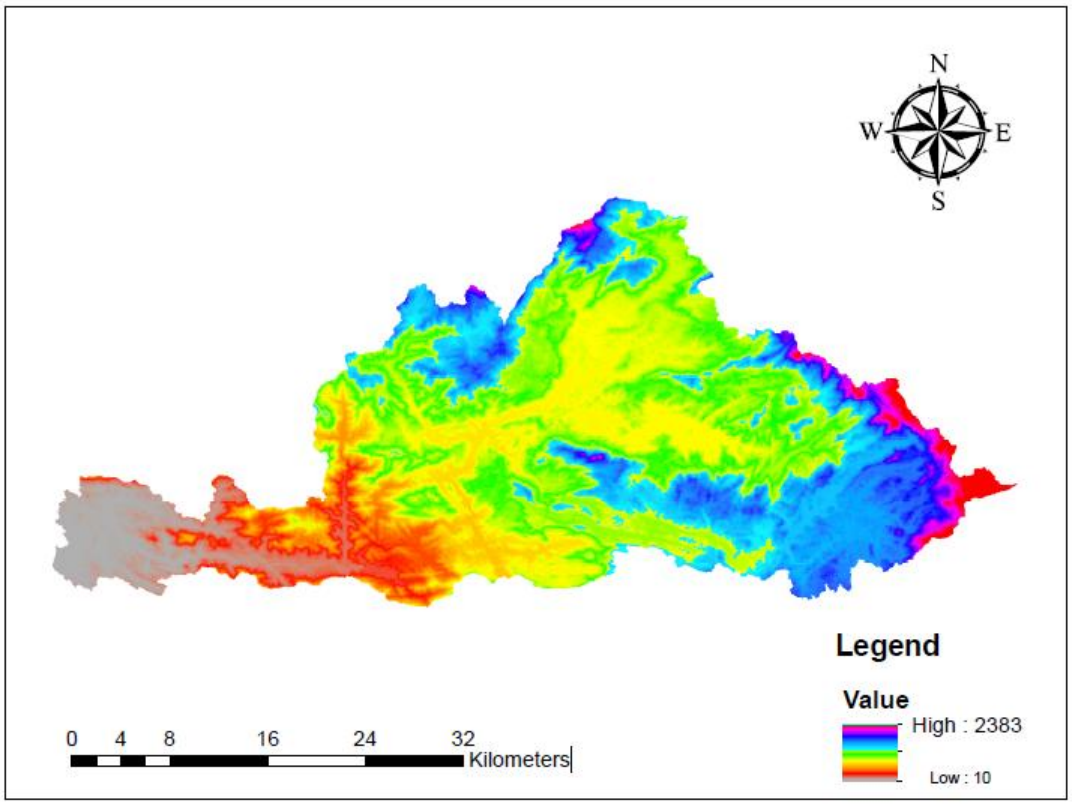

Fig. 4.1 DEM of Chalakudy basin

4.1.2 Rainfall data

In almost every month, rainfall recorded in upstream gauge locations of the basin like Parambikulam and Kerala Sholayar Dam (KSD) indicate higher values than the downstream regions of the basin. The South-West monsoon season, which extends from June to September, has the highest average rainfall of 909.40 mm, followed by the North-East monsoon season, which occurs from October to November and has a maximum of 370.75 mm. The daily rainfall data collected is given in appendix I.

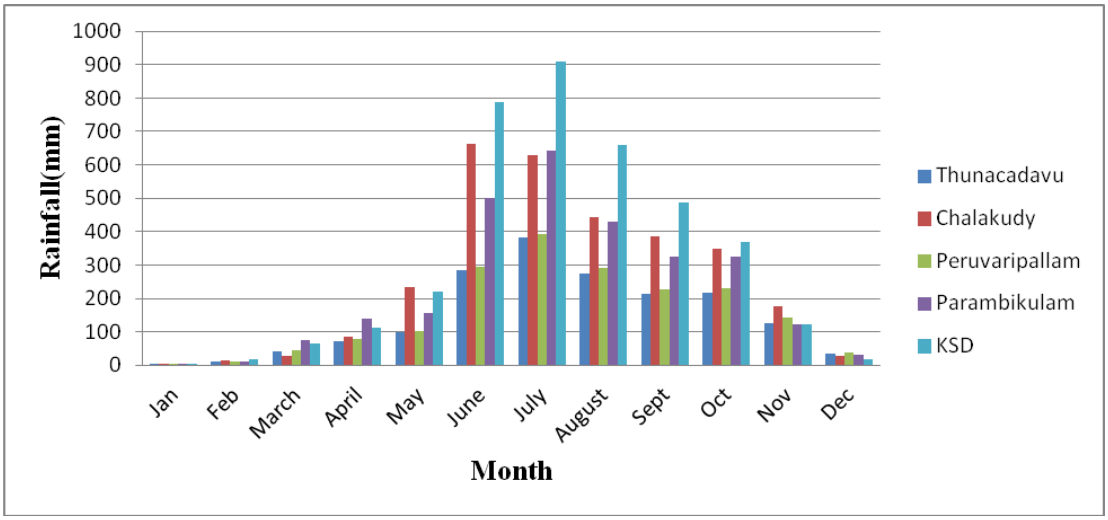

Fig.4.2. Average monthly rainfall recorded by different rain gauge stations

4.1.3 Land use / Land cover map

One of the most important components influencing the surface runoff of a basin is the land use/land cover. The land use map of the basin was prepared by Unsupervised classification in ERDAS IMAGINE software for the year 2020, and the information gathered was based mainly on cloud-free satellite images and ground truthing. The land use map prepared for the year 2020 is given in Fig.4.2. In this study, the land use classes taken were seven *viz* water body, forest, urban area, barren land, tea/oil palm, paddy and coffee/cardamom.

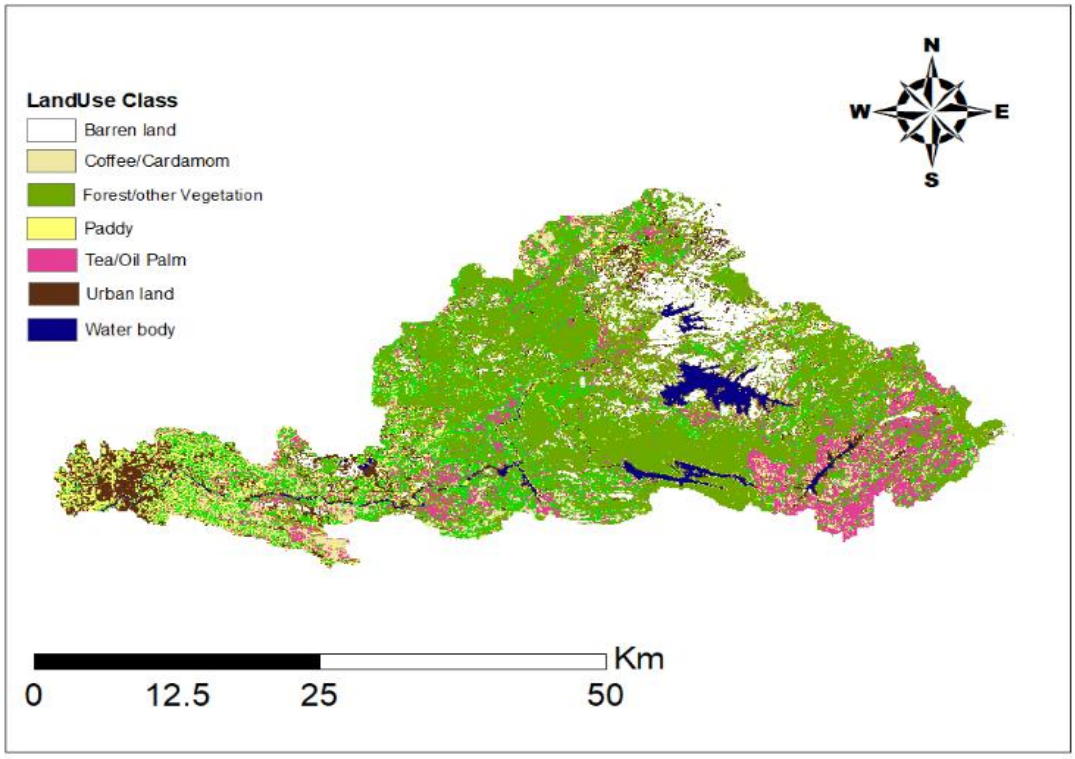

Fig. 4.3 Land use land cover map of Chalakduy river basin for 2020

Table 4.1 Areal distribution of different land use/land covers classes

Land use class	**Area (km^2)**	**Area (%)**
Water body	30	2.18
Forest/other vegetation	780	56.93
Barren land	157	12.77
Paddy	150	10.94
Tea and oil palm	90	6.56
Urban land	122	8.90
Coffee/cardamom	41	2.99
Total	1370	100

In the study area, urban lands covers 122 km^2 as seen in the 2020 LULC map. According to Nchumbeni and Rema K.P (2020), area coverage of 100.1 km^2 for urban lands was noticed for year 2017. The highest area coverage was for the forest class which was 803.09 km^2 for the year 2017 (Nchumbeni, 2020). The present study also shows highest area coverage by forest lands that it is 780 km^2 for the year 2020, which shows slightly lesser value compared to 2017 year. The reduction in the forest area might be a result of populace increment. The highest decrease in percentage area was found to be for forest class which was found to decrease consistently in between the three years from 63.01% to 55.67% respectively. The comparison of results reveals that the forest zone, barren land and tea plantation showed reduction of area from 2017-2020. An increase of water body, palm, paddy area and urban area was also found after comparing the LULC maps of 2017 and 2020. These changes reflect the alternations in Land Use land cover (LULC) after flood of August 2018.

4.1.4 Soil map

The study area was divided into four hydrological soil mapping units based on soil characteristics: HSG A, HSG B, HSG C, and HSG D (USDA, soil texture class). The code HSG ‘O' was assigned to areas such as water bodies and human settlements.

Different colour shades in the soil map represent different HSGs. The HSG A soil has a low runoff potential and a high infiltration rate, such as gravelly sands, while the HSG B soil has a moderate infiltration rate and a moderately fine to coarse texture, and the HSG C soil has a moderately fine to fine texture. The clayey soil is an example of the HSG D, which has a high runoff potential due to low infiltration rate. The soil map of the basin is shown in Fig. 4.4 and it depicts the different units and spatial distribution of each soil type in the basin. The percentage area cover rage by HSG ‘O’, HSG A, HSG B, HSG C and HSG D is 11.5%, 40.25%, 23.5%, 15.5% and 9.25 %.

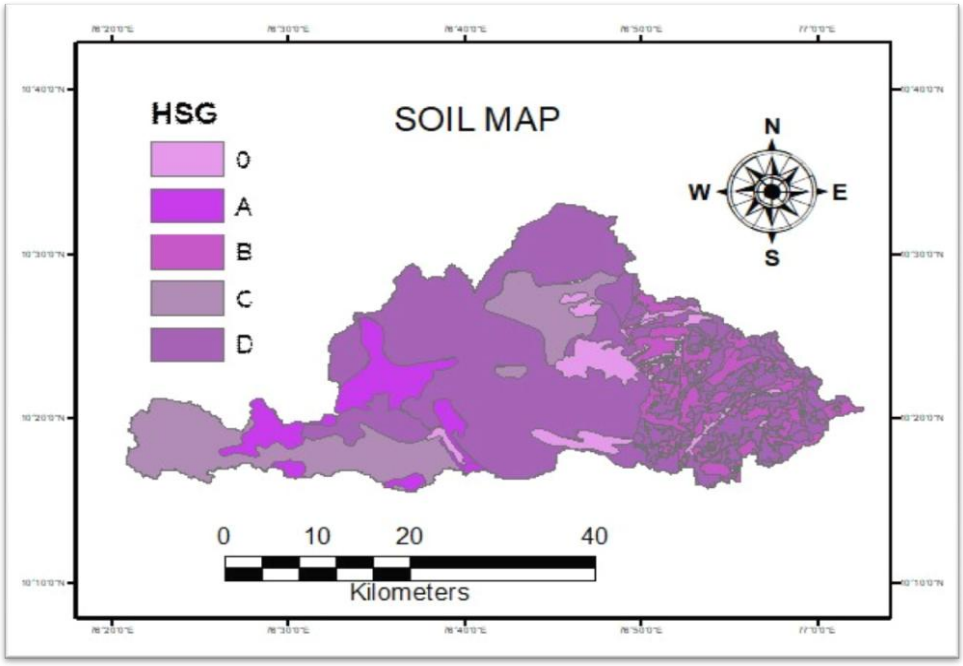

Fig. 4.4 Soil map of Chalakudy river basin

Table 4.2 Percentage area coverage by Hydrological soil group in Chalakudy basin

Hydrological Soil Group(HSG)	Area(Km^2)	% of Area
HSG 'O'	157.55	11.5
HSG 'A'	568.55	40.25
HSG 'B'	332.91	23.30
HSG 'C'	228.79	15.7
HSG ' D'	140.425	9.25

4.2 MODELLING WITH HEC-GEOHMS

4.2.1 Pre-processing:

The different input data for the HEC-HMS model setup for flood modelling studies in the Chalakudy basin included Digital Elevation Model (DEM), rainfall data, stream flow data, soil type and land use/land cover (LULC) data. The input data

files were prepared using HEC-GeoHMS, ERDAS Imagine and Arc-GIS. The data describing the terrain was in vector format. Therefore, DEM was initially analyzed through the HEC-GeoHMS (which function in Arc-GIS software platform) for creating the input file. The stream network and subbasin regions within the basin were created using DEM data. In Projected Coordinate System, all data layers were projected to the WGS 1984 Northern Hemisphere.

The preprocessing tool was used to generate eight datasets for stream and sub basin delineation before starting the hydrologic modelling in the HEC-HMS software. The HEC-GeoHMS extension tool in Arc-Map was utilized to carry out the delineation process. All the outputs from the HEC-GeoHMS toolbar is shown in Fig.4.5 (a-h) below: The datasets derived under pre processing menu are:

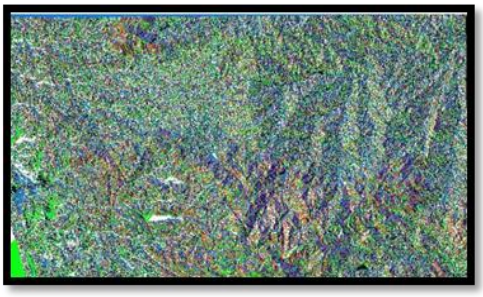

a. Flow Accumulation output

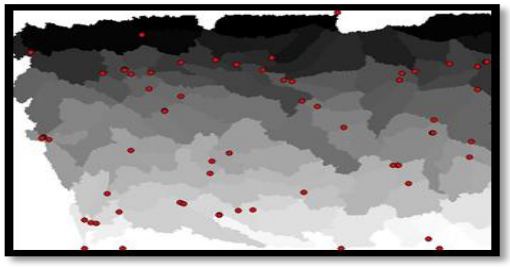

d. Catchment Grid Delineation

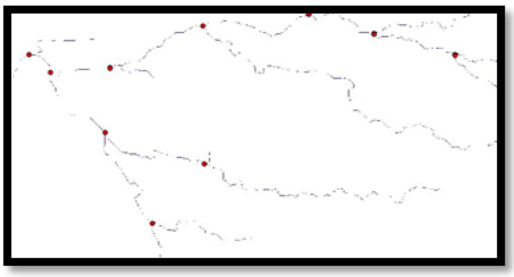

b. Stream Definition output

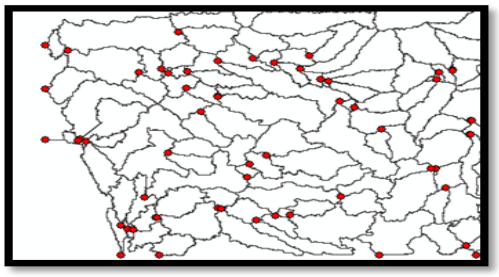

e. Catchment Polygon processing

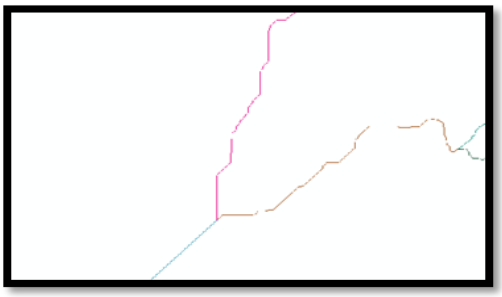

c. Stream Segmentation

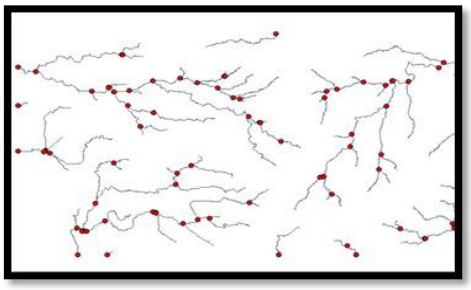

f. Drainage Line Processing

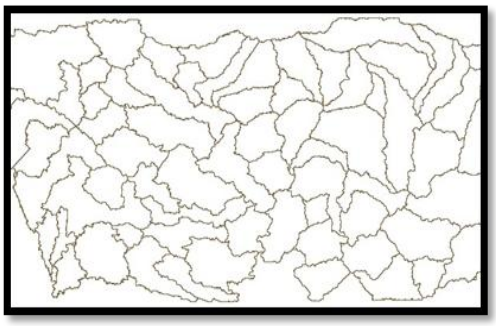

g. Ad joint Catchment Processing

Fig. 4.5 View of the results obtained from Pre-processing menu

4.2.2 Project setup

After the preprocessing operations, the delineated area represents the HEC-HMS project's working boundary. The watershed outlet was specified at the downstream area once the delineation operation was completed. Fig.4.6 represents the defined basin with the specified outlet.

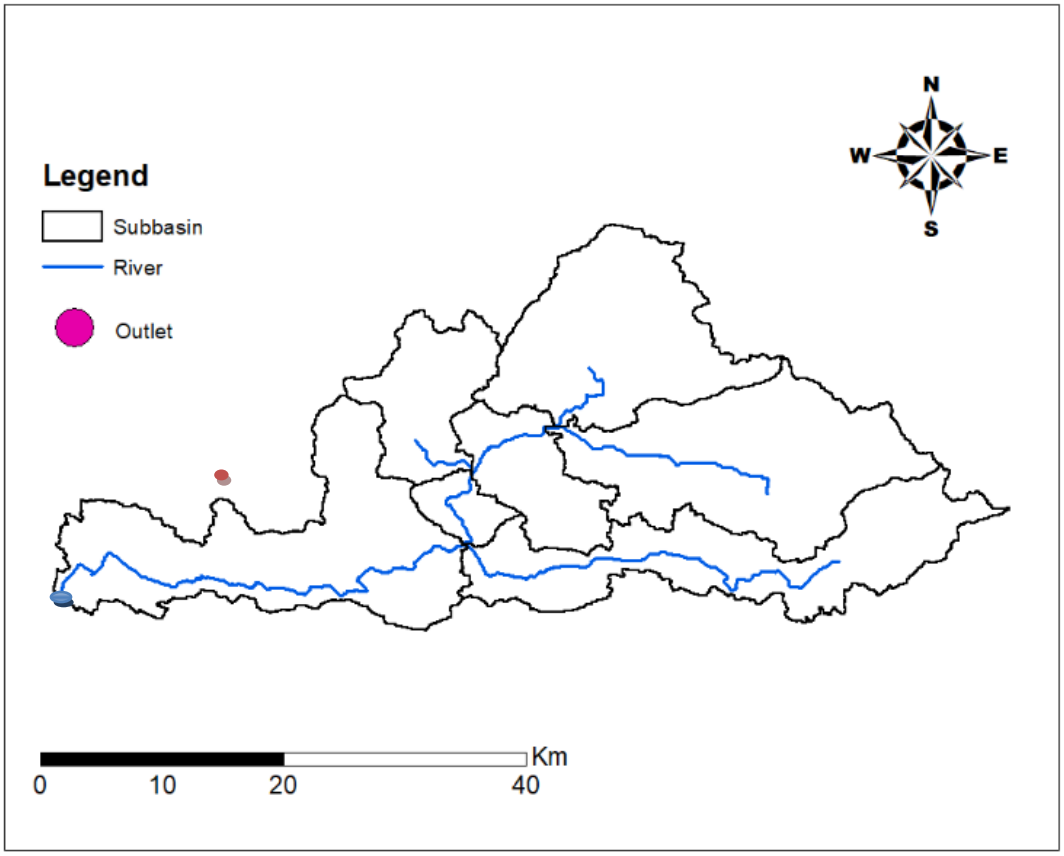

Fig. 4.6 Delineated basin shape file

4.2.3 Characteristics

Basin processing option included Sub-basin merge, the River length and Slope, Basin slope, Sub-basin centroid and the Longest flow path map. All the above processes mentioned, were used to extract the physical characteristics of streams and sub basins and to develop the hydrological parameters and HEC-HMS inputs. The following images (Fig.4.6– 4.9) demonstrate the generated output shape files:

a) *River length*

The river length tool calculates river segment lengths and saves them in the river length field. Select the river length and confirm the river name before clicking OK. Characteristics. The river length field may be found in the input river1 (or

whatever name we've given it) and observe that the feature class has been completed in. The map document has been saved.

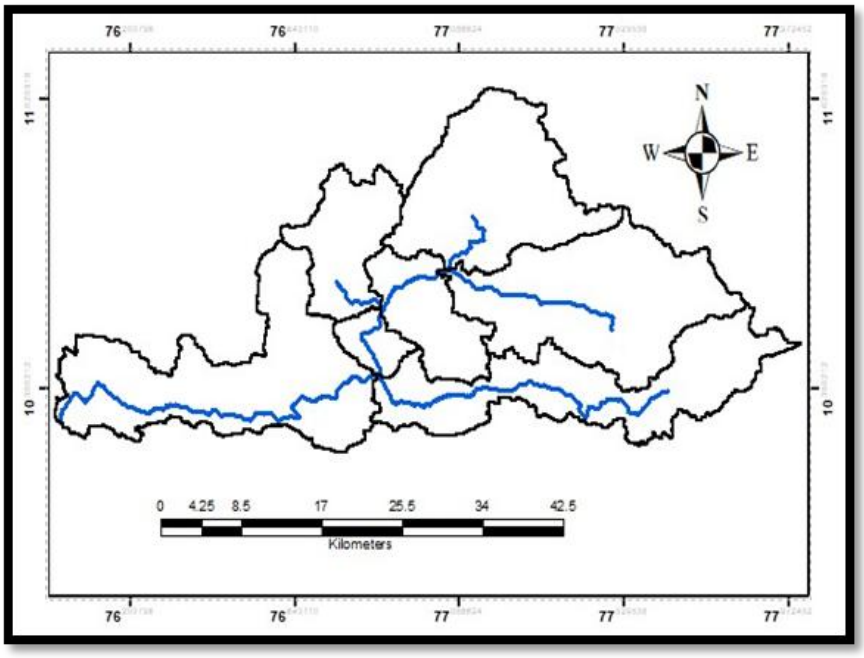

Fig.4.7 River length characteristics of Chalakudy basin

b) *River slope and basin slope*

The river slope tool calculates and saves the slopes of river segments in a slope field. The input river1 feature class's slope field has been populated. During this operation, ElevUP and ElevDS are also populated. (Elev UP – Elev DS)/River Length = Slope. Using the slope grid and sub-basin polygon, the basin slope tool calculates the average slope for the sub-basin.

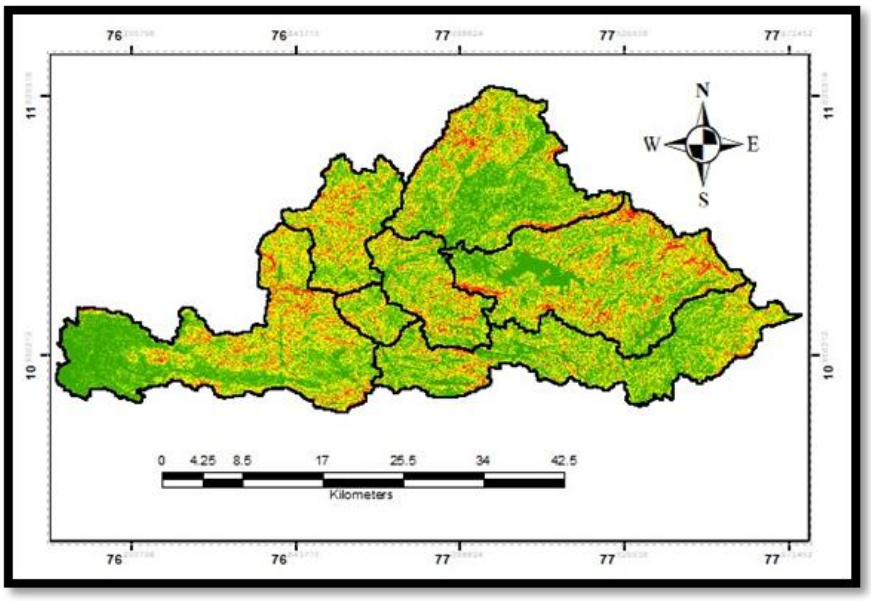

Fig.4.8 River and basin slope

c) *Longest flow path*

This Fig. 4.9 gives the longest flow path for the basin tool.

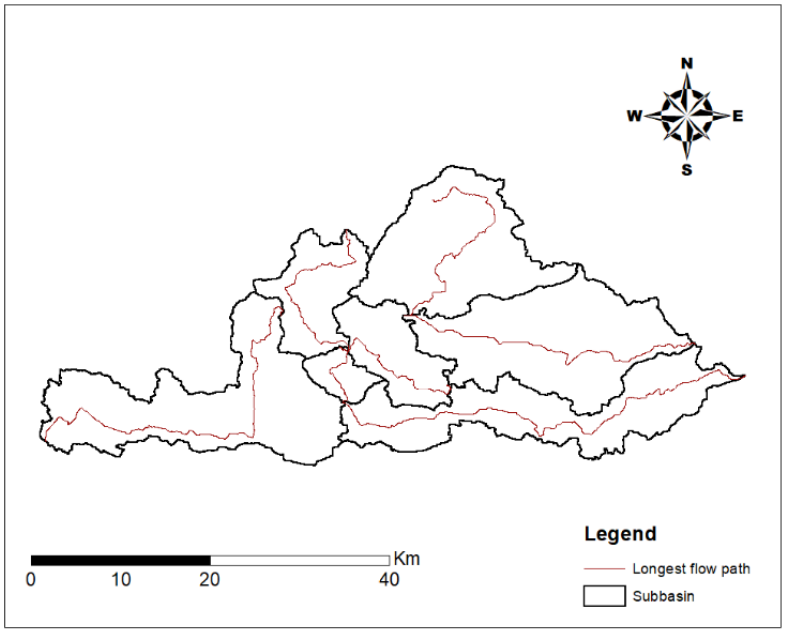

Fig.4.9 Longest flow path map of Chalakudy basin

d) *Sub-basin centroid*

Fig 4.10 creates a centroid point feature class to store the centroid of each sub-basin.

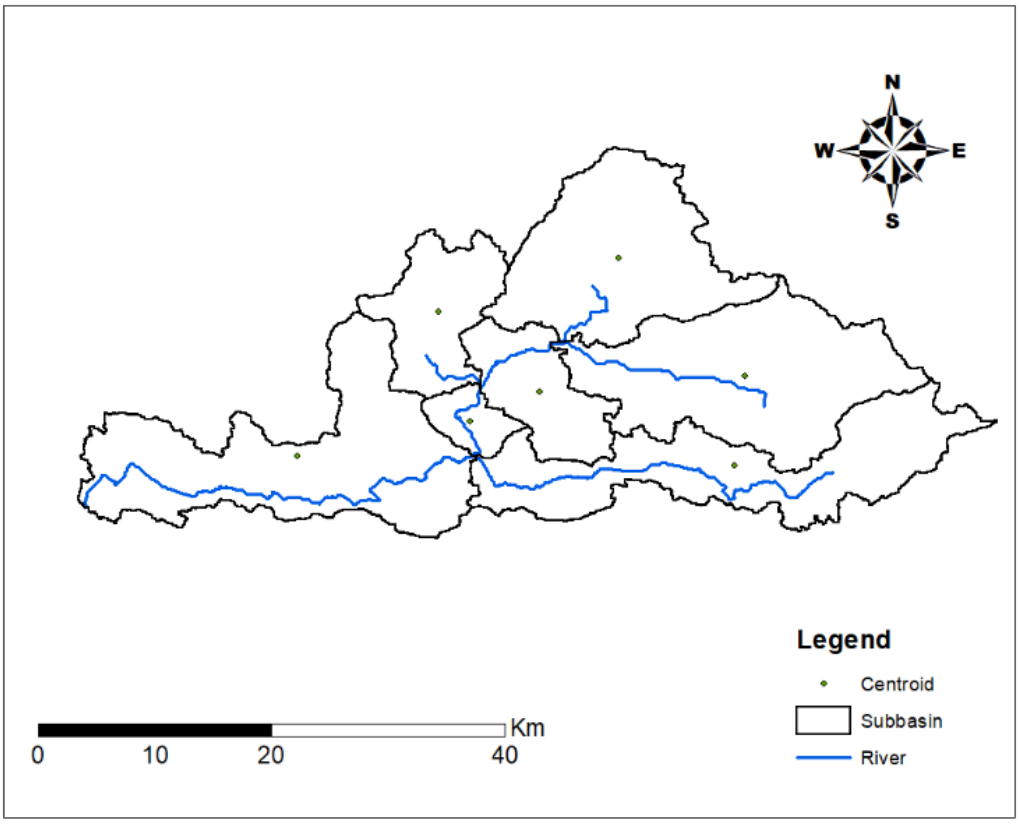

Fig.4.10 Sub-basin Centroid map of Chalakudy basin

4.2.4 HMS schematic

This tool creates a GIS representation of the basin using a schematic network with basin elements and their connectivity, which are represented as source, sink, junction, diversion, subbasin and reservoir. In this study, seven sub basins, one discharge gauging outlet which is represented as sink, three reservoirs, three junctions which was represented where one subbasin connection with another subbasin. The HMS schematic obtained from the HMS menu is shown below (Fig. 4.11).

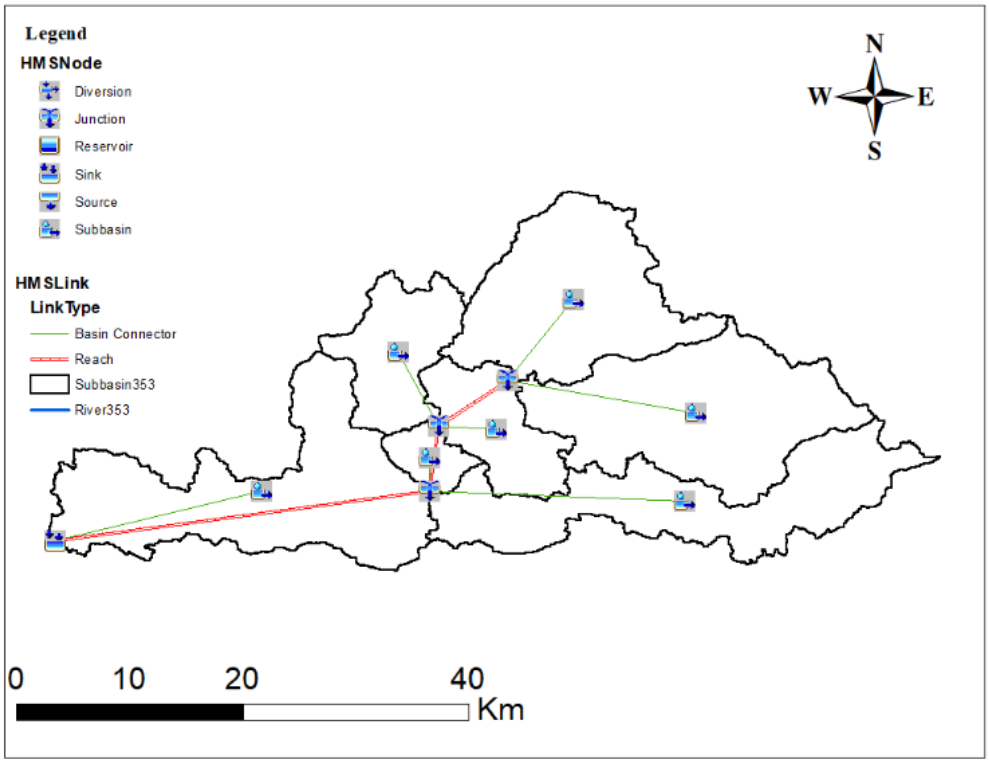

Fig. 4.11 HMS Schematic view of Chalakudy basin

4.2.5 Utility

The 'Utility' menu was used for generating the Theissen polygon map and the CN Grid map. The results obtained from the generated maps are discussed below.

4.2.5.1 *Theissen polygon map*

Fig.4.12 shows the generated Theissen polygon map as well as the five rainfall gauging stations. The contributing area of each gauging station is shown by a variety of coloured polygons. The Theissen polygon map was made using the HEC-GeoHMS extension tool to calculate the average rainfall over the entire basin.The rainfall data for the gauging stations were collected from ARS Chalakudy and IMD, Pune for the years 1990-2017.

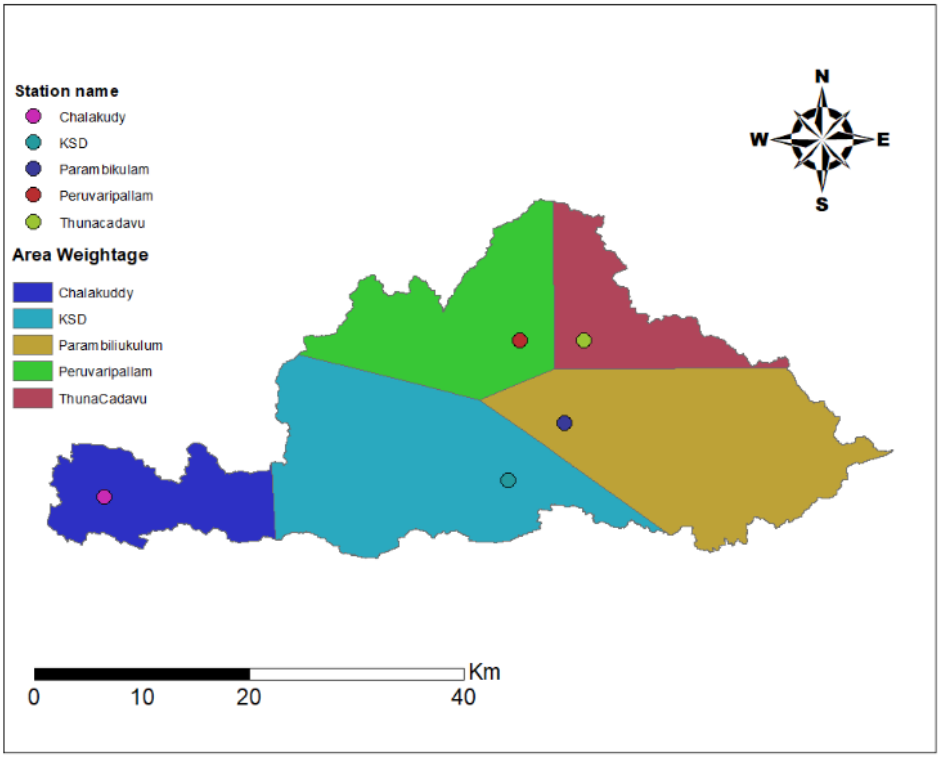

Fig. 4.12 Theissen polygon map

The above Fig. 4.12 shows that all five gauging stations are located within the basin, and each station has varying influence on the rainfall in the basin, as given in table 4.4, with different areas of influence and weights. The point rainfall data of gauging station at KSD has the largest area influencing the average rainfall of the basin, with an area of 415 km^2 and a weight of 0.302, while Thunacadavu has the smallest area influencing the average rainfall of the basin, with an area of 147 km^2 and a weight of 0.107, respectively. The influential area of each station is placed in the increasing order in table 4.3. Table 4.4 shows the total monthly average rainfall of the basin computed by Theissen polygon method.

Table 4.3 Gauging station influential area along with their weights

Sl. No.	Gauging station	Area (km^2)	Weights
1	**Thunacadavu**	137	0.107
2	**Chalakudy**	144	0.113
3	**Peruvaripallam**	230	0.18
4	**Parambikulam**	380	0.298
5	**KSD**	385	0.302
Total		1276	

Table 4.4 Monthly average rainfall (mm) computed by Theissen Polygon method (1997- 2017)

Month	**Jan**	**Feb**	**March**	**April**	**May**	**June**
Average Rainfall(mm)	2.03	13.72	57.58	107.95	168.40	545.57
Month	**July**	**August**	**Sept**	**Oct**	**Nov**	**Dec**
Average Rainfall(mm)	649.03	458.94	313.21	132.73	28.55	313.21

Table 4.5 Month wise rainfall and its departure from normal for 2018

Period	**Normal rainfall in mm**	**Actual rainfall in mm**	**%Departure from normal**
June 2018	649.8	749.6	15
July 2018	726.1	857.4	18
1-19 Aug 2018	287.6	758.6	164
Total	1649.5	2346.6	42

Source: (CWC, 2018).

From computed monthly average rainfall (mm) by Theissen Polygon method (1997-2017), July had the highest monthly average rainfall (649.03mm), followed by June (545.57mm). The month of January had the least amount of rainfall (2.03mm). Comparison was made between the 2018 climatological conditions reported by CWC to the long-term average records (1997-2017) collected in this study, As per CWC month of july had 857.4 mm, which is much above the average value of long term values. This gave a clear indication of the anomalous nature of the 2018 precipitation event. Kerala received significantly high rainfall from 1 June 2018 to 19 August 2018 (2346.6 mm), which is roughly 42% above the normal rainfall. During the first 19 days of August 2018, Kerala received 164% above normal rainfall, of which the major share was from two Extreme Rainfall Events (EREs) during 8 to 10 and 14 to 19 August 2018 (Sudheer *et al.*, 2019).

Mishra *et al.* 2018 estimated 1 and 2-day extreme precipitation in Kerala in August 2018 to get a sense of the magnitude of the state's extreme hydroclimatic conditions, which resulted in widespread flooding. They observed that 1-day maximum precipitation in Kerala ranged between 100 and 400 mm in August 2018, which is much greater than the long-term average. They also discovered that the 15th of August had the most precipitation in Kerala in 2018. In August 2018, the two-day maximum precipitation was more than 400 mm in several parts of the state, with some sections receiving more than 600 mm. Kerala's two-day maximum precipitation happened on the 15th and 16th of August, resulting in huge floods across the state. Extreme rainstorm events have wreaked havoc on the study region, inflicting considerable property destruction.

4.2.5.2 *CN grid map*

The polygons from both the soil map and the LULC map were merged to create the CN grid map. Since, the SCS loss method was selected, the CN grid map was mainly created to generate the curve number for each sub basin, which is a required parameter for running the model. The CN grid map for the year 2020 is shown in Fig.

4.13. Table 4.5 represents an overview of the ‘CN Lookup table,' whereas table 4.6 represents the CN and area of each sub basin.

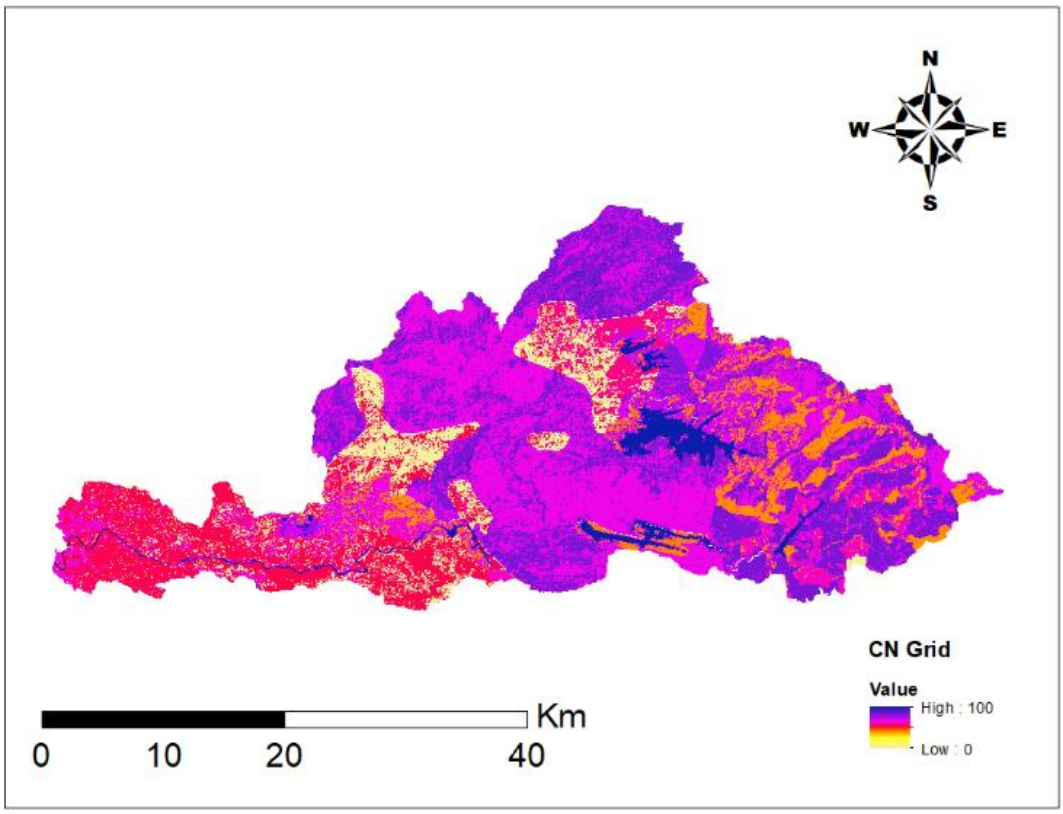

Fig. 4.13 CN grid map of Chalakudy basin

4.2.6 Basin model in HEC-HMS

The basin model includes hydrologic elements, their connectivity and the related geographic information that can be loaded into an HEC-HMS project. Basin model represents the physical characteristics of Chalakudy Sub basin and it is shown in Fig.4.14. The drainage area of subbasins is shown in the Table 4.6. The Chalakudy basin was modelled by dividing it into 7 sub basins: W140, W130, W120, W110, W100, W90 and W80.

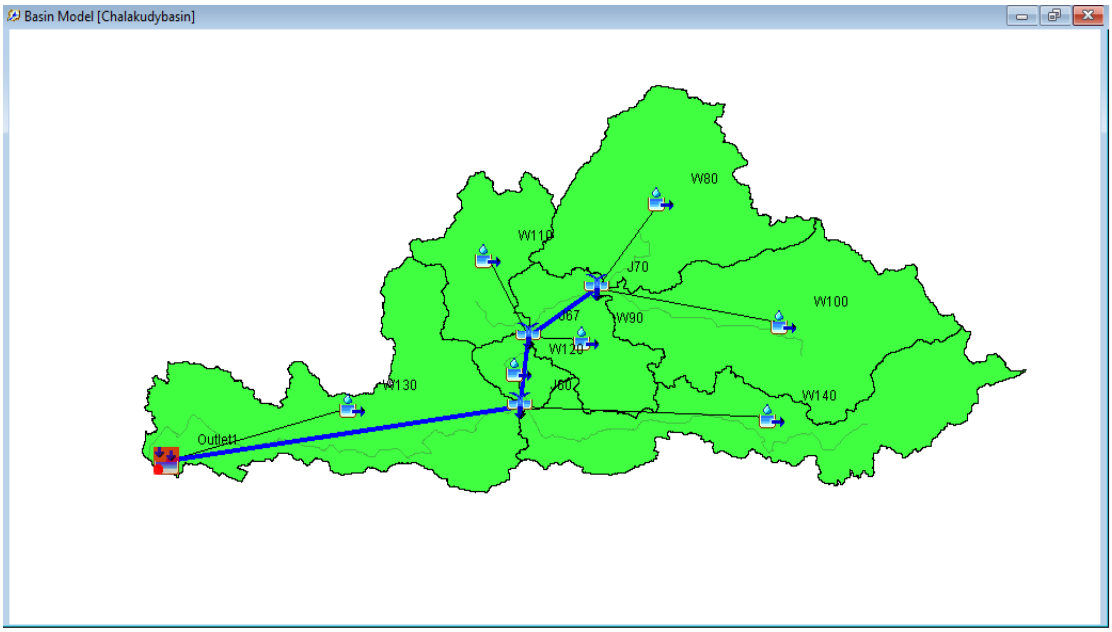

Fig. 4.14 Basin model of Chalakudy river basin in HEC-HMS

Table 4.6 Sub basins with their drainage area

Sl. no.	Sub- basin	Drainage area (Km^2)
1	W140	237.21
2	W130	319.69
3	W120	41.43
4	W110	104.57
5	W100	297.14
6	W90	110.49
7	W80	259.47

4.2.7 Optimization of model parameters

Using the optimization tool in HEC-HMS, the model parameters were adjusted to match the simulated and observed discharge. Sub basin and reach parameters included Initial Abstraction (Ia), Curve Number (CN), and Lag Time (LT), among

several others. Optimization trials were used to automatically optimize these parameters. The optimization was carried out in such a way that the output hydrograph computed at the outlet matched with the simulated/observed hydrograph closely. Minimization of the function, *i.e.,* minimization of the difference between computed and observed discharge, was selected as the objective function for optimization. To analyze the minimization function, 'first lag auto correlation statistics' was used.

Table 4.7 Initial and optimized parameter values for different Subbasins

Subbasin	**Initial abstractions (I_a)**		**Basin CN**		**Lag time(min)**	
	I	**O**	**I**	**O**	**I**	**O**
W140	15	7.71	90.95	98.16	1500	2617.40
W130	15	7.62	98.32	84.57	1500	2666.60
W120	15	8.63	92.23	73.47	1500	2912.70
W110	15	9.77	96.61	57.73	1500	3019.90
W100	15	10.60	94.23	44.42	1500	2943.70
W90	15	11.09	89.02	35.66	1500	3104.40
W80	15	11.46	92.78	33.27	1500	2695.60

Table 4.8 Initial and optimized parameter values of coefficients in Muskingum equation

River	**X**		**K**	
	I	**O**	**I**	**O**
R70	0.2	0.15	0.5	0.50
R50	0.4	0.16	0.5	0.50
R30	0.2	0.17	0.5	0.50

The NSE values slightly increased after using the optimized parameters, as shown in Table 4.9, indicating that the model generated satisfactory results for the simulation of rainfall-runoff for the sub basin.

Table 4.9 NSE values before and after optimization

Year	N.S.E value	
	Before optimization	**After optimization**
2005	0.413	0.762
2006	0.403	0.751
2007	0.542	0.812

4.2.8 Calibration of HEC-HMS model

Daily rainfall and other hydro-meteorological data from 2005 to 2007 were used for calibration. The model's calibration input was initially set to the estimated initial parameters, as shown in Table 4.7. The discharge hydrograph, peak runoff, total volume, time to peak, and total volume were all simulated. When observed discharge values were compared to model simulated discharge values, it was found that there was a significant difference between observed and predicted values in all sub basins. The initial parameters were optimized using the model's automatic optimization tool to obtain satisfactory results. The model was re-calibrated using optimum parameters (Table 4.7) to ensure peak discharge, total volume, and time to peak. It was found that the optimized value generated a simulated hydrograph that was nearly identical to the observed one. As a result, for model calibration and accurate simulation, optimized parameter values were chosen.

Fig.4.15- 4.17 represents the plot of hydrograph of simulated outflow and observed flow during the calibration. The graph showed that there is a close similarity of trend between the simulated and observed hydrograph in all the years including the calibration period. It was also seen that the peak of the hydrographs for calibration was not matching with the peak of observed hydrographs. This might be due to the fact that watershed physical characteristics change both spatially and temporarily.

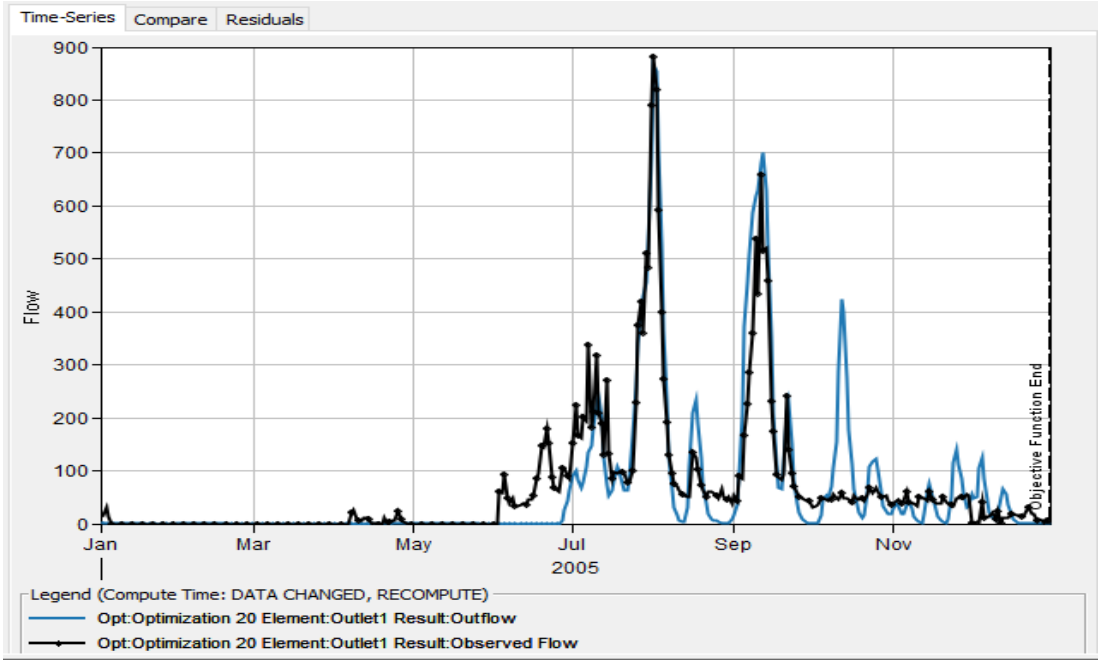

Fig. 4.15 Simulated and observed hydrograph for the year 2005

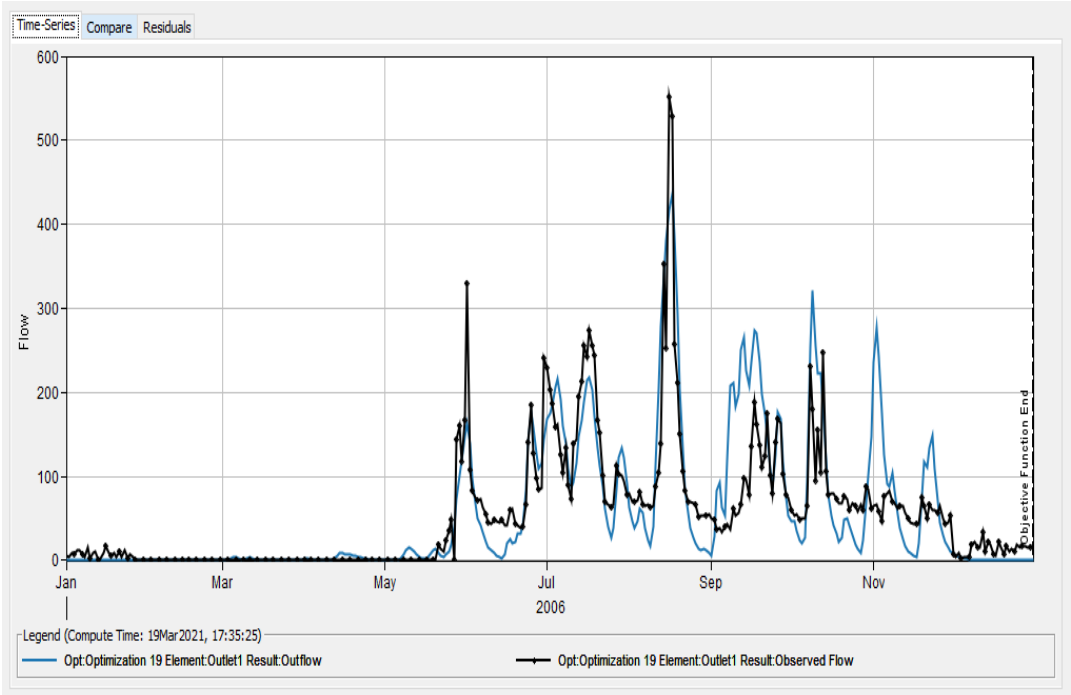

Fig. 4.16 Simulated and observed hydrograph for the year 2006

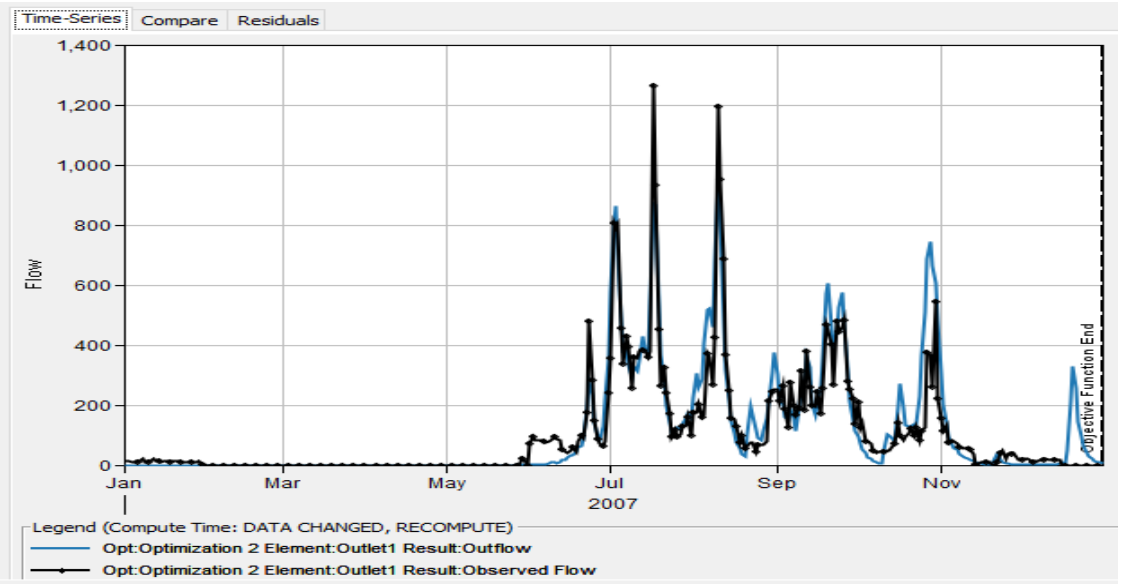

Fig. 4.17 Simulated and observed hydrograph for the year 2007

Referring to above hydrographs, it was clear that only base flow contributed to the discharge at outlet during the summer season, when there was no or little precipitation over the watershed. However, during the monsoon season, the maximum precipitation that occurred in the watershed caused a large discharge at the exit, resulting in a peak flow in the basin. During the calibration period, the largest peak discharge occurred in 2007, with a peak flow of 965.70 m^3/s.

During particular time periods in the graphs, it was also visible that the peak of the observed and simulated hydrographs of flow was not matching. This could be due to the fact that the actual basin physical parameters may not be exactly as has been simulated by the model. In addition, initial loss, imperviousness and curve number of the sub basin areas may also create some effect on the runoff in the watershed. In some parts of the watershed, areas with higher imperviousness resulted in less infiltration and thus greater surface runoff. This had an impact on the volume of discharge, the peak discharge, and the time it took to reach the peak discharge. The

time of peak was influenced by imperviousness and curve number, resulting in an increase in peak discharge and volume. That is, variations in hydrological indicators, such as time to peak, peak discharge, and volume, were highly correlated with the basin's imperviousness. In addition to these considerations, the catchment soil was predominantly clayey resulting in a large amount of storm water draining quickly into the streams. However, the initial losses including surface depressions and interception loss reduced the surface runoff at some stages of flow because of more resistance caused in flow path and the availability of more opportunity time for initial loss.

The respective R^2 values were also in the acceptable range in a scatter plot of actual and simulated flow (Fig. 4.18) for different time periods (i.e. greater than 0.7). The simulation overall results were represented as an objective function and a summary results table that provides a comparison between observed and computed flow is given. The estimation has an excellent performance rating when the RSR (Root mean square error-standard deviation ratio) is less than 0.5. Moreover, Nash Sutcliffe Efficiency (NSE) value for calibration period was obtained in the range of 0.75-0.81, which was also found satisfactory. (Table 4.10)

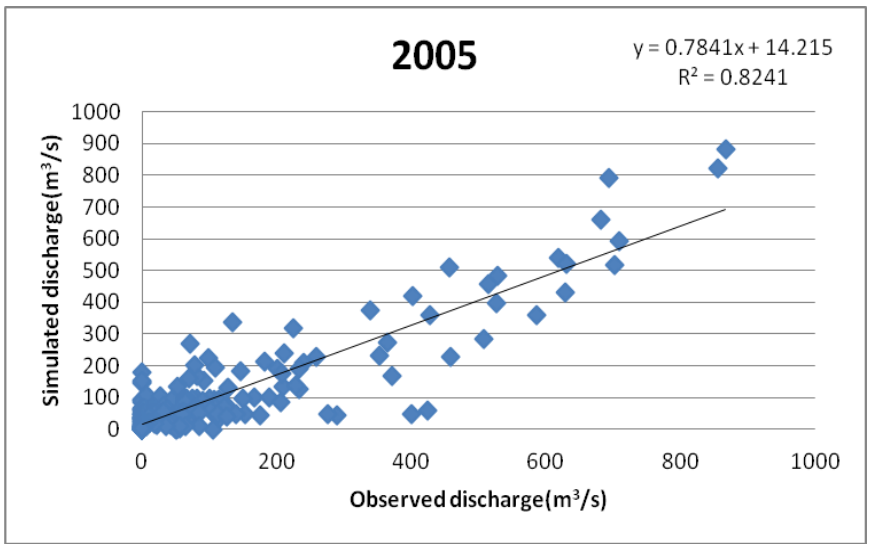

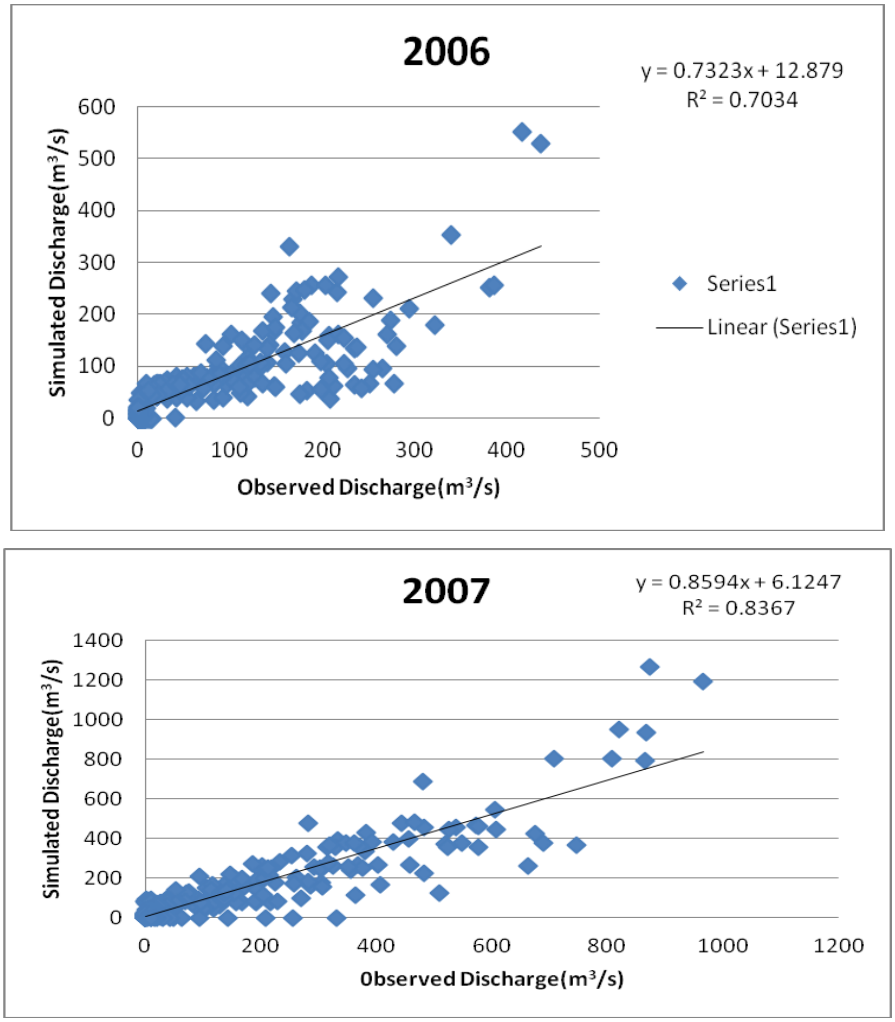

Fig. 4.18 Scatter plots of observed versus simulated flow during calibration

Table 4.10 Performance indices of the model during calibration

Year	Nash Sutcliffe Efficiency (NSE)	Percent bias(PBIAS)	Error in Peak Flow (%)	Error in Volume (%)	Coefficient of correlation (R^2)	Root mean square error-standard deviation ratio (RSR)
2005	0.762	1.72	1.73	0.46	0.8239	0.5
2006	0.751	-1.67	-1.65	-4.27	0.7034	0.5
2007	0.812	6.5	6.79	8.63	0.8367	0.5

By comparing the percent difference between simulated and observed flow, the objective function is utilized to compute model performance. Objective functions are the algorithms used in HEC-HMS to find the model parameters that produce the best value of an index (USACE, 2000). The Error in Peak Flow (percentage) and Error in Volume (percentage) were calculated using the results of the objective function. The lowest inaccuracy in Peak Flow (percent) was recorded in the simulation conducted in 2006, which was only -1.65 percent, and the highest error of 6.5 percent was observed in 2007. On the other hand, the lowest error in volume (-4.27 percent) occurred in 2006, while it was considerably greater (8.63 percent) in 2007. During the calibration period (2005-2007), the maximum volume of flow was seen in 2007, with a simulated volume of 2757.76 Mm^3 and an observed volume of 2519.68 Mm^3. Similarly, in the year 2006, the lowest volume of flow was 1401.75 Mm^3 as simulated and 1344.34 Mm^3 as observed. The summary result illustrated model performance in terms of indices like RMSE standard deviation, NSE and percent bias by comparing the simulated and observed flow of the watershed.

Rahul *et al.,* (2015), used SMA method in HEC-HMS to model the stream flow in the Vamsadhara river basin in India. He reported that during calibration period the performance indices obtained were R^2-0.71, Nash-Sutcliffe Efficiency(NSE) - 0.701, percentage error in volume PEV = 2.64% and percent error in peak PEP= 0.21%. Similar results were also reported by Najim *et al.,* (2006) and Sabzevari *et al*., (2009), with relative percent errors between observed and simulated values of less than 20%. Cheng *et al.,* (2002) also proposed that if the percent error of the runoff volume is less than 20%, the runoff model is considered satisfactory. On comparison with the above results, the statistical indices obtained in the present study were within the acceptable limits for estimating runoff over the basin. According to the statistical evaluation criterion, positive percent error numbers indicated model underestimation bias, whereas negative values indicated model overestimation bias.

4.2.9 Validation of HEC-HMS model

Figures 4.19 and 4.20 represent the comparison of simulated and observed hydrographs over the validation period (2009-2010). For relatively longer duration storms, a similarity in the trend of simulated and observed hydrographs was displayed. Simulated values were likewise found to be close to observed values. However, for short-duration storms, there was a slight variation between the recorded and observed hydrograph. This may be fact that due to differences in rainfall occurrences in specific sub basins that were not recorded by the gauge record at the time.

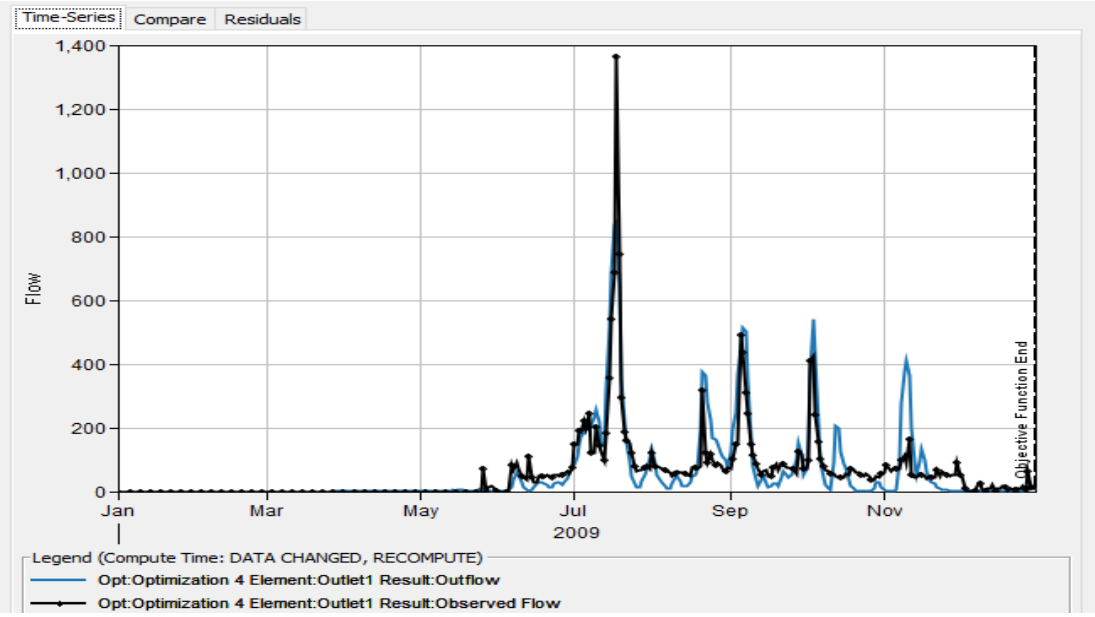

Fig. 4.19 Simulated and observed hydrograph for the year 2009

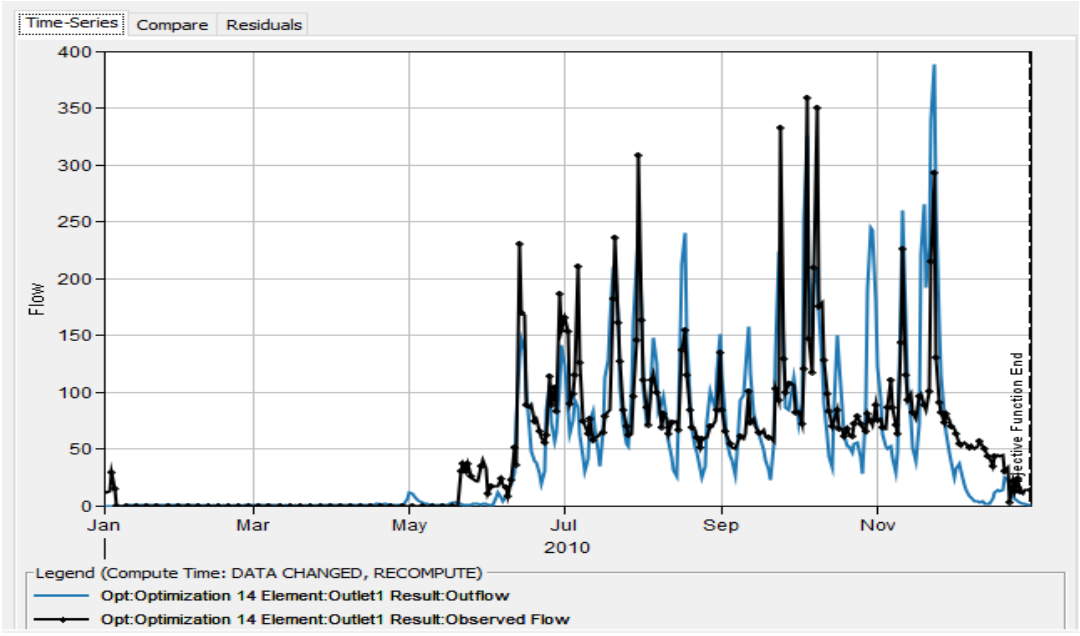

Fig. 4.20 Simulated and observed hydrograph for the year 2010

The value of coefficient of correlation (R^2) was found greater than 0.7 in all the validation years as shown in Fig. 4.21 which indicated the satisfactory performance of the model.

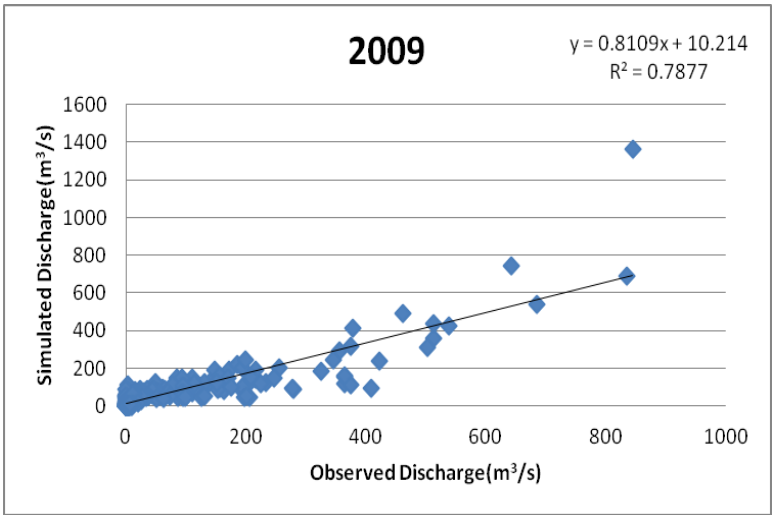

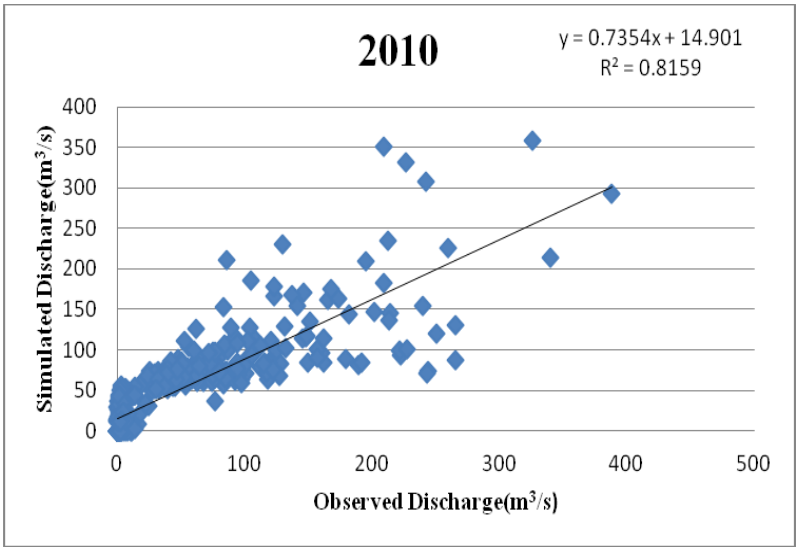

Fig. 4.21 Scatter plots of observed versus simulated flow during validation

Table 4.11 Performance indices of the model during validation

S.N.	Year	Nash Sutcliffe Efficiency (NSE)	Percent bias(PBIAS)	Error in Peak Flow (%)	Error in Volume (%)	Coefficient of correlation (R^2)	Root mean square error-standard deviation ratio (RSR)
1	2009	0.726	6.46	6.68	2.92	0.7877	0.5
2	2010	0.754	-8.18	-7.86	-2.91	0.8159	0.5

The percent error in peak flow is small and close to the observed flood peak within the permissible limit of 20%, as shown in the results. During the validation

period, the maximum peak discharge occurred between July and September. The Fig 4.15 clearly indicates that maximum peak discharge was 844.90 m^3/s which occurred in the year 2007. The total volume of discharge from the basin after settlement of all losses was computed to evaluate the volumetric error and it was found that the calibrated discharge volume was close to the observed discharge volume within the acceptable limit of 20% of total volume. It was also in the acceptable range because the RSR value was less than 0.5. Moreover, the Nash Sutcliffe Efficiency (NSE) value for the validation period was in the range of 0.71-0.76, which was acceptable. According to Roy *et al.*, (2013), the Nash-Sutcliffe efficiency, error percentage in volume, peak error percentage and net difference of observed and simulated time to peak were utilized for model efficiency analysis. The values were found to vary from (0.72 to 0.84), (4.39 to 19.47%), (1.9 to 19%) and (0 to 1 day) respectively. The results on comparison indicates good performance of the model for simulation of stream flow and thereby quantification of available water.

4.2.10 Comparison of observed and simulated measures of flow for the basin

During the simulation period (2005-2010), the maximum volume of flow was observed in 2009, with a simulated value of 2897.02 Mm^3 and an observed value of 2984.30 Mm^3. Similarly, the lowest volume of flow was seen in 2010, with a simulated value of 1284.39 Mm^3 and an observed value of 1246.99 Mm^3.

The highest peak flow of the river was obtained in 2009, with a predicted value of 1299.63 m^3/s and a measured value of 1389.50 m^3/s. The lowest peak flow was obtained in 2010, with a predicted value of 388.40 m^3/s and a measured value of 359.00 m^3/s. Overall, it was found that all of the observed and simulated values in the table showed a strong positive correlation.

Table 4.12 Comparison of observed and simulated flows

Measure	**Simulated**	**Observed**	**Year**	**Time of peak**
Peak flow rate (m^3/s)	866.60	881.80	2005	01 Aug 2005
Volume (M m^3)	1591.84	1599.33		
Peak flow rate (m^3/s)	365.00	359.00	2006	17 Aug 2006
Volume (Mm^3)	1401.75	1344.34		
Peak flow rate (m^3/s)	1181.70	1264.80	2007	10 Aug 2007
Volume (M m^3)	2519.68	2757.76		
Peak flow rate(m^3/sec)	1299.63	1389.50	2009	18 Jul 2009
Volume (M m^3)	2897.02	2984.30		
Peak flow rate (m^3/s)	388.40	359.00	2010	23 Nov 2010
Volume (M m^3)	1284.39	1246.99		

4.3 RAINFALL FREQUENCY ANALYSIS USING HEC-SSP

Meteorological data required as input to the HEC-HMS model were the precipitation depths as a function of return period over the river basin obtained from the rain-gauge point data. HEC-SSP software could be used to do various rainfall frequency analyses as needed. First, using the plotting position method, the rainfall was used to determine the return period. It was then fitted with the Log Pearson Type III distribution. In HEC-SSP software, the yearly maximum rainfall data for 29 years (1990-2019) was entered. Using this data as input, the probability distribution was generated using the software's general frequency analysis editor option. The Weibull plotting position method was used to plot the data on a probability scale. This was then followed by computing the expected probability maximum rainfall depth for different return periods using distribution functions of Log Pearson Type III distribution.

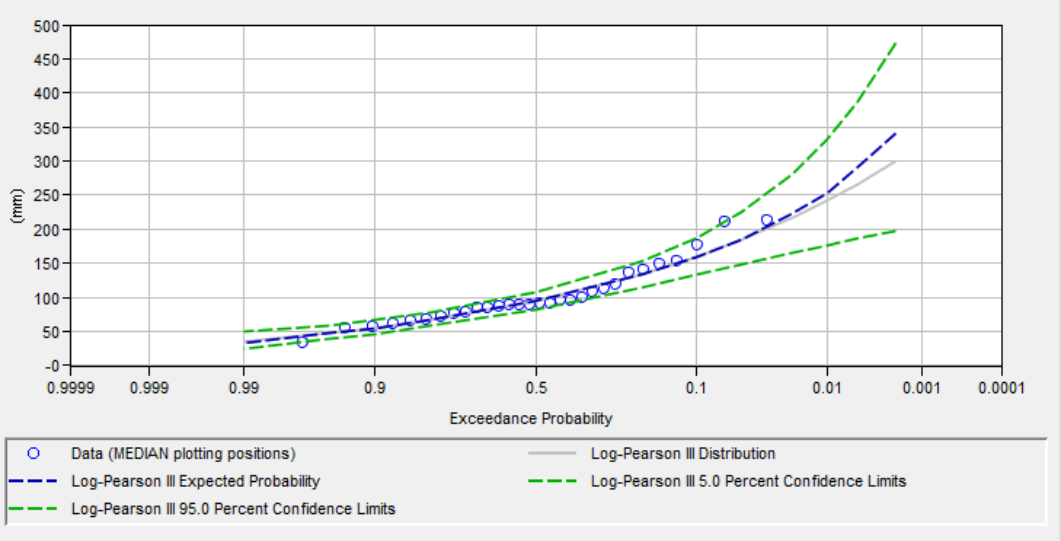

Fig. 4.22 Log-Pearson Type III distribution plot of rainfall data

Fig.4.21 shows a frequency analytical plot obtained from the Log Pearson type III distribution. The rainfall depth values are for likelihood of occurrence in the range of 0.9999 to 0.0001 in the plot. Expected probability curves with confidence limits of 5% and 95% were plotted.

Table 4.13 Statistical analysis using Log-Pearson Type III distribution

Percent chance exceedance	**T, Return Period in years**	**Expected probability Rainfall depth in mm**	**Confidence limits Rainfall depth in mm**	
			0.05	**0.95**
0.2	500	307.84	406.59	229.7
0.5	200	271.85	350.54	207.94
1.0	100	245.33	310.44	191.41
2.0	50	219.31	271.9	174.69
5.0	20	185.36	222.92	152.07
10.0	10	159.63	187.77	134.17
20.0	5	133.11	153.4	114.69

50.0	2	94.01	106.37	83.06
80.0	1.25	66.33	77.28	57.74
90.0	1.11	54.83	66.19	47.11
95.0	1.05	47.57	58.34	39.66
99.0	1.01	35.18	46.51	28.53

Table 4.13 shows the expected probability rainfall depth with confidence limits using Log Pearson Type III distribution. 159.63, 185.36, 219.31, 245.33, 271.85 and 307.84 were the estimated probability rainfall depths for 10, 20, 50, 100,200 and 500 year return periods, respectively. The design precipitation values obtained from the Log Pearson type III probability plots were used to determine the rainfall intensities for the 10, 20, 50, 100, 200 and 500 year return period over 24 hours rainfall duration.

4.4 MODELLING BY FREQUENCY STORM METHOD IN HEC-HMS

The HEC-HMS model was simulated for rainfall intensities of 10, 20, 50, 100,200 and 500 year return period storms utilizing the input from HEC-GeoHMS and some addition from the HEC-HMS.

Table 4.14 Design precipitation depths as a function of return periods

Return Period(Year)	10	20	50	100	200	500
Rainfall Depth(mm) for 24 hr duration	159.63	185.36	219.31	245.33	271.85	307.84
Rainfall Intensity (mm/hr)	6.65	7.72	9.13	10.22	11.32	12.82

Table 4.15 Design precipitation depths for different durations for different return periods

Duration (Min)	Depth (mm)	Depth (mm)	Depth (mm)	Depth (mm)	Depth (mm)	Depth (mm)
	10 Yr	20 Yr	50 Yr	100 Yr	200 Yr	500 Yr
5	0.55	0.64	0.76	0.85	0.94	1.06
15	1.66	1.93	2.28	2.55	2.83	3.20
60	6.65	7.72	9.13	10.22	11.32	12.82
120	13.30	15.44	18.27	20.44	22.65	25.65
180	19.95	23.17	27.41	30.66	33.98	38.48
360	39.90	46.34	54.82	61.33	67.96	76.96
720	79.81	92.68	109.65	122.66	135.92	153.92
1440	159.63	185.36	219.31	245.33	271.85	307.84

4.4.1. Simulation runs for different return period storms

The model may produce and generate values for a variety of flow conditions (return periods). The flow values are calculated based on the above input parameters. According to the results in table 4.16, the minimum peak flow for the Chalakudy river basin occurred for a 10 year return period for a 24 hour storm duration, while the maximum was obtained for the same duration with a 500 year frequency storm. The minimum and maximum flood value being 1173.2 m^3/s and 2732.5 m^3/s for 10 year and 500 year frequency respectively.

Table 4.16 Simulated flood magnitude values for different return periods

Return period (year)	**Flood Magnitude (m^3/s)**
10	1173.2
20	1415.6
50	1742.8
100	1985.3
200	2335.9
500	2732.5

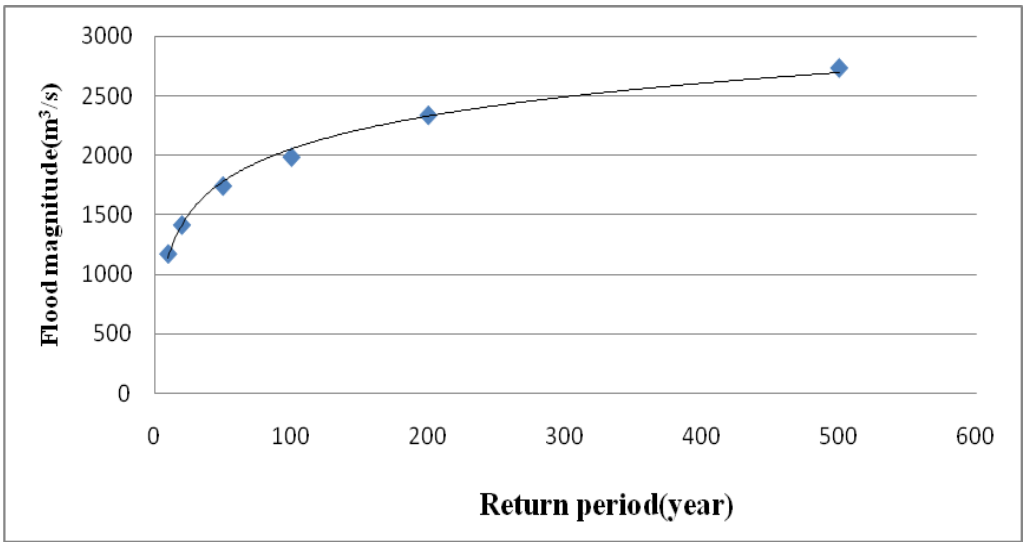

Fig. 4.23 Relationship between flood magnitude and Return period

4.5 FLOOD FREQUENCY ANALYSIS USING HEC-SSP

Flood frequency analysis is an estimation of how often a certain amount of flow is occurring. Such a estimation is pre-requisite for carrying out hydraulic computation of river and developing water surface profiles. A frequency analysis was also conducted in order to compare the flood values for different return period storms obtained from HEC-HMS simulations. The study was carried out by fitting a probability distribution to a sample of yearly severe flood values collected for the Chalakudy river basin over a lengthy period of time. The developed model parameters can then be utilised to forecast severe occurrences with a large recurrence interval. Frequency analysis was achieved using the HEC-SSP software for examination of the statistical distribution and functions.

4.5.1 General frequency analysis editor

To avoid any errors, the yearly maximum discharge data for 28 years (1990-2017) was entered into the HEC-SSP software. The probability distribution was generated using maximum discharge data as input using the software's general frequency analysis editor option. With the use of the Weibull plotting position method, data was plotted on a probability scale. This was then followed by

computing the expected probability discharge using distribution functions of Log-Pearson Type III, Gumbel and Log Normal distributions.

The minimum and maximum discharge values were found to be 204.220 m^3/s and 1880.741 m^3/s, respectively, in 28 years of stream flow data. The measures of central tendency *i.e*, mean, median, and mode, were computed as 712.326 m^3/s, 639.895 m^3/s, and 204.221 m^3/s, respectively. The skewness or asymmetry of the probability distribution of a variable with respect to the mean was computed as 1.488. Sharpness of the central peak relative to a standard bell curve termed as the kurtosis value was calculated as 2.830. This showed that the distribution has shorter and thinner tails than the normal distribution. Besides, the peak is lower and also broader than the normal distribution.

4.5.1.1 *Log- Pearson Type III distribution*

'Log transformation' option was enabled in the Log- Pearson Type III distribution for the analysis. The following findings were obtained using the Weibull plotting position method and the Log Pearson type III distribution, as shown in Table 4.17. The estimated probability discharge for various percent chance exceedance values are depicted in the results. It was discovered that there was only a 0.2 percent probability that the discharge value would be 2812.8 m^3/s and that there was a 99 percent chance that the discharge value would be 139.6 m^3/s. Among the various discharge values, the discharge value of 99 percent chance exceedance has the highest possibility of occurrence. However, discharge values of percent possibility exceedance larger than 1% are commonly chosen for design purposes, and this varies depending on the type of hydraulic structure to be built.

Table 4.17 Statistical analysis using Log-Pearson Type III distribution

Percent chance exceedance	**Computed curve discharge based on sample statistics in m^3/s**	**Expected probability discharge in m^3/s**	**Confidence limits discharge in m^3/s**	
			0.05	**0.95**
0.2	2524.6	2812.8	4369.4	1510.8
0.5	2186.6	2380.0	3432.1	1413.1
1.0	1941.7	2032.0	2843.2	1328.4
2.0	1705.2	1744.8	2339.9	1232.1
5.0	1402.9	1408.8	1780.5	1084.5
10.0	1179.2	1175.7	1431.7	952.9
20.0	955.2	958.9	1128.5	797.5
50.0	637.7	639.3	745.8	543.6
80.0	425.1	421.1	508.7	359.0
90.0	343.7	330.1	425.1	282.0
95.0	288.3	284.6	371.9	225.8
99.0	207.2	139.6	302.1	140.7

Fig. 4.24 shows a frequency analytical plot based on the Log Pearson type III distribution. The discharge values are for likelihood of occurrence in the range of 0.9999 to 0.0001 on the plot. Expected probability curves with confidence limits of 5% and 95% were plotted. The graphs also showed the curves of computed and observed occurrences.

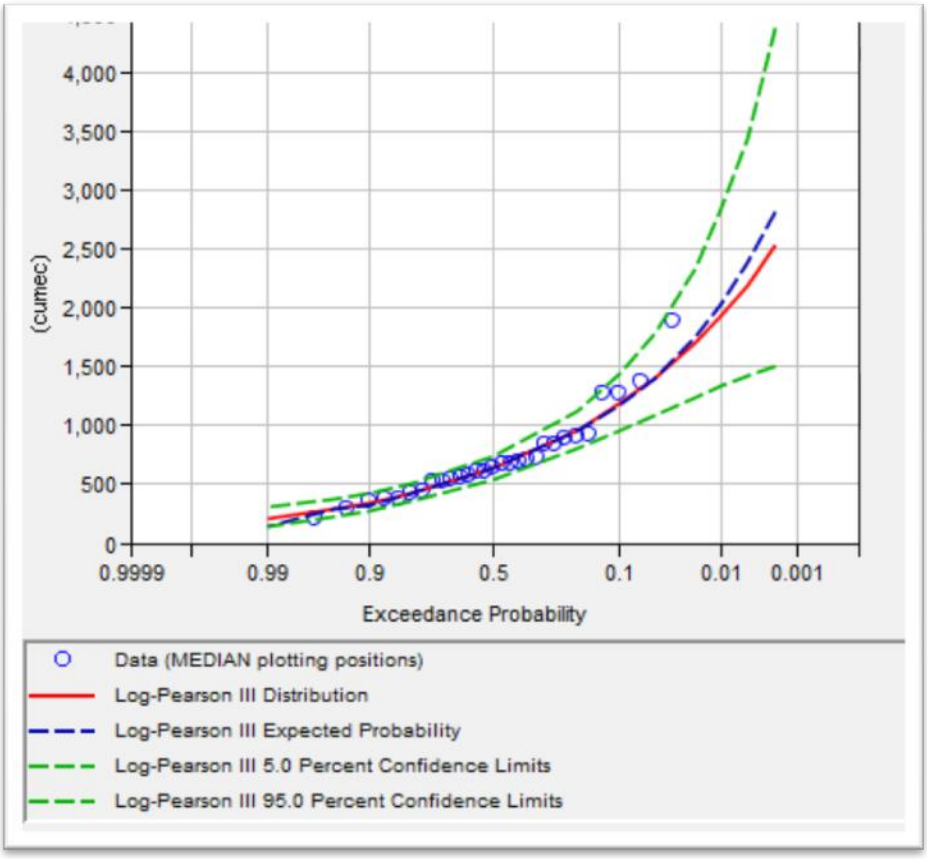

Fig. 4.24 General frequency analytical plot of Log-Pearson type III distribution

4.5.1.2 *Gumbel distribution*

Discharge values of Gumbel probability distribution differ mainly with respect to their parameters, such as location and scale. Location indicates the mean or average of the distribution and scale indicates the standard deviation or variability.

Table 4.18 shows the expected probability discharge with confidence limits using Gumbel probability distribution. 1741.8 m^3/s, 950.9 m^3/s and 638.2 m^3/s were the estimated probability discharges for 2, 20 and 50 percent annual chance of exceedance, respectively. With a confidence limit of 0.05 and 0.95, an estimated probability discharge of 2701.5 m^3/s was recorded for a 0.2 percent chance of exceedance. The probability discharge was found to be 179 m^3/s with a 99 percent chance of exceedance. The discharges with the confidence limits of 0.05 and 0.95 were discovered in the range of 279.7 m^3/s to 156.3 m^3/s.

Table 4.18 Expected probability discharge using Gumbel distribution

Percent Chance Exceedance	Median curve discharge (m^3/s)	Expected probability discharge (m^3/s)	Confidence limits discharge (m^3/s)	
			0.05	0.95
0.2	2543.3	2701.5	3551.7	1793.0
0.5	2199.1	2304.0	2982.3	1595.3
1.0	1950.4	2024.2	2590.7	1448.8
2.0	1710.7	1741.8	2214.5	1303.3
5.0	1405.3	1412.9	1755.1	1109.6
10.0	1180.0	1174.6	1433.8	959.0
20.0	955.0	950.9	1129.4	800.2
50.0	637.1	638.2	739.4	548.8
80.0	425.0	426.3	506.9	357.9
90.0	343.9	341.0	422.7	281.7
95.0	288.8	275.8	364.8	230.1
99.0	208.1	179.0	279.7	156.3

Fig. 4.25 shows a Gumbel plot that includes both the cumulative distribution function (CDF) and a plotting position histogram with the predicted probability. The annual peaks were highlighted by blue circular dots on the plot, according to the probability assigned to them by the Weibull method. The Gumbel Theoretical Distribution Curve' was represented by the red line. The percent likelihood exceedance calculated in this investigation was helpful in determining the flow return period. This helps in the selection of flood design value while constructing flood-control structures.

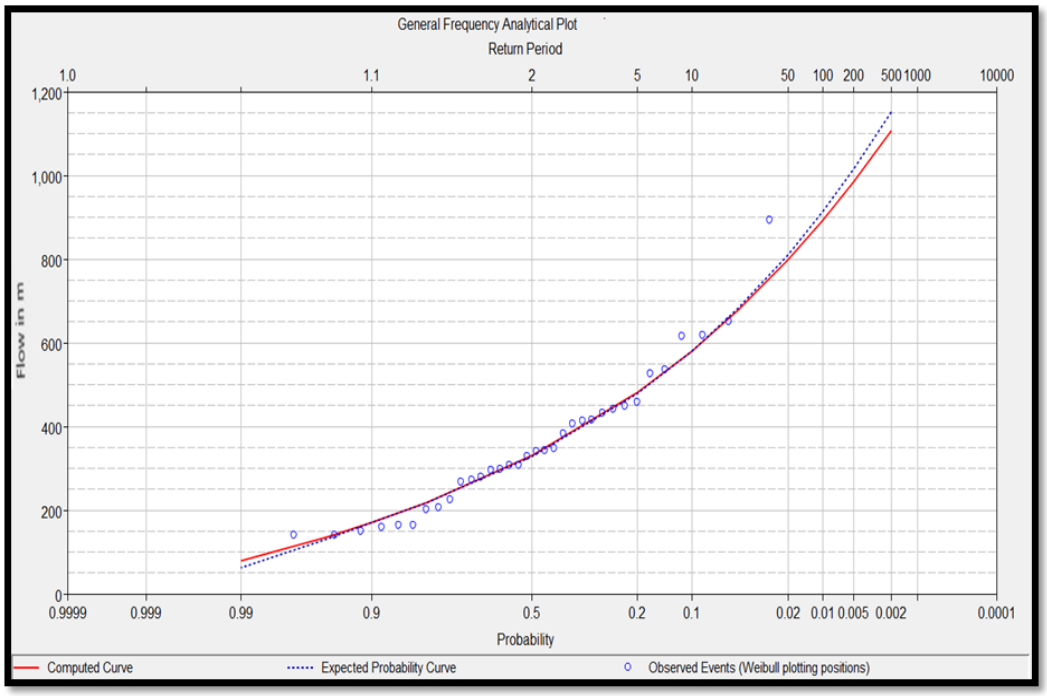

Fig. 4.25 Gumbel plot of flood frequency analysis

4.5.1.3 *Log Normal distribution*

Discharge values of Log normal probability distribution differ mainly with respect to their parameters, such as location and scale.

Table 4.19 shows the expected probability discharge with confidence limits using the Log Normal distribution. 1753.1 m^3/s, 950.3 m^3/s, and 637.4 m^3/s were the expected probability discharges for 2, 20, and 50% chance exceedance, respectively. With a confidence limit of 0.05 and 0.95, an expected probability discharge of 2753.0 m^3/s was measured for a 0.2 percent chance exceedance. The discharge confidence limit was found to be between 3550.7 m^3/s and 1792.1 m^3/s. The probability discharge was found to be 279.4 m^3/s with a 99 percent chance exceedance. The discharges with the confidence limits of 0.05 and 0.95 were found in the range of 279.4 m^3/s and 156.7 m^3/s.

Table 4.19 Expected probability discharge using Log Normal distribution

Percent Chance Exceedance	Median curve discharge (m^3/s)	Expected probability discharge (m^3/s)	Confidence limits discharge (m^3/s)	
			0.05	0.95
0.2	2543.3	2753.0	3550.7	1792.1
0.5	2199.1	2342.0	2982.3	1596.4
1.0	1950.4	1999.6	2589.5	1450.1
2.0	1710.7	1753.1	2217.1	1304.7
5.0	1405.3	1429.5	1759.2	1110.4
10.0	1180.0	1183.8	1438.6	959.9
20.0	955.0	950.3	1134.5	800.8
50.0	637.1	637.4	738.2	549.5
80.0	425.0	423.2	507.2	358.3
90.0	343.9	343.0	422.1	282.3
95.0	288.8	276.1	365.2	230.4
99.0	208.1	178.7	279.4	156.7

Fig.4.26 shows a log Normal distribution plot that includes the annual peaks occupying their positions were highlighted by blue circular dots on the plot, according to the probability assigned to them by the 'Weibull method.' The Log Normal 'Theoretical Distribution Curve' was represented by the red line. The percent likelihood exceedance calculated in this investigation was helpful in determining the flow return period. This helps in the selection of flood design while constructing flood-control structures.

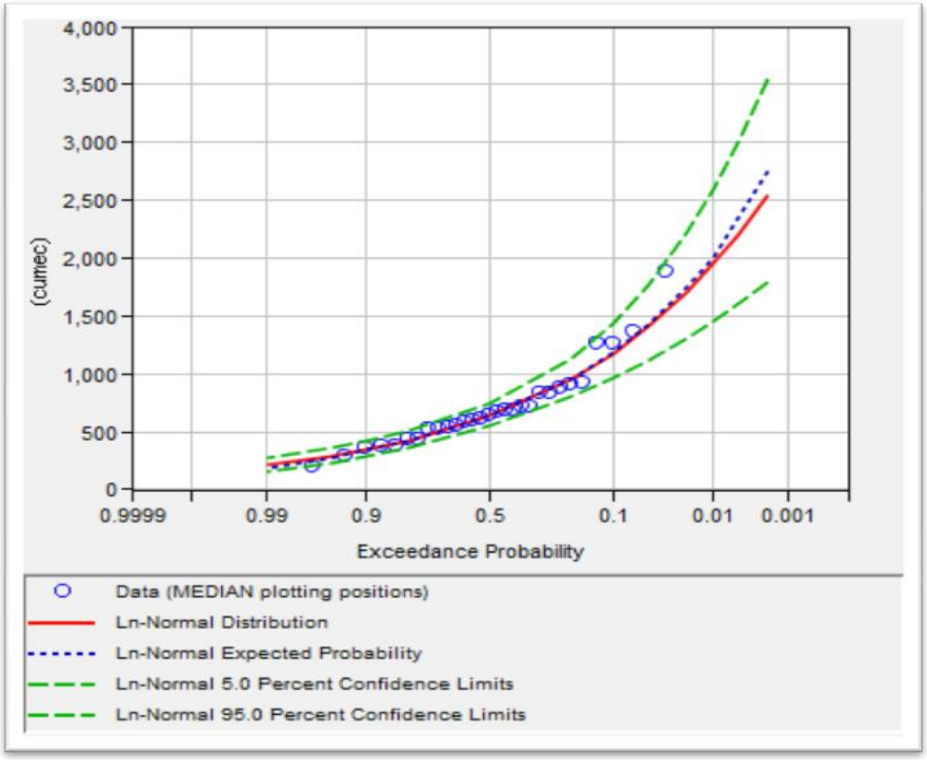

Fig. 4.26 Log Normal distribution plot of flood frequency analysis

The parameters of the fitted probability distribution functions of Log-Pearson III, Gumbel and Log Normal distribution for the annual discharge is shown in Table 4.20. The parameters of Log Pearson III were shape, scale and location while the parameters for Gumbel were scale and location.

Table 4.20 Parameters of the fitted probability distribution of annual discharge

Sl. No	Distribution	Parameters
1.	Log-Pearson III	α=-0.010 β=0.210 γ=2.804
2.	Gumbel	σ =549.53 μ=282.030
3.	Log Normal distribution	σ =361.72 μ=712.33

4.5.2 Goodness of Fit Test

Goodness of fit test ensures the reliability of Log Pearson type III, Gumbel and Log Normal distributions to represent the sample. The goodness of fit summary statistics using Chi-Square test and Kolmogorov Smirnov test are shown in Table 4.21.

Table 4.21 Goodness of fit test statistics

Sl. No.	**Type of Distribution**	**Test statistics**	
		Standard Product Moments	
		Chi – Square	Kolmogorov-Smirnov
1.	Log-Pearson III	0.094	2.312
2	Gumbel	0.087	2.706
3.	Log Normal distribution	0.096	2.552
Table value		0.23	47.4

The statistical table value for Chi-Square and Kolmogorov-Smirnov test were obtained as 0.23 and 47.4 respectively. The computed value, also called as the test statistic values, obtained for Chi-Square and Kolmogorov-Smirnov tests were found less than that of the statistical table value. Therefore, by statistical theory, the hypothesis was accepted and it indicated the best fit of both distributions for the sub basin (Thomas and Mark, 2015).

4.5.3 Expected probability discharge of Log Pearson Type III, Gumbel and Log Normal distributions

The results obtained as expected probability flood peak values from Log – Pearson Type III, Gumbel and Log Normal distributions are shown in Table 4.22. The expected probability flood peak value shown by Log–Pearson type III distribution were 1175.7 m^3/s, 1408.8 m^3/s, 1744.8 m^3/s, 2032 m^3/s, 2380 m^3/s and

2812.8 for the return periods 10, 20, 50, 100, 200 and 500 year respectively. Slightly lesser flood peak values were got using Gumbel and Log Normal distributions for the same return periods. Design flood peak values for the required return periods can be used further for matching with HEC-HMS flood peak values.

Table 4.22 Expected discharge values of Gumbel, Log –Pearson type III and Log Normal distributions

Percent Chance Exceedance	**T, Return Period in year**	**Expected probability discharge in m^3/s**		
		Log Pearson III	**Gumbel**	**Log Normal**
0.2	500	2812.8	2701.5	2753.0
0.5	200	2380.0	2304.0	2342.0
1.0	100	2032.0	2024.2	1999.6
2.0	50	1744.8	1741.8	1753.1
5.0	20	1408.8	1412.9	1429.5
10.0	10	1175.7	1174.6	1183.8
20.0	5	958.9	950.9	950.3
50.0	2	639.3	638.2	637.4
80.0	1.25	421.1	426.3	423.2
90.0	1.11	330.1	341.0	343.0
95.0	1.05	284.6	275.8	276.1
99.0	1.01	139.6	179.0	178.7

4.6 COMPARISON BETWEEN LOG–PEARSON TYPE III, GUMBEL AND LOG NORMAL DISTRIBUTIONS VERSUS HEC-HMS MODEL PREDICTED VALUES

Finally, the HEC-HMS model result was compared with the frequency analysis results obtained from different frequency distributions. The methodologies used in this study were chosen for their effectiveness and simplicity. The correlation with the simulated flow data of the Chalakudy river basin, however, is the most important requirement. For return periods of 10, 20, 50, 100, 200 and 500, the Log Pearson type-III method had the best correlation with model predicted flood peak values. Muhammad Shahzad *et al., (*2016) conducted a study on the application of HEC-RAS model to the development of floodplain maps for the part of Kabul river that lies in Pakistan. He did a work on conventional flood frequency analysis for calculating extreme flows with different return periods involving Log-Normal, Gumbel, and Log-Pearson type III (LP3) distributions. He reported that the LP3 was found to be the best distribution for the Kabul river using Kolmogorov–Smirnov (KS) test. Abera (2011) made a study on flood mapping and modelling on Fogera flood plain of Ribb river. He used the hydrologic model HEC-HMS calibrated for hourly time series data for return periods of 2, 10, 50 and 100 years. He derived frequency discharge values involving Normal, Gumbel, Log-Pearson type-III (LP3) extreme value distributions. The LP3 distribution using the hourly data was the best comparable with HEC-HMS results. The result of hydrologic model by HEC-HMS gives discharge values of 91.8 m^3/s, 202.4 m^3/s, 273.1 m^3/s, and 308.4 m^3/s for return periods of 2, 10, 50 and 100 respectively. Frequency discharge values derived using LP3 distribution showed high similarity with the HEC-HMS derived values. The other three distributions gave values that were much lower than the result from HEC-HMS. The above two authors reported that LP3 distribution was giving good similarity with HEC-HMS results.

In this study also results show that LP3 was giving good similarity with HEC-HMS discharge values. This analysis was conducted to verify that LP3 discharge

values directly could be used as input into HEC-RAS model instead of using HEC-HMS discharge values.

Table 4.23 Comparison between model predicted and flood peak values from frequency distributions

Method	$Q_t(m^3/s)$					
	10	**20**	**50**	**100**	**200**	**500**
Log Pearson III	1175.7	1408.8	1744.8	2032	2380	2812.8
Gumbel	1186.5	1418	1755.2	2026.5	2317.8	2769.1
Log Normal	1183.8	1429.5	1753.1	1999.6	2342	2753
HEC-HMS	1173.2	1415.6	1742.8	1985.3	2335.9	2732.5

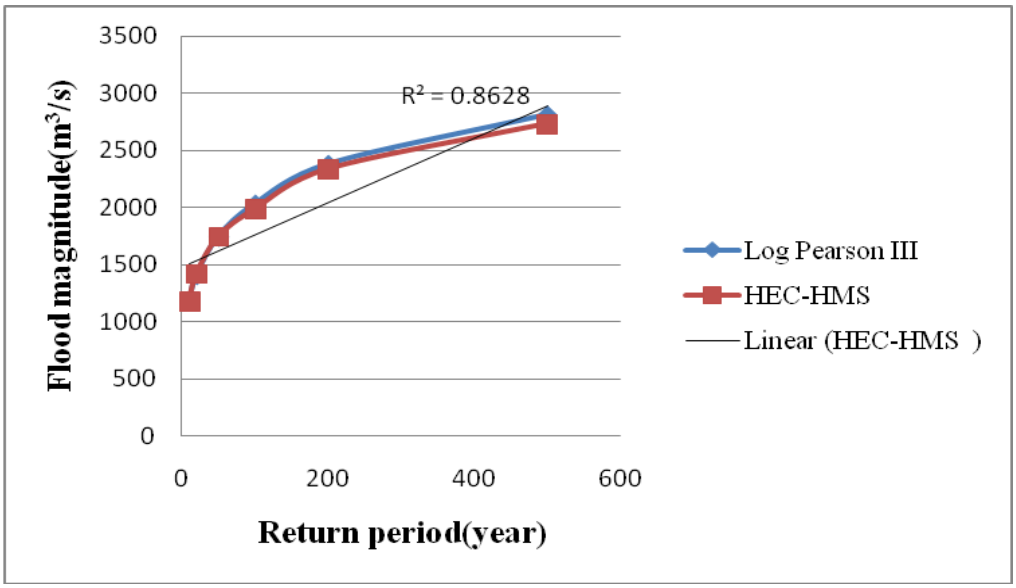

Fig. 4.27 Scatter plot of flow values of HEC-HMS versus Log Pearson III method

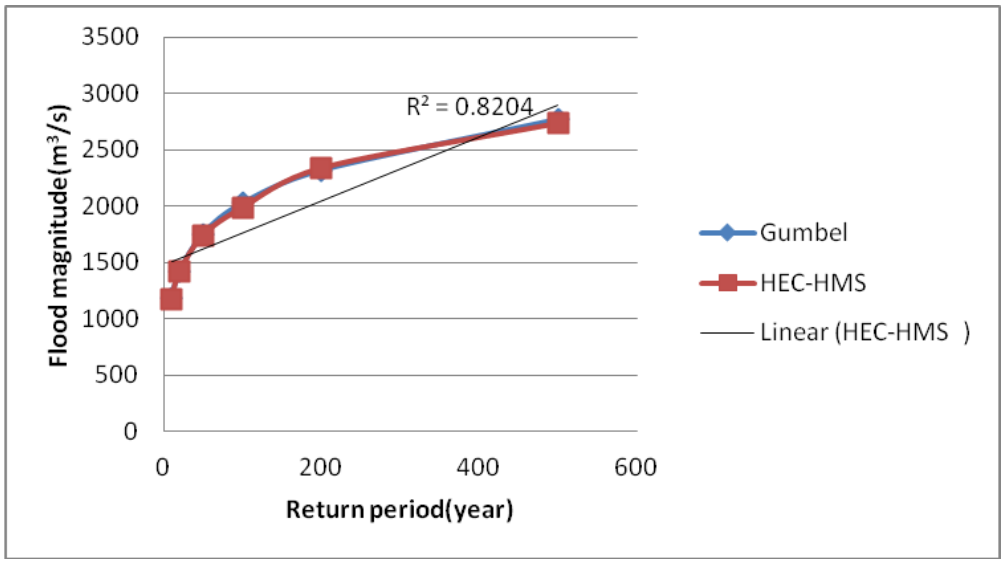

Fig. 4.28 Scatter plot of flow values of HEC-HMS versus Gumbel

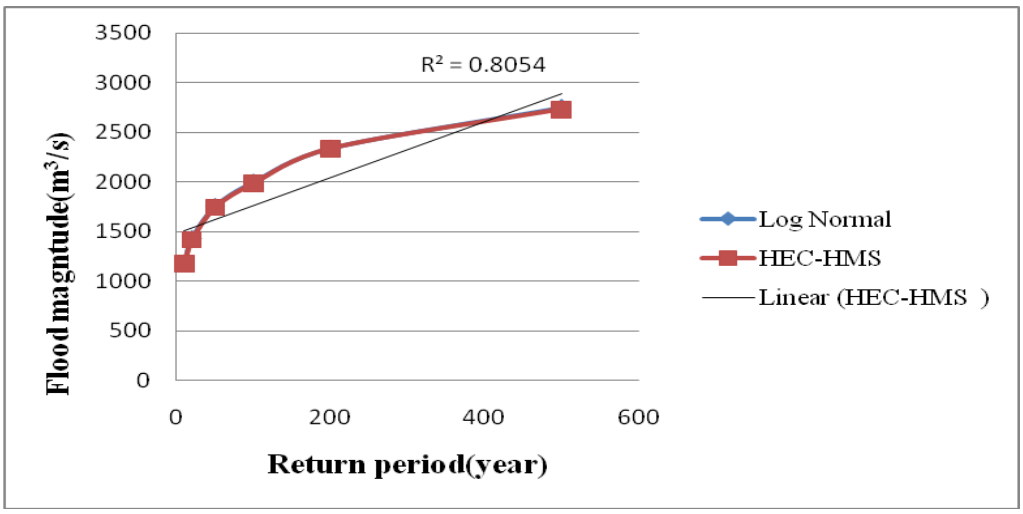

Fig. 4.29 Scatter plot of flow values of HEC-HMS versus Log Normal method

The frequency discharge value derived using Log Pearson type-III show high similarity to the HEC-HMS with higher correlation coefficient (R^2) value of 0.8628 as shown in Fig. 4.27. The other two methods give results lower than the values obtained using the HEC-HMS as shown in Fig. 4.28 and 4.29. In most flood studies,

either the model result or that found by the frequency analysis may be taken based on different considerations.

But in this study area, frequent washing and sedimentation of the channel has its effect on the gauge recording of the river. Because of the deviation in gauge readings caused by sedimentation and human error, the river's historical data is less reliable. The HEC-HMS result is considered as a good representative of discharge scenarios for flood mapping studies on and around the area for the aforementioned and other minor situations.

HEC-HMS model was already calibrated and validated for the river basin. The model simulation runs have also given good correlation between observed and simulated flows. In this study, even though the LP3 distribution gave similar results as the model predicted values, the HMS model output discharge values for different return periods were used for flood mapping using HEC-RAS.

4.7 MODELLING USING HEC-RAS

HEC-RAS is a one-dimensional steady flow hydraulic model for channel flow study and floodplain determination used extensively by hydraulic engineers. The results of the model can be used in floodplain management and insurance investigations. The conditions of steady flow are those in which a channel's depth and velocity do not alter over time. Minor fluctuations in water depth and velocity from cross-section to cross-section characterise gradually variable flow. The direct step approach is the principal method used by HEC-RAS to compute water surface profiles. It assumes a steady, gradually varied flow situation.

4.7.1 Geometric data development for Chalakudy river

The RAS Mapper window in the HEC-RAS software was used to input a projection file that was freely available on the ESRI website for geospatial projection coordinates. To produce geometry for flood mapping, run the GIS file via terrain data. To give stream centre line, bank line, flow line, and cross section line, the geometry was preserved as river name.

1. ***Stream center line:*** The river is characterized by the stream centerline.

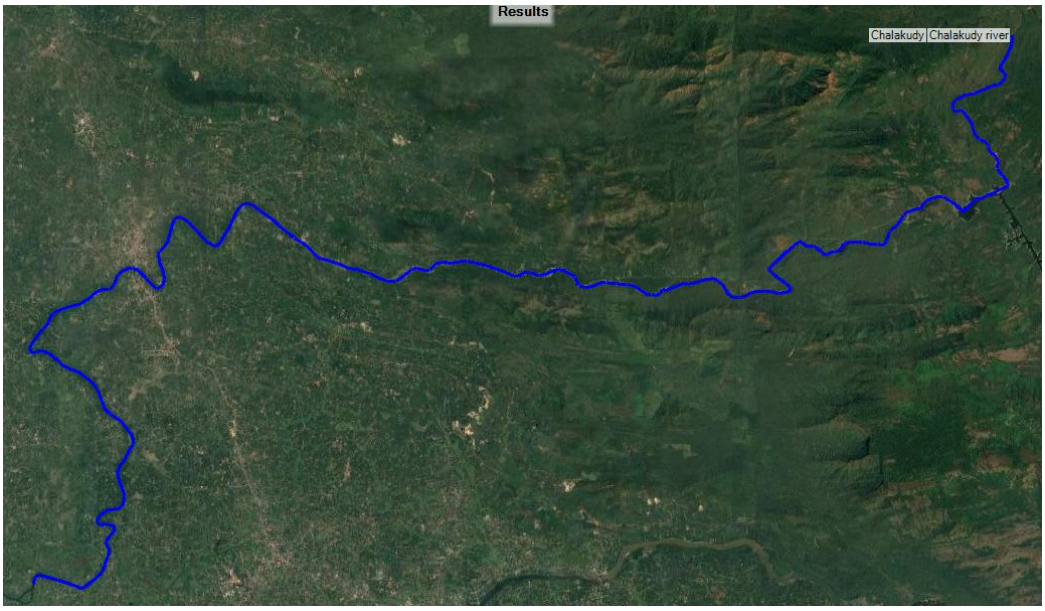

Fig.4.30 River centre line as viewed in RAS Mapper

2. ***Main Channel Bank***:

The primary stream line is separated from the left bank or right bank of the floodplain lands within which the stream is contained by main channel bank lines.

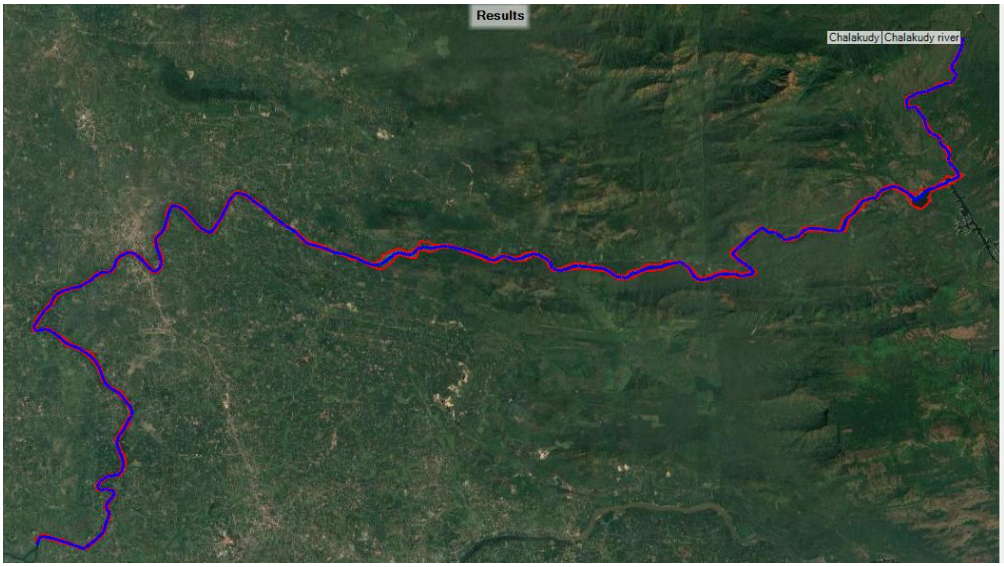

Fig.4.31 River bank lines as viewed in RAS Mapper

3. ***Flow path center line:***

It is the stream way to define flow from upstream to downstream. Flow path lines are indicated in white colour in Fig.4.32

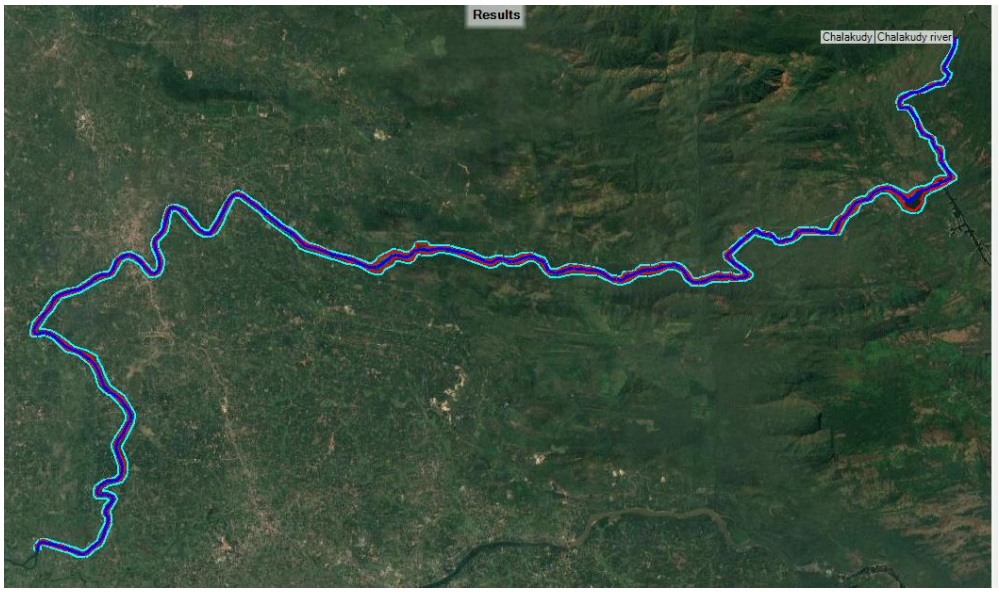

Fig.4.32 Flow path lines as viewed in RAS Mapper

4. ***Cross section cutline:***

Cross sections are located at the interval along a stream to characterize the flow carrying capability of the stream and its adjacent floodplain. The general approach to laying out cross sections is to ensure that the cross sections are perpendicular to flow lines. In the Fig. 4.33, the blue colour indicates the "Stream centerline", red colour indicates the "Main channel bank line", yellow colour indicates the "Flow path" of the Chalakudy river from upstream to downstream. Upstream region cross section is indicated as station no.75600 and downstream region station is indicated as 600. The number of cross sections is 119. The length and spacing of cross sections is 1600 m and 600 m. Final geometry data is opened in main window of HEC-RAS geometry for model execution.

Fig.4.33 Geometry data as viewed in RAS Mapper

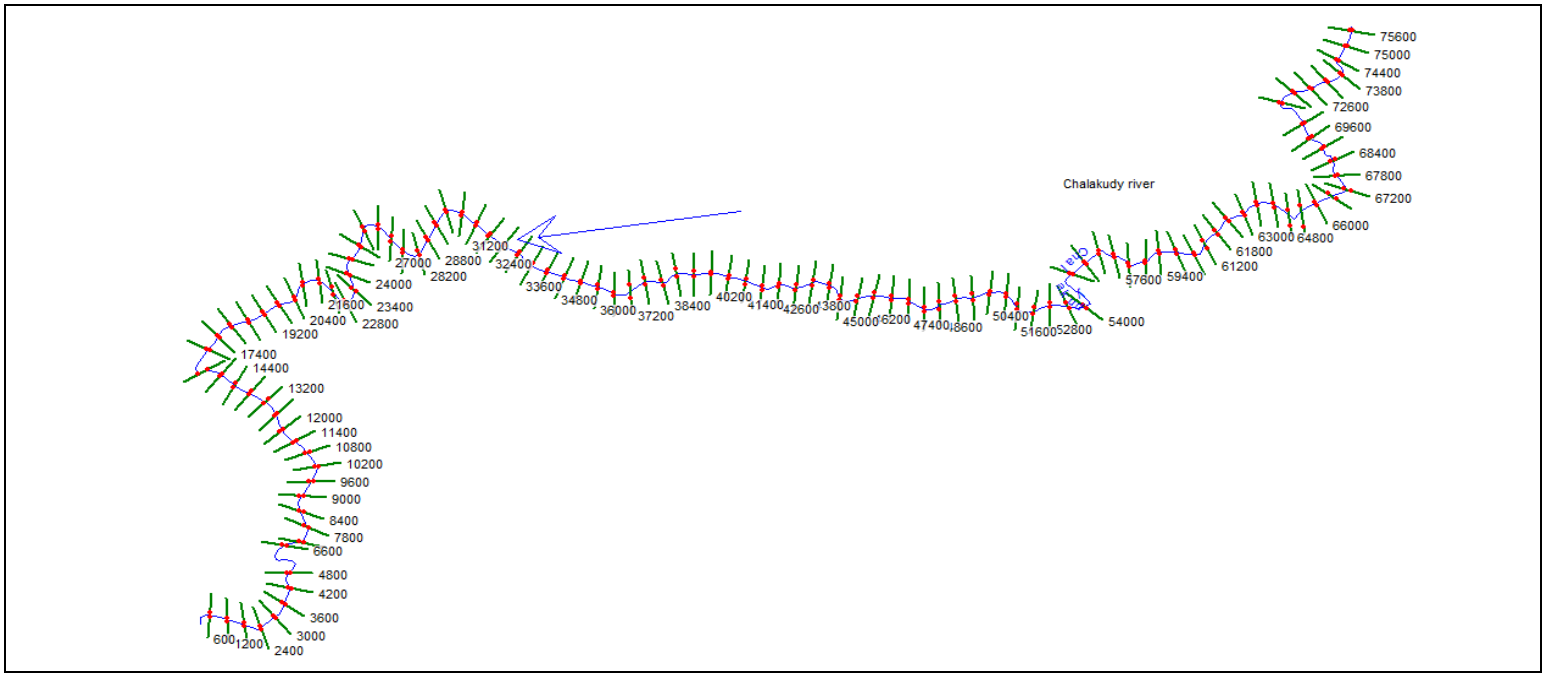

Fig.4.34 Geometry data as viewed in HEC-RAS

4.7.2 Flood inundation mapping in RAS Mapper

The elevation of the floodplain will determine whether the water surface profiles obtained for different return period floods will inundate it. The water surface must be overlaid on the topography to obtain the actual water depth in the river channel and floodplain. RAS Mapper can be used to achieve this.

RAS Mapper can be opened from the main HEC-RAS window. In the data layer window (left pane), we will notice that there are new layers under the results group called steady flow (or whatever name you gave to your plan when running the steady flow analysis). There are four additional groups under steady flow: geometry, depth, velocity, and WSE. Each layer can be selected by clicking on the respective name in the left pane.

4.7.2.1 *Steady flow analysis*

Using HEC-RAS, steady flow analysis showed discharges of 1173.2, 1415.6, 1742.8, 1985.3, 2335.9 and 2732.5m^3/s, inundating 1882.5, 2022.17, 2195.06, 2310.34, 2470.07 and 2638 ha respectively for different return periods. There was only a slight increase in inundated area as a result of the variations in flow (Fig.4.35).

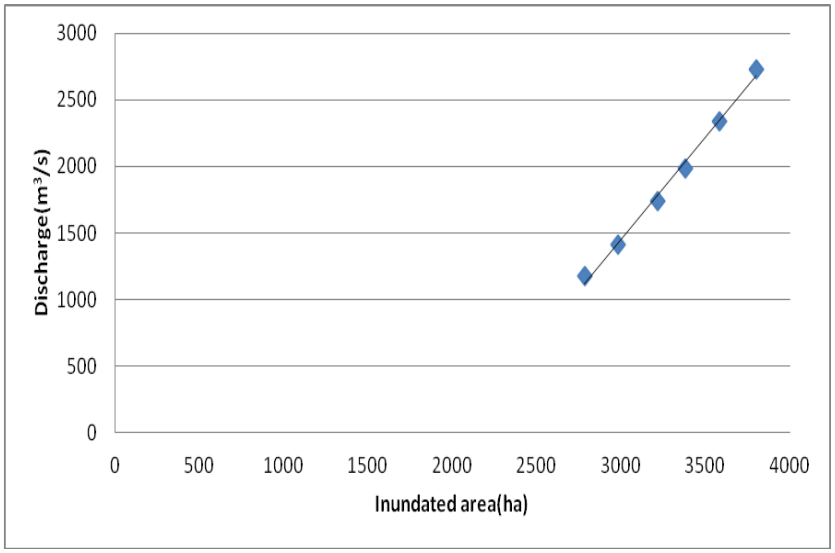

Fig. 4.35 Discharge versus inundated area relationship

4.7.3 Flood inundation maps

Maps are effective tools for displaying the spatial distribution of flood risk. Based on peak discharges simulated in HEC-HMS hydrologic modeling and by using the DEM of the study area, flood hazard maps for 10, 20, 50-, 100-, 200- and 500-year return periods were generated in this study. RAS Mapper was used to visualize the results. Flood maps were created for various return periods. Fig. 4.36- 4.41 displays the extent of water flow along the river during various return periods. As can be seen, the water has overflown the river banks, flooding the barren lands, the forest around the Chalakudy region, agricultural land and some areas where people live. In the following part, the variation of water level in the respective over banks will be analyzed.

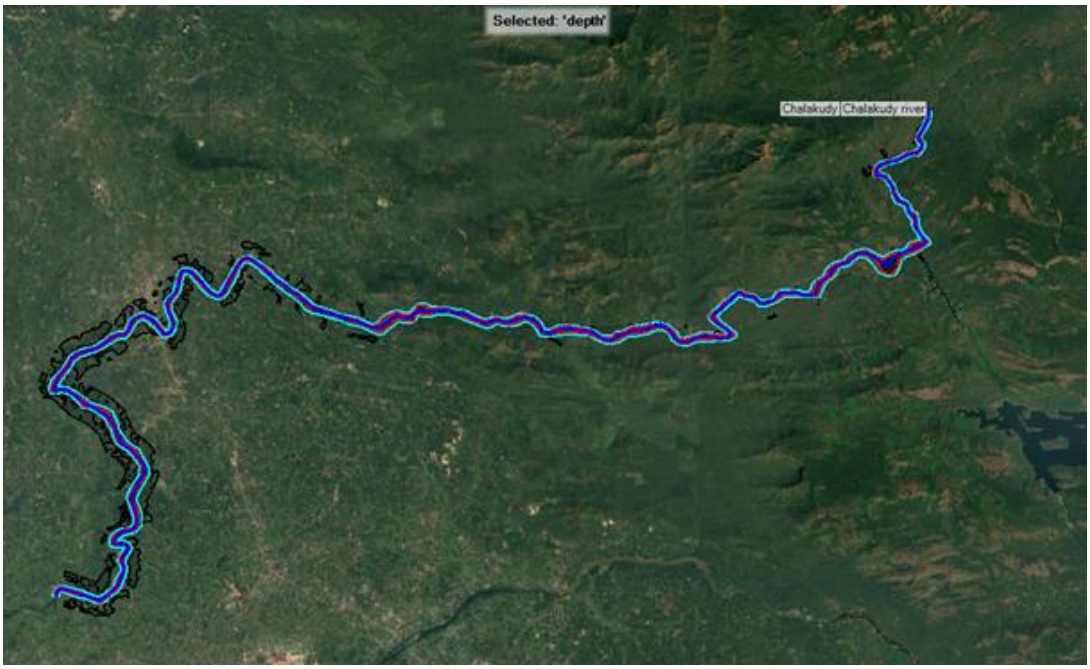

Fig. 4.36 Flood inundation map for 10 year return period as viewed in RAS Mapper

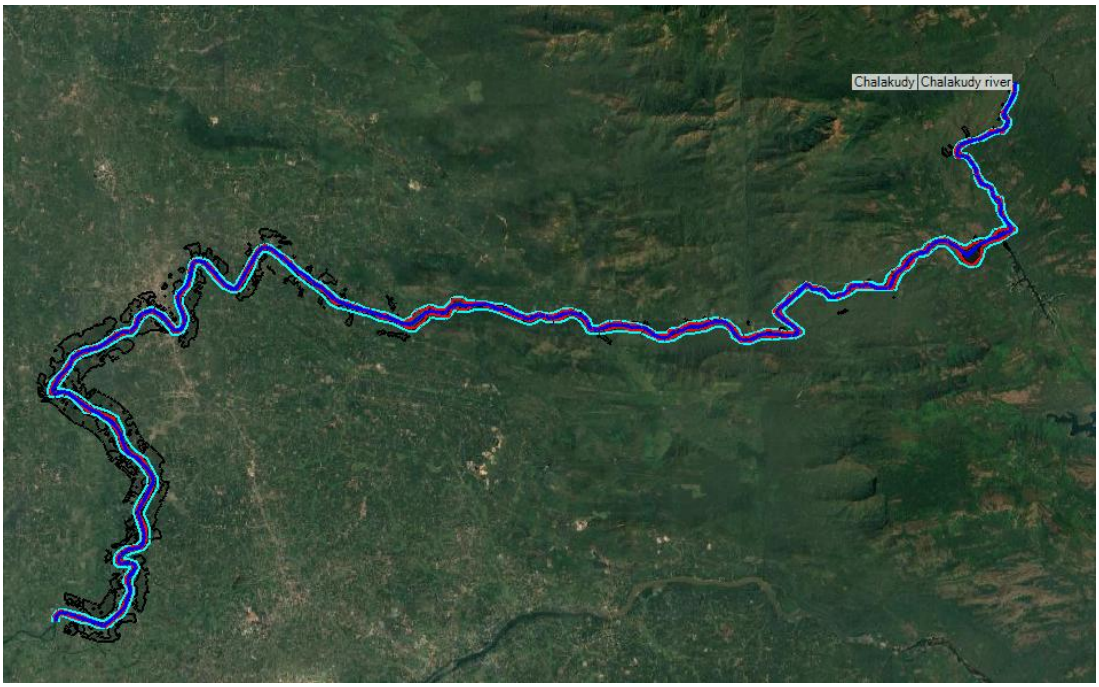

Fig. 4.37 Flood inundation map for 20 year return period view in RAS Mapper

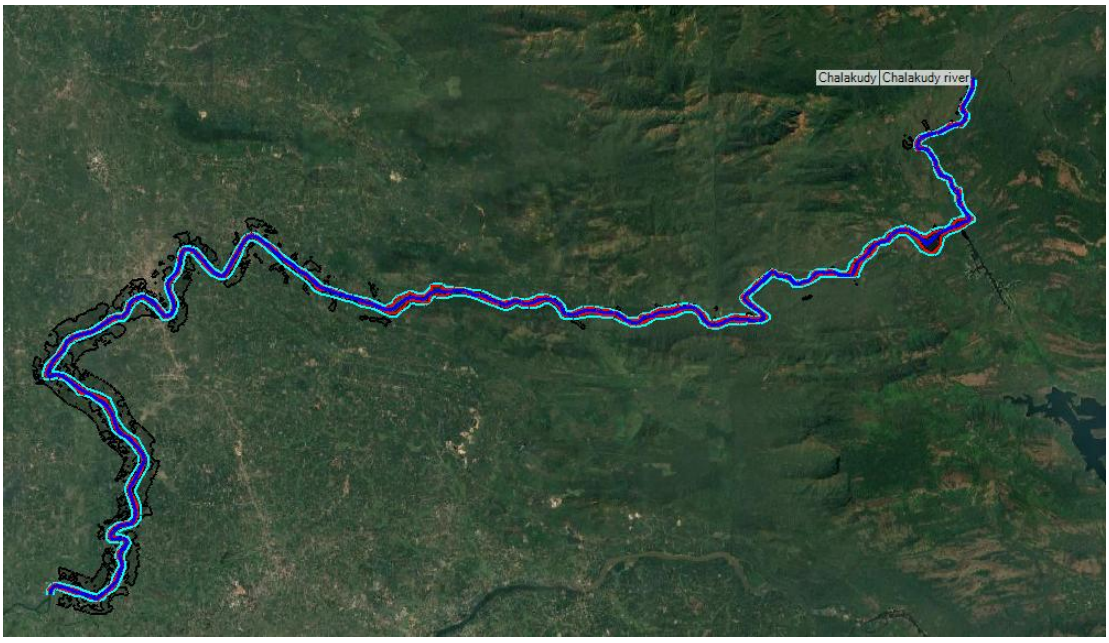

Fig. 4.38 Flood inundation map for 50 year return period view in RAS Mapper

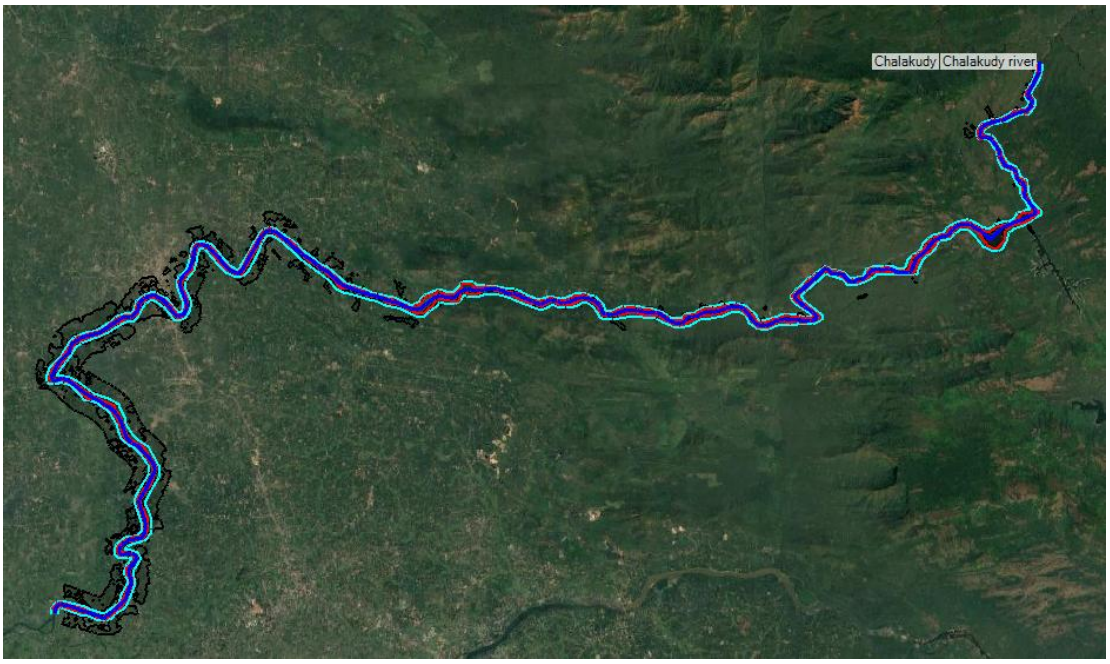

Fig. 4.39 Flood inundation map for 100 year return period view in RAS Mapper

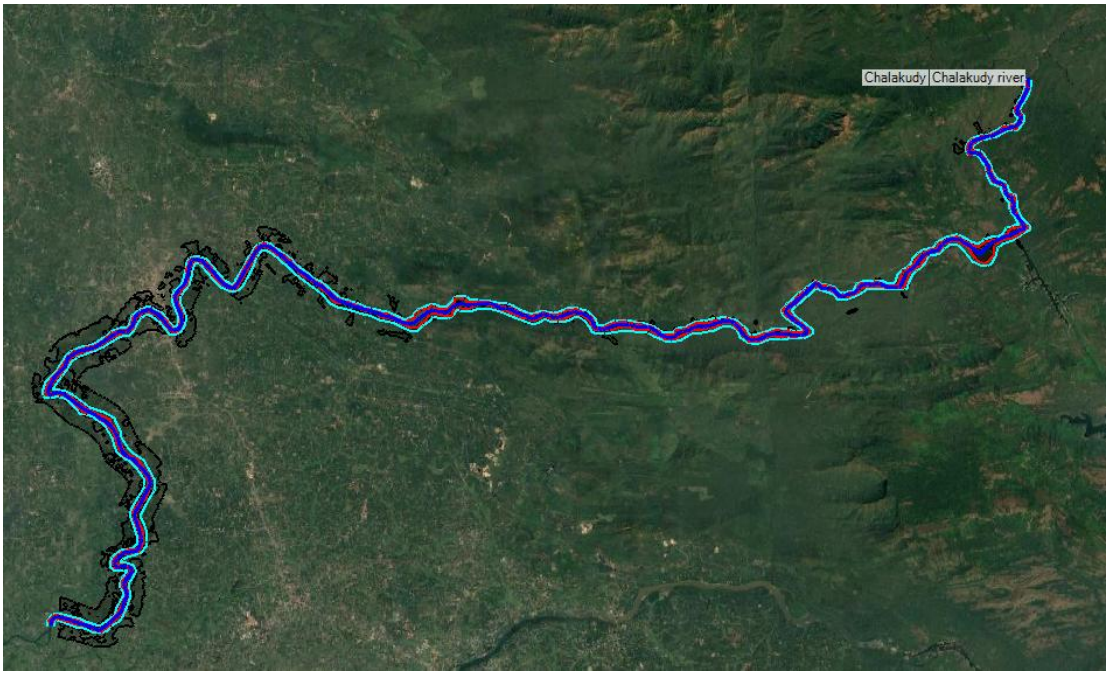

Fig. 4.40 Flood inundation map for 200 year return period view in RAS Mapper

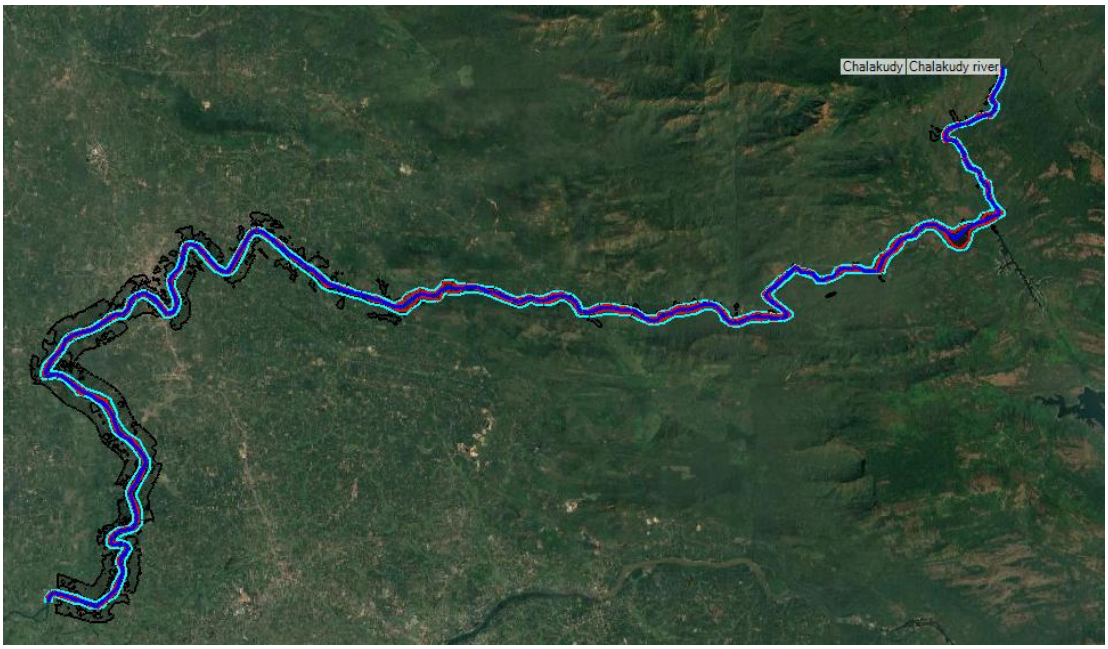

Fig. 4.41 Flood inundation map for 500 year return period view in RAS Mapper

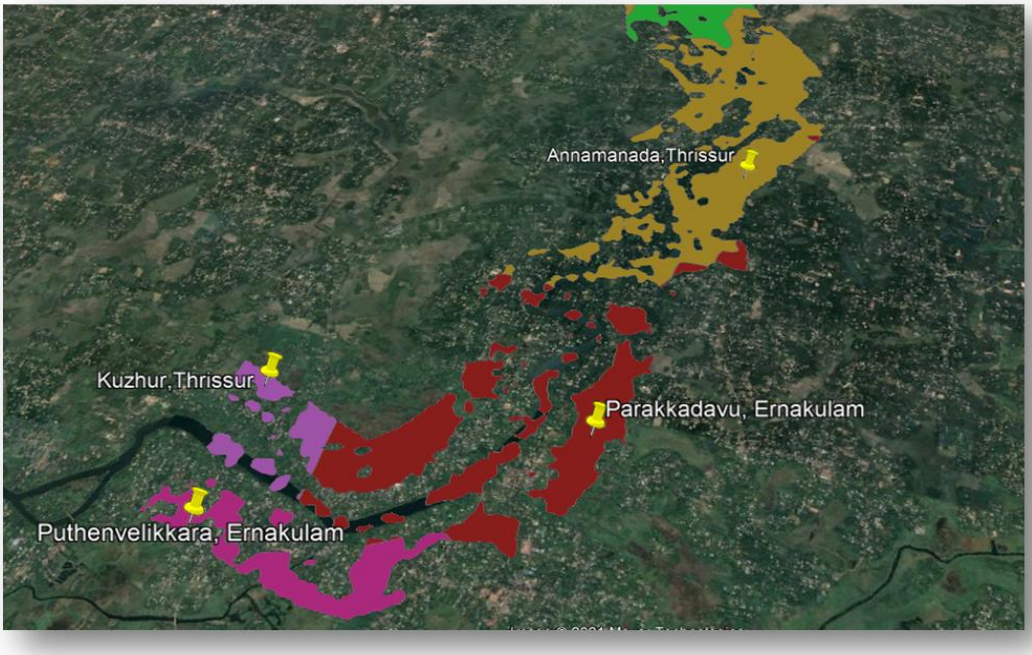

Fig. 4.42 Flood Inundated Panchayaths for 10 year return period in downstream region

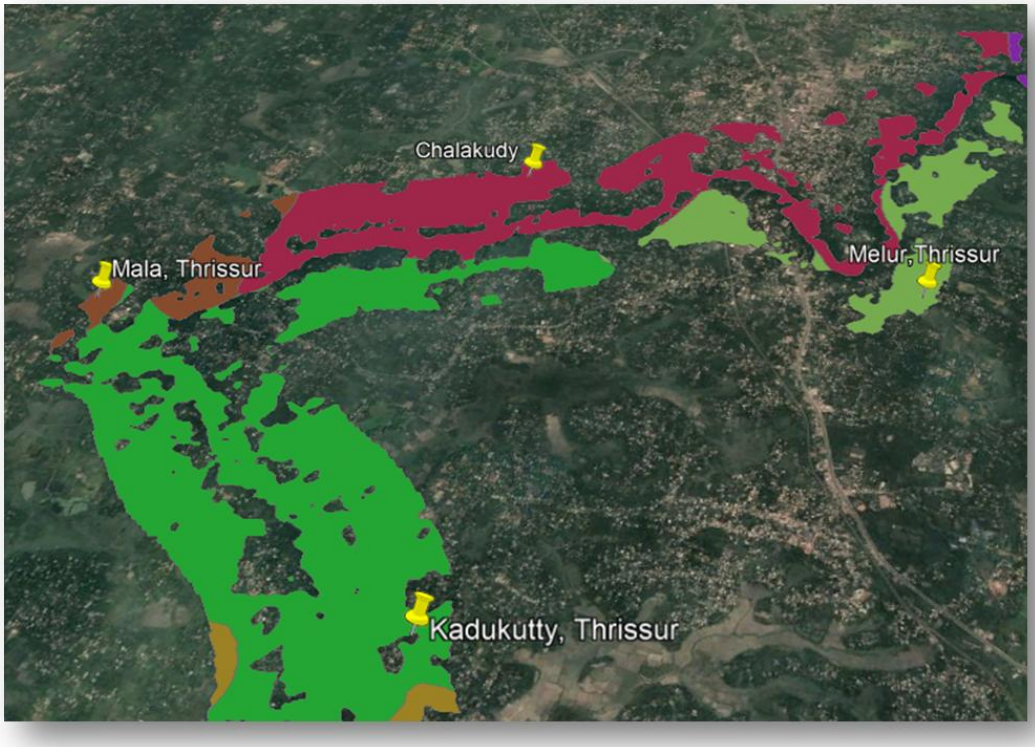

Fig.4.43 Flood Inundated Panchayaths for 10 year return period in middle region

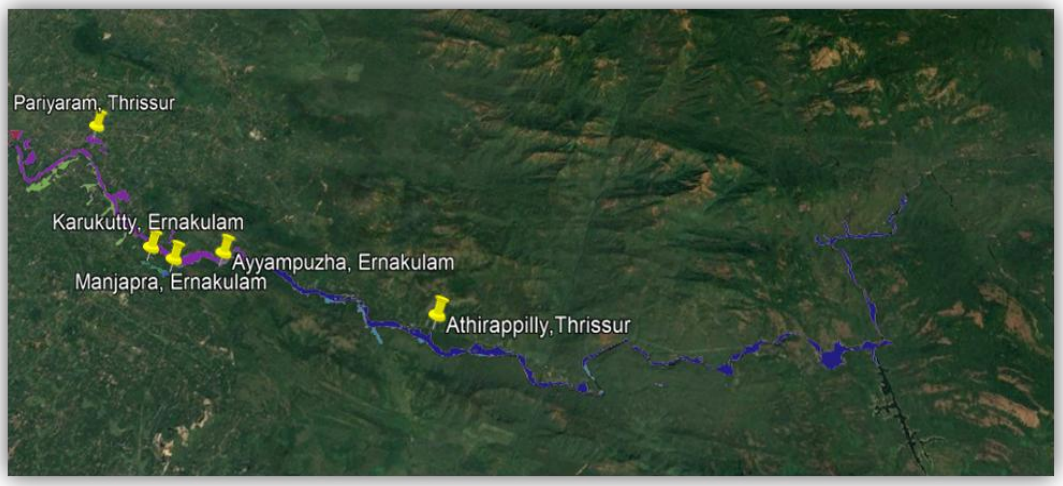

Fig.4.44 Flood Inundated Panchayaths for 10 year return period in upstream region

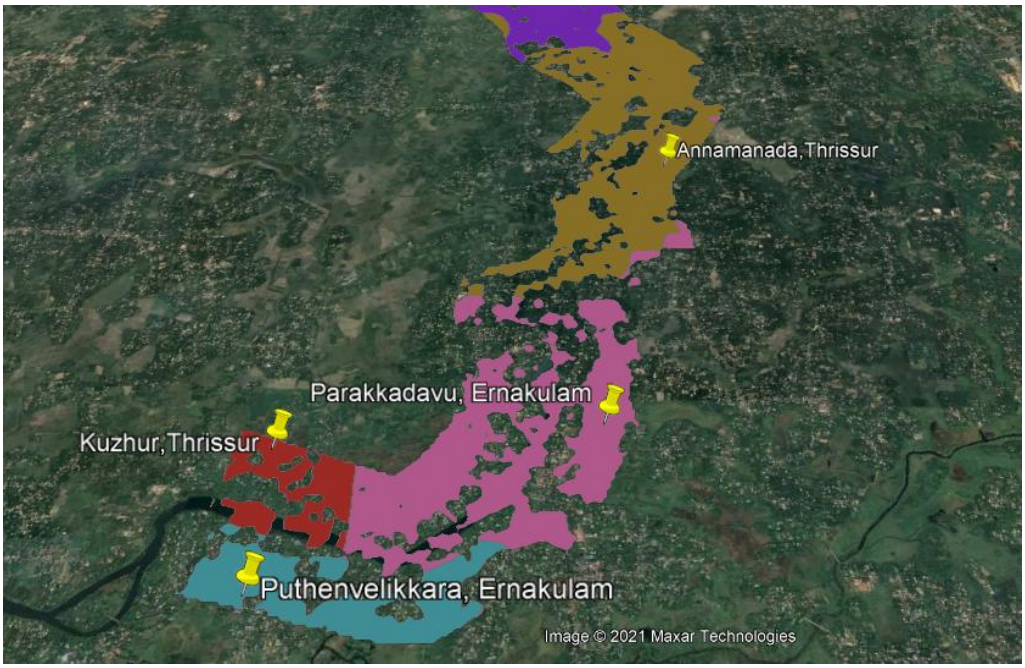

Fig.4.45 Flood Inundated Panchayaths for 200 year return period in downstream region

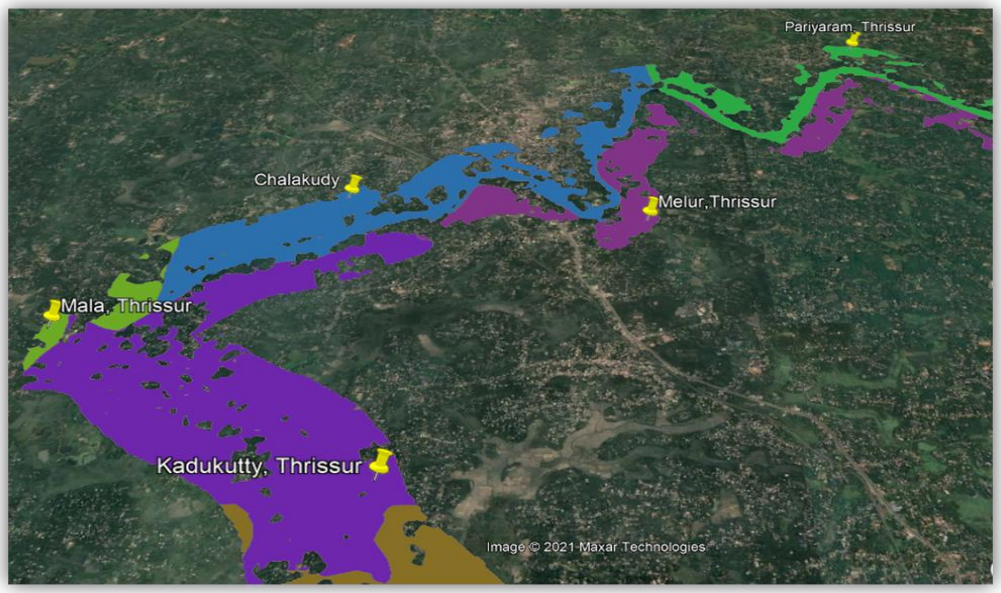

Fig.4.46 Flood Inundated Panchayaths for 200 year return period in middle region

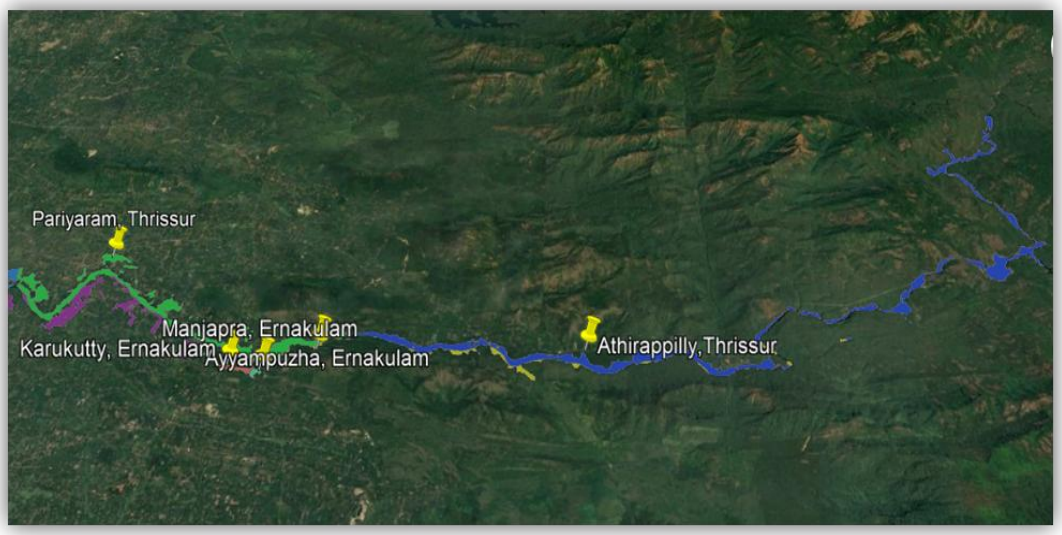

Fig.4.47 Flood Inundated Panchayaths for 200 year return period in upstream region

The above maps (Fig.4.36- 4.47) clearly indicate that flood inundation area increases when return period increases.

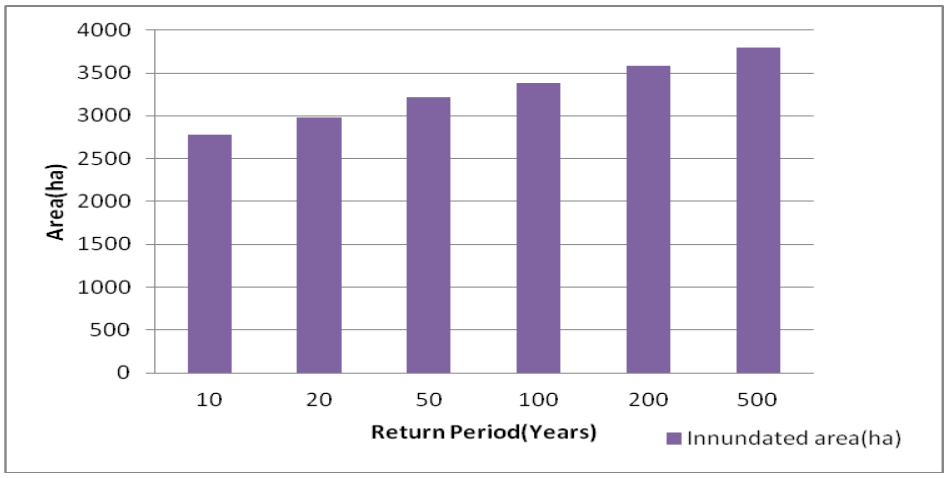

Fig. 4.48 Return period and area inundation relationship

The 500-year return period flood has inundated a total area of around 2,638 ha along the river. Inundated areas were estimated for various scenarios (return periods) and are shown in table 4.23. In general, the total inundated area is less than 3000 ha for all return periods, with vegetation, paddy, and urban areas being the most flooded. Collin *et al*., (2012) studied the river inundation and hazard mapping of Susan river–Kumasi, Ghana. HEC-RAS & Arc-GIS were used as tools for flood analysis. On a topographic map, the flood results were marked. The total flooded area calculated was 2.93 km^2, with a maximum inundation depth of 4.01 m. Khalil *et al*., (2015) made a study on assessment of flood using geospatial techniques for Indus river reach: Chashma – Taunsa. He used HEC-RAS as the hydraulic modelling software. During the 2020 flood, the flood inundated area computed in the model had an excellent agreement with satellite observed data, indicating that the computed flood extents were trustworthy. The simulated flooded area owing to the 2010 flood was calculated to be 1900 km^2, with depths in the research region ranging from 0.15 m to 8.1 m. Bikram (2010) has done studies on hydraulic modelling for flood inundation area of Lothar Khola, Nepal. He found out flood inundated areas for different return periods using HEC-RAS model. It was observed that the flood inundation areas were 230, 240, 247, 250 and 253 ha for 2-year, 10-year, 50-year, 100-year and 200-year return periods respectively. The above three authors have reported that mapping of the flood inundation areas will be helpful for planners for the preparation of evacuation plans in future. In this study also flood inundation areas were mapped to aid the preparation of suitable mitigation measures in the future.

Table 4.24 Panchayath wise inundated areas for different return periods

Name of the Panchayath	10 year flood	20 year flood	50 year flood	100 year flood	200 year flood	500 year flood
	Inundated areas – High (ha)					
Athirappilly,Thrssur	496	524	556	577	605	633
Annamanada,Thrissur	372	399	429	451	478	506
Kadukutty,Thrssur	557	590	627	653	681	707
Chalakudy,Thrissur	373	394	422	440	463	489
Melur,Thrissur	254	277	304	323	348	377
Pariyaram, Thrissur	317	340	364	381	403	435
Parakkadavu, Ernakulam	209	228	257	277	301	326
% High risk area	92.63	92.34	91.95	91.74	91.49	91.37
	Inundated areas – Medium (ha)					
Ayyampuzha, Ernakulam	40	45	52	56	62	67
Mala,Thrissur	48	50	53	55	58	60
Kuzhur,Thrissur	37	43	51	56	62	68
Puthenvelikara, Ernakulam	63	71	82	89	97	104
% Medium risk area	6.75	7.01	7.39	7.57	7.78	7.86
	Inundated areas – less (ha)					
Manjapra,Ernakulam	6	7	7	8	9	10
Karukutty, Ernakulam	11	12	14	15	17	19
%Low risk area	0.61	0.63	0.65	0.68	0.72	0.76
Total	**2783**	**2980**	**3218**	**3381**	**3584**	**3801**

Table 4.24 shows results after superimposing of Cadastral level map of Chalakudy river basin with flooded area polygons obtained from HEC-RAS output for different return periods. The flood inundated areas Panchayath wise were classified into three categories such as high, medium and less inundated. Kadukutty was found to be a high flood inundated area for 10 and 500 year return period with 557 and 707 ha, followed by Athirappilly, Chalakudy, Annamanada, Pariyaram, Melur and

Parakkadavu. Puthenvelikara was found to be medium inundated area for 10 and 500 return periods with 63 and 104 ha followed by Mala, Ayyampuzha and Kuzhur. Karukutty was found to be a less inundated area for 10 and 500 year return period with inundated areas of 11 and 19 ha, followed by Manjapra. The 2018 floods in Chalakudy river basin has also experienced inundation in the same panchayaths as obtained in this study.

4.7.4 Overflow water depth in the banks

Fig.4.43 to 4.48 shows the overflow water depth in the right bank and the left bank for various return periods. The overflow water depth in the banks appear to be higher and it rises in increasing order as the return period increases. The water depth ranges from 0 to 23.5 m with the maximum depth happening along the main channel. The depth of the water, on the other hand, gradually reduces as it expands. When the return period extends, the water depth and flood extent rises.

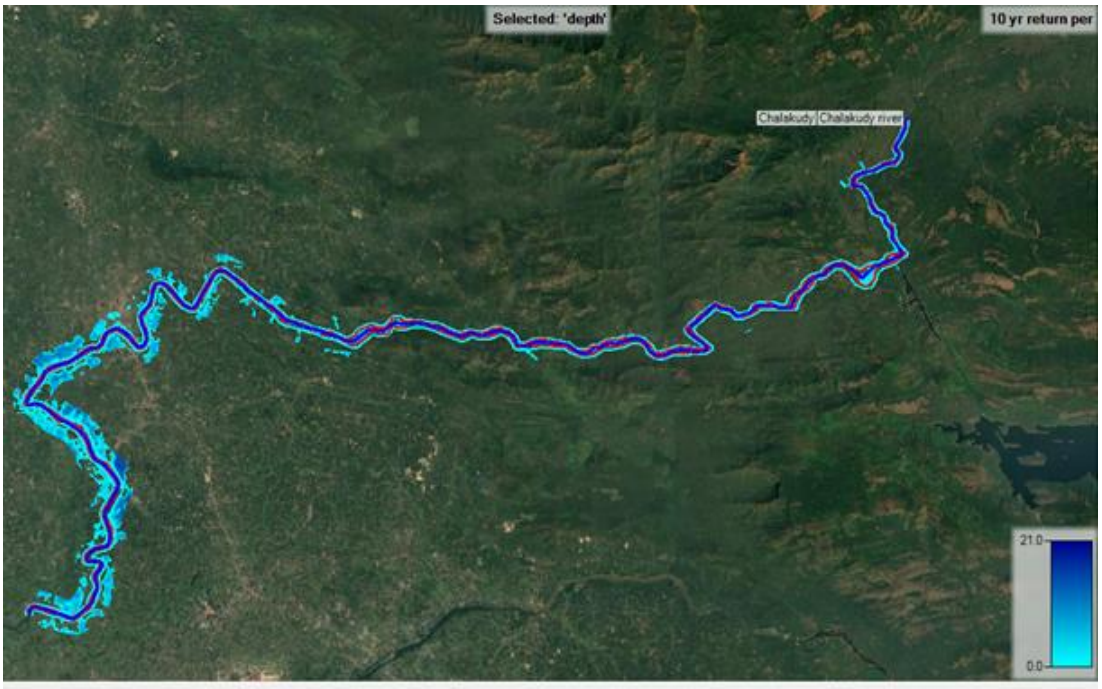

Fig. 4.49 Flood depth map for 10 year return period as viewed in RAS Mapper

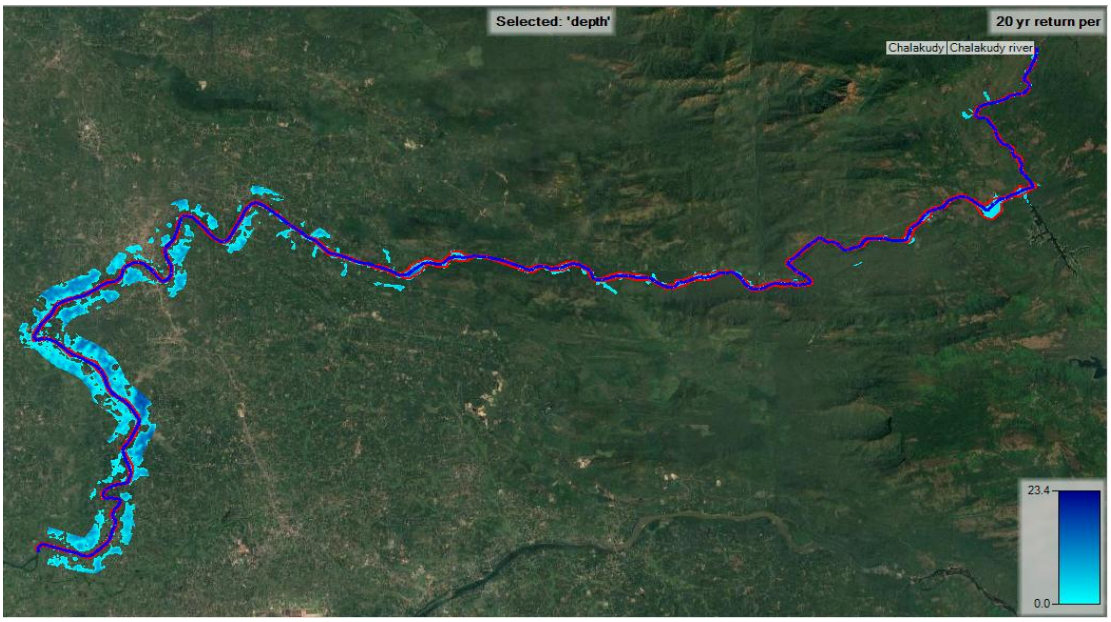

Fig. 4.50 Flood depth map for 20 year return period view in RAS Mapper

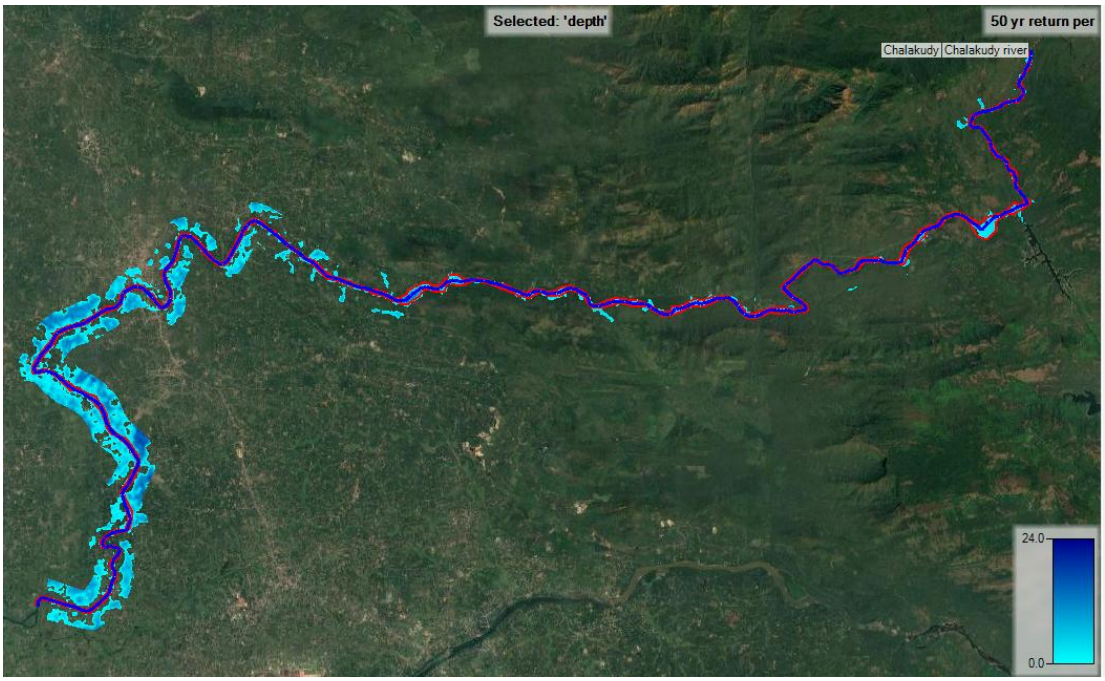

Fig. 4.51 Flood depth map for 50 year return period view in RAS Mapper

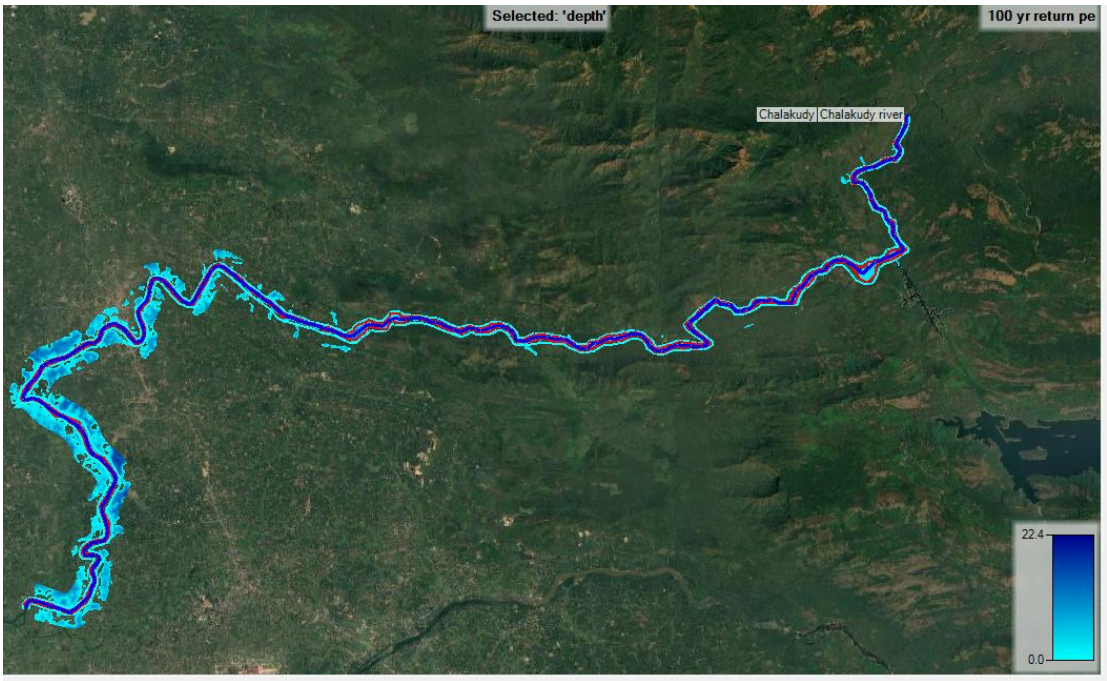

Fig. 4.52 Flood depth map for 100 year return period view in RAS Mapper

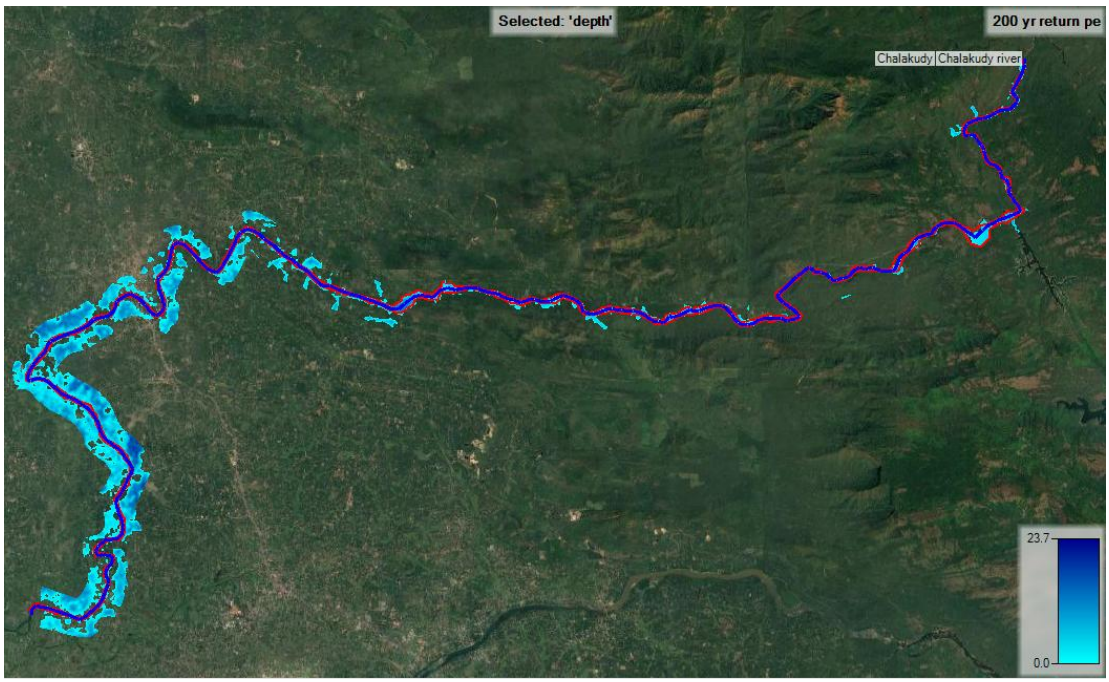

Fig. 4.53 Flood depth map for 200 year return period view in RAS Mapper

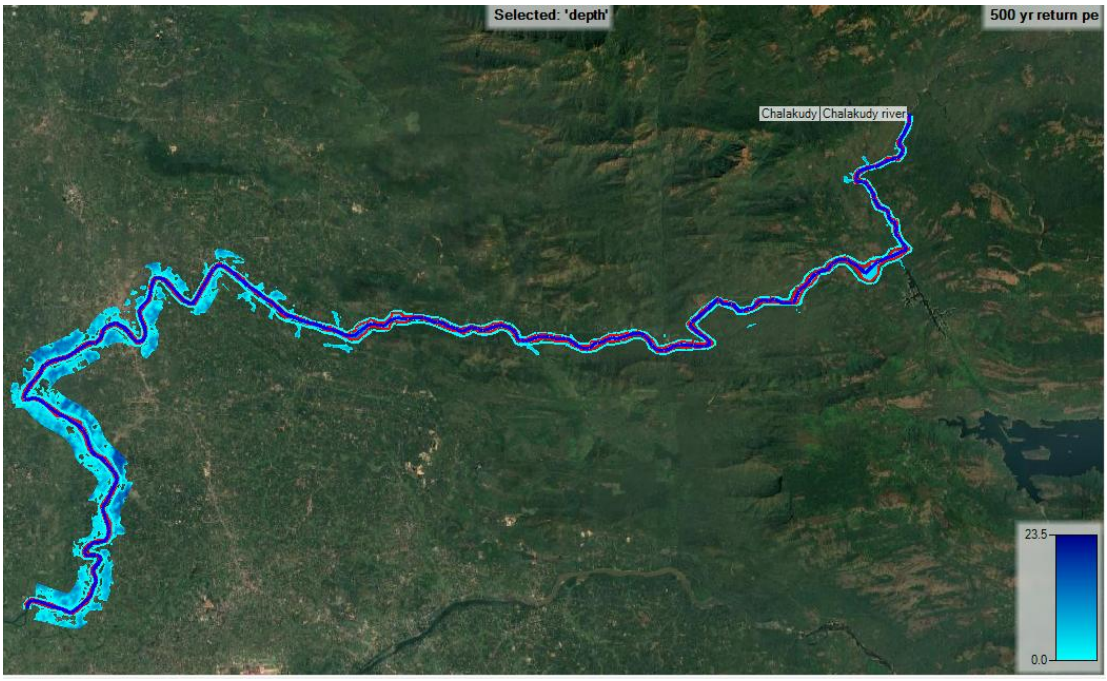

Fig. 4.54 Flood depth map for 500 year return period view in RAS Mapper

Fig. 4.49 - 4.54 shows that the main channel had the highest depth, while the over banks (both left and right) and the main channel had depths ranging from 0 to 21 m for 10 year return period, 0 to 21.4 m for 20 year, 0 to 22 m for 50 year return period 0 to 22.4 m for 100 year, 0 to 23.7m for 200 year and 0 to 23.5 m for the 500 year return period storms.

4.7.5 Flood velocity maps

Despite the fact that maximum water depth is the most significant parameter when analyzing flood hazard, other characteristics such as velocity are also significant because water flows at a scouring velocity during flood events, which can cause damage to channel bed as well as the banks.

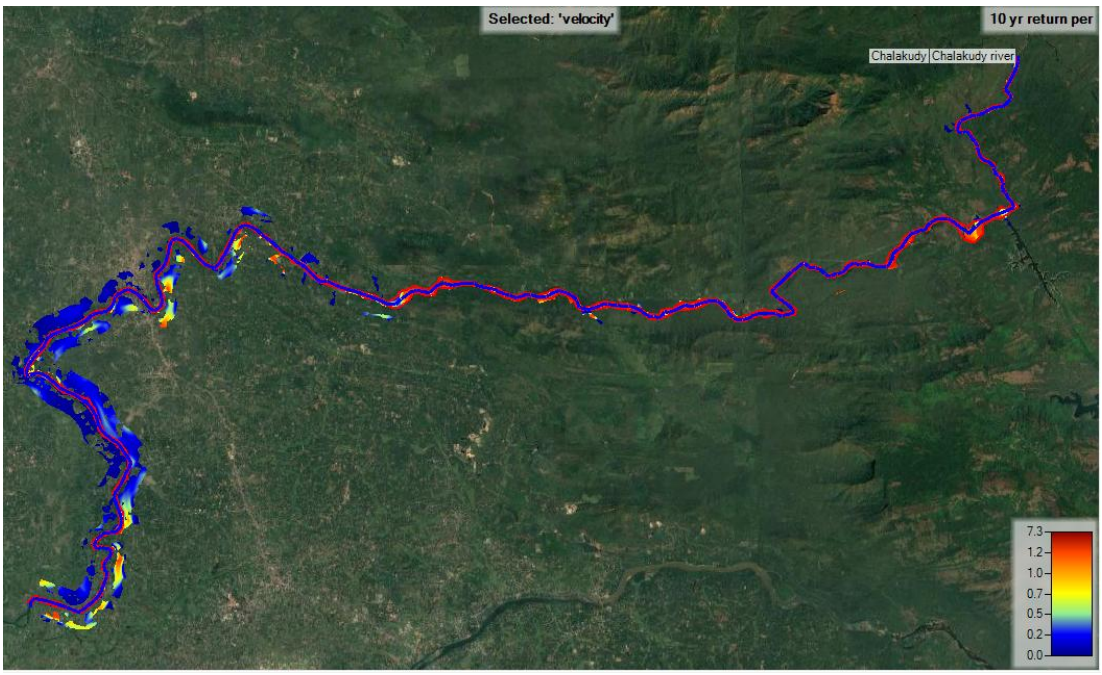

Fig. 4.55 Velocity map for 10 year return period as viewed in RAS Mapper

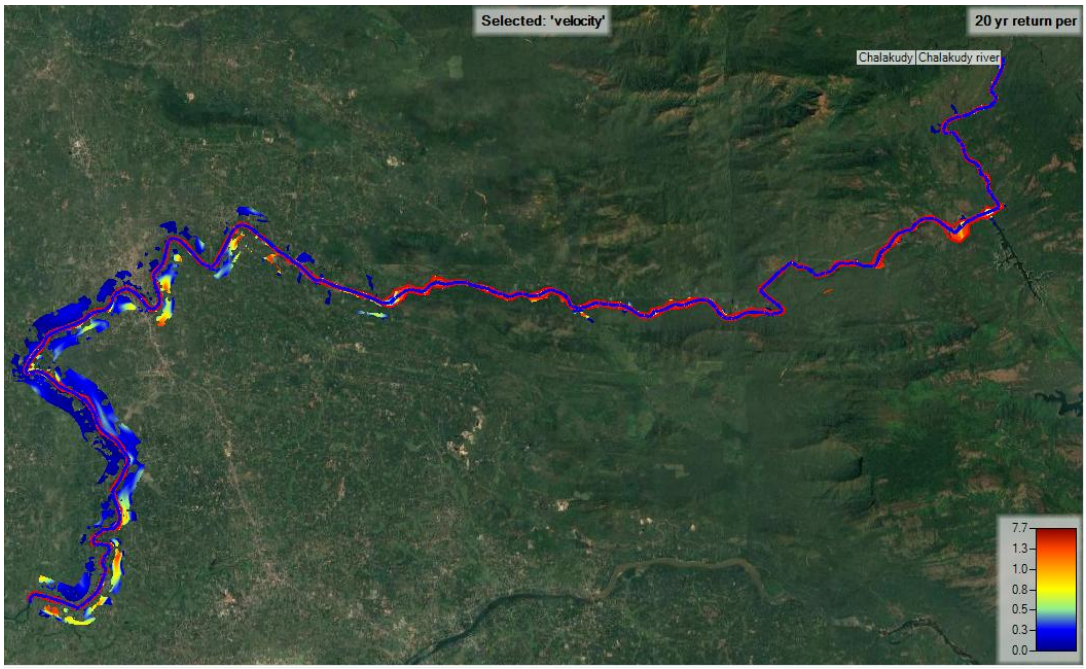

Fig. 4.56 Velocity map for 20 year return period as viewed in RAS Mapper

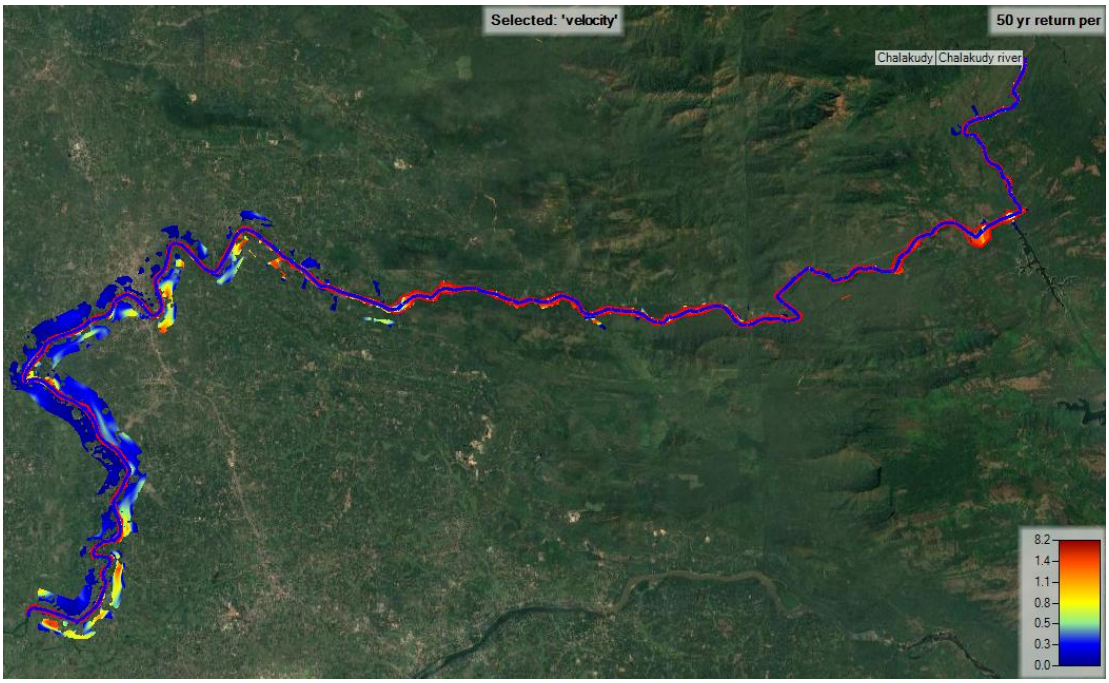

Fig. 4.57 Velocity map for 50 year return period as viewed in RAS Mapper

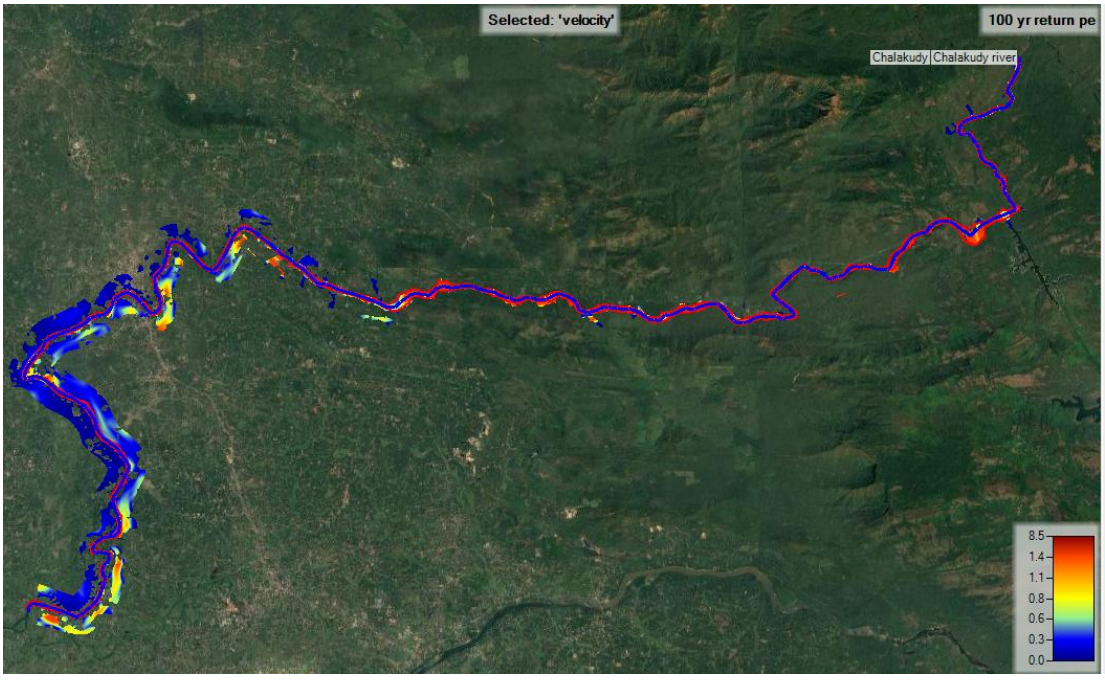

Fig. 4.58 Velocity map for 100 year return period as viewed in RAS Mapper

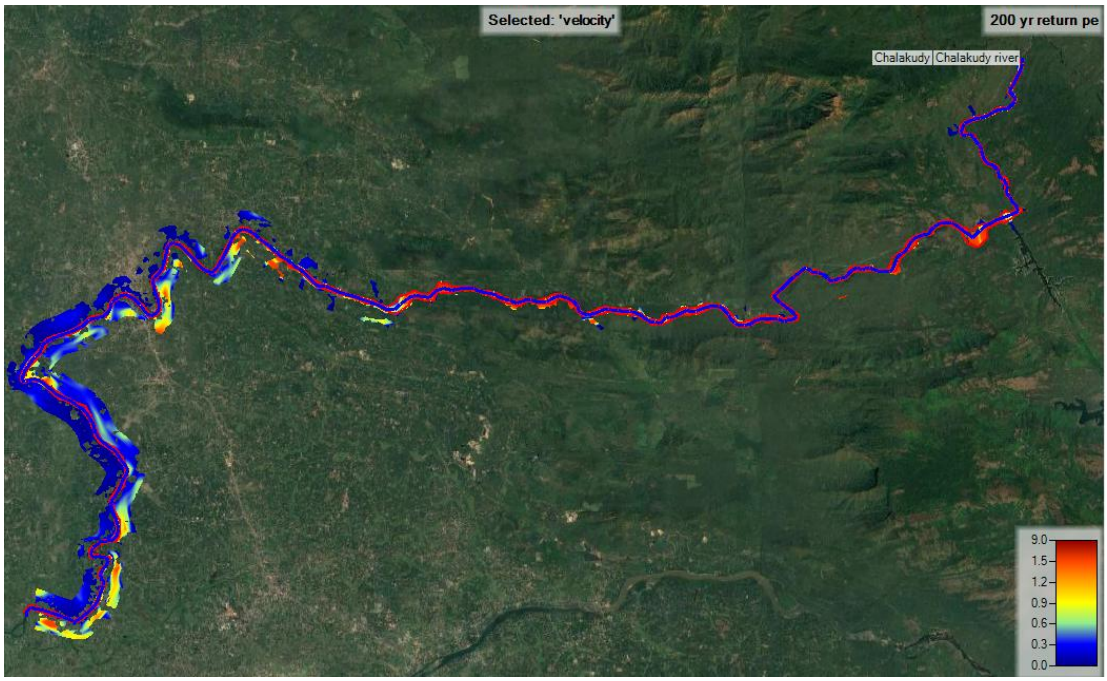

Fig. 4.59 Velocity map for 200 year return period as viewed in RAS Mapper

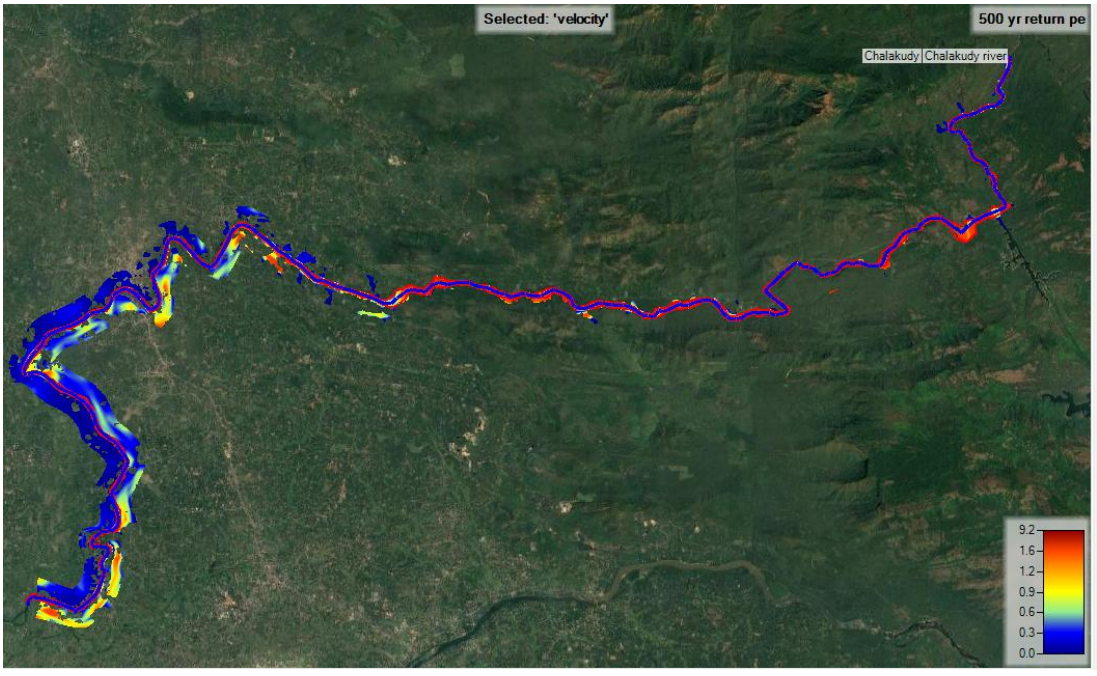

Fig. 4.60 Velocity map for 500 year return period as viewed in RAS Mapper

Fig. 4.55 - 4.60 shows that the main channel had the highest velocities, while the over banks (both left and right) had velocities ranging from 0 to 7.3 m/s for the 10 year return period, 0 to 7.7 m/s for the 20 year return period, 0 to 8.2 m/s for the 50 year return period and 0 to 8.5 m/s for the 100 year, 0 to 9.0 m/s for the 200 year return period and 0 to 9.2 m/s for 500 year return periods. The spatial distribution of flow velocities simulated by HEC-RAS was seen using RAS Mapper. We can see that the velocities are very close to zero near the water edge. A similar result has been described by Shroder *et al.,* 2015. They discovered that water velocity in areas where water comes near inhabited areas varied between 0 and 5 m/s, whereas in the main channel it was around 10 m/s, using the LISFLOOD model for hydraulic modelling at the Carlisle location in the United Kingdom.

4.7.6 Visualizing HEC-RAS results

The HEC-RAS results can be viewed in a variety of ways. One of these is to use the option 'View Cross-sections' to see the water surface in each cross-section and then browse through any cross-section along a specified river/reach as shown in Fig 4.61&4.65. In Fig 4.61, Cross sectional view at river station 3600 for lower reach with X – axis indicating cross sectional length 1600m and Y axis indicating Water Surface Elevation (WSE). Total cross sectional length is divided into three subsections: middle portion indicates channel, left side as Left Over Bank (LOB), right side as Right Over Bank (ROB). Blue shaded line indicates the water surface elevations and green dotted lines indicate energy grade line for 10, 20, 50, 100, 200 and 500 year return periods.

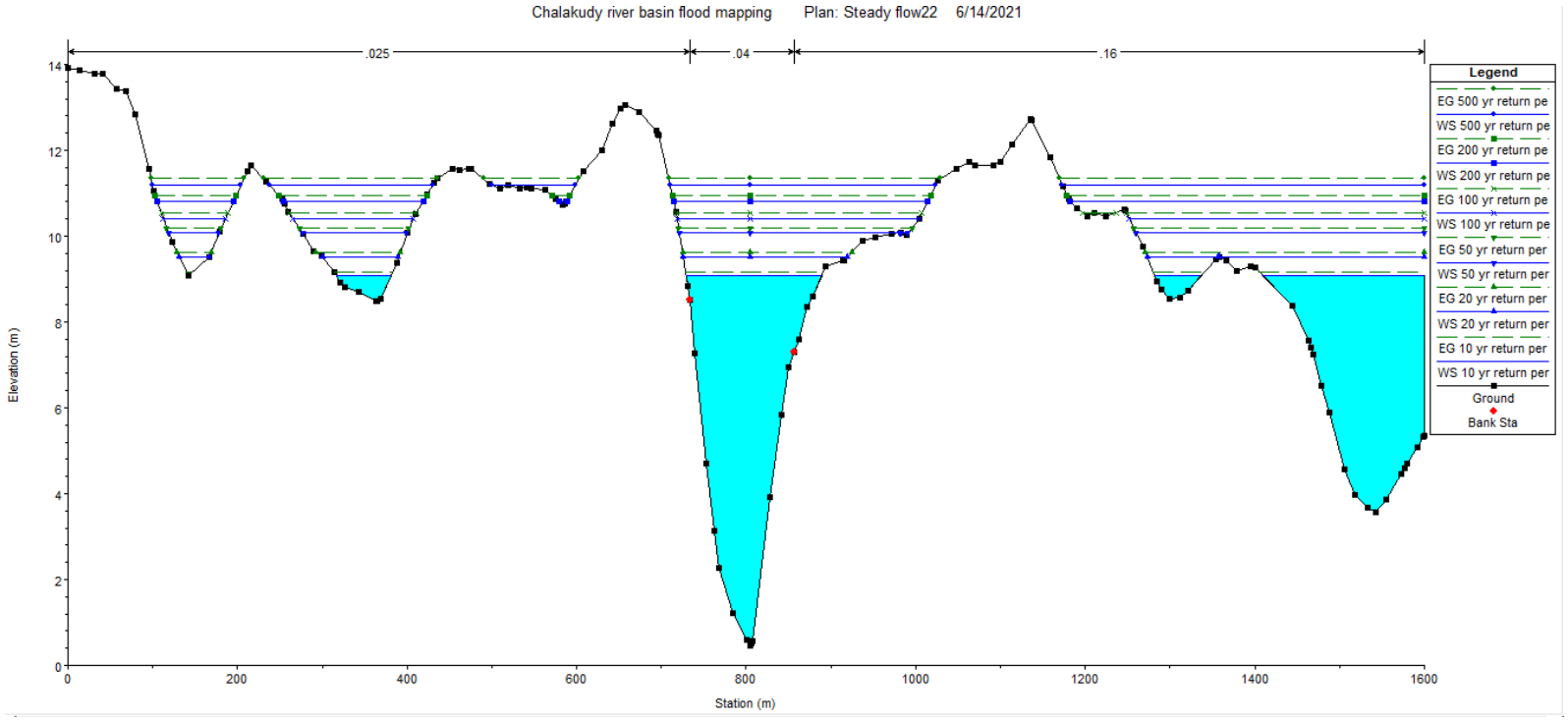

Fig 4.61 Cross section view at river station 3600 in the lower reach

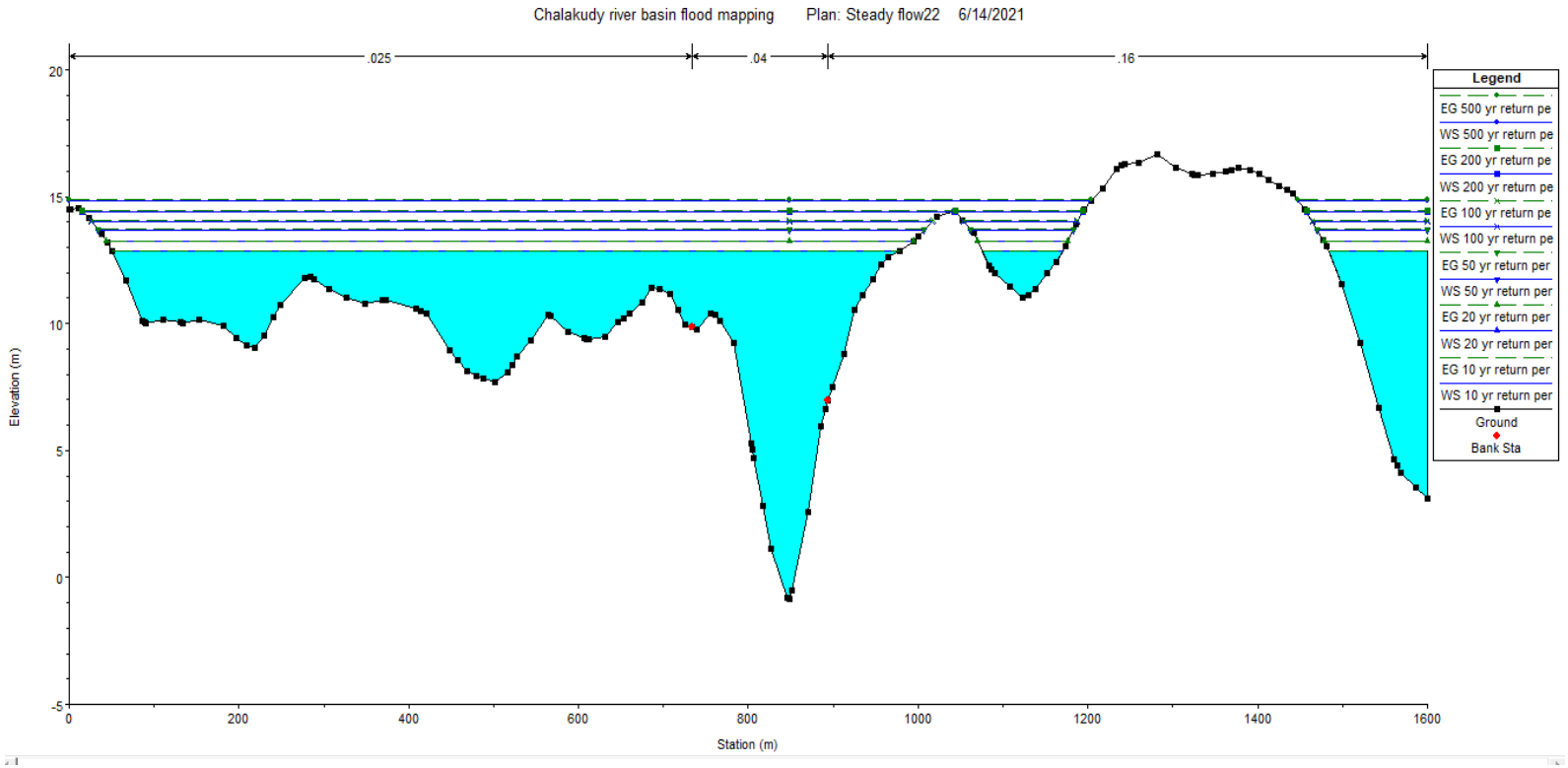

Fig. 4.62 Cross section view at river station 12000 in the lower reach

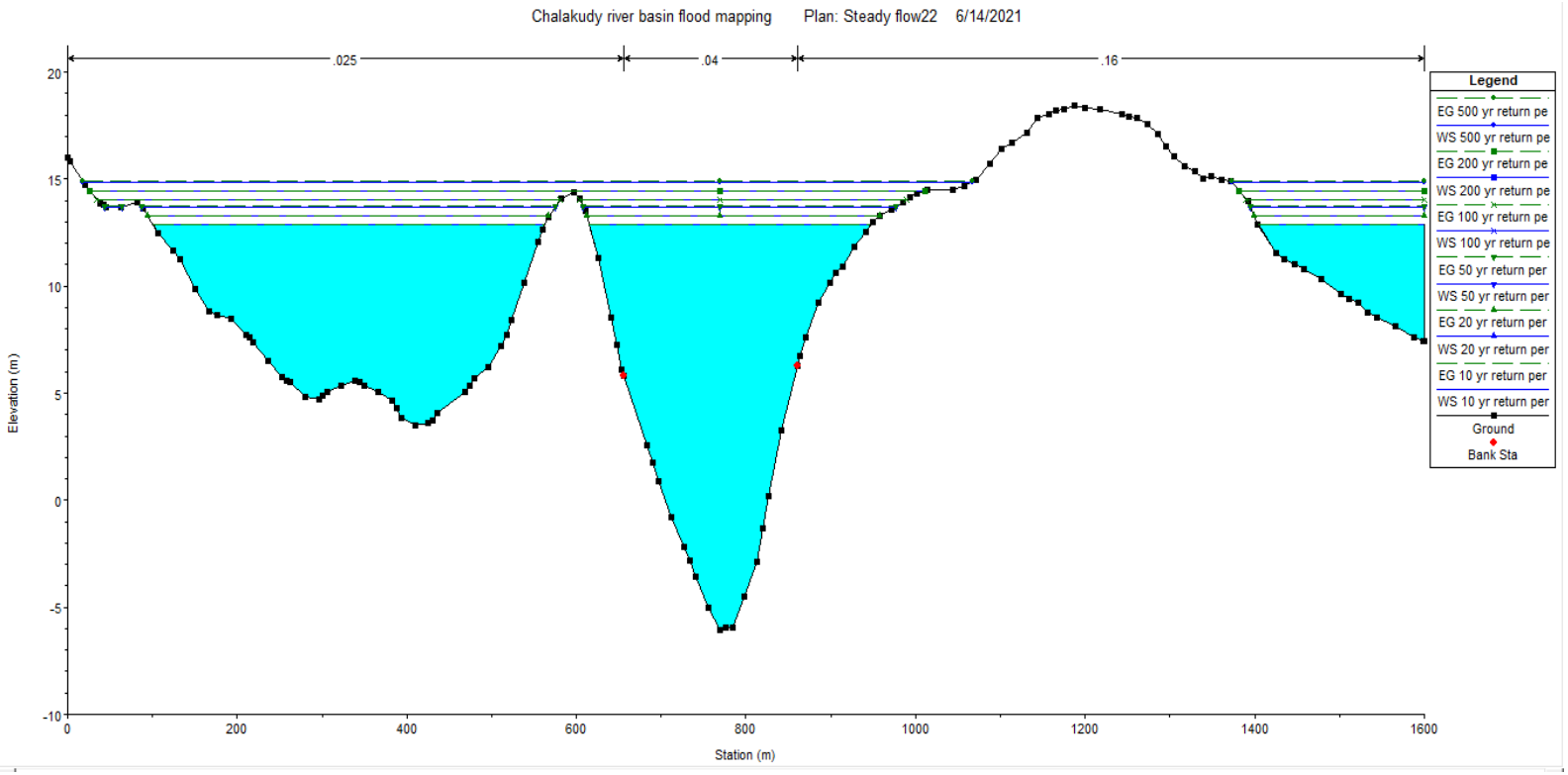

Fig.4.63 Cross section view at river station 13200 in the middle reach

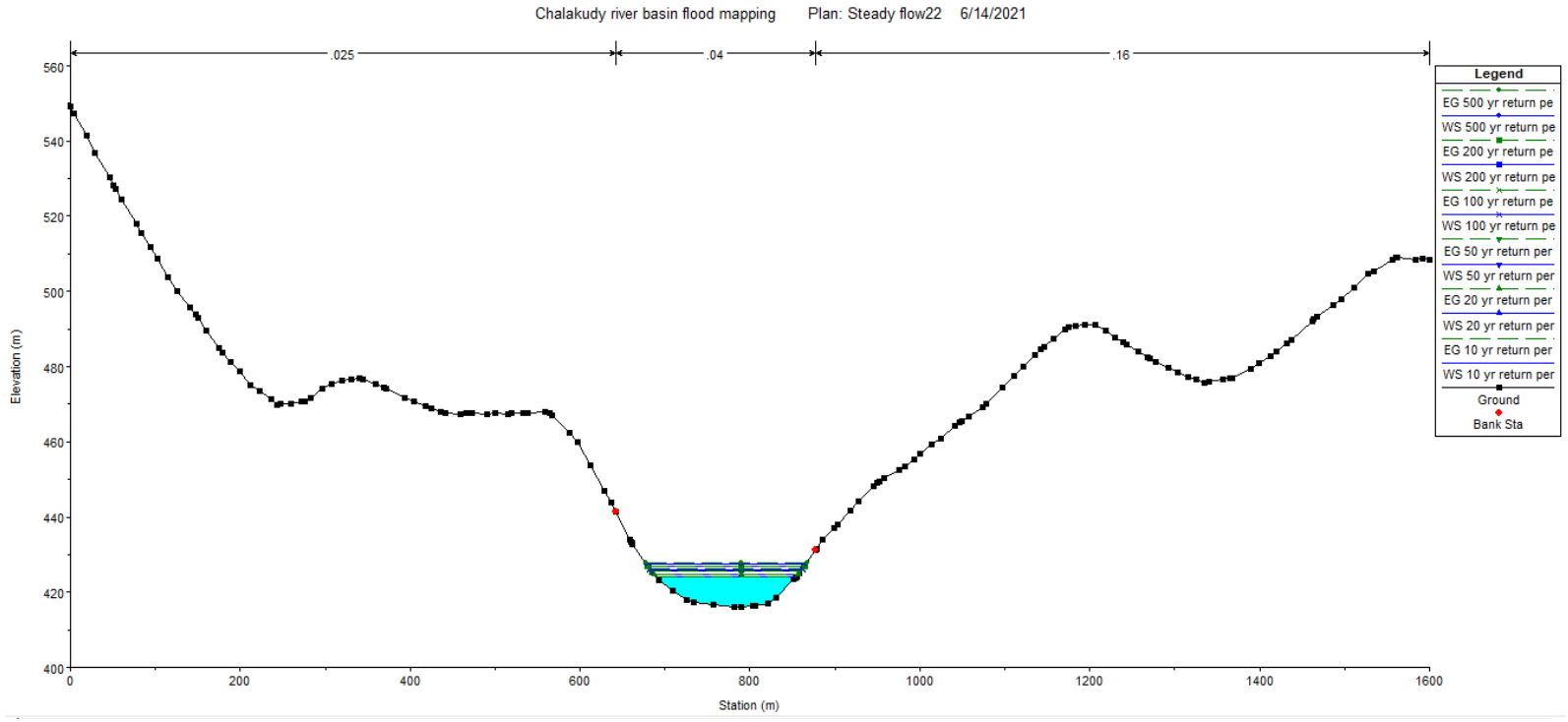

Fig 4.64 Cross section view at river station 67200 in the upper reach

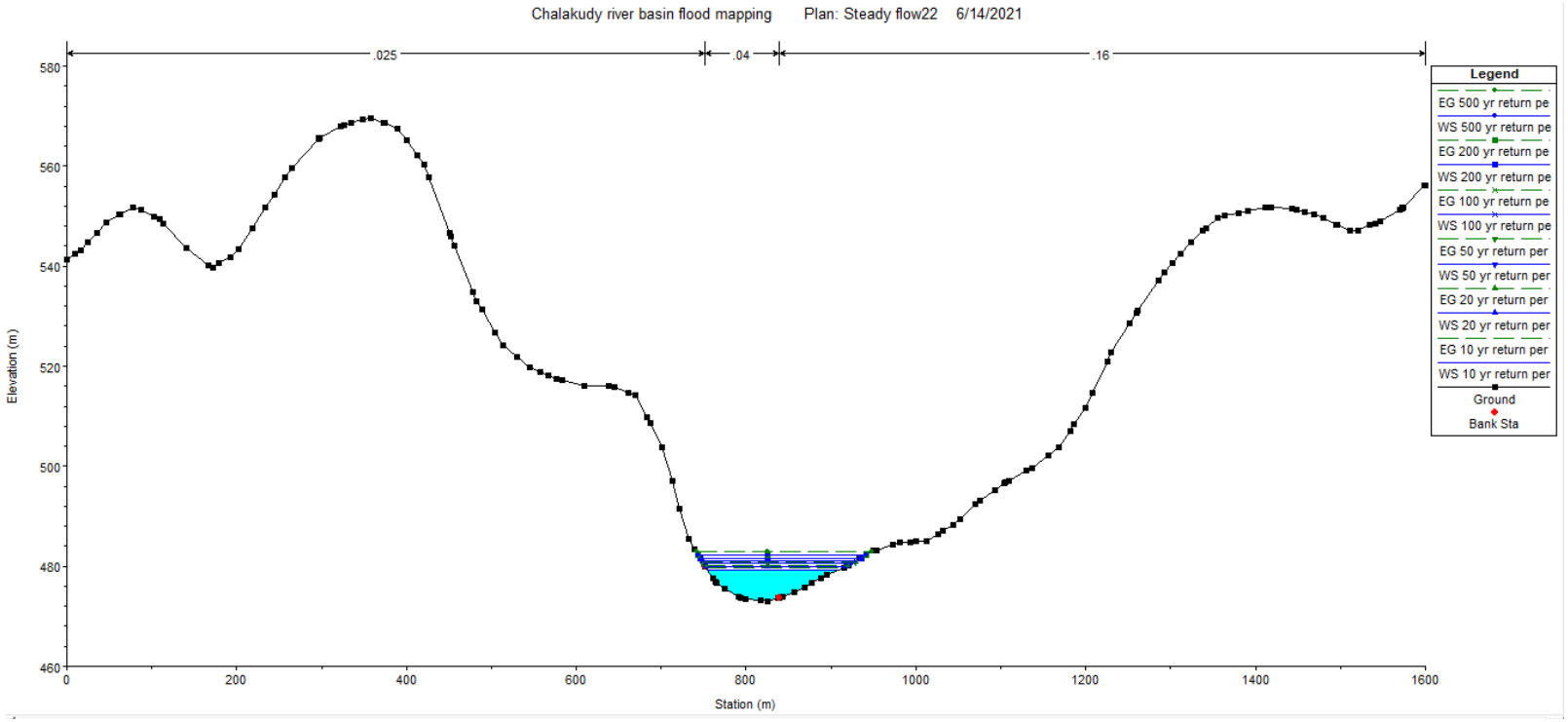

Fig 4.65 Cross section view at river station 75600 in the upper reach

It can be observed from Figs. 4.55 to 4.59 that the slope of Chalakudy river in the upper region is steep as compared to the slope of the lower region. The upstream areas are mostly forested catchments and some portions lie in Tamil Nadu region. The dams in the basin are all concentrated in the upper reaches and hence some amount of flow gets store in these structures. Consequently, the inundated area and depth of flow in the upper reach is relatively less as compared to the lower reach and middle reach. It is clearly indicated by the comparison between two cross sectional views in upstream and downstream regions, that the maximum affected area lies in the lower regions of the basin.

4.8 CADASTRAL LEVEL FLOOD RISK ASSESSMENT

Based on the data of flood depth variability along the river channel and over banks, flow velocity and water surface elevation the risk assessment of Chalakudy river basin was performed. The Panchayaths which are severely affected were categorized as high risk, medium risk and low risk areas based on the depth of flood water flow. This was done for different return period storms in order to analyze the variations in risk based on storm frequency.

Table 4.25 Cadastral level risk areas of Chalakudy river basin for 10 year return period

Station No.	**Name of Panchayat**	**Depth (m)**	**Velocity (m/s)**	**WSE (m)**
	High risk areas(Depth > 20 m)			
LOB 6600-11400	Annamanada,Thrissur	0.2-28.1	0-5	10.39 - 12.85
LOB&ROB12000-19800	Kadukutty, Thrissur	0.5-29.2	0.01-2.7	12.86 - 13.29
ROB 20400-34800	Melur,Thrissur	0.21-24.7	0.12-4.8	13.28 - 16.99
LOB 27000-39600	Pariyaram, Thrissur	0.13-24.6	0.11-1.6	13.57- 34.19
	Medium risk areas (Depth 10 – 20 m)			
ROB 600-3000	Puthenvelikkara,Ernakulam	0.12 -10.4	0.01-2.5	7.56 - 8.96

LOB 600-1800	Kuzhur,Thrissur	0.1- 10.1	0.0-0.9	7.56 - 8.91
ROB 3000-9600	Parakkadavu, Ernakulam	0.3-16.7	0- 5	8.96 - 12.84
LOB 16800-18000	Mala, Thrissur	0.24-15.2	0.03-1.6	13.20 - 13.24
LOB18000-26400	Chalakudy, Thrssur	0.15-18.2	0.13-1.2	13.24 - 13.51
ROB 35400-37200	Karukutty, Ernakulam	0-16.5	0.1-0.9	17.04 - 17.17
	Low risk areas(Depth <10 m)			
ROB 37200-37800	Manjapra, Ernakulam	0-7.5	0-0.5	17.17 - 17.01
ROB 37800-58800	Ayyampuzha, Ernakulam	0-4.6	0-1.6	17.01 -207.19
LOB 39600-75600	Athirappilly,Thrissur	0-5.9	0-0.1	34.19 -479.60

Table 4.26 Cadastral level risk areas of Chalakudy river basin for 20 year return period

Station No.	Name of Panchayat	Depth (m)	Velocity (m/s)	WSE (m)
	High risk areas (Depth > 20 m)			
LOB 6600-11400	Annamanada,Thrissur	0.3-28.5	0-5.3	10.70-13.25
LOB &ROB12000-19800	Kadukutty, Thrissur	0.4-29.6	0.01-2.8	13.26-13.71
ROB 20400-34800	Melur,Thrissur	0.31-25.1	0.14-5	13.71-17.39
LOB 27000-39600	Pariyaram, Thrissur	0.23-25	0.03-5.4	14.03-34.56
	Medium risky areas (Depth 10 – 20 m)			
ROB 600-3000	Puthenvelikkara, Ernakulam	0.14-10.8	0.02-2.4	8.25-9.40
LOB 600-1800	Kuzhur, Thrissur	0-10.3	0-1	8.25-9.33
ROB 3000-9600	Parakkadavu, Ernakulam	0.2-17.1	0-5.3	9.40-13.23
LOB 16800-18000	Mala, Thrissur	0.32-15.6	0.12-1.7	13.60-13.66
LOB18000-26400	Chalakudy, Thrissur	0.21-18.6	0.3-1.3	13.66-13.95
ROB 35400-37200	Karukutty, Thrissur	0.01-17	0.13-1.2	17.45-17.61
	Low risky areas(Depth <10 m)			
ROB 37200-37800	Manjapra, Ernakulam	0-7.9	0-0.6	17.61-17.47
ROB 37800-58800	Ayyampuzha, Ernakulam	0-4.9	0-1.7	17.47-207.51
LOB 39600-75600	Athirappilly,Thrissur	0-6.4	0-0.2	34.56-479.85

Table 4.27 Cadastral level risk areas of Chalakudy river basin for 50 year return period

Station No.	Name of Panchayat	Depth (m)	Velocity (m/s)	WSE (m)
	High risk areas (Depth > 20 m)			
LOB 6600-11400	Annamanada,Thrissur	0.4-29	0-5.6	11.11-13.69
LOB &ROB12000-19800	Kadukutty, Thrissur	0.32-30.1	0.02-2.9	13.70-14.18
ROB 20400-34800	Melur,Thrissur	0.23-25.6	0.14-5.2	14.18-17.87
LOB 27000-39600	Pariyaram, Thrissur	0.31-25.7	0.02-5.7	14.54-35.01
	Medium risk areas (Depth 10 – 20 m)			
ROB 600-3000	Puthenvelikkara, Ernakulam	0.1-11.3	0.01-2.3	8.93-9.96
LOB 600-1800	Kuzhur,Thrissur	0-10.9	0-1	8.93-9.87
ROB 3000-9600	Parakkadavu,Ernakulam	0.3-17.6	0-5.6	9.96-13.69
LOB 16800-18000	Mala, Thrissur	0.21-16	0.12-1.8	14.06-14.12
LOB18000-26400	Chalakudy, Thrissur	0.32-19.1	0.17-1.3	14.12-14.12
ROB 35400-37200	Karukutty, Ernakulam	0.3-17.5	0.13-1.4	17.95-18.16
	Low risky areas(Depth <10 m)			
ROB 37200-37800	Manjapra, Ernakulam	0-8.5	0-0.7	18.16-18.02
ROB 37800-58800	Ayyampuzha, Ernakulam	0-5.3	0-1.8	18.02-207.90
LOB 39600-75600	Athirappilly,Thrissur	0-7	0-0.2	35.01-480.53

Table 4.28 Cadastral level risk areas of Chalakudy river basin for 100 year return period

Station No.	Name of Panchayat	Depth (m)	Velocity (m/s)	WSE (m)
	High risk areas (Depth > 20 m)			
LOB 6600-11400	Annamanada,Thrissur	0.35-29.3	0-5.9	11.31-14.02
LOB &ROB12000-19800	Kadukutty, Thrissur	0.32-30.4	0.17-2.8	14.03-14.51
ROB 20400-34800	Melur,Thrissur	0.13-26	0.14-5.3	14.51-18.19
LOB 27000-39600	Pariyaram, Thrissur	0.13-25.9	0.12-5.8	14.89-35.32
	Medium risk areas (Depth 10 – 20 m)			
ROB 600-3000	Puthenvelikkara, Ernakulam	0.1-11.7	0.01-2.3	9.34-10.30
LOB 600-1800	Kuzhur,Thrissur	0-11.2	0-1.1	9.34-10.22
ROB 3000-9600	Parakkadavu,Ernakulam	0.23-17.9	0-5.9	10.30-14
LOB 16800-18000	Mala, Thrissur	0.21-16.3	0.01-1.8	14.37-14.45
LOB18000-26400	Chalakudy, Thrssur	0.4-19.4	0.17-1.4	14.45-14.81
ROB 35400-37200	Karukutty, Thrissur	0.1-17.9	0.12-1.5	18.29-18.53
	Low risk areas(Depth <10 m)			
ROB 37200-37800	Manjapra, Ernakulam	0-8.8	0-0.8	18.53-18.40
ROB 37800-58800	Ayyampuzha,Ernakulam	0-5.5	0-1.9	18.40-208.15
LOB 39600-75600	Athirappilly, Thrissur	0-7.4	0-0.2	35.32-480.99

Table 4.29 Cadastral level risk areas of Chalakudy river basin for 200 year return period

Station No.	Name of Panchayat	Depth (m)	Velocity (m/s)	WSE (m)
	High risk areas (Depth > 20 m)			
LOB 6600-11400	Annamanada,Thrissur	0.6-29.7	0-5.9	11.81-14.42
LOB&ROB12000 -19800	Kadukutty, Thrissur	0.32-30.8	0.04-2.6	14.42-14.91
ROB 20400-34800	Melur,Thrissur	0.32-26.4	0.06-5.2	14.90-18.60
LOB 27000-39600	Pariyaram, Thrissur	0.21-26.3	0.14-5.6	15.32-35.73
	Medium risk areas (Depth 10 – 20 m)			
ROB 600-3000	Puthenvelikkara, Ernakulam	0.1-12.1	0.02-2.4	9.47-10.69
LOB 600-1800	Kuzhur,Thrissur	0-11.6	0-1.4	9.74-10.60
ROB 3000-9600	Parakkadavu,Ernakulam	02-18.3	0-5.9	10.69-14.38
LOB 16800-18000	Mala, Thrissur	0.3-16.7	0.2-1.7	14.75-14.83
LOB18000-26400	Chalakudy, Thrssur	0.37-19.8	0.17-1.4	14.83-15.23
ROB 35400-37200	Karukutty, Thrissur	0.01-18.3	0.01-1.7	18.73-19.02
	Low risk areas(Depth <10 m)			
ROB 37200-37800	Manjapra, Ernakulam	0-9.3	0-0.8	19.02-18.90
ROB 37800-58800	Ayyampuzha, Ernakulam	0-5.9	0-2	18.90-208.49
LOB 39600-75600	Athirappilly,Thrissur	0-8	0-0.2	35.73-481.60

Table 4.30 Cadastral level risk areas of Chalakudy river basin for 500 year return period

Station No.	Name of Panchayat	Depth (m)	Velocity (m/s)	WSE (m)
	High risk areas (Depth > 20 m)			
LOB 6600-11400	Annamanada,Thrissur	0.7-30.1	0-6.1	12.19-14.85
LOB&ROB12000-19800	Kadukutty, Thrissur	0.12-31.2	0.02-2.4	14.85-15.34
ROB 20400-34800	Melur,Thrissur	0.25- 26.9	0.03-4.6	15.33-19.09
LOB 27000-39600	Pariyaram, Thrissur	0.31-26.8	0.01-5.9	15.78-36.15
	Medium risk areas (Depth 10 – 20 m)			
ROB 600-3000	Puthenvelikkara, Ernakulam	0.12-12.4	0.01- 2.5	10.11-11.06
LOB 600-1800	Kuzhur,Thrissur	0-12	0-1.7	10.11-10.96
ROB 3000-9600	Parakkadavu,Ernakulam	0.2-18.7	0-6.1	11.06-14.80
LOB 16800-18000	Mala, Thrissur	0.31-17.1	0.2-1.7	15.17-15.26
LOB18000-26400	Chalakudy,Thrssur	0.3-2.3	0.13-1.4	15.26-15.68
ROB 35400-37200	Karukutty, Thrissur	0.5-18.8	0.012-1.8	19.23-19.56
	Low risk areas(Depth <10 m)			
ROB 37200-37800	Manjapra, Ernakulam	0-9.9	0-0.9	19.56-19.42
ROB 37800-58800	Ayyampuzha, Ernakulam	0-6.2	0-2.1	19.42-208.84
LOB 39600-75600	Athirappilly,Thrissur	0-8.8	0-0.2	36.15-482.83

Table 4.25- 4.30, shows the cadastral level classification of Chalakudy basin into three categories such as high risk when flood depth is greater 20 m, medium risk areas when flood flow depth between 10-20 m and low risk areas when depth is less than 10 m. Annamanada, Kadukutty, Melur and Pariyaram Panchayats come under high risk areas for different return periods. In high risk areas, Kadukutty, Thrissur lying between Left Over Bank(LOB) and Right Over Bank(ROB) station nos.12000-19800, is identified as most vulnerable area with the depth, velocity and water surface elevation varying from 0.12 – 31.2 m, 0.02- 2.4 m/s and 14.85-15.34 m .

Puthenvelikkara, Kuzhur, Parakkadavu, Mala, Chalakudy and Karukutty panchayats come under medium risk areas for different return periods with only slight variation in depth, velocity and water surface elevation. Manjapra, Ayyampuzha and Athirappilly are identified as low risk areas for different return periods. Considering the devastating effect of the 2018 floods, the Kerala Agricultural University has prepared a comprehensive flood map for the Chalakudy river basin. The worst flood affected block Panchayats were Mala, Vellangalloor and Parakkadavu. Out of these Poomangalam Grama Panchayat in Vellangalloor block and Kuzhoor Grama Panchayat of Mala block were mostly affected ones, to the tune of 42.49% and 41.83% respectively (The Hindu, June 02, 2020). Emergency Action Plan has been prepared by Kerala State Electricity Board Limited (KSEBL, 2020) in collaboration with Central Project Management Unit (CPMU) and Central Water Commission (CWC), Government of India. Flood inundation areas likely to be affected by the failure of Poringalkuthu Dam were prepared based on the Dam Break Analysis carried out using digital elevation model (DEM). They found that flood prone Panchayaths were Athirappilly, Pariyaram, Melur, Kodassery, Chalakudy, Koratty, Alur, Mala, Kadukutty, Annamanada, Kuzhur, Poyya, Puthenchira, Ayyampuzha, Manjapra, Karukutty, Parakkadavu, Puthenvelikara, Kunnukara, Karumalloor, Nedumbassery, Chendamangalam, North Paravoor, Angamali and Chengamanad.The flood prone area mapping of Chalakudy basin conducted using HEC-RAS model also shows similar results.

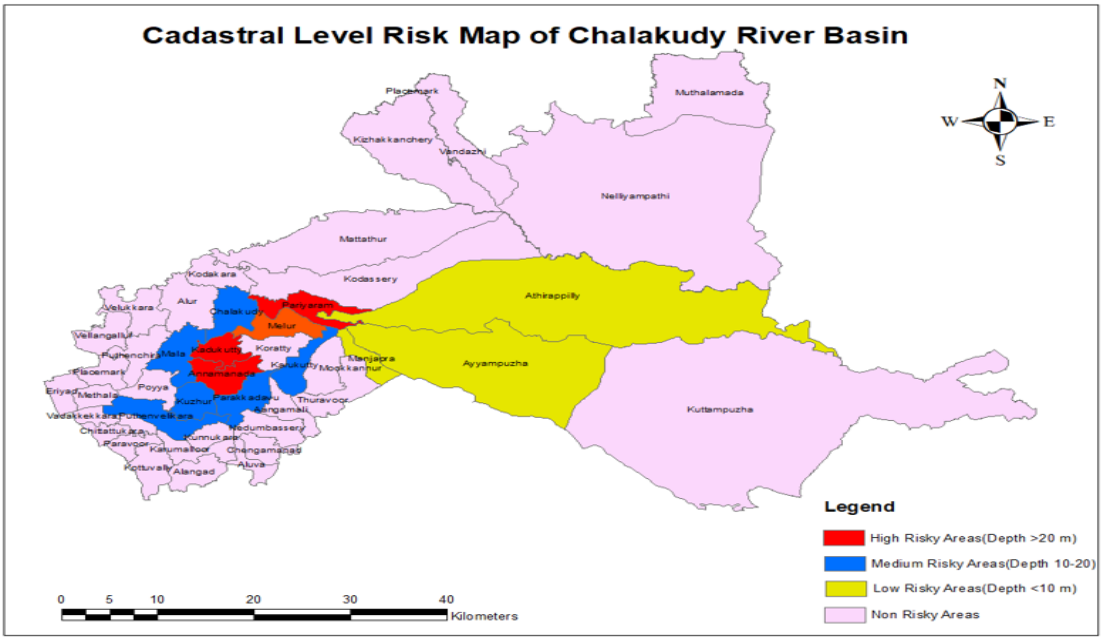

Fig.4.66 Cadastral level risk map of Chalakudy river basin

As shown in Fig.4.66, Panchayaths were divided into three classes based on depth such as high risk areas when depth is greater than 20 m indicated as red colour, Medium risk areas when depth varies from 10 – 20 m indicated as blue colour and low risk areas when depth is less than 10 m indicated as yellow colour. Remaining Panchayaths come under non risk areas.

4.9. FLOOD VULNERABILITY ANALYSIS

For each of the flood events being modelled, maps showing the areas vulnerable to flooding were created by intersecting the land use map of the floodplains with the flooded area polygons. As a binary model, this represents the flood risk vulnerability component in a certain land use in terms of the presence or absence of floods over a specific return period. Flood prone paddy land varied from 949 to 1361 ha, forest/ other vegetation from 528 to 805 ha, barren land from 201 to 304 ha, urban land from 127 to 172 ha, water body from 762 to 873 ha, tea/oil palm from 53 to 95 ha, and coffee/cardamom from 162 to 191 ha.

Table 4.31 Flood vulnerability classification of different land uses

Land use type (ha)	Total Vulnerable Area (ha)											
	10 year flood		20 year flood		50 year flood		100 year flood		200 year flood		500 year flood	
	Area	%	Area	%	Area	%	Area	%	Area	%	Area	%
Water body	762	27.39	788	26.43	816	25.35	833	24.63	854	23.83	873	22.96
Forest/other vegetation	528	18.97	579	19.42	641	19.91	687	20.31	742	20.70	805	21.17
Barren land	201	7.22	220	7.38	244	7.58	260	7.69	281	7.84	304	7.99
Paddy	949	34.11	1030	34.55	1126	34.99	1192	35.2	1274	35.55	1361	35.80
Urban land	127	4.56	135	4.52	145	4.50	152	4.49	161	4.49	172	4.52
Tea/Oil palm	53	1.90	60	2.01	70	2.17	77	2.27	85	2.37	95	2.49
Coffee/ Cardamom	162	5.82	169	5.66	176	5.46	180	5.32	186	5.19	191	5.02
Total	**2782**	**100.00**	**2981**	**100.00**	**3218**	**100.00**	**3381**	**100.00**	**3583**	**100.00**	**3801**	**100.00**

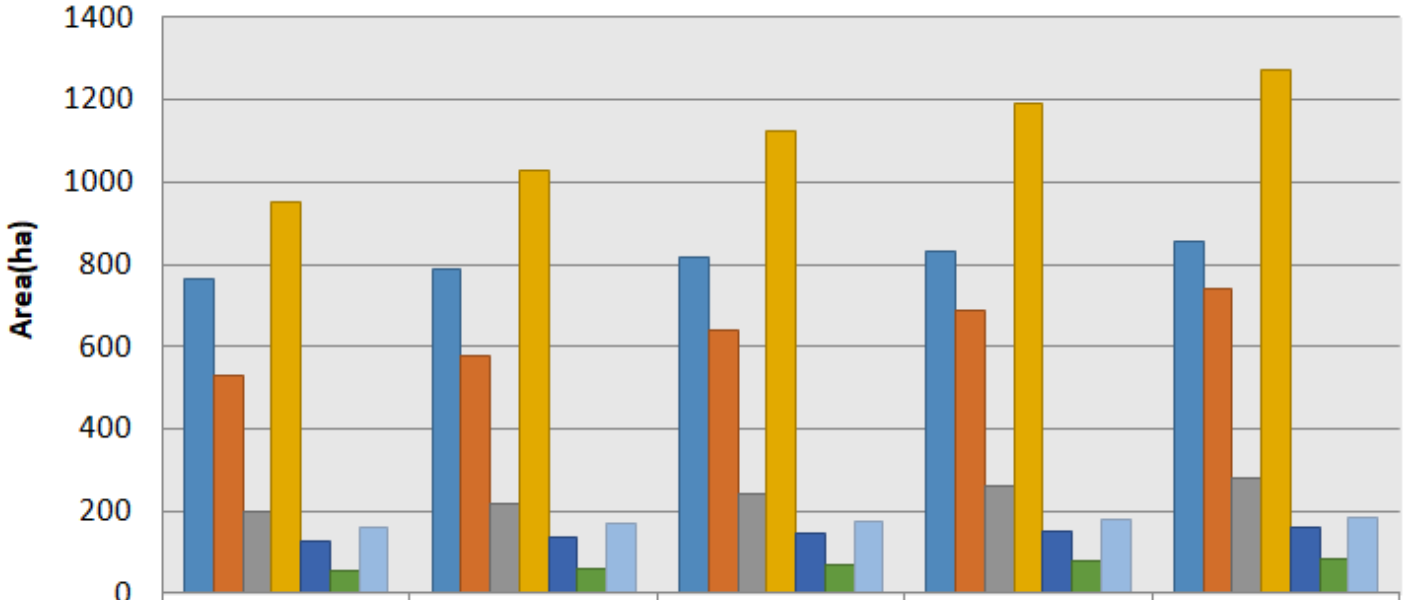

	10yrs	20yrs	50yrs	100yrs	200yrs
Water body	762	788	816	833	854
Forest	528	579	641	687	742
Barren land	201	220	244	260	281
Paddy	949	1030	1126	1192	1274
Urban land	127	135	145	152	161
Tea/Oil Palm	53	60	70	77	85
Coffee/Cardamom	162	169	176	180	186

Fig. 4.67 Vulnerability classification for different year return period flood

The table 4.31 showed that 762, 528, 201, 949, 127, 53 and 162 ha of water body, forest/other vegetation, barren land, paddy, urban land tea/oil palm and coffee/cardamom are respectively inundated by 10-year flood. Similarly, 873, 805, 304, 1361, 172, 95 and 191 ha of water body, forest/ other vegetation, barren land, paddy, urban land, tea/oil palm and coffee/cardamom area, are respectively inundated by 500-year flood. The flooded area increased with increase in flooding intensity, mostly paddy area was inundated by different return period floods, which was followed by forest/other vegetation and barren area. The flood prone panchayaths lie Pariyaram, Kadukutty, Chalakudy, *etc.*, have lot of areas under Nutmeg cultivation. Hence flooding of these panchayaths will affect the nutmeg grown areas specifically and the farmers dependent on nutmeg cultivation are severely affected.

Bikram (2010) performed steady flow analysis in HEC-RAS for Lothar Khola, Nepal. According to the results, a 2-year flood inundated 42, 53, 26 and 108 ha of agricultural, forest, river, and sand area, respectively. Similarly, 200-year floods submerged 50, 62, 27 and 114 ha of cultivation area, forest, river, and sand area, respectively, showing that flooded area increased with higher flooding severity. The flooded area was mostly sand area, which was followed by forest and cultivation area.

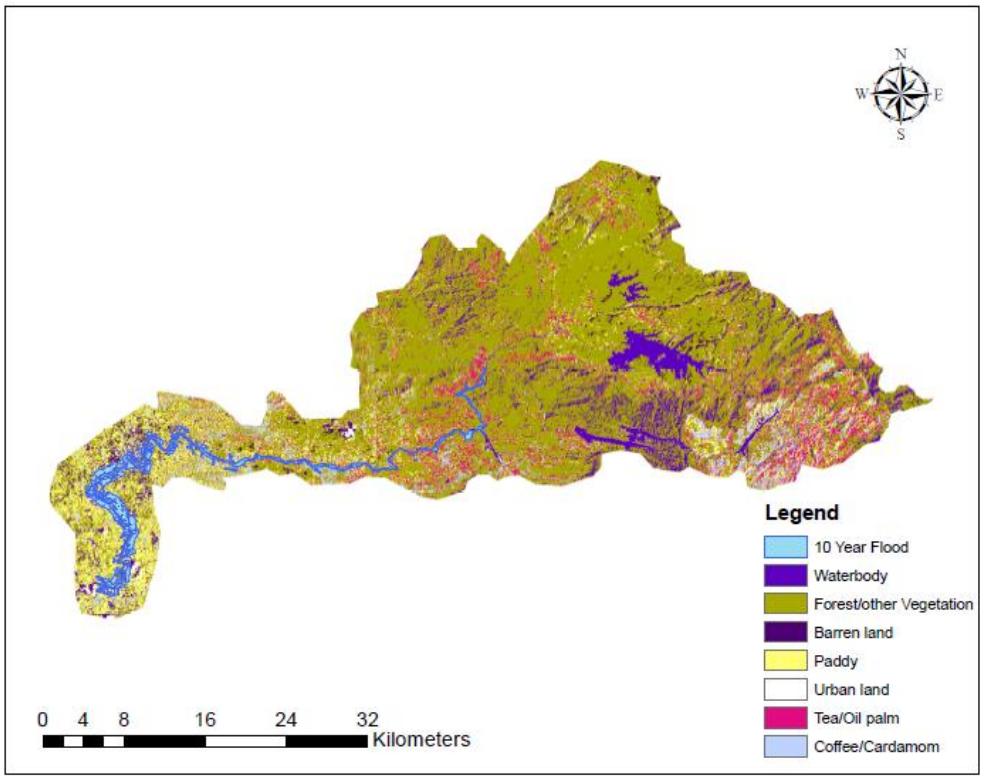

Fig. 4.68 Flood vulnerability map for 10 year return period

Fig 4.68 shows results by superimposing of land use land cover map with flooded area polygon for 10 year return period flood. It shows that paddy land was the largest area flooded with 949 ha followed by water body 762 ha, forest/other vegetation 528 ha, Barren land 201 ha, coffee/cardamom 162 ha, Urban land 127 ha, and Tea/Oil palm 53 ha. Among the other vegetations, nutmeg cultivated lands were severely affected during the 2018 floods in this basin.

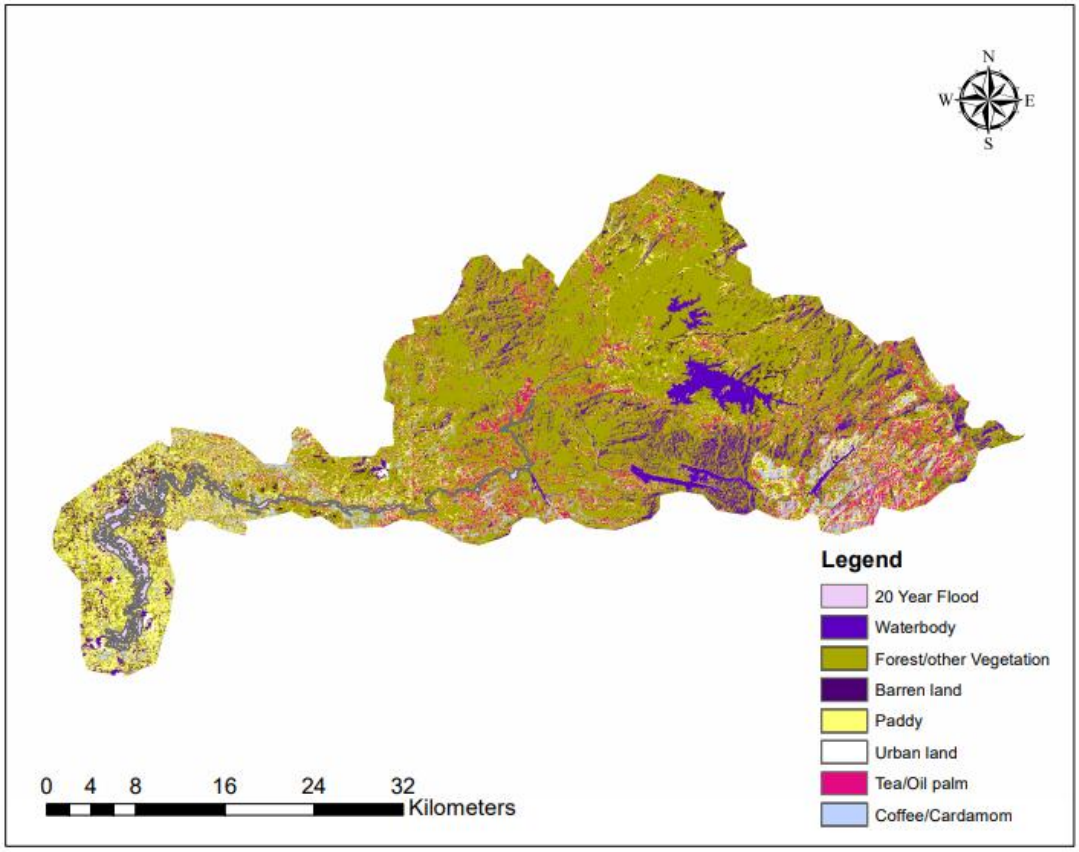

Fig. 4.69 Flood vulnerability map for 20-year return period

Fig 4.69 shows results by superimposing of land use land cover map with flooded area polygon for 20-year return period flood. It shows that paddy lands were the highest flooded area with 1030 ha, followed by water body 788 ha, forest/other vegetation 579 ha, barren land 220 ha, coffee/cardamom 169 ha, urban land 135 ha and tea/oil palm 60 ha.

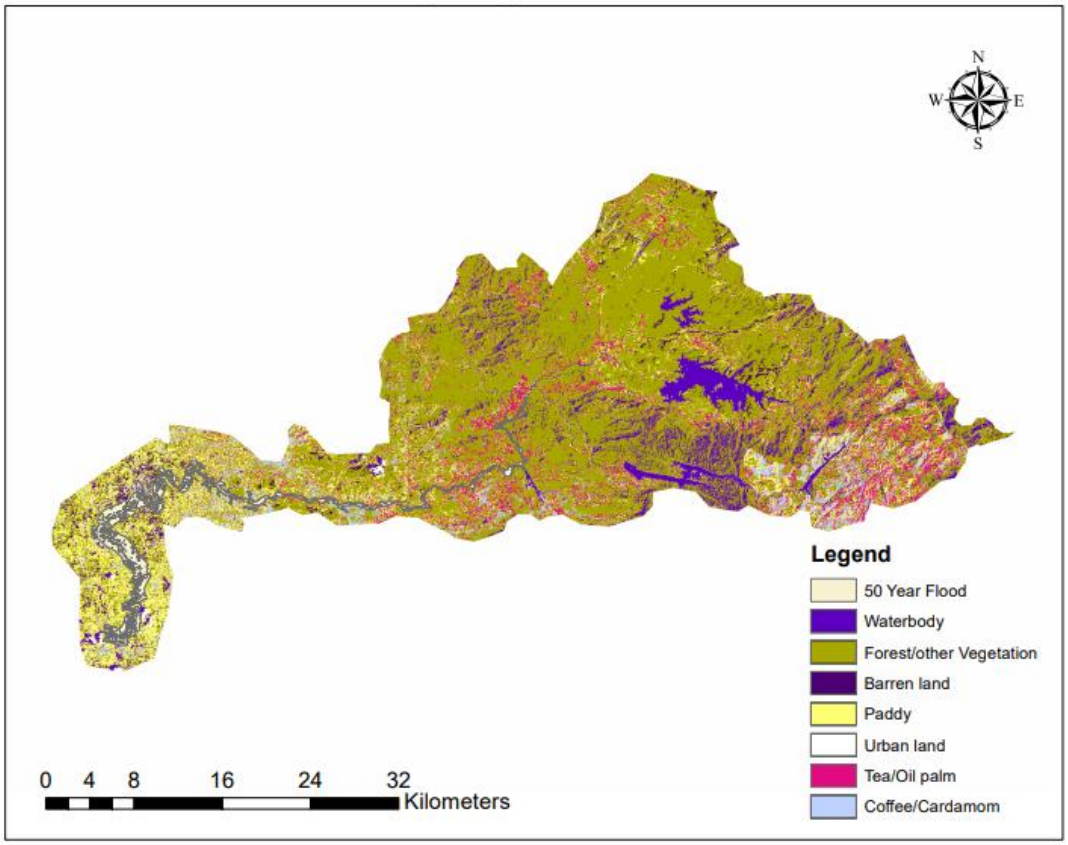

Fig. 4.70 Flood vulnerability map for 50 year return period

In Fig 4.70, superimposing of land use land cover with flooded area polygons for 50 year return period is shown. It indicates that paddy was the largest area flooded with 1126 ha followed by water body 816 ha, forest/other vegetation 579 ha, barren land 244 ha, coffee/cardamom 176 ha, urban land 145 ha an tea/oil palm 70 ha.

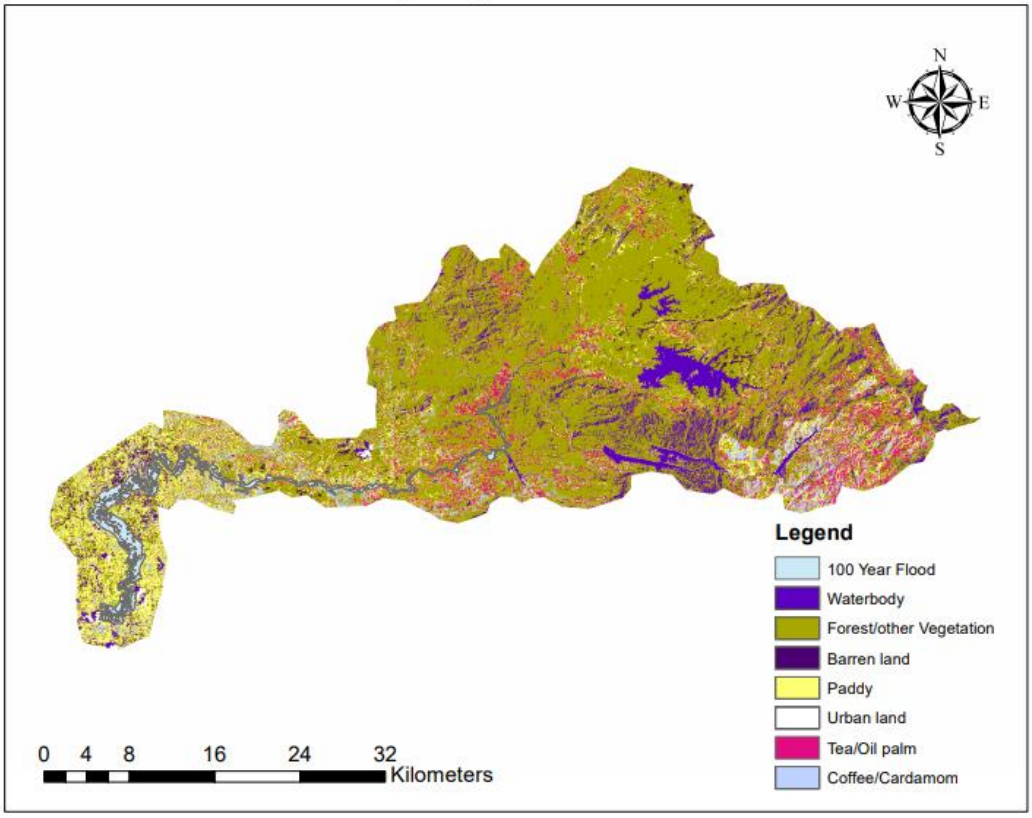

Fig. 4.71 Flood vulnerability map for 100 year return period

In Fig 4.71, superimposing of land use land cover with flooded polygon for 100-year return period is shown. It indicates that paddy was the largest area flooded with 1192 ha followed by water body 833 ha, forest/other vegetation 687, barren land 260, coffee/cardamom 180 ha, urban land 157 ha, tea/oil palm 77 ha.

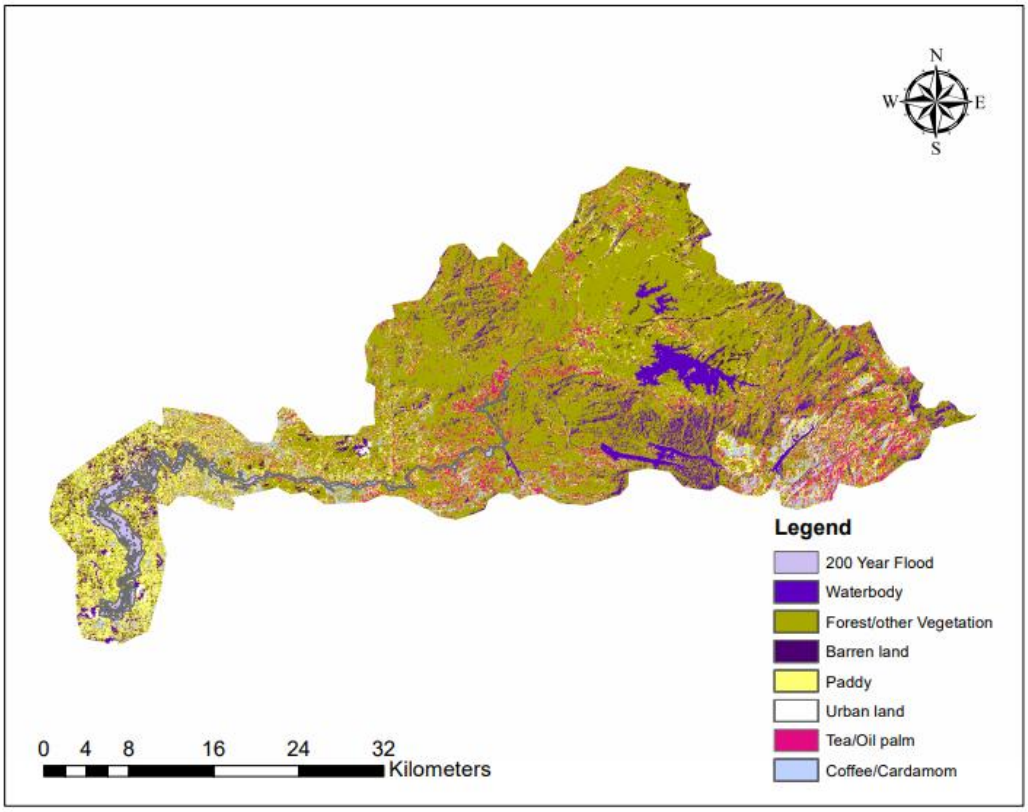

Fig. 4.72 Flood vulnerability map for 200 year return period

In Fig 4.72, superimposing of land use land cover with flooded polygon for 200-year return period is shown. It is evident that paddy was the largest area flooded with 1361 ha followed by water body 873 ha, forest/other vegetation 805, barren land 304, coffee/cardamom 191 ha, urban land 172 ha and tea/oil palm 95 ha.

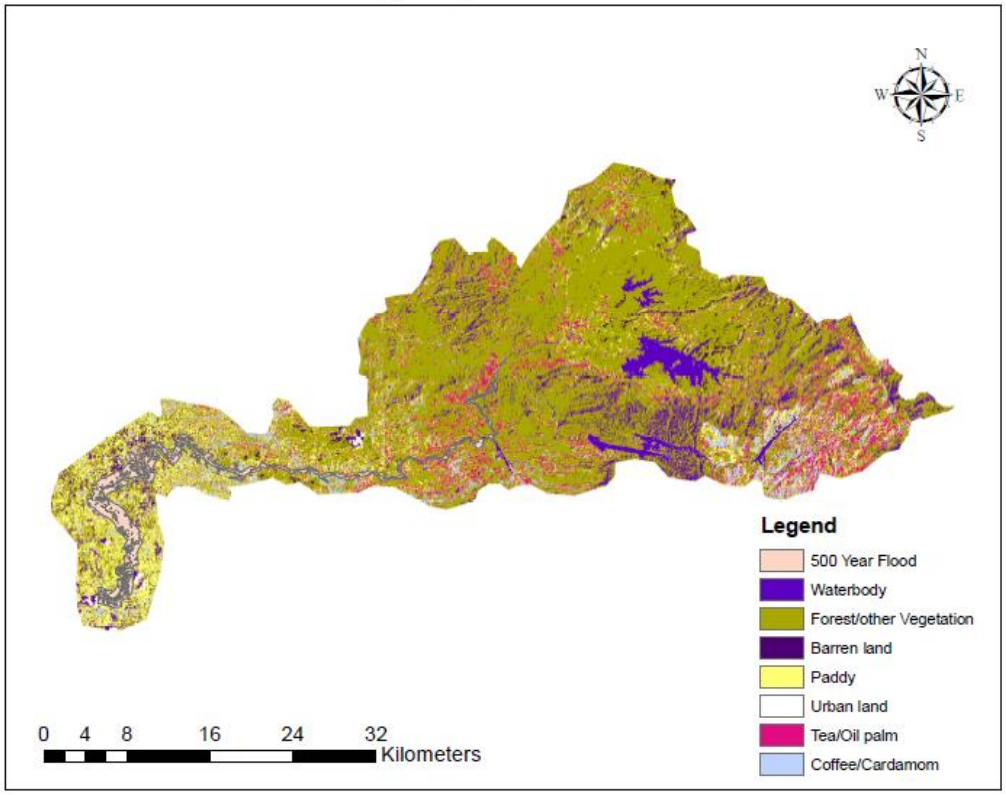

Fig. 4.73 Flood vulnerability map for 500-year return period

In Fig 4.73, superimposing of land use land cover with flooded polygon for 500-year return period is shown. In this case also, paddy was the largest area flooded with 949 ha followed by water body 762 ha, forest/other vegetation 528, barren land 201, coffee/cardamom 162 ha, urban land 127 ha and tea/oil palm 53 ha.

The 2018 floods in Chalakudy river basin due to a high return period storm caused flooding in the Panchayats like Kadukutty, Pariyaram, Mala, Chalakudy, etc as obtained in this study. Among the cultivated lands, Nutmeg, Paddy, Oil palm and many other high value crops grown by farmers were severely affected. The entire inhabited areas including towns were flooded and people had to be evacuated to relief camps. In addition to high return period storms, back flows from small streams

joining the Chalakudy river due to the high flood water depth in the river, as well as the overflowing of bridges, culverts *etc.*, were all reasons for flooding to human inhabited areas. The results obtained from this study can be used as a guideline in the preparation of cadastral level action plans for flood protection in this area. The local level initiatives lead by the people in collaboration with Government bodies and other research and development agencies can effectively address the issues related to climate change and related adversities like floods in this basin.

CHAPTER V
SUMMARY AND CONCLUSIONS

Chalakudy river basin in Kerala was selected for hydrological and hydraulic modelling studies for flood prone area mapping in this research. The basin lies between 10°05' to 10°35' North Latitude and 76°15' to 76°55' East Longitude. The total length of the river is about 130 km and the catchment area is about 1,704 km^2. Out of the total catchment area, about 300 k m^2 lies in Tamil Nadu and the remaining in Kerala. It is an area liable to flood and principally dominated by agricultural land. The area comes under the humid tropical zone, where water resources planning and management is necessary for irrigation scheduling, flood control and design of engineering structures. In view of the importance of water management in this humid region, it is necessary to understand the rainfall-runoff relationship of the basin along with its land characteristics. The HEC-HMS model which is a widely used rainfall-runoff model was chosen for the simulation of watershed responses and generation of flood hydrographs in this study. The simulated runoff is useful for well-planned programmes in water resource management, conservation and future prediction of runoff for flood mitigation strategies in the catchment. Chalakudy river is highly hazardous and wild during flood seasons as a result of depth of the river and illegal sand mining in it. This was one of the worst affected basins in the Kerala floods of 2018 and most of its basin areas were severely affected.

In order to address these issues, an attempt was made to calibrate and validate HEC-HMS model for simulating the flood hydrograph for the Chalakudy river basin. Flood frequency analysis was carried out to find the flood peak values for different return periods using various frequency distributions in HEC-SSP software. The results were compared with the estimated flood peak values for different return periods obtained from the HEC-HMS model. Hydraulic modelling was done in HEC-RAS model and flood inundation maps were developed to study the water surface

profiles of velocity and depth of flood flow and its characteristics. Flood vulnerable land use areas were identified and vulnerability maps were developed according to the land use pattern of Chalakudy river basin.

During the calibration period (2005-2007), the highest flow volume was seen in 2007, with a simulated flow of 2519.68 Mm^3/year and an actual flow of 2757.76 Mm^3/year. Similarly, the lowest flow volume was observed in 2006, with 1401.75 Mm^3/year simulated and 1344.34 Mm^3/year observed. During the validation period (2009-2010), the highest volume of flow was seen in 2009, with a simulated flow of 2984.30 Mm^3/year and an actual flow of 2897.02 Mm^3/year. Similarly, the lowest volume of flow was seen in 2010, with a simulated flow of 1284.39 Mm^3/year and an observed flow of 1246.99 Mm^3/year. The maximum peak flow of the river was seen in 2009, with the predicted value as 1299.63 m^3/s and the actual value as 1389.00 m^3/s. The predicted value was acceptable because the peak flow error was in the range of 20%. Statistical performance indices of the model, Nash-Sutcliffe efficiency (NSE) and Coefficient of correlation (R^2) values were obtained above 0.7, Error in Peak Flow (%) and Error in Volume (%) were obtained below 20% and Root Mean Square Error-Standard Deviation Ratio (RSR) was got as 0.5 and below. These values indicated that HEC-HMS model simulation performed well in both calibration and validation. The model performance in rainfall-runoff transformation indicated its applicability for the study area.

The results obtained for flood frequency analysis from HEC-SSP software matched with HEC-HMS model predicted flood values. The expected probable discharges obtained by Log – Pearson type III distribution were 1175.7 m^3/s, 1408.8 m^3/s, 1744.8 m^3/s, 2032 m^3/s , 2380 m^3/s and 2812.8 m^3/s for the return periods 10, 20, 50, 100, 200 and 500 year respectively, while the discharges obtained by Gumbel distribution were 1186.5 m^3/s, 1418.0 m^3/s, 1755.2 m^3/s, 2026.5 m^3/s, 2317.8 m^3/s and 2769.1 m^3/sec respectively and the discharges got by Log Normal distribution were 1183.8 m^3/s, 1429.5 m^3/s, 1753.1 m^3/s, 1999.6 m^3/s, 2342 m^3/s and 2753 m^3/s

respectively for the same return periods. The measured flood peak values of HEC-HMS model for the same return periods were 1173.2 m³/s, 1415.6 m³/s, 1742.8 m³/s, 1985.3 m³/s, 2335.9 m³/s and2732.5 m³/s. The frequency discharge values calculated using Log Pearson type-III indicated a high degree of similarity to the HEC-HMS predicted values with an R^2 value of 0.862. The results of the other two methods were significantly lower than those of the HEC-HMS predicted values. For all return periods of 10, 20, 50, 100, 200 and 500, it was found that Log Pearson Type-III distribution had a good correlation with model predicted flood peak values.

This study presents a systematic approach in the preparation of flood vulnerability map with the application of steady flow models and GIS. The major tools/models used in this method were one-dimensional model HEC-RAS and Arc-GIS for spatial data processing and geometric data generation by RAS Mapper. HEC-RAS for steady flow analysis showed discharges of 1173.2 m³/s, 1415.6 m³/s, 1742.8 m³/s, 1985.3 m³/s, 2335.9 m³/s, and 2732.5m^3/s, inundating 2783.25, 2980.46, 3217.72, 3381.27, 3582.65 and 3800.83 ha respectively. The assessment of the vulnerability to flooding was done with regard to the land use pattern and cadastral map of Chalakudy river basin in the flood areas for different return periods. Superimposing of cadastral level map of the river basin and flood inundated area polygons for different return periods gave Panchayath wise flood risk areas. Kadukutty Panchayath located in the downstream of Chalakudy river basin was found to be a maximum flood inundated area for 10 year return period (557 ha) and for 200 year return period (681 ha). Manjapra Panchayath located in the upstream was found to be the least flood inundated area for 10 return period (6 ha) and for 200 year return period (9 ha). Annamanada, Kadukutty, Melur and Pariyaram panchayaths were under high risk areas, with depths greater than 20 m. Ayyampuzha, Chalakudy, Mala, Kuzhur, Parakkadavu and Puthenvelikara panchayaths were under medium risk area with depths varying from 10 to 20 m. Athirappilly, Manjapra and Karukutty panchayaths were under low risk areas with depths less than 10 m.

The flood vulnerability maps were generated by intersecting the flood plain land use map with the flooded area polygons. The assessment of the flood area indicates that the paddy land varies from 949 to 1361 ha, forest/other vegetation ranges from 528 to 805 ha, barren land varies from 201 to 304 ha, urban land varies from 127 to 172 ha, water body varies from 762 to 873 ha, tea/oil palm varies from 53 to 95 ha and coffee/cardamom ranges from 162 to 191 ha. It was observed that as flooding intensity increased, the flooded area increased, with paddy being the first lan use class to be inundated by different year floods, followed by forest/other vegetation, barren land and other land use classes.

The study area risk map indicates that even a 10-year flood has a major impact on agriculture, which is increased by a 100-year storm flood. Even with a 10-year return period storm, flooding in the Chalakudy river basin is devastating. This indicates the need for engineering structures such as dykes and levees to be built along the river channel and lower reaches of the flood plain. Topographic analysis based on GIS and RAS Mapper data is much more efficient in accurately representing terrain nature. The higher the DEM resolution, the more accurate will be the geometric data of the river and more accurate flood maps can be generated. Flood plain study highly depends on hydrologic data. The availability of hourly time series data improves model accuracy. In regions where the river meanders, additional cross sections are used to prevent errors during interpolation.

The study concluded that the infrastructure development and planning should be integrated giving due consideration to flood hazard and risk reduction. It is important that such maps be updated on a regular basis. According to the flood maps created for this study, heavy settlement and agricultural lands are present around flood prone areas in the Chalakudy river basin. In such cases, developing and implementing flood management measures for raising awareness, preparedness and developing coping strategies is crucial. Communities' capacity to withstand floods should be strengthened by non-structural measures at the local level. To ensure flood

risk and hazard reduction, a network of emergency operation centers could be established at the district and municipal levels. Dams, levees, embankments and barrages are examples of structural flood management projects. Flood protection for residential and agricultural areas should also be implemented. However, such structures are normally designed to withstand a 1-in-10-year flood as higher values may not be economical.

Local area action plans are required to address flood management issues in the basin. The excess flood waters of Chalakudy basin can be diverted to the rain shadow belt of Bharathapuzha basin by Inter Basin Water Transfer (IBWT). Revisiting the operational schedules of dams in Chalakudypuzha basin linked with the PAP-IBWT project and reducing the inflows to the basin can be thought of. The possibility of building medium to minor scale control structures in the uncontrolled catchments of Chalakudy basin is yet another solution to be consiered. Flood protection for residential and agricultural areas should also be implemented. Integrated Water Resources Management (IWRM) is the most effective tool for managing floods as well as droughts. Building adequate institutional arrangements for implementing IWRM at the basin scale of Chalakudy river must be the policy intervention that the Government and planners should consider. The concepts –'Room for river' and 'living with water' –the pillars of IWRM should be practiced effectively.

Scope for future work

- The geometry of the river can be developed using high resolution DEM or real field survey data so that the topography of the flood channel and flood plains could be better represented.
- Long term discharge data can be used to model the floods on a continuous time scale.
- TINs obtained using new technologies such as LIDAR (Light Detection and Ranging), which improves the quality of the digital terrain representations can be used for better results.

REFERENCES

Abbott, M. B. and Refsgaard, J. C. 1996. *Distributed Hydrological Modeling*. In: Water Science and Technology Library (Eds.). doi: 10.1007/978-94-009 0257-2.

Abdessamed, D., Abderrazak, B. and Kamila, B. 2018. Modelling rainfall runoff relations using HEC-HMS in a semi-arid region: Case study in Ain Sefra watershed, Ksour Mountains (SW Algeria). *J. water land Dev*. 36 (3): 45–55.

Abed, N. A., Abdulla, F. and Khayarah, A. A. 2005. GIS-hydrologic models for managing water resources in the Zarqa river basin. *Environ. Geol*. 47: 405-411.

Abera, Z. 2011. Flood Mapping and Modeling on Fogera Flood Plain: A Case Study of Ribb river, Ethiopia. M. Tech (Hydraulic Engineering) thesis, Addis Ababa Institute of Technology.

Abood, M. M., Mohammed, T. A., Ghazali, A. H., Mohamud, A. R. and Sidek, L. M. 2012. Impact of infiltration methods on the accuracy of rainfall-runoff simulation. *Res. J. Appl. Sci. Eng. Tech*. 4(12): 1708-1713.

Abhas K. J., Robin, B. and Jessica, L. (2012). Cities and Flooding; A Guide to integrated urban flood risk management for the 21st Century, electronic document.Retrieved fromhttp://www.gfdrr.org/gfdrr/sites/gfdrr.org/files/urban floods/pdf/Cities%20and%20Floodi ng%20Guidebook.pdf.Accessed21 November 2012.

Adnan, N.A. and Atkinson, P.M. 2018.Disentangling the effects of long-term changes in precipitation and land use on hydrological response in a monsoonal catchment. *J. Flood Risk Manag*. 11: 1063–1077.

Ahmad, U. N., Shabri, A. and Zakaria, Z. A. 2011. Flood frequency analysis of annual maximum stream flows using L-Moments and TL-Moments. *Appl. Math. Sci*. 5: 243– 253.

Akbarpour, M. 2004. Simulation of Rainfall-Runoff Process by Artificial Neural Networks and HEC- HMS Models in Zard River Basin. In: *Proceedings of the Fourth International Iran and Russia Conference*. pp. 1143-1148.

Alaghamand, S., Abullah, R. and Abustan, I. 2011. Selecting the best set value in calibration process for the validation of hydrological modelling(Kayu Ara river basin, Malaysia.*Res. J. Environ. Sci.* 5(4): 354-365.

Alemaw, B. S. F. and Chaukra, T. R. 2003. A continental water balance model: a GIS approach for southern Africa. *Phys. Chem. Earth Parts*. 20 (28): 957-966.

Alfredo, R. N., Larissa, F. D., Romão, B. and Roberto Q.C. 2016. Methodologies for generation of hazard indicator maps and flood prone areas.*Revista Brasileira de Recursos Hídricos*,21: 377 – 390.

Ali, M. Khan, S. J., Aslam, I., and Khan, Z. 2011. Simulation of the impacts of land-use change on surface runoff of Lai Nullah basin in Islamabad, Pakistan. Landscape and Urban Planning. 102. 271-279. 10.1016/j.landurbplan.2011.05.006.

Ali, E. N. and Jaber, M. 2018. Flood plain analysis using ArcGIS, HEC GeoRAS and HEC-RAS in Attarat Um Al-Ghudran Oil Shale Concession Area, Jordan. *Civil Environ Eng.* 8: 323.

Arekhi, S. 2012. Runoff modeling by HEC-HMS Model (case study: Kan watershed, Iran). *Int. J. Agric. Crop Sci*. 4(23): 1807-1811.

Arturo, V. M. 2018. Effect of climatic oscillations on flood occurrence on Papaloapan river, México, during the 1550–2000 period. *Nat. Hazards*. 94: 167–180.

Asadi A. and Boostani F. 2013. Application of HEC-HMS for flood forecasting in Kabkian basin and Delibajak sub basin in Iran. *IOSR J. Eng*. 3 (9): 2250-3021.

Avanti, W., Aarti, P., Pragati, B. and Rajashri, B. 2020. Flood modeling and flood forecasting using HEC-RAS. *International Journal of Advance Scientific Research and Engineering Trends.* 5(6).

Bakir, M. and Xingnan, Z. 2008. *GIS-based hydrological modelling: A comparative study of HEC-HMS And the Xinanjiang model*. Int. water Tech. conf.IWTC12 Alexandria, Egypt.

Bartles, M. and Fleming, M. 2017. Estimation of flow, volume, and stage-frequency for use in dam and levee safety studies within HEC-SSP and HEC-HMS. *World Environmental and Water Resources Congress*. pp.78-91.doi:10.1061/9780784480601.008.

Birkhead, A. and James, C. S. 2002. Muskingum river routing with dynamic bank storage. *J. Hydrol*. 264 (1):113-132.

Bikram, M. Mohan, K. B., Ripendra,A. and Biswombher, M.P. *Floodplain analysis and risk assessment of Lothar Khola.* 11th ESRI India User Conference 2010.

Boyaj, A., Ashok, K., Ghosh, S., Devanand, A. and Dandu, G. 2018. The Chennai extreme rainfall event in 2015: The Bay of Bengal connection. Climate Dynamics. DOI:10.1007/s00382-017-3778-7.

Butler, D. and Davies, J. W. 2004. Urban drainage.11 New Fetter Lane, London EC4P 4EE: Spon Press, Taylor & Francis e-Library

Cheng, C. T., Ou, C. and Chau, K. 2002. Combining a fuzzy optimal model with a genetic algorithm to solve multi-objective rainfall–runoff model calibration. *J. Hydrol*. 268: 72–86.

Choudhari, K., Panigrahi, B. and Paul, J. C. 2014. Simulation of rainfall-runoff process using HEC- HMS model for Balijore Nala watershed, Odisha, India. *Int. J. Geomatics Geosciences*. 5 (2): 253-264.

Christopher, T. 1999. Floodplain mapping using HEC-RAS and ArcView GIS, Austin. Ph.D thesis, The University of Texas at Austin.

Chow, V. T. 1951. A generalized formula for hydrologic frequency analysis. *Trans. Am. Geophys. Union*. 32 (2): 231–237.

Clay, H.E., Claire, W.and Travere, R.G. 2005.Watershed scale evaluation of a system of storm water detention basin. *J. Hydrol. Eng*. 3: 237-242.

CWC. 2018. Basin Report: West flowing rivers from Tadri to Kanyakumari.

Demetrio, A. Z., Antonino, L., Domenico, M. and Santo, M. Z. 2016.Comparing Different Infiltration Methods of the HEC-HMS Model: The Case Study of the Mésima Torrent (Southern Italy*). Land degradation and Dev*. 28(1): 294-308.

Department for International Development (DFID).Source book for sustainable flood mitigation strategies, electronic document. http://www.dfid.gov.uk/r4d/PDF/Outputs/Water/R8159-Source_Book.pdf. Accessed 21. November 2012.

Drissia, T. K., Jothiprakash, V. and Anitha, A. B.2019. Flood Frequency Analysis Using L Moments: a Comparison between At-Site and Regional Approach. *Water Resour. Manag*. 33: 1013–1037.

Fisherman, L. 2015. Probability analysis of flow volumes using the joke-SSP software tool. Diploma thesis, Faculty of Civil Engineering and Geodesy, 70 p.

Fleming, M. 2004. Description of the Hydrologic Engineering Center's Hydrologic Modelling System (HEC-HMS) and application of watershed studies. *Smart Tech. Notes Collection*, ERDC/TN SMART: 4-3.

George, S. L. and Gary, D. T. 2000. *Flood-Frequency Prediction Methods for Unregulated Streams of Tennessee*. U.S. Geological Survey Water-Resources Investigations Report 03-4176, Nashville, Tennessee, U.S. pp.1-79.

Gupta, A. K. and Nair, S. S. 2011. Urban floods in Bangalore and Chennai: Risk management challenges and lessons for sustainable urban ecology. Curr. Sci. DOI:10.1016/j.ajodo.2005.02.022.

Haan, C. T. 1977. *Statistical Methods in Hydrology*. Iowa State University Press, Iowa.

Hakim, F. A., Alam, A., Sultan, B. M. and Shabir A. 2016.One dimensional steady flow analysis using HECRAS – A case of River Jhelum, Jammu and Kashmir. *European Scientific Journal*. 12(32): 340-350.

Halwatura, D. and Najim, M. M. M. 2013. Application of the HEC_HMS model for runoff simulation in a tropical catchment. *J. Environ. Modeling Software*. 46: 155-162.

Hammouri, N. and Naqa, A. E. 2007. Hydrological modeling of ungauged wadis in arid environments using GIS. *Revista Mexicana de Geologicas*. 24(2): 185-196.

Hilbert, A. A. 2015. Rainfall runoff simulation using modified SCS-CN and HEC-HMS model in Kuantan watershed. B.Eng (Civil) thesis, Universiti Malaysia Pahang, 82p.

Hoblit, B. C. and Curtis, D. C. 2001. Integrating radar rainfall estimates with digital elevation models and land use data to create an accurate hydrological model. In: *Flood Plain Management Association Spring 2001 Conference*. 13-16 March 2001, San Diego, California.

Horritt, M. S. and Bates, P. D. 2002. Evaluation of 1D and 2D numerical models for predicting river flood inundation. J. Hydrol. 268, 87–99.

Hu, H. H., Kreymborg, L. R., Doeing, B. J., Baron, K. S. and Jutila, S. A. 2006. Gridded snowmelt and rainfall-runoff CWMS hydrologic modeling of the Red river of the North basin. *J. Hydrol. Eng.* 11(2): 91-100.

Interagency Advisory Committee on Water Data. 1982.Guidelines for determining flood flow frequency: U.S. Geological Survey, Office of Water Data Coordination Bulletin 17B. 186p.

Islam, R. 2015. A review on watershed delineation using GIS tools. https://www.researchgate.net/publication/240626931.

Ismael, O., Joseph, K. S. and Patrick, G. P. 2017. HEC-HMS model for runoff simulation in Ruiru reservoir watershed. *American J. of Eng. Res.* 6(4):1-7.

Izinyon, O. C. and Igbinoba, E. 2011. Flood Frequency Analysis of Ikpoba River Catchment at Benin City using Log Pearson Type III distribution. *J. Emerging Trends Eng. and Appl. Sci*. 2 (1): 50-55.

Joan, C. C., Maurice, D., Rosa, D. L. R. and Julie, C. U. 2019. Potential of the Molawin creek for micro hydro power generation: An assessment. *Sustain. Energy Technol. Assess*. 32: 111-120.

Joo, J., Kjeldsen, T., Kim, H. and Lee, H. 2013. A comparison of two event-based flood models (ReFH-rainfall runoff model and HEC-HMS) at two Korean catchments, Bukil and Jeungpyeong. *KSCE J. Civil Eng*. 18: 330–343.

Kabiri. 2014. Simulation of the runoff using modified SCS-CN method using GIS system. *Res. J. Environ. Sci*. 8(4): 178-192.

Kamali, B. and Mousavi, S. J. 2014. Automatic calibration of HEC-HMS model using multi-objective fuzzy optimal models. *Civil Eng. Infrastructures J.* 47(1):1–12.

Kaur, R., Kumar,S and Gurung, H. P. 2002. A pedo-transfer function (PTF) for estimating soil bulk density from basic soil data and its comparison with existing PTFs**.***Australian J. of Soil Res.* 40(5) :847 – 858.

Kerala state electricity board Ltd. May 2020. Emergency action plan for Sholayar main/Flanking/Saddle dams.

Khaleghi, S. Mahmoodi, M and Sorayya, K. 2015. Integrated application of HEC-RAS and GIS and RS for flood risk assessment in Lighvan Chai River. *International Journal of Engineering Science Invention*. 4(4):38-45.

Khan, M. 2015. The comparison of Normal, Lognormal, Log Pearson Type III and Gumbel Distribution for Krishna river and evaluation of best distribution. *Eur. J. Environ. Ecol.* 2: 146-150.

Khalil, U., Muhmmad, N. and Habib, R. (2015). Assessment of flood using geospatial technique for Indus river reach: Chashma-Taunsa. *Science International*. 27(3).

Kite, G. W. and Pietroniro, A.1996. Remote sensing applications in hydrological modelling. *Hydrol. Sci. J*. 41 (4): 63-591.

Knebl, M. R., Yang, Z. L. Hutchison, K. and Maidment, D. R. 2005. Regional scale flood modeling using NEXRAD rainfall, GIS, and HEC-HMS/RAS: a case study for the San Antonio River Basin Summer 2002 storm event. *J. Environ. Manag*. 75 (4): 325- 336.

Koneti, S., Sunkara, S. L. and Roy, P. S. 2018.Hydrological modelling with respect to impact of land-use and land-cover change on the runoff dynamics in Godavari river basin using the HEC-HMS model. *Int. J. for Geo-Inf.* 7,206.

Kristi, R. and Tatiana, H. P. 2010. *Hydrologic analysis of flash floods in Sana'a, Yemen*. Watershed Management Conference.Washington University, St. Louis, Missouri. pp 1248-1259. https://doi.org/10.1061/41143(394)112.

Kumar, A. 2013. Demystifying a Himalayan tragedy: study of 2013 Uttarakhand disaster. *Jour. Indian Res.*, 1(3):106–116. Retrieved from http://mujournal.mewaruniversity.in/jir3/jir3.pdf#page=114

Law, G. S. and Tasker, G. D. 2003. Flood-frequency prediction methods for unregulated streams of Tennessee. *Water Resources Investigations Report No. 03-4176, Nashville, Tennessee*.

Legesse, D., Vallet, C. C. and Gasse, F. 2003. Hydrological response of a catchment to climate and land used changes in Tropical Africa: case study South Central Ethiopia. *J. Hydrol*. 275:67-85.

Linsley, R. K., Kohler, M. A. and Paulhus, J. L. H. 1982. *Hydrology for Engineers*. Third Edition, McGraw-Hill.

Majidi, A. and Shahedi, K. 2012. Simulation of rainfall-runoff process Using Green-Ampt method and HEC-HMS model (Case Study: Abnama Watershed, Iran). *Int. J. Hydraulic Eng*. 1 (1): 5-9.

Majidi, A. and Vagharfard, H. 2013. Surface runoff simulation with two methods using HEC-HMS model. *Curr. Advantages Environ. Sci*. 1 (1): 7-11.

Maya, K. 2005. Studies on the nature and chemistry of sediments and water of periyar and Chalakudy rivers, Kerala, India. PhD. (Marine geology) thesis, The Cochin University of Science and Technology. 129p.

McCarthy, G. T. 1938. The unit hydrograph and flood routing. Conference North Atlantic Division, US Army Corps of Engineers, New London, Connecticut, USA.

Melo, I., Tomasik, B., Torrieri, G., Vogel, S., Bleicher, M., Korony, S. and Gintner, M. 2009. Kolmogorov-Smirnov test and its use for the identification of fireball fragmentation. *Phys. Rev. C*. 80 (2): 1-8.

Mihalik, E. N., Levine, S. N. and Amatya, M. D. 2008. Rainfall-runoff modeling of Chapel Branch Creek watershed using GIS-based Rational and SCS-CN method. *ASABE Annual International Meeting,* June 29 – July 2, 2008, ASABE Rhode Island Convention Center Providence, Rhode Island, USA. pp. 1-15.

Mike, B. and Matthew, F. 2019. Paleo flood enhancements within HEC-SSP. *AGU's Fall Meeting*. December 9 – 13, 2019. Moscone South - Poster Hall, San Francisco.

Mishra, V. and Harsh, L. S. 2018. Hydroclimatological Perspective of the Kerala Flood of 2018. *Journal Geological Society of India*. 92: 645-650.

Mishra, V., Aadhar, S., Shah, Harsh, Kumar, Rahul , Pattanaik, D., Tiwari, and Amar. 2018. The Kerala flood of 2018: combined impact of extreme rainfall and reservoir storage. *Hydrology and Earth System Sciences Discussions.* 1-13.

Muhammad, S. I., Zakir, H. D., Erik, P. Q., Asif, K. and Nynke, H. 2016. Impact of climate change on flood frequency and intensity in the Kabul river basin. *Geosciences.* 8(114): 2-16. doi:10.3390/geosciences8040114.

Mujere, N. 2011. Flood frequency analysis using the Gumbel distribution. *International J. Comput. Sci. and Eng*. 3: 2774-2778.

Mukherjee, S., Aadhar, S., Stone, D. and Mishra, V. 2018. Increase in extreme precipitation events under anthropogenic warming in India. Weather and Climate Extremes. DOI:10.1016/j.wace.2018.03.005

Najim, M. M. M., Babelb, M. S. and Loofb, R. 2006. AGNPS Model Assessment for a Mixed Forested Watershed in Thailand. *Sci. Asia*. 32: 53–6.

Nareth, Nand, P. V. 2015. Flood plain mapping using HEC-RAS and GIS in Nam Phong river basin, Thailand. *International Journal of Environmental and Rural Development* . 6-1.

Narasayya, K. 2015. A Geo-Informatic approach to estimate stream flow of an un developed catchment-a hypothetical research. *Int. J. Advmtin Remote Sensing GIS and Geography*. 3(1): 22-31.

Nchumbeni, M. O. and Rema, K. P. 2020. Impact of land use land cover change on runoff processes of Chalakudy river basin. *IJCMAS.* 5(3):456-464.

Olayinka, D., N. and Hudson E. I. 2017. Flood modelling and risk assessment of Lagos Island and Part of Eti-Osa local government areas In Lagos State. *Journal of Civil and Environmental Systems Engineering.* 15(1): 106- 121.

Pampaniya, N. K., Tiwari, M. K. and Gaur, M. L. 2015. Hydrological modeling of an agricultural watershed using HEC-HMS hydrological model, remote sensing and geographical information system. *16th Esri India User Conf.*

Parvathy, S and Thomas, R. 2021. *Impact of urbanization on flooding in Chalakudy river*. IOP Conf. Series: Materials Science and Engineering. doi:10.1088/1757-899X/1114/1/012025.

Paudel, R. C., Basnet, K. and Sherchan, B. 2019. Application of HEC-HMS model for runoff simulation: A case study of Marshyangdi river basin in Nepal. *Proceedings of IOE Graduate Conf., 2019-Winter*.

Pickands, J. 1975. Statistical inference using extreme order statistics. *Ann Stat*. 3:119–131.

Praful, K.V. Timbadiya, P. L. P., Prakash, D. and Porey. 2011. Calibration of HEC-RAS model on prediction of flood for Lower Tapi River. India. *Journal of Water Resource and Protection.* 3: 805-811.

Prabeer, K. P. 2017. Flood management in Mahanadi Basin using HEC-RAS and Gumbel's Extreme Value Distribution. *Journal of the Institution of Engineers.* 99(4):751–755.

Praveen, R., Kalpesh, B. and Manekar, V. L. 2015. Simulation of Rainfall - Runoff Process using HEC-HMS (Case Study: Tapi River, India). *Hydro 2015 International*, 20th International Conference on Hydraulics, Water Resources and River Engineering, 17-19 December, IIT Roorkee, India.

Rahman, A., Zaman, M. A. and Haddad, K. 2015. Applicability of Wakeby distribution in flood frequency analysis: a case study for Eastern Australia. *Hydrol. Process*. 29: 602–614.

Rathod, P., Kalpesh, B. and Vivek, M. 2015.Simulation of rainfall-runoff process using HEC-HMS. *20th Int. Conf. on Hydraulics, Water Resour. and River Eng.*

Razi, M. A. M., Ariffin. J., Tahir. W. and Arish, M. A. M. 2010. Flood estimation studies using hydrological modelling system (HEC-HMS) in Johor river, Malaysia. *J. Appl. Sci.* 10(11): 930-939.

Reshma, T., Venkata, R. K. and Deva, P. 2013. Simulation of event based runoff using HEC-HMS model for an Experimental Watershed. *Int. J. of Hydraulic Eng.* 2(2):28-33.

Rossi, C. G., Dybala, T. J., Moriasi, D. N., Arnold, J. G., Amonett, C. and Marek, T. 2008. Hydrologic calibration and validation of the Soil and Water Assessment Tool for the Leon river watershed. *J. Soil and Water Conserv.* 63(6): 533-541.

Sabzevari, T., Ardakanian, R., Shamsaee, A. and Talebi, A. 2009. Estimation of flood hydrograph in no statistical watersheds using HEC-HMS model and GIS (Case study: Kasilian watershed). *J. Water Eng.* 4:1–11.

Sai, V. K., Muthappa, K. J, Gowtham, P. M. E, Shruthi, H.G., Shivaprasad, H. and Nagaraj, S. R. 2017. Applicability of HEC-HMS tool to Western Ghats - Nethravathi river basin. *Int. J. Advanced Res. Eng. Manag*. 3(4): 70-79.

Salajegheha, A., Bakhshaeib , M., Chavoshic , S. , Keshtkara , A. R. and Najafi, H. M. 2009. Flood plain mapping using HEC-RAS and GIS in semi-arid regions of Iran. *Desert*. 14 : 83-93.

Sampath, D. S., Weerakoon, S. B. and Herath, S. 2015. HEC-HMS model for runoff simulation in a tropical catchment with Intra-Basin diversions - Case study of the Deduru Oya river basin, Sri Lanka. *Inst. Eng.*1: 1-9.

Santillan, J., Makinano, M. and Paringit, E. 2011. Integrated Landsat image analysis and hydrologic modeling to detect impacts of 25-year land-cover change on surface runoff in a Philippine watershed. *Remote Sensing*. 3: 1067–1087.

Sandhyarekha. and Shivapur, A. V. 2017. Flood plain mapping of river Krishna using HEC-RAS model at two streaches namely Kudachi and Ugar villages of Belagavi district, Karnataka. *International Research Journal of Engineering and Technology (IRJET)*.04(08): 1524-1529.

Sardoii, E. R., Rostami, N., Sigaroudi, S. K. and Taheri, S. 2012. Calibration of loss estimation methods in HEC-HMS for simulation of surface runoff. *Adv. Environ. Biol*. 6(1): 343-348.

Sarma, P. 1999. Flood risk zone mapping of Dikrong sub basin in Assam, available at: http://www.gisdevelopment.net/application/natural_hazards/floods.

Sathya, A. and Santosh G. T. 2021. Flood Inundation Mapping of Cauvery River Using HEC- RAS and GIS. *Advances in Civil Engineering*.83: 15-23.

Scharffenberg, W. and Harris, J. 2008. Hydrologic Engineering Center Hydrologic Modeling System, HEC-HMS: interior flood modeling. In: *World Environmental and Water Resources Congress*, 12-16, May 2008, Honolulu,Hawaii, U.S.A [On-line]. Available: https://doi.org/10.1061/40976(316)632.

Selman, O. and Fevzi, O. 2020. Flood analysis with HEC-RAS: A case study of Tigris river. *Advances in Civil Engineering.*10:1-13.

Serede,I. J., Raude, J. M. and Mutua, B. M. 2015. Hydraulic Analysis of Irrigation Canals using HEC-RAS Model: A Case Study of Mwea Irrigation Scheme, Kenya. International Journal of Engineering Research & Technology (IJERT).04(09).

Seth, I., Soonthornnonda, P. and Christensen, E. R. 2006. Use of GIS in urban storm-water modelling. *J. Environ. Eng.* Vol 132. 12p.

Shahzad ,M. K., Anwar, F., Usman, T. S., Sharif , M., Sheraz, Khurram. and Ahmed, A.2016. Floodplain mapping using HEC-RAS and Arc-GIS: A Case Study of Kabul river. *Arab J Sci Eng.* 41:1375–1390.

Singh, P., Gupta, A. and Singh, M. 2014.Hydrological inferences from watershed analysis for water resource management using remote sensing and GIS techniques. *Egyptian J. Remote Sensing Space Sci.* 17 (2): 111-121.

Skhakhfa, I. D. and Ouerdachi, L. 2016. Hydrological modelling of wadi Ressoul watershed, Algeria, by HEC-HMS model. *J. Water and Land Dev*. 31 (1): 139-147.

Subramanya, K. 2008. *Engineering Hydrology*. Tata McGraw-Hill Publishing Company Limited, New Delhi, India.

Su, Z., Neumann, P., Schumann F. A. and Schultz G. A. 1992. Application of remote sensing and geographic information system in hydrological modeling. *Earsel. Adv.remote sensing. 1: 3-7.*

Sudheer, K. P., Thomas, J., Bhallamudi, M. and Bindhu, V. M. 2019. Role of dams on the floods of August 2018 in Periyar river basin, Kerala. *Curr. sci. 116(5):* 780-794.

Sunilkumar, P. and Vargheese K, O. 2017. Flood modelling of mangalam river using GIS and HEC-RAS. *International Journal of Advance Research in Science and Technology*. 6(06): 159-169.

Supe, M. S., Taley, S. M. and Kale, M. U. 2015. Rainfall-runoff modelling using HEC- HMS for Wan river basin. *Int. J. Res. Eng. Sci.Tech.* 1(8): 21-28.

Tassew, B. G., Belete, A. M. and Miegel, K. 2019. Application of HEC-HMS Model for Flow Simulationin the Lake Tana Basin: The Case of Gilgel Abay Catchment, Upper Blue Nile Basin, Ethiopia. *Hydrol*. 6 (21):1-17.

Thakur, J. K., Singh, S. K. and Ekanthalu, V. S. 2016. Integrating remote sensing, geographic information systems and global positioning system techniques with hydrological modeling. *Appl. Water Sci*. 34 (3): 1-14.

The Hindu, 02 June 2020. https://www.thehindu.com/news/national/kerala/kerala-agricultural-university-prepares-flood-map-for-chalakudy-river-basin/article31728976.ece.

Thomas, D. G. and Mark,E. H. 2015. *Introduction to Environmental Forensics* (3rd Ed.), *Statistical Methods*. Academic Press, pp. 99-148.

Tumbare, M. J. 2000. Sustainable Use of Water Resources. Mitigating floods in Southern Africa. In: *1st WARSFA/Water Net Symposium*. Maputo: Univ. of Zimbabwe Press. pp. 1-8.

Tunas, I. G. Arafat, Y. and Azikin, H. 2019. *Integration of Digital Elevation Model (DEM) and HECRAS Hydrodynamic model for flood routing*. IOP Conf. Series: Materials Science and Engineering.

USACE. 2000. *HEC-HMS Hydrologic Modeling System Technical Reference Manual*. Hydrologic Engineering Center, Davis, California. 103p.

USACE. 2000. *HEC-HMS* Hydrologic Modeling System User's Manual. Hydrologic Engineering Center, Davis, California.

USACE. 2008. Hydrological modeling system, HEC-HMS, user's manual, version *3.3*. Davis, CA, USA.

Vahdettin, D. and Kisi, O. 2016. Flood hazard mapping by using geographic information system and hydraulic model: Mert river, Samsun, Turkey. *Advances in Meteorology*. 1- 9.

Verma, A. K., Jha, M. K. and Mahana, R. K. 2009. Evaluation of HEC-HMS and WEPP for simulating watershed runoff using remote sensing and geographical information system. *Paddy and Water Environ*. 8 (2): 131-144.

Wai, J. X. 2015. *Comparative Study of Flood Frequency Method on Selective Rivers.* Other thesis, INTI International University, Malaysia, 2p.

Waikhom, R. S. and Manoj, K. J. 2015. Continuous Hydrological Modeling using Soil Moisture Accounting Algorithm in Vamsadhara River Basin, India. *J. Water Resour. Hydraulic Eng.* 4 (4): 398-408.

Wang, F. G. and Wang, X. D. 2010. Fast and robust modulation classification via Kolmogorov- Smirnov Test. *IEEE Trans. Commun*. 58(8): 2324- 2332.

Yao, C., Chang, L., Ding, J., Li, Z., An, D. and Zhang, Y. 2014. *Evaluation of the effects of underlying surface change on catchment hydrological response using the HEC-HMS model.* Proceedings of the International Association of Hydrological Sciences. 364: 145-150.

Yener, M. K., Şorman, A. U.,Şorman, A. A., Şensoy, A. and Gezgin, T. 2008. Modeling studies with HEC-HMS and runoff scenarios in Yuvacik basin, Turkiye. *Int. Congr. River Basin Manag.* 623-634.

Zelenhasic, E. 1970.Theoretical probability distributions for flood peaks. Colorado University Press, Colorado.

Zeng, X., Dong, W. and Jichun, W. 2015. Evaluating the three methods of Goodness of Fit Test for frequency analysis. *J. Risk Anal. Crisis Response*. 5: 178-187.

Zhang, D. P. and Luo, Y. L. 2000. Applied Probability and Statistic. Higher Education Press, Beijing.

APPENDIX I

Average daily rainfall (mm) over the Chalakudy basin (1997-2017)

Day	Jan	Feb	Mar	Apr	May	Jun	Jul	Aug	Sep	Oct	Nov	Dec
1	0.11	0.3	0	1.39	4.27	5.64	20.21	16.54	12.44	10.96	8.3	2.11
2	0.13	1.3	0.14	1.54	3.15	13.25	24.56	17.12	13.14	8.72	9.83	1.42
3	0.12	0.02	0.91	0.66	2.54	9.42	21.24	14.45	13.02	16.07	4.36	1.26
4	0.23	0.06	2.67	2.51	6.09	8.25	19.96	22.92	7.93	11.7	3.59	0.91
5	0	0.17	0.9	1.45	7.07	11.99	19.13	18.28	8.69	9.11	4.15	0.12
6	0	0.17	1.55	4.58	6.39	15.84	17.03	19.9	11.23	7.89	6.25	0.15
7	0	0.26	2.38	3.19	7.07	17.43	15.75	16.15	11.72	8.08	8.85	0.66
8	0	0.02	0.73	2.72	8.93	16.08	13.81	15.39	10.16	11.38	8.35	1.05
9	0.19	0.12	0.27	2.76	7.46	12.09	15.55	15.99	10.82	6.3	7.27	1.51
10	0.52	0	3.6	2.48	2.05	11.79	22.41	17.09	9.17	5.8	9.92	1.47
11	0.02	0.62	0.48	1.58	3.44	13.71	21.02	15.61	8.94	8.25	3.57	2.36
12	0	0.34	0.71	1.7	1.88	20.28	22.85	13.03	8.36	11.17	3.89	1.12
13	0.08	0.87	2.18	2.48	5.41	20.99	16.26	11.36	6.77	11.28	2.02	1.22
14	0.43	0	2.52	2.78	2.78	18.76	22.01	9.96	9.17	15.77	1.54	1.44
15	0.06	0.56	2.25	2.62	1.61	18.34	19.97	9.42	8.41	13.91	3.23	0.87
16	0	1.07	3.33	1.83	4.38	14.88	26.03	13.51	11.57	11.46	3.17	0.5
17	0.07	0	1.86	4.19	4.87	17.96	29.53	14.56	12.33	8.23	1.91	0.38
18	0	0.17	1.82	3.94	6.22	18.44	27.74	13.49	10.32	8.21	4.93	0.59
19	0	1.47	2.05	3.58	6.85	17.77	18.27	9.35	9.75	8.19	3.42	2.7
20	0.02	0	1.54	3.19	1.84	16.14	15.51	12.97	7.11	10.54	2.48	1.99
21	0	0.01	1.58	6.12	3.05	15.77	14.69	15.57	5.44	8.36	4.15	1.56
22	0.02	0.14	1.42	3.73	2.27	20.54	13.19	14.7	5.82	8.06	6.96	0.29
23	0.05	0.16	1.13	2.85	3.66	23.01	13.07	12.57	8.86	6.14	5.48	0.05
24	0	0.63	0.87	5.69	5.58	22.59	16.03	10.15	9.54	9.39	4.7	0.02
25	0	1.39	0.4	4.73	7.73	17.29	13.34	9.59	8.05	8.81	1.26	0
26	0	1.78	1.54	3.13	6.82	16.81	15.3	9.79	9.77	10.54	3.53	0
27	0	1.95	2.42	5.46	6.81	22.76	16.36	9.3	7.13	9	2.39	0.15
28	0.02	0.5	0.69	3.98	8.11	23.34	19.44	9.56	7.91	12.67	1.08	1.86
29	0.2	0.17	2.75	2.91	7.86	22.87	14.86	11.31	8.25	11.54	1.85	0.72
30	0		3.37	2.4	8.89	25.35	15.15	12.47	9.13	7.94	2.92	0.49
31	0		3.24		7.6		11.85	13.43		8.39		0.19

APPENDIX II

Average daily flow (cumec) of Chalakudy basin (1997-2017)

Day	January	February	March	April	May	June
1	9.27	3.05	2.53	1.57	5.13	35.74
2	8.91	2.71	3.28	1.68	5.17	39.18
3	9.78	3.92	3.44	2	4.75	33.81
4	9.41	3.38	2.17	3.39	4.49	31.68
5	9.11	4.38	2.05	3.55	6.57	53.78
6	8.3	4.84	2.9	3.25	9.63	60.65
7	8.4	5.8	3.08	5.69	9.52	56.01
8	9.08	4.58	2.76	3.4	11.23	61.44
9	6.83	5.49	2.82	4.53	8.44	51.13
10	6.41	5.4	2.1	2.98	7.35	53.41
11	6.19	3.57	2.39	3.74	6.49	55.36
12	7.55	5.07	1.9	3.81	7.41	58.54
13	6.5	3.75	1.88	3.16	6.18	82.47
14	6.77	3.11	1.74	4.1	9.77	83.63
15	6.53	3.05	1.87	2.39	7.74	87.84
16	6.93	4.34	1.96	4.51	7.11	83.11
17	6.32	3.75	2.67	2.53	7.26	88.58
18	6.04	4.73	2.17	2.58	7.75	95.73
19	6.37	2.94	3.35	4.62	11.47	94.53
20	4.95	3.1	1.66	5.05	9.44	94.81
21	4.85	2.87	2.95	3.84	13.02	109.56
22	4.74	2.6	3.47	6.32	12.39	100.61
23	4.4	2.95	2.36	3.88	15.22	121.59
24	4.15	2.78	2.3	3.47	15.52	132.82
25	4.34	2.78	1.87	6.12	17.44	117.2
26	3.99	2.52	2.03	5.4	17.43	89.67
27	6.36	3.41	2.02	5.99	8.96	113.95
28	3.72	3.43	2.1	6.39	15.79	102.21
29	3.72	5.27	2.13	5.52	21.66	102.83
30	3.43		1.99	6.16	22.51	128.27
31	3.17		1.87		21.88	

Average daily flow (cumec) of Chalakudy basin (1997-2017)

Day	July	August	September	October	November	December
1	127.51	233.57	116.49	77.02	61.23	19.66
2	154.67	222.37	111.38	68.49	58.7	16.14
3	151.19	189.49	126.64	86.7	53.58	11.65
4	152.79	223.35	112.59	114.97	51.31	11.94
5	144.97	199.69	121.23	79.36	52.51	14.51
6	130.29	183.89	117.01	74.18	52.66	13.46
7	150.21	167.1	115.51	71.55	56.24	12.42
8	125.27	160.23	103.31	82.96	53.88	13.81
9	122.87	144.15	130.83	68.78	62.7	15.31
10	130.33	171.23	122	60.07	63.19	12.24
11	143.37	163.95	108.81	69.9	68.64	15.01
12	160.8	136.67	117.75	93.96	55.92	12.11
13	151.29	127.68	106.99	98.76	47.05	11.46
14	167.99	116.58	106.45	85.58	44.76	10.78
15	160.07	96.97	93.5	93.08	43.14	10.21
16	158.08	127.47	101.82	83.23	43.13	11.58
17	230.65	154.62	101.4	76.06	42.14	12.19
18	264.82	122.11	88.34	84.32	40.73	12.02
19	218.43	108.55	100.19	77.15	41.42	12.89
20	168.25	87.37	91.36	79.08	40.36	10.63
21	157.26	92	94.11	72.43	40.34	10.51
22	175.76	95.35	82.98	66.72	49.21	11.04
23	149.52	99.64	89.09	60.21	50.61	8.81
24	144.73	122.01	99.25	62.09	46.76	9.98
25	164.81	128.74	86.88	60.19	45.34	9.52
26	157.21	102.79	84.55	66.67	41.81	10.9
27	159.54	95.39	74.38	75.71	38.05	8.43
28	164.1	82.18	79.49	73.08	40.72	10.81
29	165.47	87.78	72.24	65.24	39.14	8.27
30	165.4	104.36	84.26	76.37	37.16	8.32
31	183.98	111.27		61.56		9.59

APPENDIX III

Average daily maximum and minimum temperature (^{o}C) from 1997-2017

Day	January		February		March		April		May		June	
	Max	Min	Max	Min	Max	Min	Max	Min	Max	Min	Max	Min
1	32.1	22.5	33.7	22.6	35.6	23.5	35.4	25.2	34.6	24.9	31.6	24.1
2	31.9	22.1	33.2	22.2	35.9	23.4	35.0	24.7	34.0	24.8	31.5	24.2
3	32.1	21.8	33.3	22.4	35.8	23.8	35.2	25.2	34.2	25.2	31.5	24.2
4	32.4	22.0	33.9	22.8	35.5	23.4	34.7	24.6	33.8	24.9	31.7	24.1
5	32.7	22.6	34.1	22.7	35.8	23.4	34.9	25.0	33.7	24.8	31.3	24.0
6	32.5	22.9	34.3	22.7	35.8	24.2	35.1	24.9	33.3	24.9	30.0	23.6
7	32.8	22.8	34.3	22.4	35.4	23.9	34.9	24.7	33.3	25.0	30.7	23.5
8	32.2	22.8	34.2	22.5	35.6	23.9	34.9	24.8	33.5	24.5	30.2	23.5
9	32.7	23.5	34.3	22.4	35.6	23.8	34.8	25.2	33.7	24.9	30.1	23.5
10	32.5	23.4	34.2	22.9	35.5	23.9	35.0	25.2	33.9	25.2	30.4	23.5
11	32.7	23.0	34.4	23.0	35.6	24.1	34.8	25.1	33.8	24.8	29.8	23.6
12	32.7	22.6	33.9	23.1	35.7	24.0	34.3	25.0	33.2	25.0	29.7	23.5
13	32.5	21.9	34.3	22.7	35.7	23.9	34.3	24.9	33.3	24.8	29.3	23.4
14	32.6	21.9	34.9	22.3	35.6	23.7	34.6	24.7	33.4	25.2	29.7	23.3
15	32.5	21.6	34.6	22.5	35.8	24.2	34.5	24.9	33.6	25.1	30.2	23.5
16	32.7	22.1	34.7	22.6	35.6	24.2	34.7	25.1	33.2	24.9	29.8	23.3
17	32.7	22.1	34.8	22.5	35.6	24.2	34.4	25.5	32.5	24.8	29.3	23.3
18	33.2	22.2	35.0	22.8	35.9	24.1	34.6	25.2	32.4	24.8	29.5	23.0
19	33.2	22.3	34.6	22.6	35.5	24.0	34.7	25.0	32.8	24.3	29.9	23.1
20	32.9	21.8	35.1	22.8	35.6	24.5	34.9	25.5	32.5	24.6	29.8	23.2
21	33.3	21.9	35.0	23.4	35.3	24.7	34.6	25.0	32.5	24.6	29.3	23.3
22	33.4	22.4	34.9	23.1	34.9	25.1	34.6	24.6	32.7	24.7	29.5	23.2
23	33.6	22.0	35.3	22.9	35.2	24.5	34.6	25.5	32.9	25.1	29.6	23.1
24	33.7	22.4	35.2	22.7	35.4	24.8	34.4	24.7	33.1	25.1	29.8	23.1
25	33.5	22.6	34.9	23.0	35.1	24.6	34.7	25.1	32.7	24.9	29.6	23.3
26	33.2	22.7	35.2	22.8	35.4	24.5	34.7	25.1	32.5	24.7	29.4	23.0
27	33.0	22.8	35.4	22.8	35.8	24.6	34.3	25.4	31.9	24.3	29.7	22.9
28	33.1	22.8	35.5	23.1	35.3	24.8	34.0	25.4	31.6	24.1	29.2	23.0
29	33.4	22.7	8.3	5.6	35.4	25.0	34.1	25.2	31.7	24.2	29.5	22.9
30	33.7	22.9			35.4	25.1	34.3	25.4	31.3	24.2	29.3	23.1
31	33.3	22.8			35.3	24.9			31.9	24.1		

Average daily maximum and minimum temperature (^{o}C) from 1997-2017

Day	July		August		September		October		November		December	
	Max	Min	Max	Min	Max	Min	Max	Min	Max	Min	Max	Min
1	28.9	22.8	29.3	23.0	30.0	23.2	31.1	22.9	31.3	23.2	31.5	22.9
2	29.4	22.6	29.3	23.1	30.5	23.4	30.8	22.8	31.1	23.0	31.5	23.1
3	29.5	23.0	29.3	23.2	30.2	23.2	31.0	23.0	31.9	23.2	32.1	23.1
4	29.2	23.0	29.3	23.1	30.3	23.3	30.7	22.8	31.9	23.4	31.8	23.2
5	29.4	23.1	29.2	23.0	30.4	23.3	30.8	23.3	31.8	23.4	31.8	23.2
6	29.8	23.0	29.2	22.7	30.1	23.2	30.3	23.0	31.5	23.2	31.8	23.0
7	29.4	23.0	29.4	23.0	29.7	23.0	30.9	23.0	31.3	23.0	31.6	22.9
8	29.7	23.0	29.1	23.0	30.3	23.0	31.5	22.8	31.6	23.2	31.7	22.1
9	29.3	32.5	29.5	23.1	29.8	23.1	31.0	22.6	31.9	23.4	31.8	22.8
10	29.2	22.8	29.3	23.1	29.8	22.9	31.2	23.0	31.7	22.6	31.9	22.6
11	29.3	22.9	29.4	23.0	30.5	23.2	31.3	23.2	31.7	23.0	32.0	22.5
12	28.9	22.7	29.4	23.0	30.6	23.1	30.8	23.4	31.6	22.9	31.8	22.6
13	29.1	22.7	29.7	23.3	30.6	23.4	31.3	23.5	31.9	22.8	31.8	23.1
14	29.6	23.0	30.2	23.3	30.1	23.2	31.6	23.3	32.1	23.4	31.2	23.2
15	29.5	23.1	30.0	23.5	30.0	23.2	30.9	23.3	32.1	22.5	31.8	22.9
16	29.0	23.1	29.8	23.3	30.3	23.2	31.5	23.3	31.9	22.1	31.9	23.1
17	29.1	22.7	29.4	23.3	30.2	23.2	31.3	23.4	31.9	22.8	31.8	22.9
18	29.1	22.7	29.7	23.3	30.3	23.2	31.6	23.3	32.0	23.1	31.3	23.2
19	29.0	22.8	30.3	23.0	30.4	23.1	31.2	23.1	31.6	23.5	31.7	23.1
20	29.0	22.8	30.2	23.3	30.6	23.2	31.1	23.1	32.1	23.2	31.7	22.9
21	29.0	23.0	29.8	23.5	30.3	23.2	31.5	23.2	32.0	23.3	31.8	22.9
22	29.2	23.2	29.8	23.1	31.0	23.1	31.2	23.1	31.9	23.8	31.7	22.5
23	29.4	23.0	29.9	23.3	31.0	23.0	31.3	23.2	31.5	23.6	32.0	22.3
24	29.6	22.9	30.1	23.2	31.1	23.1	31.4	23.0	31.5	23.1	32.1	22.5
25	29.2	22.8	29.9	23.1	30.8	23.0	31.2	23.3	31.8	23.3	32.2	21.6
26	29.4	22.9	29.8	23.0	31.5	23.1	31.8	23.3	31.5	22.9	32.3	21.5
27	29.2	23.1	29.8	23.3	31.4	23.2	31.4	23.5	32.1	22.8	32.0	21.7
28	29.3	23.0	29.8	23.2	31.4	23.3	31.3	23.2	32.0	22.5	31.7	22.3
29	29.2	23.1	30.0	23.4	31.3	23.3	31.4	23.1	31.8	23.0	31.9	22.5
30	29.4	23.0	29.5	23.2	30.6	23.2	31.6	23.3	32.0	23.0	32.1	22.3
31	29.7	23.5	29.9	23.3			31.3	23.3			31.7	21.9

APPENDIX IV

Average daily relative humidity (RH, %) from 1997-2017

Day	January		February		March		April		May		June	
	8:00 AM	2:00 PM	8:00 AM	2:00 PM	8:00 AM	2:00 PM	8:00 AM	2:00 PM	8:00 AM	2:00 PM	8:00 AM	2:00 PM
1	43	73	38	71	39	79	55	87	60	87	69	92
2	42	74	36	70	38	78	57	88	56	87	70	93
3	41	74	37	73	38	78	53	88	60	88	70	91
4	41	74	40	71	36	80	56	88	61	87	70	91
5	42	71	39	75	40	81	54	88	63	89	75	93
6	42	74	38	75	40	83	52	87	60	86	79	93
7	41	72	37	78	42	85	53	86	62	87	79	94
8	45	75	40	75	40	84	58	87	63	88	80	94
9	44	72	38	73	42	84	56	89	60	88	76	95
10	43	72	39	77	44	82	54	87	59	87	78	94
11	42	76	37	78	45	84	56	87	60	89	80	94
12	41	73	40	75	40	86	56	88	60	88	80	94
13	39	73	38	74	42	82	58	87	64	91	86	95
14	38	70	35	74	48	87	58	87	59	88	77	94
15	40	69	37	80	43	85	58	88	61	90	73	94
16	39	71	38	78	45	87	56	87	65	88	77	94
17	39	72	39	76	45	86	56	87	62	90	78	94
18	39	72	41	80	43	83	57	86	64	90	77	95
19	41	72	39	74	49	82	55	87	65	91	76	94
20	39	72	39	79	48	86	59	86	67	91	79	94
21	38	75	41	81	49	89	57	87	65	90	77	95
22	36	71	36	82	54	89	58	88	64	91	81	95
23	39	73	38	79	53	88	58	86	63	89	83	96
24	39	73	40	80	49	89	56	87	67	90	77	94
25	40	76	42	82	51	128	57	87	68	91	78	94
26	40	71	37	79	46	87	57	87	68	91	77	95
27	41	72	35	77	51	85	59	86	66	91	79	95
28	42	75	38	80	50	88	60	88	71	92	83	95
29	39	77	12	21	53	87	59	88	71	91	79	94
30	38	75			56	89	58	86	96	92	79	94
31	39	72			51	86			67	92		

Average daily relative humidity (RH, %) from 1997-2017

Day	July		August		September		October		November		December	
	8:00 AM	2:00 PM	8:00 AM	2:00 PM	8:00 AM	2:00 PM	8:00 AM	2:00 PM	8:00 AM	2:00 PM	8:00 AM	2:00 PM
1	81	95	77	94	71	94	70	93	66	90	58	80
2	77	95	77	95	73	93	70	92	63	88	57	79
3	79	93	79	95	73	93	67	93	63	87	54	79
4	79	94	80	95	70	94	68	92	65	87	52	77
5	79	95	80	95	71	94	69	94	64	87	53	76
6	79	94	76	95	76	94	69	92	63	87	49	76
7	76	95	76	95	71	94	69	92	64	86	47	76
8	77	94	78	95	73	93	68	93	60	87	52	79
9	80	94	73	95	75	93	71	92	62	86	50	79
10	78	95	76	95	72	92	69	92	60	85	51	79
11	81	95	76	94	70	94	68	91	60	86	53	80
12	81	95	76	95	69	94	71	93	60	86	50	80
13	78	94	76	94	73	93	74	92	59	86	57	77
14	76	96	70	94	73	93	72	93	59	84	52	76
15	77	94	73	94	72	94	72	92	53	81	51	75
16	78	95	76	95	73	94	68	91	52	81	47	76
17	79	95	76	96	73	93	71	92	55	80	47	73
18	76	95	75	94	71	94	68	91	58	79	52	74
19	77	95	74	93	69	93	69	93	57	79	50	76
20	78	94	73	94	69	93	72	92	59	81	49	74
21	80	95	74	94	69	93	69	129	57	82	47	74
22	77	95	73	94	68	132	66	89	58	79	46	74
23	77	94	71	93	69	92	69	90	58	81	47	74
24	76	95	72	94	68	92	66	89	61	80	45	74
25	80	95	75	95	72	93	68	89	57	82	45	75
26	76	95	75	94	67	91	65	89	52	79	42	72
27	77	95	74	93	65	93	70	91	55	79	45	74
28	78	95	73	94	68	92	65	90	58	81	47	73
29	79	95	73	93	70	92	66	90	56	79	46	72
30	76	94	76	95	70	92	66	89	56	78	44	77
31	74	94	71	94			68	90			47	76

APPENDIX V

Average daily wind speed (km/h) from 1997-2017

Day	Jan	Feb	Mar	Apr	May	Jun	Jul	Aug	Sep	Oct	Nov	Dec
1	9.47	9.38	6.22	5.55	6.22	5.90	6.61	6.92	5.77	4.97	6.57	8.67
2	9.26	9.00	5.40	5.59	5.72	6.14	6.18	7.19	6.43	4.85	6.78	8.25
3	8.97	8.44	5.31	5.09	5.82	5.77	7.32	5.92	6.30	4.88	5.89	8.71
4	8.70	7.76	5.61	5.84	5.94	5.97	7.07	6.12	6.66	5.40	6.14	9.74
5	8.51	7.50	5.68	5.98	6.26	6.33	6.27	6.47	6.74	5.42	6.85	9.51
6	8.60	7.16	6.01	5.84	6.04	6.02	6.90	5.69	6.66	5.47	6.21	8.74
7	9.28	5.90	5.69	6.30	5.76	6.24	6.25	5.33	6.44	5.22	5.60	8.79
8	9.58	6.29	5.63	5.79	5.50	5.30	6.13	5.25	5.76	5.24	6.37	8.09
9	9.34	5.85	5.78	5.32	5.56	6.17	6.56	6.03	6.90	5.33	6.10	7.57
10	9.20	5.94	6.64	5.90	5.19	6.75	6.33	6.08	6.75	6.00	6.30	8.83
11	9.33	6.36	6.80	5.88	5.57	5.90	6.41	5.80	6.54	5.61	6.24	9.71
12	9.00	5.53	6.56	6.12	5.44	5.68	5.67	6.75	6.23	5.17	7.19	8.98
13	8.45	5.53	6.69	5.98	6.12	6.95	5.44	7.04	6.61	5.90	7.72	8.33
14	7.90	5.31	5.11	6.19	5.51	6.53	5.76	6.40	6.00	5.97	7.34	9.07
15	8.60	7.12	4.50	6.01	5.73	6.29	6.35	5.96	6.13	5.52	7.40	9.58
16	8.60	7.19	4.71	5.83	5.32	6.62	7.16	5.64	5.76	4.77	6.99	8.46
17	7.90	6.98	5.62	5.87	5.54	6.73	7.24	6.02	5.49	5.21	6.91	10.09
18	8.74	7.43	4.67	5.88	5.20	6.89	5.79	5.49	5.42	5.21	7.10	10.81
19	8.60	6.82	4.49	4.96	5.33	6.96	6.14	5.57	5.51	6.35	7.00	10.27
20	7.72	5.51	5.60	7.02	5.13	7.13	7.20	5.41	6.54	6.33	6.66	10.87
21	8.12	7.00	5.40	5.63	5.39	6.82	5.75	5.52	5.88	6.61	8.07	10.58
22	7.91	6.52	5.24	5.34	5.11	6.99	6.48	5.58	5.41	5.86	8.31	9.80
23	7.52	6.36	5.54	5.99	5.26	6.07	6.25	5.89	5.09	6.44	8.88	10.04
24	7.67	6.67	5.49	5.49	5.18	6.67	7.09	5.93	5.46	6.00	8.08	8.63
25	7.82	5.15	5.22	5.71	5.04	6.68	6.89	5.64	4.79	6.61	8.04	8.06
26	8.66	4.75	5.72	5.91	6.17	6.14	6.49	5.51	5.00	6.12	7.25	7.87
27	8.88	4.44	5.50	6.25	5.82	6.31	6.19	5.80	5.43	5.94	7.16	8.27
28	8.96	4.94	5.44	5.77	6.25	6.98	6.86	5.90	5.31	5.66	7.27	8.95
29	9.27	1.22	5.41	5.69	5.55	6.04	6.02	6.27	5.70	5.77	7.58	9.61
30	9.33		5.67	6.30	6.18	6.73	6.89	5.87	4.95	6.49	9.25	8.18
31	10.37		5.42		6.78		7.24	6.03		5.68		7.68

APPENDIX VI

Average daily sunshine hours from 1997-2017

Day	Jan	Feb	Mar	Apr	May	Jun	Jul	Aug	Sep	Oct	Nov	Dec
1	8.7	9.0	9.2	8.2	8.1	5.3	1.5	3.3	4.5	5.8	5.0	6.6
2	9.1	8.6	9.1	6.9	7.7	4.7	3.0	3.3	5.2	5.9	6.7	6.4
3	8.8	8.8	8.7	7.3	6.7	4.8	2.9	2.2	4.2	6.1	6.1	7.6
4	9.2	8.9	8.1	7.3	5.9	5.5	2.6	2.4	4.0	5.5	6.2	7.6
5	9.1	8.9	8.8	7.1	6.5	4.4	2.2	2.4	5.1	5.2	5.0	7.7
6	8.9	8.9	8.9	7.3	6.2	2.4	2.3	3.0	3.6	5.2	4.4	8.0
7	9.1	9.2	8.5	7.0	5.5	3.9	2.2	3.5	3.4	6.0	5.5	7.8
8	7.8	8.4	8.5	7.0	6.5	2.3	3.1	2.2	4.9	6.5	6.7	7.6
9	8.5	8.8	8.0	7.2	7.1	3.3	2.4	4.0	3.8	5.6	6.0	7.3
10	8.5	9.3	8.1	6.9	6.7	3.5	2.0	3.0	4.4	5.7	6.1	7.3
11	9.0	8.9	8.6	7.1	6.4	3.4	2.4	2.9	6.0	6.1	5.9	7.6
12	9.2	8.0	8.6	6.5	6.0	2.8	1.6	3.5	5.1	5.1	6.7	7.1
13	8.9	9.2	9.2	7.2	5.7	1.9	1.8	3.8	5.3	4.3	7.2	7.1
14	9.1	9.5	8.7	6.9	6.4	2.1	2.6	4.2	4.0	4.8	6.9	6.4
15	9.2	9.3	8.4	6.9	6.3	2.9	2.4	3.7	4.8	4.2	6.6	6.9
16	9.0	9.7	7.7	7.7	6.0	2.9	3.1	4.5	5.7	5.1	7.2	7.9
17	9.3	9.5	7.9	7.3	5.3	2.0	2.4	3.5	4.9	5.0	7.5	8.2
18	9.0	9.2	8.6	8.0	5.7	2.5	2.0	3.4	5.3	5.6	7.0	6.6
19	9.1	8.9	8.8	7.7	5.4	3.0	1.8	4.6	4.9	4.9	6.9	7.7
20	8.9	8.9	8.2	7.2	5.9	2.9	2.3	5.2	5.8	4.5	6.3	7.1
21	8.9	8.7	8.1	7.0	5.7	2.5	1.8	4.6	5.0	5.1	5.9	8.5
22	8.8	8.7	7.5	7.2	5.8	2.7	2.5	4.4	6.3	4.9	5.9	8.0
23	9.1	9.1	8.1	7.0	7.0	2.8	2.8	3.9	5.9	5.4	5.1	8.4
24	9.3	9.4	8.0	6.8	5.4	2.2	2.6	5.0	6.2	5.4	6.3	8.6
25	9.0	8.7	8.0	7.4	5.1	2.5	2.3	4.5	5.4	5.1	6.9	8.4
26	8.5	8.5	7.8	7.0	4.6	2.7	2.7	4.4	5.7	6.3	7.6	8.4
27	8.0	8.8	8.5	6.6	4.6	2.9	1.9	4.0	6.4	4.9	6.8	8.1
28	7.8	9.2	7.5	6.4	4.8	1.9	2.2	3.9	6.3	5.3	6.4	7.8
29	8.9	2.1	7.9	6.3	5.1	2.2	2.5	4.4	5.9	5.1	6.8	7.5
30	9.2		7.9	7.0	5.0	2.6	2.9	4.1	4.6	5.6	7.0	8.2
31	9.2		7.5		5.4		2.6	4.3		5.3		7.7

APPENDIX VII

Summary Output Tables in HEC-RAS

Reach	River Station	Profile	Q Total	Min Ch El	W.S. Elev	Crit W.S.	E.G. Elev	E.G. Slope	Vel Chnl	Flow Area	Top Width	Froude # Chl
			(m^3/s)	(m)	(m)	(m)	(m)	(m/m)	(m/s)	(m^2)	(m)	
Chalakudy river	75600	10 yr	1173.20	472.93	479.27		479.60	0.001383	2.64	609.58	154.44	0.38
Chalakudy river	75600	20 yr	1415.60	472.93	479.85		480.22	0.001405	2.82	701.18	163.85	0.39
Chalakudy river	75600	50 yr	1742.80	472.93	480.53		480.96	0.001412	3.05	815.74	174.36	0.40
Chalakudy river	75600	100 yr	1985.30	472.93	480.99		481.46	0.001411	3.21	897.86	180.97	0.41
Chalakudy river	75600	200 yr	2335.90	472.93	481.60		482.14	0.001412	3.41	1012.18	189.69	0.41
Chalakudy river	75600	500 yr	2732.50	472.93	482.23		482.83	0.001424	3.63	1134.14	198.27	0.42
Chalakudy river	75000	10 yr	1173.20	471.86	476.32	476.32	477.88	0.006961	4.53	223.61	72.16	0.81
Chalakudy river	75000	20 yr	1415.60	471.86	476.79	476.79	478.49	0.006715	4.72	258.60	76.38	0.80
Chalakudy river	75000	50 yr	1742.80	471.86	477.36	477.36	479.23	0.006458	4.93	303.94	81.53	0.80
Chalakudy river	75000	100 yr	1985.30	471.86	477.73	477.73	479.74	0.006400	5.09	334.63	84.84	0.80
Chalakudy river	75000	200 yr	2335.90	471.86	478.25	478.25	480.41	0.006251	5.25	380.35	90.20	0.80
Chalakudy river	75000	500 yr	2732.50	471.86	478.82	478.82	481.11	0.005998	5.36	433.10	95.89	0.79
Chalakudy river	74400	10 yr	1173.20	468.86	473.13		473.88	0.004746	3.91	349.65	117.67	0.67
Chalakudy river	74400	20 yr	1415.60	468.86	473.69		474.48	0.004275	4.02	417.82	124.96	0.65
Chalakudy river	74400	50 yr	1742.80	468.86	474.38		475.23	0.003855	4.16	507.47	134.11	0.63
Chalakudy river	74400	100 yr	1985.30	468.86	474.85		475.73	0.003639	4.26	571.80	139.23	0.62
Chalakudy river	74400	200 yr	2335.90	468.86	475.48		476.41	0.003416	4.39	661.72	146.10	0.61
Chalakudy river	74400	500 yr	2732.50	468.86	476.14		477.13	0.003260	4.52	761.36	154.63	0.61
Chalakudy river	73800	10 yr	1173.20	464.35	472.14		472.48	0.001209	2.59	477.62	134.39	0.36
Chalakudy river	73800	20 yr	1415.60	464.35	472.77		473.15	0.001170	2.75	569.48	155.59	0.36
Chalakudy river	73800	50 yr	1742.80	464.35	473.53		473.96	0.001141	2.95	695.94	178.64	0.37
Chalakudy river	73800	100 yr	1985.30	464.35	474.03		474.50	0.001130	3.08	788.50	190.93	0.37
Chalakudy river	73800	200 yr	2335.90	464.35	474.69		475.21	0.001120	3.25	920.34	205.87	0.37
Chalakudy river	73800	500 yr	2732.50	464.35	475.38		475.95	0.001111	3.43	1066.88	219.69	0.38
Chalakudy river	73200	10 yr	1173.20	463.20	471.88		472.04	0.000403	1.80	826.49	160.36	0.22
Chalakudy river	73200	20 yr	1415.60	463.20	472.49		472.69	0.000449	1.99	932.08	182.51	0.23
Chalakudy river	73200	50 yr	1742.80	463.20	473.23		473.46	0.000500	2.21	1073.53	201.65	0.25
Chalakudy river	73200	100 yr	1985.30	463.20	473.72		473.98	0.000534	2.35	1175.09	211.59	0.26
Chalakudy river	73200	200 yr	2335.90	463.20	474.37		474.68	0.000578	2.54	1316.16	221.88	0.27
Chalakudy river	73200	500 yr	2732.50	463.20	475.05		475.40	0.000620	2.73	1469.52	232.03	0.29
Chalakudy river	72600	10 yr	1173.20	463.49	471.30		471.63	0.001166	2.55	471.00	101.81	0.35
Chalakudy river	72600	20 yr	1415.60	463.49	471.85		472.25	0.001239	2.78	537.69	157.30	0.37
Chalakudy river	72600	50 yr	1742.80	463.49	472.52		472.98	0.001314	3.04	651.69	188.35	0.39
Chalakudy river	72600	100 yr	1985.30	463.49	472.96		473.48	0.001341	3.21	738.62	199.12	0.40
Chalakudy river	72600	200 yr	2335.90	463.49	473.56		474.14	0.001367	3.43	860.19	209.05	0.41
Chalakudy river	72600	500 yr	2732.50	463.49	474.18		474.83	0.001389	3.65	993.29	219.60	0.41

Reach	River Station	Profile	Q Total	Min Ch El	W.S. Elev	Crit W.S.	E.G. Elev	E.G. Slope	Vel Chnl	Flow Area	Top Width	Froude # Chl
			(m^3/s)	(m)	(m)	(m)	(m)	(m/m)	(m/s)	(m^2)	(m)	
Chalakudy river	72000	10 yr	1173.20	463.44	470.39		470.77	0.001807	2.73	432.51	109.32	0.43
Chalakudy river	72000	20 yr	1415.60	463.44	470.92		471.35	0.001802	2.92	491.70	114.04	0.43
Chalakudy river	72000	50 yr	1742.80	463.44	471.55		472.05	0.001825	3.16	565.33	119.66	0.44
Chalakudy river	72000	100 yr	1985.30	463.44	471.98		472.54	0.001842	3.31	617.66	124.13	0.45
Chalakudy river	72000	200 yr	2335.90	463.44	472.55		473.18	0.001868	3.52	690.74	130.14	0.46
Chalakudy river	72000	500 yr	2732.50	463.44	473.15		473.86	0.001896	3.73	770.47	136.40	0.47
Chalakudy river	71400	10 yr	1173.20	459.24	470.33		470.41	0.000199	1.29	944.97	151.18	0.15
Chalakudy river	71400	20 yr	1415.60	459.24	470.84		470.95	0.000236	1.45	1024.96	158.76	0.17
Chalakudy river	71400	50 yr	1742.80	459.24	471.47		471.60	0.000272	1.64	1139.64	210.71	0.18
Chalakudy river	71400	100 yr	1985.30	459.24	471.90		472.05	0.000295	1.77	1233.87	229.58	0.19
Chalakudy river	71400	200 yr	2335.90	459.24	472.47		472.66	0.000326	1.95	1373.02	254.22	0.21
Chalakudy river	71400	500 yr	2732.50	459.24	473.07		473.30	0.000355	2.12	1534.85	288.90	0.22
Chalakudy river	70200	10 yr	1173.20	465.36	468.73	468.73	469.93	0.010527	4.89	247.94	109.68	0.96
Chalakudy river	70200	20 yr	1415.60	465.36	469.07	469.07	470.40	0.009980	5.16	286.04	113.53	0.96
Chalakudy river	70200	50 yr	1742.80	465.36	469.48	469.48	470.99	0.009544	5.50	333.70	118.00	0.95
Chalakudy river	70200	100 yr	1985.30	465.36	469.77	469.77	471.40	0.009274	5.73	367.93	121.52	0.95
Chalakudy river	70200	200 yr	2335.90	465.36	470.16	470.16	471.95	0.008918	6.01	416.59	126.35	0.95
Chalakudy river	70200	500 yr	2732.50	465.36	470.58	470.58	472.54	0.008579	6.29	470.37	131.48	0.95
Chalakudy river	69600	10 yr	1173.20	455.81	460.70		461.50	0.005140	3.94	297.53	90.34	0.69
Chalakudy river	69600	20 yr	1415.60	455.81	461.16		462.05	0.005074	4.16	339.96	94.11	0.70
Chalakudy river	69600	50 yr	1742.80	455.81	461.73		462.73	0.004997	4.42	394.59	98.76	0.71
Chalakudy river	69600	100 yr	1985.30	455.81	462.12		463.19	0.004947	4.58	433.58	101.97	0.71
Chalakudy river	69600	200 yr	2335.90	455.81	462.56		463.77	0.005142	4.87	479.52	105.73	0.73
Chalakudy river	69600	500 yr	2732.50	455.81	463.00		464.37	0.005405	5.19	526.63	109.60	0.76
Chalakudy river	69000	10 yr	1173.20	449.98	455.46	455.46	457.06	0.011011	5.61	209.23	65.96	1.01
Chalakudy river	69000	20 yr	1415.60	449.98	455.93	455.93	457.69	0.010725	5.87	241.24	69.57	1.01
Chalakudy river	69000	50 yr	1742.80	449.98	456.50	456.50	458.45	0.010379	6.18	281.87	73.20	1.01
Chalakudy river	69000	100 yr	1985.30	449.98	456.90	456.90	458.97	0.010147	6.38	311.12	75.68	1.01
Chalakudy river	69000	200 yr	2335.90	449.98	457.54	457.41	459.67	0.009011	6.47	361.00	79.73	0.96
Chalakudy river	69000	500 yr	2732.50	449.98	458.26	457.94	460.44	0.007764	6.53	420.30	84.29	0.91
Chalakudy river	68400	10 yr	1173.20	440.74	456.25		456.28	0.000042	0.76	1693.10	237.89	0.08
Chalakudy river	68400	20 yr	1415.60	440.74	456.86		456.90	0.000051	0.86	1841.48	245.67	0.08
Chalakudy river	68400	50 yr	1742.80	440.74	457.62		457.67	0.000062	0.99	2029.88	253.49	0.09
Chalakudy river	68400	100 yr	1985.30	440.74	458.13		458.19	0.000070	1.07	2161.62	258.60	0.10
Chalakudy river	68400	200 yr	2335.90	440.74	458.82		458.89	0.000081	1.19	2341.86	265.15	0.11

Reach	River Station	Profile	Q Total	Min Ch El	W.S. Elev	Crit W.S.	E.G. Elev	E.G. Slope	Vel Chnl	Flow Area	Top Width	Froude # Chl
			(m^3/s)	(m)	(m)	(m)	(m)	(m/m)	(m/s)	(m^2)	(m)	
Chalakudy river	68400	500 yr	2732.50	440.74	459.55		459.63	0.000091	1.31	2536.55	272.55	0.12
Chalakudy river	67800	10 yr	1173.20	449.69	454.54	454.54	456.04	0.011188	5.43	216.05	72.46	1.00
Chalakudy river	67800	20 yr	1415.60	449.69	454.98	454.98	456.63	0.010786	5.70	248.40	75.29	1.00
Chalakudy river	67800	50 yr	1742.80	449.69	455.50	455.50	457.36	0.010516	6.04	288.74	78.67	1.01
Chalakudy river	67800	100 yr	1985.30	449.69	455.86	455.86	457.85	0.010324	6.25	317.77	81.02	1.01
Chalakudy river	67800	200 yr	2335.90	449.69	456.37	456.37	458.52	0.009957	6.49	359.98	84.28	1.00
Chalakudy river	67800	500 yr	2732.50	449.69	456.88	456.88	459.22	0.009663	6.78	402.92	87.12	1.00
Chalakudy river	67200	10 yr	1173.20	415.93	424.04		424.12	0.000228	1.22	963.49	164.98	0.16
Chalakudy river	67200	20 yr	1415.60	415.93	424.71		424.80	0.000240	1.32	1075.53	170.00	0.17
Chalakudy river	67200	50 yr	1742.80	415.93	425.54		425.64	0.000251	1.43	1217.85	175.77	0.17
Chalakudy river	67200	100 yr	1985.30	415.93	426.10		426.21	0.000258	1.51	1317.34	179.25	0.18
Chalakudy river	67200	200 yr	2335.90	415.93	426.85		426.98	0.000266	1.61	1454.33	183.93	0.18
Chalakudy river	67200	500 yr	2732.50	415.93	427.64		427.79	0.000274	1.71	1601.56	188.84	0.19
Chalakudy river	66600	10 yr	1173.20	418.00	424.04		424.06	0.000039	0.48	2237.76	429.92	0.07
Chalakudy river	66600	20 yr	1415.60	418.00	424.72		424.73	0.000038	0.51	2530.18	434.95	0.07
Chalakudy river	66600	50 yr	1742.80	418.00	425.55		425.57	0.000037	0.55	2894.73	441.47	0.07
Chalakudy river	66600	100 yr	1985.30	418.00	426.12		426.14	0.000037	0.57	3146.25	445.91	0.07
Chalakudy river	66600	200 yr	2335.90	418.00	426.88		426.90	0.000037	0.61	3488.79	451.90	0.07
Chalakudy river	66600	500 yr	2732.50	418.00	427.68		427.71	0.000037	0.64	3852.43	458.04	0.07
Chalakudy river	66000	10 yr	1173.20	418.00	422.12	422.12	423.80	0.010908	5.75	204.12	60.88	1.00
Chalakudy river	66000	20 yr	1415.60	418.00	422.61	422.61	424.47	0.010581	6.04	234.38	63.29	1.00
Chalakudy river	66000	50 yr	1742.80	418.00	423.20	423.20	425.28	0.010304	6.39	272.80	66.22	1.01
Chalakudy river	66000	100 yr	1985.30	418.00	423.62	423.62	425.84	0.010033	6.59	301.26	68.32	1.00
Chalakudy river	66000	200 yr	2335.90	418.00	424.19	424.19	426.58	0.009759	6.86	340.58	71.10	1.00
Chalakudy river	66000	500 yr	2732.50	418.00	424.76	424.76	427.37	0.009627	7.16	381.89	73.92	1.01
Chalakudy river	65400	10 yr	1173.20	417.18	420.03		420.06	0.000418	0.80	1581.51	862.25	0.18
Chalakudy river	65400	20 yr	1415.60	417.18	420.23		420.26	0.000442	0.87	1750.30	867.59	0.19
Chalakudy river	65400	50 yr	1742.80	417.18	420.47		420.51	0.000471	0.97	1958.12	873.00	0.20
Chalakudy river	65400	100 yr	1985.30	417.18	420.63		420.68	0.000489	1.03	2101.40	876.53	0.21
Chalakudy river	65400	200 yr	2335.90	417.18	420.85		420.91	0.000513	1.11	2296.61	881.84	0.21
Chalakudy river	65400	500 yr	2732.50	417.18	421.09		421.16	0.000534	1.19	2505.58	887.66	0.22
Chalakudy river	64800	10 yr	1173.20	416.62	418.85	418.85	419.27	0.017347	2.88	407.95	499.46	1.02
Chalakudy river	64800	20 yr	1415.60	416.62	418.97	418.97	419.44	0.016573	3.05	464.69	505.13	1.01
Chalakudy river	64800	50 yr	1742.80	416.62	419.11	419.11	419.65	0.015731	3.25	537.12	511.78	1.01
Chalakudy river	64800	100 yr	1985.30	416.62	419.21	419.21	419.79	0.014970	3.36	591.35	516.23	1.00

Reach	River Station	Profile	Q Total	Min Ch El	W.S. Elev	Crit W.S.	E.G. Elev	E.G. Slope	Vel Chnl	Flow Area	Top Width	Froude # Chl
			(m^3/s)	(m)	(m)	(m)	(m)	(m/m)	(m/s)	(m^2)	(m)	
Chalakudy river	64800	200 yr return pe	2335.90	416.62	419.35	419.35	419.99	0.014435	3.54	661.71	521.68	1.00
Chalakudy river	64800	500 yr return pe	2732.50	416.62	419.48	419.48	420.20	0.014239	3.74	732.90	527.13	1.01
Chalakudy river	64200	10 yr return per	1173.20	400.07	403.06	403.06	403.99	0.013139	4.26	275.46	151.76	1.01
Chalakudy river	64200	20 yr return per	1415.60	400.07	403.33	403.33	404.35	0.012531	4.47	316.85	156.77	1.00
Chalakudy river	64200	50 yr return per	1742.80	400.07	403.65	403.65	404.79	0.012061	4.73	368.66	162.84	1.00
Chalakudy river	64200	100 yr return pe	1985.30	400.07	403.88	403.88	405.10	0.011786	4.90	405.51	167.01	1.00
Chalakudy river	64200	200 yr return pe	2335.90	400.07	404.18	404.18	405.51	0.011473	5.11	457.06	172.95	1.00
Chalakudy river	64200	500 yr return pe	2732.50	400.07	404.50	404.50	405.95	0.011178	5.32	513.99	179.77	1.00
Chalakudy river	63600	10 yr return per	1173.20	350.24	355.50	355.50	357.04	0.011041	5.49	213.69	69.80	1.00
Chalakudy river	63600	20 yr return per	1415.60	350.24	355.95	355.95	357.64	0.010697	5.76	245.63	72.75	1.00
Chalakudy river	63600	50 yr return per	1742.80	350.24	356.50	356.50	358.38	0.010334	6.07	287.00	76.47	1.00
Chalakudy river	63600	100 yr return pe	1985.30	350.24	356.87	356.87	358.89	0.010224	6.29	315.53	79.01	1.01
Chalakudy river	63600	200 yr return pe	2335.90	350.24	357.39	357.39	359.57	0.009899	6.53	357.77	82.62	1.00
Chalakudy river	63600	500 yr return pe	2732.50	350.24	357.93	357.93	360.27	0.009637	6.77	403.51	86.37	1.00
Chalakudy river	63000	10 yr return per	1173.20	267.84	272.80	272.80	274.56	0.010376	5.88	200.24	58.03	0.99
Chalakudy river	63000	20 yr return per	1415.60	267.84	273.33	273.33	275.24	0.009831	6.14	231.99	61.43	0.98
Chalakudy river	63000	50 yr return per	1742.80	267.84	273.98	273.98	276.07	0.009309	6.44	273.10	65.56	0.97
Chalakudy river	63000	100 yr return pe	1985.30	267.84	274.41	274.41	276.63	0.009066	6.64	301.91	68.31	0.97
Chalakudy river	63000	200 yr return pe	2335.90	267.84	274.99	274.99	277.38	0.008722	6.89	342.96	71.79	0.97
Chalakudy river	63000	500 yr return pe	2732.50	267.84	275.58	275.58	278.15	0.008457	7.15	386.39	74.96	0.96
Chalakudy river	62400	10 yr return per	1173.20	247.74	251.30	251.30	252.38	0.012302	4.60	254.80	118.77	1.00
Chalakudy river	62400	20 yr return per	1415.60	247.74	251.61	251.61	252.80	0.011897	4.84	292.53	123.39	1.00
Chalakudy river	62400	50 yr return per	1742.80	247.74	252.00	252.00	253.33	0.011450	5.11	341.08	128.80	1.00
Chalakudy river	62400	100 yr return pe	1985.30	247.74	252.26	252.26	253.68	0.011185	5.28	375.71	132.55	1.00
Chalakudy river	62400	200 yr return pe	2335.90	247.74	252.67	252.67	254.15	0.010442	5.40	434.56	153.78	0.98
Chalakudy river	62400	500 yr return pe	2732.50	247.74	253.08	253.08	254.63	0.009504	5.53	500.01	167.45	0.95
Chalakudy river	61800	10 yr return per	1173.20	237.73	244.26		244.70	0.001971	2.96	396.69	89.82	0.45
Chalakudy river	61800	20 yr return per	1415.60	237.73	244.51		245.09	0.002448	3.37	419.76	91.83	0.50
Chalakudy river	61800	50 yr return per	1742.80	237.73	244.72		245.52	0.003276	3.97	438.83	93.42	0.59
Chalakudy river	61800	100 yr return pe	1985.30	237.73	244.82		245.82	0.004000	4.43	448.45	94.21	0.65
Chalakudy river	61800	200 yr return pe	2335.90	237.73	244.88		246.23	0.005341	5.14	454.25	94.68	0.75
Chalakudy river	61800	500 yr return pe	2732.50	237.73	244.85	244.41	246.72	0.007440	6.05	451.37	94.45	0.88
Chalakudy river	61200	10 yr return per	1173.20	240.86	242.21	242.21	242.82	0.004965	1.44	388.99	339.33	0.53
Chalakudy river	61200	20 yr return per	1415.60	240.86	242.43	242.38	243.05	0.004451	1.53	464.24	356.73	0.52
Chalakudy river	61200	50 yr return per	1742.80	240.86	242.80	242.59	243.37	0.003337	1.52	602.67	393.25	0.47

Reach	River Station	Profile	Q Total	Min Ch El	W.S. Elev	Crit W.S.	E.G. Elev	E.G. Slope	Vel Chnl	Flow Area	Top Width	Froude # Chl
			(m^3/s)	(m)	(m)	(m)	(m)	(m/m)	(m/s)	(m2)	(m)	
Chalakudy river	61200	100 yr return pe	1985.30	240.86	243.07	242.74	243.61	0.002761	1.50	713.52	421.10	0.43
Chalakudy river	61200	200 yr return pe	2335.90	240.86	243.45	242.95	243.94	0.002165	1.51	877.68	447.23	0.40
Chalakudy river	61200	500 yr return pe	2732.50	240.86	243.88		244.33	0.001714	1.50	1078.47	482.09	0.36
Chalakudy river	60600	10 yr return per	1173.20	233.79	238.67		239.56	0.005332	4.22	308.57	99.93	0.72
Chalakudy river	60600	20 yr return per	1415.60	233.79	239.10		240.12	0.005508	4.52	352.99	107.10	0.74
Chalakudy river	60600	50 yr return per	1742.80	233.79	239.62		240.80	0.005723	4.87	410.50	116.20	0.76
Chalakudy river	60600	100 yr return pe	1985.30	233.79	239.95		241.25	0.005920	5.12	450.07	122.12	0.78
Chalakudy river	60600	200 yr return pe	2335.90	233.79	240.41		241.86	0.006081	5.41	508.18	129.31	0.80
Chalakudy river	60600	500 yr return pe	2732.50	233.79	240.83	240.24	242.47	0.006314	5.78	563.78	135.76	0.83
Chalakudy river	60000	10 yr return per	1173.20	230.32	234.49	234.21	235.51	0.008806	4.47	262.47	104.13	0.88
Chalakudy river	60000	20 yr return per	1415.60	230.32	234.83	234.60	235.99	0.008810	4.76	303.11	127.57	0.89
Chalakudy river	60000	50 yr return per	1742.80	230.32	235.24	235.06	236.57	0.008836	5.12	358.77	148.87	0.91
Chalakudy river	60000	100 yr return pe	1985.30	230.32	235.53	235.37	236.96	0.008715	5.33	404.09	162.66	0.91
Chalakudy river	60000	200 yr return pe	2335.90	230.32	235.89	235.79	237.49	0.008792	5.64	465.59	177.87	0.93
Chalakudy river	60000	500 yr return pe	2732.50	230.32	236.28	236.23	238.04	0.008725	5.93	538.60	192.52	0.94
Chalakudy river	59400	10 yr return per	1173.20	223.83	228.09	228.09	229.51	0.011283	5.28	222.36	78.71	1.00
Chalakudy river	59400	20 yr return per	1415.60	223.83	228.52	228.52	230.07	0.010979	5.51	257.14	83.64	1.00
Chalakudy river	59400	50 yr return per	1742.80	223.83	229.04	229.04	230.74	0.010604	5.76	302.52	89.51	1.00
Chalakudy river	59400	100 yr return pe	1985.30	223.83	229.37	229.37	231.19	0.010530	5.99	331.67	92.12	1.01
Chalakudy river	59400	200 yr return pe	2335.90	223.83	229.84	229.84	231.80	0.010120	6.21	376.16	95.86	1.00
Chalakudy river	59400	500 yr return pe	2732.50	223.83	230.32	230.32	232.45	0.009871	6.46	422.98	99.61	1.00
Chalakudy river	58800	10 yr return per	1173.20	199.86	207.19	207.19	208.25	0.005118	4.97	324.19	141.43	0.72
Chalakudy river	58800	20 yr return per	1415.60	199.86	207.51	207.51	208.65	0.005363	5.23	370.03	149.73	0.75
Chalakudy river	58800	50 yr return per	1742.80	199.86	207.90	207.90	209.13	0.005462	5.45	431.58	160.15	0.76
Chalakudy river	58800	100 yr return pe	1985.30	199.86	208.15	208.15	209.45	0.005609	5.63	471.43	166.45	0.77
Chalakudy river	58800	200 yr return pe	2335.90	199.86	208.49	208.49	209.89	0.005674	5.82	529.52	174.92	0.78
Chalakudy river	58800	500 yr return pe	2732.50	199.86	208.84	208.84	210.34	0.005689	5.97	591.90	182.20	0.79
Chalakudy river	58200	10 yr return per	1173.20	183.62	188.55	188.55	190.21	0.010854	5.70	205.81	62.24	1.00
Chalakudy river	58200	20 yr return per	1415.60	183.62	189.05	189.05	190.86	0.010549	5.96	237.56	65.74	1.00
Chalakudy river	58200	50 yr return per	1742.80	183.62	189.66	189.66	191.65	0.010212	6.24	279.18	70.24	1.00
Chalakudy river	58200	100 yr return pe	1985.30	183.62	190.05	190.05	192.18	0.010150	6.46	307.42	73.15	1.01
Chalakudy river	58200	200 yr return pe	2335.90	183.62	190.60	190.60	192.90	0.009719	6.72	348.02	77.03	1.00
Chalakudy river	58200	500 yr return pe	2732.50	183.62	191.13	191.13	193.65	0.009449	7.03	390.56	80.81	1.00
Chalakudy river	57600	10 yr return per	1173.20	167.60	174.44		174.76	0.001312	2.48	473.27	103.16	0.37
Chalakudy river	57600	20 yr return per	1415.60	167.60	175.13		175.47	0.001262	2.60	545.23	107.49	0.37

Reach	River Station	Profile	Q Total	Min Ch El	W.S. Elev	Crit W.S.	E.G. Elev	E.G. Slope	Vel Chnl	Flow Area	Top Width	Froude # Chl
			(m^3/s)	(m)	(m)	(m)	(m)	(m/m)	(m/s)	(m^2)	(m)	
Chalakudy river	57600	50 yr return period	1742.80	167.60	175.97		176.35	0.001208	2.73	638.66	112.87	0.37
Chalakudy river	57600	100 yr return period	1985.30	167.60	176.56		176.96	0.001174	2.81	705.87	116.59	0.37
Chalakudy river	57600	200 yr return period	2335.90	167.60	177.36		177.80	0.001122	2.91	801.70	121.69	0.36
Chalakudy river	57600	500 yr return pe	2732.50	167.60	178.16		178.63	0.001072	3.04	900.20	126.73	0.36
Chalakudy river	57000	10 yr return per	1173.20	164.81	170.82	170.82	172.79	0.012802	7.00	300.22	85.09	1.12
Chalakudy river	57000	20 yr return per	1415.60	164.81	171.40	171.40	173.56	0.012186	7.34	351.47	91.28	1.11
Chalakudy river	57000	50 yr return per	1742.80	164.81	172.10	172.10	174.49	0.011719	7.76	417.57	98.70	1.10
Chalakudy river	57000	100 yr return pe	1985.30	164.81	172.60	172.60	175.14	0.011313	8.01	468.82	105.06	1.09
Chalakudy river	57000	200 yr return pe	2335.90	164.81	173.18	173.18	176.00	0.011418	8.46	531.81	112.58	1.11
Chalakudy river	57000	500 yr return pe	2732.50	164.81	174.06	174.06	176.93	0.010156	8.55	639.09	128.92	1.06
Chalakudy river	56400	10 yr return per	1173.20	146.69	152.89	152.32	154.21	0.006565	5.09	236.00	64.53	0.80
Chalakudy river	56400	20 yr return per	1415.60	146.69	153.31	152.83	154.88	0.007036	5.56	263.28	67.61	0.84
Chalakudy river	56400	50 yr return per	1742.80	146.69	153.78	153.45	155.71	0.007712	6.17	296.37	71.17	0.90
Chalakudy river	56400	100 yr return pe	1985.30	146.69	154.07	153.87	156.29	0.008330	6.62	317.28	73.33	0.94
Chalakudy river	56400	200 yr return pe	2335.90	146.69	154.49	154.49	157.10	0.008995	7.18	348.40	76.42	0.98
Chalakudy river	56400	500 yr return pe	2732.50	146.69	155.10	155.10	157.95	0.008778	7.52	396.66	81.23	0.99
Chalakudy river	55800	10 yr return per	1173.20	144.01	147.78	147.78	148.99	0.011911	4.87	240.81	100.44	1.00
Chalakudy river	55800	20 yr return per	1415.60	144.01	148.15	148.15	149.46	0.011617	5.07	279.23	107.65	1.01
Chalakudy river	55800	50 yr return per	1742.80	144.01	148.57	148.57	150.03	0.011273	5.34	326.39	114.62	1.01
Chalakudy river	55800	100 yr return pe	1985.30	144.01	148.85	148.85	150.42	0.010842	5.54	359.30	119.25	1.00
Chalakudy river	55800	200 yr return pe	2335.90	144.01	149.23	149.23	150.95	0.010383	5.80	405.93	125.28	1.00
Chalakudy river	55800	500 yr return pe	2732.50	144.01	149.63	149.63	151.51	0.010136	6.08	456.07	131.14	1.00
Chalakudy river	54000	10 yr return per	1173.20	127.37	130.71	130.71	131.82	0.012158	4.66	251.64	114.13	1.00
Chalakudy river	54000	20 yr return per	1415.60	127.37	131.04	131.04	132.25	0.011818	4.88	290.34	120.52	1.00
Chalakudy river	54000	50 yr return per	1742.80	127.37	131.45	131.45	132.78	0.011430	5.11	340.74	128.36	1.00
Chalakudy river	54000	100 yr return pe	1985.30	127.37	131.72	131.72	133.14	0.011212	5.28	376.18	133.26	1.00
Chalakudy river	54000	200 yr return pe	2335.90	127.37	132.08	132.08	133.61	0.010915	5.49	425.58	139.27	1.00
Chalakudy river	54000	500 yr return pe	2732.50	127.37	132.46	132.46	134.11	0.010610	5.69	479.94	145.51	1.00
Chalakudy river	53400	10 yr return per	1173.20	81.48	86.74	85.18	87.09	0.002321	2.61	449.25	140.08	0.47
Chalakudy river	53400	20 yr return per	1415.60	81.48	87.13	85.51	87.53	0.002421	2.80	505.16	146.22	0.48
Chalakudy river	53400	50 yr return per	1742.80	81.48	87.60		88.07	0.002536	3.03	575.70	153.62	0.50
Chalakudy river	53400	100 yr return pe	1985.30	81.48	87.95		88.46	0.002556	3.15	629.89	159.13	0.51
Chalakudy river	53400	200 yr return pe	2335.90	81.48	88.49		89.03	0.002646	3.24	722.83	195.89	0.52
Chalakudy river	53400	500 yr return pe	2732.50	81.48	88.94		89.53	0.002579	3.40	813.42	206.58	0.52
Chalakudy river	52800	10 yr return per	1173.20	79.48	83.12	83.11	84.34	0.011620	4.89	240.08	97.90	1.00

Reach	River Station	Profile	Q Total	Min Ch El	W.S. Elev	Crit W.S.	E.G. Elev	E.G. Slope	Vel Chnl	Flow Area	Top Width	Froude # Chl
			(m^3/s)	(m)	(m)	(m)	(m)	(m/m)	(m/s)	(m^2)	(m)	
Chalakudy river	52800	20 yr return per	1415.60	79.48	83.60	83.48	84.83	0.010093	4.91	288.19	104.87	0.95
Chalakudy river	52800	50 yr return per	1742.80	79.48	84.16	83.91	85.44	0.008566	5.01	348.96	113.16	0.89
Chalakudy river	52800	100 yr return pe	1985.30	79.48	84.49	84.20	85.85	0.008170	5.17	387.17	117.80	0.89
Chalakudy river	52800	200 yr return pe	2335.90	79.48	84.94	84.58	86.41	0.007728	5.37	441.46	123.78	0.88
Chalakudy river	52800	500 yr return pe	2732.50	79.48	85.41	85.01	87.00	0.007333	5.58	501.88	129.68	0.87
Chalakudy river	52200	10 yr return per	1173.20	75.24	82.53		82.69	0.000911	1.79	655.32	178.26	0.30
Chalakudy river	52200	20 yr return per	1415.60	75.24	83.05		83.23	0.000902	1.89	750.86	187.61	0.30
Chalakudy river	52200	50 yr return per	1742.80	75.24	83.69		83.89	0.000893	1.99	873.59	199.07	0.30
Chalakudy river	52200	100 yr return pe	1985.30	75.24	84.11		84.33	0.000857	2.07	960.29	206.62	0.30
Chalakudy river	52200	200 yr return pe	2335.90	75.24	84.66		84.90	0.000836	2.19	1075.53	215.48	0.30
Chalakudy river	52200	500 yr return pe	2732.50	75.24	85.22		85.49	0.000824	2.31	1199.23	223.06	0.31
Chalakudy river	51600	10 yr return per	1173.20	77.08	82.10		82.21	0.000656	1.50	1045.09	298.62	0.25
Chalakudy river	51600	20 yr return per	1415.60	77.08	82.65		82.76	0.000618	1.56	1211.03	309.86	0.25
Chalakudy river	51600	50 yr return per	1742.80	77.08	83.31		83.43	0.000585	1.64	1418.58	322.00	0.25
Chalakudy river	51600	100 yr return pe	1985.30	77.08	83.75		83.89	0.000570	1.70	1564.23	330.83	0.25
Chalakudy river	51600	200 yr return pe	2335.90	77.08	84.32		84.46	0.000559	1.79	1753.33	342.69	0.25
Chalakudy river	51600	500 yr return pe	2732.50	77.08	84.90		85.06	0.000540	1.89	1957.09	356.53	0.25
Chalakudy river	51000	10 yr return per	1173.20	75.33	81.56		81.73	0.000992	1.98	852.81	216.83	0.32
Chalakudy river	51000	20 yr return per	1415.60	75.33	82.10		82.30	0.001002	2.09	974.83	228.85	0.32
Chalakudy river	51000	50 yr return per	1742.80	75.33	82.76		82.98	0.001009	2.22	1129.58	242.50	0.33
Chalakudy river	51000	100 yr return pe	1985.30	75.33	83.20		83.44	0.001011	2.30	1239.13	251.98	0.33
Chalakudy river	51000	200 yr return pe	2335.90	75.33	83.76		84.02	0.000986	2.44	1382.13	263.52	0.33
Chalakudy river	51000	500 yr return pe	2732.50	75.33	84.34		84.63	0.000966	2.58	1537.86	275.24	0.33
Chalakudy river	50400	10 yr return per	1173.20	74.39	78.78	78.78	80.20	0.010891	5.31	237.57	92.16	0.99
Chalakudy river	50400	20 yr return per	1415.60	74.39	79.21	79.21	80.76	0.010508	5.56	277.93	98.68	0.99
Chalakudy river	50400	50 yr return per	1742.80	74.39	79.73	79.73	81.44	0.010109	5.83	332.48	107.24	0.99
Chalakudy river	50400	100 yr return pe	1985.30	74.39	80.09	80.09	81.89	0.009921	6.01	371.37	112.79	0.99
Chalakudy river	50400	200 yr return pe	2335.90	74.39	80.56	80.56	82.50	0.009705	6.24	426.31	120.19	0.99
Chalakudy river	50400	500 yr return pe	2732.50	74.39	81.05	81.05	83.13	0.009477	6.47	487.65	127.95	0.99
Chalakudy river	49800	10 yr return per	1173.20	71.82	76.01		76.15	0.001029	1.67	781.32	277.45	0.31
Chalakudy river	49800	20 yr return per	1415.60	71.82	76.31		76.47	0.001101	1.83	864.49	281.81	0.32
Chalakudy river	49800	50 yr return per	1742.80	71.82	76.67		76.87	0.001185	2.03	967.60	287.13	0.34
Chalakudy river	49800	100 yr return pe	1985.30	71.82	76.91		77.14	0.001249	2.16	1036.79	290.64	0.35
Chalakudy river	49800	200 yr return pe	2335.90	71.82	77.24		77.51	0.001326	2.34	1132.57	295.49	0.37
Chalakudy river	49800	500 yr return pe	2732.50	71.82	77.56		77.88	0.001419	2.53	1229.84	300.52	0.38

Reach	River Station	Profile	Q Total	Min Ch El	W.S. Elev	Crit W.S.	E.G. Elev	E.G. Slope	Vel Chnl	Flow Area	Top Width	Froude #Chl
			(m^3/s)	(m)	(m)	(m)	(m)	(m/m)	(m/s)	(m^2)	(m)	
Chalakudy river	49200	10 yr return per	1173.20	72.04	73.78	73.78	74.45	0.020508	3.90	402.21	322.08	1.17
Chalakudy river	49200	20 yr return per	1415.60	72.04	73.96	73.96	74.71	0.018415	4.09	463.07	331.12	1.14
Chalakudy river	49200	50 yr return per	1742.80	72.04	74.19	74.19	75.04	0.016647	4.33	540.15	343.04	1.11
Chalakudy river	49200	100 yr return pe	1985.30	72.04	74.36	74.36	75.26	0.015300	4.45	599.68	351.75	1.08
Chalakudy river	49200	200 yr return pe	2335.90	72.04	74.58	74.58	75.56	0.014325	4.65	675.76	361.25	1.07
Chalakudy river	49200	500 yr return pe	2732.50	72.04	74.83	74.83	75.88	0.012975	4.80	766.90	369.68	1.04
Chalakudy river	48600	10 yr return per	1173.20	62.32	67.96		68.10	0.000741	1.68	747.18	216.37	0.27
Chalakudy river	48600	20 yr return per	1415.60	62.32	68.42		68.58	0.000991	1.78	859.61	285.36	0.31
Chalakudy river	48600	50 yr return per	1742.80	62.32	68.95		69.13	0.001083	1.86	1030.78	346.24	0.32
Chalakudy river	48600	100 yr return pe	1985.30	62.32	69.31		69.49	0.001036	1.91	1155.13	358.76	0.32
Chalakudy river	48600	200 yr return pe	2335.90	62.32	69.77		69.97	0.000973	1.99	1325.40	370.54	0.31
Chalakudy river	48600	500 yr return pe	2732.50	62.32	70.26		70.47	0.000928	2.07	1507.27	383.57	0.31
Chalakudy river	48000	10 yr return per	1173.20	58.88	67.76		67.84	0.000253	1.29	987.72	229.33	0.17
Chalakudy river	48000	20 yr return per	1415.60	58.88	68.15		68.26	0.000298	1.46	1080.42	239.75	0.19
Chalakudy river	48000	50 yr return per	1742.80	58.88	68.64		68.77	0.000354	1.66	1198.77	252.39	0.20
Chalakudy river	48000	100 yr return pe	1985.30	58.88	68.96		69.12	0.000393	1.80	1281.59	258.89	0.22
Chalakudy river	48000	200 yr return pe	2335.90	58.88	69.39		69.59	0.000447	1.98	1395.87	268.30	0.23
Chalakudy river	48000	500 yr return pe	2732.50	58.88	69.83		70.07	0.000505	2.18	1515.16	277.78	0.25
Chalakudy river	47400	10 yr return per	1173.20	62.10	67.38		67.54	0.001310	2.00	1053.42	373.98	0.35
Chalakudy river	47400	20 yr return per	1415.60	62.10	67.74		67.92	0.001369	2.15	1187.53	383.75	0.36
Chalakudy river	47400	50 yr return per	1742.80	62.10	68.17		68.39	0.001432	2.33	1357.08	395.76	0.38
Chalakudy river	47400	100 yr return pe	1985.30	62.10	68.47		68.70	0.001472	2.45	1474.93	403.79	0.39
Chalakudy river	47400	200 yr return pe	2335.90	62.10	68.86		69.13	0.001515	2.61	1638.03	413.00	0.40
Chalakudy river	47400	500 yr return pe	2732.50	62.10	69.27		69.57	0.001538	2.78	1805.22	421.31	0.41
Chalakudy river	46800	10 yr return per	1173.20	61.64	65.51	65.06	66.01	0.006632	3.23	450.96	232.97	0.73
Chalakudy river	46800	20 yr return per	1415.60	61.64	65.74	65.29	66.32	0.006804	3.50	504.39	237.42	0.75
Chalakudy river	46800	50 yr return per	1742.80	61.64	66.01	65.57	66.71	0.007033	3.83	570.84	242.96	0.78
Chalakudy river	46800	100 yr return pe	1985.30	61.64	66.21	65.76	66.99	0.007102	4.03	619.41	246.76	0.79
Chalakudy river	46800	200 yr return pe	2335.90	61.64	66.46	66.01	67.35	0.007357	4.34	681.16	251.45	0.82
Chalakudy river	46800	500 yr return pe	2732.50	61.64	66.72	66.31	67.75	0.007588	4.65	747.79	256.41	0.84
Chalakudy river	46200	10 yr return per	1173.20	56.56	59.66	59.66	60.47	0.013559	3.98	297.12	190.32	1.00
Chalakudy river	46200	20 yr return per	1415.60	56.56	59.89	59.89	60.79	0.013053	4.20	340.31	195.89	1.00
Chalakudy river	46200	50 yr return per	1742.80	56.56	60.16	60.16	61.18	0.012457	4.47	395.11	200.96	1.00
Chalakudy river	46200	100 yr return pe	1985.30	56.56	60.35	60.35	61.46	0.012290	4.67	431.95	204.30	1.01
Chalakudy river	46200	200 yr return pe	2335.90	56.56	60.62	60.62	61.83	0.011722	4.89	488.02	209.27	1.00
Chalakudy river	46200	500 yr return pe	2732.50	56.56	60.90	60.90	62.23	0.011268	5.11	548.41	214.50	1.00

Reach	River Station	Profile	Q Total	Min Ch El	W.S. Elev	Crit W.S.	E.G. Elev	E.G. Slope	Vel Chnl	Flow Area	Top Width	Froude # Chl
			(m^3/s)	(m)	(m)	(m)	(m)	(m/m)	(m/s)	(m^2)	(m)	
Chalakudy river	45600	10 yr return per	1173.20	52.07	58.01		58.11	0.000603	1.29	852.36	333.75	0.24
Chalakudy river	45600	20 yr return per	1415.60	52.07	58.40		58.51	0.000581	1.31	984.77	353.11	0.23
Chalakudy river	45600	50 yr return per	1742.80	52.07	58.88		59.00	0.000542	1.34	1161.44	374.74	0.23
Chalakudy river	45600	100 yr return pe	1985.30	52.07	59.17		59.30	0.000532	1.39	1270.68	387.19	0.23
Chalakudy river	45600	200 yr return pe	2335.90	52.07	59.55		59.70	0.000525	1.45	1421.01	403.29	0.23
Chalakudy river	45600	500 yr return pe	2732.50	52.07	59.96		60.12	0.000509	1.53	1588.66	417.46	0.23
Chalakudy river	45000	10 yr return per	1173.20	51.47	57.69		57.81	0.000430	1.55	947.02	217.52	0.22
Chalakudy river	45000	20 yr return per	1415.60	51.47	58.03		58.18	0.000509	1.75	1022.55	233.84	0.24
Chalakudy river	45000	50 yr return per	1742.80	51.47	58.46		58.65	0.000612	2.01	1139.43	323.90	0.26
Chalakudy river	45000	100 yr return pe	1985.30	51.47	58.68		58.92	0.000719	2.22	1217.07	351.60	0.29
Chalakudy river	45000	200 yr return pe	2335.90	51.47	59.00		59.29	0.000832	2.46	1329.42	355.75	0.31
Chalakudy river	45000	500 yr return pe	2732.50	51.47	59.35		59.70	0.000944	2.70	1453.58	360.28	0.34
Chalakudy river	44400	10 yr return per	1173.20	52.85	56.35	56.35	57.06	0.008414	3.93	358.15	240.46	0.84
Chalakudy river	44400	20 yr return per	1415.60	52.85	56.60	56.60	57.33	0.008668	4.01	419.67	266.35	0.85
Chalakudy river	44400	50 yr return per	1742.80	52.85	56.80	56.80	57.65	0.009853	4.31	478.55	298.71	0.91
Chalakudy river	44400	100 yr return pe	1985.30	52.85	57.12	57.12	57.86	0.007980	4.09	584.77	366.83	0.83
Chalakudy river	44400	200 yr return pe	2335.90	52.85	57.30	57.30	58.11	0.007906	4.26	650.42	370.94	0.83
Chalakudy river	44400	500 yr return pe	2732.50	52.85	57.45	57.45	58.38	0.008284	4.53	707.34	374.46	0.86
Chalakudy river	43800	10 yr return per	1173.20	46.91	50.46		50.69	0.001823	2.17	564.94	265.02	0.41
Chalakudy river	43800	20 yr return per	1415.60	46.91	50.81		51.05	0.001727	2.25	661.78	289.28	0.40
Chalakudy river	43800	50 yr return per	1742.80	46.91	51.23		51.48	0.001612	2.32	798.48	336.26	0.39
Chalakudy river	43800	100 yr return pe	1985.30	46.91	51.52		51.78	0.001497	2.33	897.02	343.25	0.38
Chalakudy river	43800	200 yr return pe	2335.90	46.91	51.91		52.17	0.001369	2.34	1032.42	352.84	0.37
Chalakudy river	43800	500 yr return pe	2732.50	46.91	52.31		52.59	0.001262	2.36	1177.20	361.95	0.36
Chalakudy river	43200	10 yr return per	1173.20	45.72	50.12		50.19	0.000408	1.27	1051.71	368.87	0.20
Chalakudy river	43200	20 yr return per	1415.60	45.72	50.47		50.56	0.000413	1.35	1184.74	378.32	0.21
Chalakudy river	43200	50 yr return per	1742.80	45.72	50.90		51.00	0.000418	1.45	1349.09	387.30	0.21
Chalakudy river	43200	100 yr return pe	1985.30	45.72	51.19		51.31	0.000421	1.51	1463.81	392.88	0.21
Chalakudy river	43200	200 yr return pe	2335.90	45.72	51.59		51.72	0.000423	1.59	1620.46	399.54	0.22
Chalakudy river	43200	500 yr return pe	2732.50	45.72	52.00		52.15	0.000427	1.68	1786.01	406.21	0.22
Chalakudy river	42600	10 yr return per	1173.20	45.03	48.54	48.52	49.42	0.010868	4.20	282.21	157.15	0.94
Chalakudy river	42600	20 yr return per	1415.60	45.03	48.78	48.78	49.77	0.010731	4.45	320.73	163.03	0.95
Chalakudy river	42600	50 yr return per	1742.80	45.03	49.10	49.10	50.20	0.010140	4.67	374.59	169.98	0.94
Chalakudy river	42600	100 yr return pe	1985.30	45.03	49.31	49.31	50.50	0.009928	4.84	411.06	174.52	0.94
Chalakudy river	42600	200 yr return pe	2335.90	45.03	49.60	49.60	50.90	0.009624	5.04	462.54	180.75	0.94

Reach	River Station	Profile	Q Total	Min Ch El	W.S. Elev	Crit W.S.	E.G. Elev	E.G. Slope	Vel Chnl	Flow Area	Top Width	Froude # Chl
			(m^3/s)	(m)	(m)	(m)	(m)	(m/m)	(m/s)	(m^2)	(m)	
Chalakudy river	42600	500 yr return pe	2732.50	45.03	49.92	49.92	51.32	0.009184	5.21	521.60	187.81	0.93
Chalakudy river	42000	10 yr return per	1173.20	41.04	45.24		45.66	0.003818	2.91	421.69	201.79	0.58
Chalakudy river	42000	20 yr return per	1415.60	41.04	45.79		46.17	0.002738	2.80	541.89	231.31	0.50
Chalakudy river	42000	50 yr return per	1742.80	41.04	46.45		46.80	0.001958	2.69	704.09	254.43	0.44
Chalakudy river	42000	100 yr return pe	1985.30	41.04	46.90		47.24	0.001669	2.68	828.71	302.19	0.41
Chalakudy river	42000	200 yr return pe	2335.90	41.04	47.50		47.81	0.001306	2.59	1017.01	329.04	0.37
Chalakudy river	42000	500 yr return pe	2732.50	41.04	48.11		48.40	0.001043	2.50	1224.69	347.42	0.34
Chalakudy river	41400	10 yr return per	1173.20	35.12	45.36		45.40	0.000082	0.85	1473.97	229.47	0.10
Chalakudy river	41400	20 yr return per	1415.60	35.12	45.86		45.91	0.000097	0.96	1590.40	235.19	0.11
Chalakudy river	41400	50 yr return per	1742.80	35.12	46.48		46.54	0.000115	1.09	1737.75	240.64	0.12
Chalakudy river	41400	100 yr return pe	1985.30	35.12	46.90		46.97	0.000127	1.18	1840.23	244.36	0.13
Chalakudy river	41400	200 yr return pe	2335.90	35.12	47.46		47.55	0.000144	1.30	1978.04	249.27	0.14
Chalakudy river	41400	500 yr return pe	2732.50	35.12	48.04		48.14	0.000162	1.43	2124.47	254.45	0.15
Chalakudy river	40800	10 yr return per	1173.20	37.81	45.06		45.26	0.000869	2.16	812.88	185.92	0.31
Chalakudy river	40800	20 yr return per	1415.60	37.81	45.50		45.75	0.000948	2.38	897.15	193.36	0.33
Chalakudy river	40800	50 yr return per	1742.80	37.81	46.05		46.36	0.001032	2.65	1005.78	202.59	0.34
Chalakudy river	40800	100 yr return pe	1985.30	37.81	46.42		46.77	0.001084	2.83	1082.69	208.94	0.36
Chalakudy river	40800	200 yr return pe	2335.90	37.81	46.91		47.32	0.001154	3.07	1187.16	217.33	0.37
Chalakudy river	40800	500 yr return pe	2732.50	37.81	47.42		47.90	0.001221	3.31	1300.31	226.26	0.39
Chalakudy river	40200	10 yr return per	1173.20	39.20	42.89	42.89	43.95	0.009463	4.65	257.58	122.20	0.91
Chalakudy river	40200	20 yr return per	1415.60	39.20	43.19	43.19	44.37	0.008957	4.86	295.39	125.98	0.90
Chalakudy river	40200	50 yr return per	1742.80	39.20	43.54	43.54	44.89	0.008685	5.16	340.26	129.54	0.91
Chalakudy river	40200	100 yr return pe	1985.30	39.20	43.78	43.78	45.26	0.008523	5.36	371.88	132.00	0.91
Chalakudy river	40200	200 yr return pe	2335.90	39.20	44.14	44.14	45.75	0.008095	5.56	419.51	135.61	0.90
Chalakudy river	40200	500 yr return pe	2732.50	39.20	44.52	44.52	46.28	0.007720	5.78	471.25	139.41	0.89
Chalakudy river	39600	10 yr return per	1173.20	30.35	34.19	34.19	35.41	0.011830	4.89	239.72	98.85	1.00
Chalakudy river	39600	20 yr return per	1415.60	30.35	34.56	34.56	35.89	0.011492	5.11	277.10	104.82	1.00
Chalakudy river	39600	50 yr return per	1742.80	30.35	35.01	35.01	36.46	0.011140	5.34	326.10	112.61	1.00
Chalakudy river	39600	100 yr return pe	1985.30	30.35	35.32	35.32	36.85	0.010952	5.48	362.06	118.78	1.00
Chalakudy river	39600	200 yr return pe	2335.90	30.35	35.73	35.73	37.36	0.010686	5.66	412.97	126.94	1.00
Chalakudy river	39600	500 yr return pe	2732.50	30.35	36.15	36.15	37.89	0.010455	5.84	467.70	134.71	1.00
Chalakudy river	39000	10 yr return per	1173.20	23.87	26.68	26.48	27.25	0.012971	3.66	452.48	275.27	0.97
Chalakudy river	39000	20 yr return per	1415.60	23.87	27.06	26.69	27.59	0.009902	3.52	560.43	297.58	0.87
Chalakudy river	39000	50 yr return per	1742.80	23.87	27.38	26.99	27.94	0.009694	3.62	659.45	326.90	0.87
Chalakudy river	39000	100 yr return pe	1985.30	23.87	27.58	27.20	28.17	0.009602	3.70	727.94	345.61	0.87

Reach	River Station	Profile	Q Total	Min Ch El	W.S. Elev	Crit W.S.	E.G. Elev	E.G. Slope	Vel Chnl	Flow Area	Top Width	Froude # Chl
			(m^3/s)	(m)	(m)	(m)	(m)	(m/m)	(m/s)	(m^2)	(m)	
Chalakudy river	39000	200 yr return pe	2335.90	23.87	27.88	27.43	28.49	0.009011	3.75	835.92	371.43	0.85
Chalakudy river	39000	500 yr return pe	2732.50	23.87	28.09	27.69	28.80	0.008990	4.00	915.92	375.04	0.86
Chalakudy river	38400	10 yr return per	1173.20	15.21	19.64	19.42	20.54	0.009477	4.18	280.34	123.97	0.89
Chalakudy river	38400	20 yr return per	1415.60	15.21	19.77	19.77	20.93	0.012007	4.79	295.67	127.60	1.00
Chalakudy river	38400	50 yr return per	1742.80	15.21	20.18	20.18	21.44	0.011691	4.97	350.62	140.21	1.00
Chalakudy river	38400	100 yr return pe	1985.30	15.21	20.46	20.46	21.77	0.011414	5.06	392.19	149.89	1.00
Chalakudy river	38400	200 yr return pe	2335.90	15.21	21.06	21.06	22.17	0.012023	4.68	499.32	223.50	1.00
Chalakudy river	38400	500 yr return pe	2732.50	15.21	21.32	21.32	22.54	0.011812	4.89	558.86	231.00	1.00
Chalakudy river	37800	10 yr return per	1173.20	14.04	17.01		17.28	0.003194	2.28	513.52	249.50	0.51
Chalakudy river	37800	20 yr return per	1415.60	14.04	17.47		17.73	0.002502	2.25	629.07	266.02	0.46
Chalakudy river	37800	50 yr return per	1742.80	14.04	18.02		18.27	0.001941	2.23	791.47	320.61	0.42
Chalakudy river	37800	100 yr return pe	1985.30	14.04	18.40		18.65	0.001625	2.22	920.84	358.94	0.39
Chalakudy river	37800	200 yr return pe	2335.90	14.04	18.90		19.14	0.001316	2.20	1119.92	421.29	0.36
Chalakudy river	37800	500 yr return pe	2732.50	14.04	19.47		19.69	0.001022	2.12	1361.80	435.25	0.33
Chalakudy river	37200	10 yr return per	1173.20	6.66	17.17		17.18	0.000011	0.33	3595.98	492.83	0.04
Chalakudy river	37200	20 yr return per	1415.60	6.66	17.61		17.62	0.000014	0.37	3816.91	507.75	0.04
Chalakudy river	37200	50 yr return per	1742.80	6.66	18.16		18.16	0.000017	0.43	4097.38	530.42	0.05
Chalakudy river	37200	100 yr return pe	1985.30	6.66	18.53		18.54	0.000020	0.47	4297.75	548.53	0.05
Chalakudy river	37200	200 yr return pe	2335.90	6.66	19.02		19.03	0.000023	0.52	4573.12	572.77	0.06
Chalakudy river	37200	500 yr return pe	2732.50	6.66	19.56		19.58	0.000026	0.57	4892.20	599.77	0.06
Chalakudy river	36600	10 yr return per	1173.20	4.72	17.14		17.16	0.000041	0.70	1820.29	331.47	0.07
Chalakudy river	36600	20 yr return per	1415.60	4.72	17.58		17.60	0.000048	0.78	1968.12	350.21	0.08
Chalakudy river	36600	50 yr return per	1742.80	4.72	18.11		18.14	0.000058	0.89	2163.87	385.93	0.09
Chalakudy river	36600	100 yr return pe	1985.30	4.72	18.47		18.51	0.000065	0.96	2309.14	409.31	0.09
Chalakudy river	36600	200 yr return pe	2335.90	4.72	18.96		19.00	0.000074	1.06	2516.04	451.73	0.10
Chalakudy river	36600	500 yr return pe	2732.50	4.72	19.49		19.55	0.000082	1.15	2791.47	538.89	0.11
Chalakudy river	36000	10 yr return per	1173.20	4.42	17.12		17.14	0.000039	0.70	2073.63	402.53	0.07
Chalakudy river	36000	20 yr return per	1415.60	4.42	17.55		17.58	0.000047	0.79	2250.44	421.33	0.08
Chalakudy river	36000	50 yr return per	1742.80	4.42	18.07		18.11	0.000057	0.91	2477.50	444.42	0.09
Chalakudy river	36000	100 yr return pe	1985.30	4.42	18.43		18.48	0.000064	0.98	2640.61	460.87	0.09
Chalakudy river	36000	200 yr return pe	2335.90	4.42	18.91		18.96	0.000074	1.08	2874.92	545.06	0.10
Chalakudy river	36000	500 yr return pe	2732.50	4.42	19.44		19.50	0.000083	1.18	3182.35	601.21	0.11
Chalakudy river	35400	10 yr return per	1173.20	5.54	17.04		17.10	0.000094	1.11	1253.47	197.78	0.11
Chalakudy river	35400	20 yr return per	1415.60	5.54	17.45		17.53	0.000117	1.27	1336.10	206.54	0.13
Chalakudy river	35400	50 yr return per	1742.80	5.54	17.95		18.05	0.000147	1.47	1441.27	217.04	0.14

Reach	River Station	Profile	Q Total	Min Ch El	W.S. Elev	Crit W.S.	E.G. Elev	E.G. Slope	Vel Chnl	Flow Area	Top Width	Froude # Chl
			(m^3/s)	(m)	(m)	(m)	(m)	(m/m)	(m/s)	(m^2)	(m)	
Chalakudy river	35400	100 yr return pe	1985.30	5.54	18.29		18.41	0.000168	1.61	1516.10	224.82	0.15
Chalakudy river	35400	200 yr return pe	2335.90	5.54	18.73		18.88	0.000200	1.80	1618.37	237.52	0.17
Chalakudy river	35400	500 yr return pe	2732.50	5.54	19.23		19.41	0.000234	2.00	1742.82	295.55	0.18
Chalakudy river	34800	10 yr return per	1173.20	3.86	16.99		17.05	0.000083	1.04	1300.10	166.87	0.11
Chalakudy river	34800	20 yr return per	1415.60	3.86	17.39		17.46	0.000105	1.20	1368.25	183.50	0.12
Chalakudy river	34800	50 yr return per	1742.80	3.86	17.87		17.96	0.000136	1.41	1463.27	214.71	0.14
Chalakudy river	34800	100 yr return pe	1985.30	3.86	18.19		18.31	0.000158	1.55	1535.69	228.37	0.15
Chalakudy river	34800	200 yr return pe	2335.90	3.86	18.61		18.76	0.000190	1.74	1635.30	242.80	0.16
Chalakudy river	34800	500 yr return pe	2732.50	3.86	19.09		19.27	0.000222	1.93	1756.13	264.96	0.18
Chalakudy river	34200	10 yr return per	1173.20	7.44	16.85		16.96	0.000294	1.48	921.34	165.47	0.19
Chalakudy river	34200	20 yr return per	1415.60	7.44	17.21		17.35	0.000368	1.68	981.43	170.98	0.21
Chalakudy river	34200	50 yr return per	1742.80	7.44	17.63		17.82	0.000469	1.94	1058.64	196.89	0.24
Chalakudy river	34200	100 yr return pe	1985.30	7.44	17.92		18.14	0.000544	2.11	1120.25	229.11	0.26
Chalakudy river	34200	200 yr return pe	2335.90	7.44	18.29		18.56	0.000646	2.35	1208.39	249.79	0.28
Chalakudy river	34200	500 yr return pe	2732.50	7.44	18.71		19.04	0.000726	2.59	1317.86	270.29	0.30
Chalakudy river	33600	10 yr return per	1173.20	1.42	16.89		16.90	0.000019	0.56	2515.40	353.40	0.05
Chalakudy river	33600	20 yr return per	1415.60	1.42	17.25		17.27	0.000024	0.65	2646.38	359.57	0.06
Chalakudy river	33600	50 yr return per	1742.80	1.42	17.69		17.72	0.000032	0.77	2806.25	366.97	0.07
Chalakudy river	33600	100 yr return pe	1985.30	1.42	17.99		18.03	0.000038	0.85	2916.36	371.98	0.08
Chalakudy river	33600	200 yr return pe	2335.90	1.42	18.37		18.42	0.000047	0.97	3062.67	397.32	0.08
Chalakudy river	33600	500 yr return pe	2732.50	1.42	18.81		18.87	0.000057	1.09	3241.38	416.70	0.09
Chalakudy river	33000	10 yr return per	1173.20	5.30	16.86		16.88	0.000053	0.80	2994.03	559.92	0.08
Chalakudy river	33000	20 yr return per	1415.60	5.30	17.21		17.25	0.000066	0.92	3198.62	579.18	0.09
Chalakudy river	33000	50 yr return per	1742.80	5.30	17.64		17.69	0.000085	1.08	3453.29	611.42	0.11
Chalakudy river	33000	100 yr return pe	1985.30	5.30	17.93		17.99	0.000100	1.19	3635.25	640.83	0.12
Chalakudy river	33000	200 yr return pe	2335.90	5.30	18.30		18.37	0.000119	1.33	3874.78	649.42	0.13
Chalakudy river	33000	500 yr return pe	2732.50	5.30	18.73		18.82	0.000139	1.48	4155.37	666.33	0.14
Chalakudy river	32400	10 yr return per	1173.20	12.28	15.81	15.81	16.69	0.008871	4.25	286.76	177.93	0.87
Chalakudy river	32400	20 yr return per	1415.60	12.28	16.09	16.09	17.03	0.008294	4.42	339.49	199.45	0.86
Chalakudy river	32400	50 yr return per	1742.80	12.28	16.42	16.42	17.43	0.007752	4.61	408.96	221.92	0.84
Chalakudy river	32400	100 yr return pe	1985.30	12.28	16.63	16.63	17.70	0.007559	4.76	456.56	235.27	0.84
Chalakudy river	32400	200 yr return pe	2335.90	12.28	17.05	16.90	18.06	0.006159	4.65	560.82	274.37	0.78
Chalakudy river	32400	500 yr return pe	2732.50	12.28	17.70	17.22	18.51	0.003987	4.18	812.88	451.37	0.64
Chalakudy river	31800	10 yr return per	1173.20	10.08	15.22		15.32	0.000490	1.35	892.56	341.81	0.22
Chalakudy river	31800	20 yr return per	1415.60	10.08	15.67		15.78	0.000434	1.37	1054.97	377.73	0.21

Reach	River Station	Profile	Q Total	Min Ch El	W.S. Elev	Crit W.S.	E.G. Elev	E.G. Slope	Vel Chnl	Flow Area	Top Width	Froude # Chl
			(m^3/s)	(m)	(m)	(m)	(m)	(m/m)	(m/s)	(m^2)	(m)	
Chalakudy river	31800	50 yr return per	1742.80	10.08	16.25		16.36	0.000379	1.39	1289.86	441.57	0.20
Chalakudy river	31800	100 yr return pe	1985.30	10.08	16.63		16.75	0.000356	1.42	1466.23	485.26	0.20
Chalakudy river	31800	200 yr return pe	2335.90	10.08	17.13		17.25	0.000347	1.49	1721.48	533.74	0.20
Chalakudy river	31800	500 yr return pe	2732.50	10.08	17.67		17.79	0.000359	1.61	2048.85	659.94	0.21
Chalakudy river	31200	10 yr return per	1173.20	8.53	14.75		14.95	0.000785	2.00	656.91	166.49	0.29
Chalakudy river	31200	20 yr return per	1415.60	8.53	15.18		15.42	0.000853	2.20	729.75	173.69	0.31
Chalakudy river	31200	50 yr return per	1742.80	8.53	15.72		16.01	0.000919	2.44	826.23	183.77	0.32
Chalakudy river	31200	100 yr return pe	1985.30	8.53	16.06		16.40	0.000971	2.61	891.37	190.95	0.34
Chalakudy river	31200	200 yr return pe	2335.90	8.53	16.50		16.89	0.001052	2.84	976.56	200.66	0.35
Chalakudy river	31200	500 yr return pe	2732.50	8.53	16.95		17.41	0.001128	3.08	1069.95	210.80	0.37
Chalakudy river	30600	10 yr return per	1173.20	8.76	14.47		14.54	0.000480	1.41	1513.73	359.14	0.22
Chalakudy river	30600	20 yr return per	1415.60	8.76	14.89		14.98	0.000508	1.55	1667.97	372.23	0.23
Chalakudy river	30600	50 yr return per	1742.80	8.76	15.41		15.52	0.000574	1.76	1876.12	430.43	0.25
Chalakudy river	30600	100 yr return pe	1985.30	8.76	15.75		15.88	0.000595	1.88	2029.55	453.60	0.26
Chalakudy river	30600	200 yr return pe	2335.90	8.76	16.19		16.34	0.000619	2.02	2231.96	470.53	0.27
Chalakudy river	30600	500 yr return pe	2732.50	8.76	16.66		16.82	0.000635	2.15	2456.34	504.78	0.27
Chalakudy river	30000	10 yr return per	1173.20	9.40	13.66		13.97	0.002405	2.46	489.17	236.81	0.47
Chalakudy river	30000	20 yr return per	1415.60	9.40	14.13		14.43	0.001876	2.41	606.30	257.16	0.42
Chalakudy river	30000	50 yr return per	1742.80	9.40	14.68		14.98	0.001524	2.40	753.62	279.76	0.39
Chalakudy river	30000	100 yr return pe	1985.30	9.40	15.06		15.35	0.001351	2.41	861.37	294.68	0.37
Chalakudy river	30000	200 yr return pe	2335.90	9.40	15.51		15.82	0.001225	2.45	999.50	312.55	0.36
Chalakudy river	30000	500 yr return pe	2732.50	9.40	16.00		16.32	0.001116	2.50	1156.80	342.27	0.35
Chalakudy river	29400	10 yr return per	1173.20	10.62	13.73		13.75	0.000076	0.27	2166.41	803.84	0.07
Chalakudy river	29400	20 yr return per	1415.60	10.62	14.21		14.23	0.000069	0.31	2559.40	831.60	0.07
Chalakudy river	29400	50 yr return per	1742.80	10.62	14.76		14.79	0.000065	0.36	3042.90	912.48	0.07
Chalakudy river	29400	100 yr return pe	1985.30	10.62	15.14		15.17	0.000067	0.40	3399.76	971.62	0.08
Chalakudy river	29400	200 yr return pe	2335.90	10.62	15.61		15.64	0.000064	0.44	3863.15	1009.90	0.08
Chalakudy river	29400	500 yr return pe	2732.50	10.62	16.10		16.13	0.000063	0.47	4376.24	1058.99	0.08
Chalakudy river	28800	10 yr return per	1173.20	-0.77	13.73		13.73	0.000010	0.34	3454.85	633.09	0.04
Chalakudy river	28800	20 yr return per	1415.60	-0.77	14.21		14.21	0.000011	0.36	3763.79	651.21	0.04
Chalakudy river	28800	50 yr return per	1742.80	-0.77	14.76		14.77	0.000013	0.40	4130.15	671.96	0.04
Chalakudy river	28800	100 yr return pe	1985.30	-0.77	15.13		15.15	0.000014	0.42	4384.40	686.99	0.04
Chalakudy river	28800	200 yr return pe	2335.90	-0.77	15.60		15.61	0.000016	0.45	4709.29	707.83	0.05
Chalakudy river	28800	500 yr return pe	2732.50	-0.77	16.10		16.11	0.000018	0.49	5066.52	747.39	0.05
Chalakudy river	28200	10 yr return per	1173.20	-0.90	13.71		13.72	0.000024	0.56	2395.53	500.21	0.06

Reach	River Station	Profile	Q Total	Min Ch El	W.S. Elev	Crit W.S.	E.G. Elev	E.G. Slope	Vel Chnl	Flow Area	Top Width	Froude # Chl
			(m^3/s)	(m)	(m)	(m)	(m)	(m/m)	(m/s)	(m^2)	(m)	
Chalakudy river	28200	20 yr return per	1415.60	-0.90	14.19		14.20	0.000027	0.61	2643.45	537.45	0.06
Chalakudy river	28200	50 yr return per	1742.80	-0.90	14.74		14.76	0.000031	0.67	2948.04	568.66	0.07
Chalakudy river	28200	100 yr return pe	1985.30	-0.90	15.11		15.13	0.000034	0.71	3164.03	597.03	0.07
Chalakudy river	28200	200 yr return pe	2335.90	-0.90	15.57		15.60	0.000038	0.76	3454.72	659.51	0.07
Chalakudy river	28200	500 yr return pe	2732.50	-0.90	16.07		16.09	0.000040	0.79	3786.34	684.36	0.07
Chalakudy river	27600	10 yr return per	1173.20	9.42	13.64		13.68	0.000667	1.43	2052.49	489.28	0.25
Chalakudy river	27600	20 yr return per	1415.60	9.42	14.10		14.15	0.000698	1.56	2284.51	506.97	0.26
Chalakudy river	27600	50 yr return per	1742.80	9.42	14.64		14.70	0.000758	1.73	2562.52	534.47	0.28
Chalakudy river	27600	100 yr return pe	1985.30	9.42	15.00		15.07	0.000796	1.84	2758.27	553.05	0.29
Chalakudy river	27600	200 yr return pe	2335.90	9.42	15.44		15.53	0.000850	1.99	3009.40	571.12	0.30
Chalakudy river	27600	500 yr return pe	2732.50	9.42	15.92		16.02	0.000894	2.13	3286.54	589.03	0.31
Chalakudy river	27000	10 yr return per	1173.20	2.77	13.57		13.60	0.000051	0.72	1754.38	293.61	0.08
Chalakudy river	27000	20 yr return per	1415.60	2.77	14.03		14.06	0.000062	0.81	1899.33	338.72	0.09
Chalakudy river	27000	50 yr return per	1742.80	2.77	14.54		14.59	0.000076	0.94	2083.40	369.67	0.10
Chalakudy river	27000	100 yr return pe	1985.30	2.77	14.89		14.95	0.000086	1.02	2227.33	456.05	0.11
Chalakudy river	27000	200 yr return pe	2335.90	2.77	15.32		15.39	0.000100	1.14	2458.12	607.11	0.12
Chalakudy river	27000	500 yr return pe	2732.50	2.77	15.78		15.86	0.000116	1.26	2762.48	693.42	0.13
Chalakudy river	26400	10 yr return per	1173.20	8.56	13.51		13.55	0.000098	0.60	1417.11	415.03	0.10
Chalakudy river	26400	20 yr return per	1415.60	8.56	13.95		14.01	0.000104	0.65	1612.44	456.57	0.10
Chalakudy river	26400	50 yr return per	1742.80	8.56	14.46		14.53	0.000113	0.72	1857.04	501.61	0.11
Chalakudy river	26400	100 yr return pe	1985.30	8.56	14.81		14.88	0.000120	0.77	2034.03	526.30	0.11
Chalakudy river	26400	200 yr return pe	2335.90	8.56	15.23		15.32	0.000130	0.83	2261.96	555.03	0.12
Chalakudy river	26400	500 yr return pe	2732.50	8.56	15.68		15.78	0.000140	0.90	2521.41	587.39	0.12
Chalakudy river	25800	10 yr return per	1173.20	3.26	13.50		13.52	0.000024	0.43	2676.92	583.54	0.05
Chalakudy river	25800	20 yr return per	1415.60	3.26	13.95		13.97	0.000027	0.47	2944.05	606.28	0.06
Chalakudy river	25800	50 yr return per	1742.80	3.26	14.46		14.48	0.000031	0.53	3260.79	631.75	0.06
Chalakudy river	25800	100 yr return pe	1985.30	3.26	14.81		14.83	0.000034	0.57	3481.90	650.23	0.07
Chalakudy river	25800	200 yr return pe	2335.90	3.26	15.23		15.26	0.000039	0.63	3767.69	717.48	0.07
Chalakudy river	25800	500 yr return pe	2732.50	3.26	15.69		15.72	0.000043	0.69	4138.76	910.61	0.07
Chalakudy river	25200	10 yr return per	1173.20	-1.33	13.47		13.50	0.000047	0.79	1660.62	362.63	0.08
Chalakudy river	25200	20 yr return per	1415.60	-1.33	13.91		13.95	0.000055	0.88	1827.81	392.52	0.09
Chalakudy river	25200	50 yr return per	1742.80	-1.33	14.41		14.46	0.000067	0.99	2037.72	462.51	0.10
Chalakudy river	25200	100 yr return pe	1985.30	-1.33	14.75		14.80	0.000073	1.06	2198.30	480.69	0.10
Chalakudy river	25200	200 yr return pe	2335.90	-1.33	15.17		15.23	0.000082	1.15	2403.34	512.96	0.11
Chalakudy river	25200	500 yr return pe	2732.50	-1.33	15.62		15.68	0.000089	1.23	2657.72	594.31	0.11

Reach	River Station	Profile	Q Total	Min Ch El	W.S. Elev	Crit W.S.	E.G. Elev	E.G. Slope	Vel Chnl	Flow Area	Top Width	Froude # Chl
			(m^3/s)	(m)	(m)	(m)	(m)	(m/m)	(m/s)	(m^2)	(m)	
Chalakudy river	24600	10 yr return per	1173.20	3.46	13.48		13.48	0.000005	0.21	5161.33	1190.77	0.02
Chalakudy river	24600	20 yr return per	1415.60	3.46	13.92		13.93	0.000006	0.24	5699.88	1225.24	0.03
Chalakudy river	24600	50 yr return per	1742.80	3.46	14.43		14.44	0.000007	0.28	6333.86	1283.94	0.03
Chalakudy river	24600	100 yr return pe	1985.30	3.46	14.77		14.78	0.000008	0.30	6775.52	1293.57	0.03
Chalakudy river	24600	200 yr return pe	2335.90	3.46	15.19		15.20	0.000009	0.32	7320.44	1303.99	0.03
Chalakudy river	24600	500 yr return pe	2732.50	3.46	15.65		15.65	0.000009	0.35	7913.40	1315.02	0.04
Chalakudy river	24000	10 yr return per	1173.20	10.66	13.41		13.47	0.000181	0.54	1134.79	417.98	0.12
Chalakudy river	24000	20 yr return per	1415.60	10.66	13.85		13.91	0.000172	0.57	1325.11	446.18	0.12
Chalakudy river	24000	50 yr return per	1742.80	10.66	14.35		14.42	0.000169	0.61	1555.59	478.35	0.12
Chalakudy river	24000	100 yr return pe	1985.30	10.66	14.68		14.76	0.000167	0.63	1720.78	499.08	0.12
Chalakudy river	24000	200 yr return pe	2335.90	10.66	15.10		15.18	0.000175	0.68	1934.65	557.62	0.13
Chalakudy river	24000	500 yr return pe	2732.50	10.66	15.54		15.63	0.000185	0.73	2216.42	697.49	0.13
Chalakudy river	23400	10 yr return per	1173.20	7.96	13.42		13.43	0.000015	0.24	2845.79	649.80	0.04
Chalakudy river	23400	20 yr return per	1415.60	7.96	13.86		13.87	0.000018	0.27	3144.92	710.73	0.04
Chalakudy river	23400	50 yr return per	1742.80	7.96	14.36		14.37	0.000022	0.27	3515.38	769.56	0.05
Chalakudy river	23400	100 yr return pe	1985.30	7.96	14.69		14.71	0.000023	0.28	3781.19	798.48	0.05
Chalakudy river	23400	200 yr return pe	2335.90	7.96	15.11		15.13	0.000024	0.28	4134.75	907.23	0.05
Chalakudy river	23400	500 yr return pe	2732.50	7.96	15.56		15.58	0.000025	0.30	4550.16	949.05	0.05
Chalakudy river	22800	10 yr return per	1173.20	7.62	13.36		13.40	0.000124	0.75	1268.40	413.40	0.11
Chalakudy river	22800	20 yr return per	1415.60	7.62	13.79		13.84	0.000129	0.82	1454.87	447.64	0.12
Chalakudy river	22800	50 yr return per	1742.80	7.62	14.28		14.34	0.000141	0.91	1697.01	567.20	0.13
Chalakudy river	22800	100 yr return pe	1985.30	7.62	14.62		14.68	0.000144	0.96	1907.61	686.05	0.13
Chalakudy river	22800	200 yr return pe	2335.90	7.62	15.03		15.09	0.000151	1.03	2210.88	773.37	0.13
Chalakudy river	22800	500 yr return pe	2732.50	7.62	15.47		15.54	0.000166	1.13	2582.07	912.30	0.14
Chalakudy river	22200	10 yr return per	1173.20	1.27	13.34		13.36	0.000041	0.59	2376.53	493.28	0.07
Chalakudy river	22200	20 yr return per	1415.60	1.27	13.77		13.79	0.000048	0.66	2596.51	530.65	0.08
Chalakudy river	22200	50 yr return per	1742.80	1.27	14.25		14.28	0.000058	0.75	2878.91	640.41	0.09
Chalakudy river	22200	100 yr return pe	1985.30	1.27	14.59		14.62	0.000063	0.81	3099.63	688.25	0.09
Chalakudy river	22200	200 yr return pe	2335.90	1.27	14.99		15.03	0.000072	0.89	3392.38	768.48	0.10
Chalakudy river	22200	500 yr return pe	2732.50	1.27	15.43		15.47	0.000081	0.98	3744.70	838.43	0.10
Chalakudy river	21600	10 yr return per	1173.20	4.70	13.29		13.32	0.000088	0.82	2193.78	824.84	0.10
Chalakudy river	21600	20 yr return per	1415.60	4.70	13.72		13.75	0.000096	0.87	2559.45	902.95	0.11
Chalakudy river	21600	50 yr return per	1742.80	4.70	14.19		14.23	0.000106	0.94	3011.11	987.01	0.11
Chalakudy river	21600	100 yr return pe	1985.30	4.70	14.52		14.57	0.000110	0.99	3346.36	1046.84	0.12
Chalakudy river	21600	200 yr return pe	2335.90	4.70	14.92		14.97	0.000117	1.05	3777.81	1117.59	0.12
Chalakudy river	21600	500 yr return pe	2732.50	4.70	15.36		15.41	0.000121	1.12	4286.50	1235.96	0.12

Reach	River Station	Profile	Q Total	Min Ch El	W.S. Elev	Crit W.S.	E.G. Elev	E.G. Slope	Vel Chnl	Flow Area	Top Width	Froude # Chl
			(m^3/s)	(m)	(m)	(m)	(m)	(m/m)	(m/s)	(m^2)	(m)	
Chalakudy river	21000	10 yr return per	1173.20	4.53	13.30		13.31	0.000003	0.15	5669.78	1072.15	0.02
Chalakudy river	21000	20 yr return per	1415.60	4.53	13.73		13.73	0.000003	0.17	6138.31	1128.03	0.02
Chalakudy river	21000	50 yr return per	1742.80	4.53	14.21		14.21	0.000005	0.21	6688.37	1160.42	0.02
Chalakudy river	21000	100 yr return pe	1985.30	4.53	14.54		14.55	0.000005	0.23	7082.57	1220.51	0.03
Chalakudy river	21000	200 yr return pe	2335.90	4.53	14.94		14.95	0.000006	0.25	7582.47	1276.05	0.03
Chalakudy river	21000	500 yr return pe	2732.50	4.53	15.38		15.38	0.000007	0.28	8150.24	1331.60	0.03
Chalakudy river	20400	10 yr return per	1173.20	2.61	13.28		13.30	0.000044	0.67	3489.00	733.78	0.07
Chalakudy river	20400	20 yr return per	1415.60	2.61	13.71		13.73	0.000051	0.74	3803.79	757.77	0.08
Chalakudy river	20400	50 yr return per	1742.80	2.61	14.18		14.21	0.000060	0.84	4168.67	784.21	0.09
Chalakudy river	20400	100 yr return pe	1985.30	2.61	14.51		14.54	0.000066	0.90	4427.67	802.36	0.09
Chalakudy river	20400	200 yr return pe	2335.90	2.61	14.90		14.94	0.000075	0.99	4748.59	824.65	0.10
Chalakudy river	20400	500 yr return pe	2732.50	2.61	15.33		15.37	0.000084	1.07	5109.09	856.25	0.11
Chalakudy river	19800	10 yr return per	1173.20	4.11	13.29		13.29	0.000005	0.19	5137.75	884.05	0.02
Chalakudy river	19800	20 yr return per	1415.60	4.11	13.71		13.72	0.000006	0.22	5517.65	914.81	0.03
Chalakudy river	19800	50 yr return per	1742.80	4.11	14.18		14.19	0.000007	0.26	5960.83	959.91	0.03
Chalakudy river	19800	100 yr return pe	1985.30	4.11	14.51		14.52	0.000008	0.29	6285.31	1047.87	0.03
Chalakudy river	19800	200 yr return pe	2335.90	4.11	14.91		14.92	0.000010	0.32	6716.58	1128.33	0.04
Chalakudy river	19800	500 yr return pe	2732.50	4.11	15.34		15.35	0.000012	0.36	7244.49	1271.45	0.04
Chalakudy river	19200	10 yr return per	1173.20	6.34	13.27		13.28	0.000087	0.63	4458.36	991.30	0.10
Chalakudy river	19200	20 yr return per	1415.60	6.34	13.69		13.71	0.000094	0.70	4884.11	1057.74	0.10
Chalakudy river	19200	50 yr return per	1742.80	6.34	14.16		14.18	0.000107	0.79	5404.36	1149.66	0.11
Chalakudy river	19200	100 yr return pe	1985.30	6.34	14.49		14.51	0.000110	0.83	5782.84	1177.73	0.11
Chalakudy river	19200	200 yr return pe	2335.90	6.34	14.88		14.90	0.000115	0.89	6250.36	1206.06	0.12
Chalakudy river	19200	500 yr return pe	2732.50	6.34	15.31		15.33	0.000118	0.94	6770.73	1230.05	0.12
Chalakudy river	18600	10 yr return per	1173.20	4.74	13.25		13.25	0.000036	0.45	6151.67	983.12	0.06
Chalakudy river	18600	20 yr return per	1415.60	4.74	13.66		13.67	0.000042	0.51	6585.12	1091.50	0.07
Chalakudy river	18600	50 yr return per	1742.80	4.74	14.13		14.13	0.000051	0.59	7139.03	1302.53	0.08
Chalakudy river	18600	100 yr return pe	1985.30	4.74	14.45		14.46	0.000054	0.63	7566.75	1339.83	0.08
Chalakudy river	18600	200 yr return pe	2335.90	4.74	14.84		14.85	0.000059	0.68	8097.85	1385.59	0.08
Chalakudy river	18600	500 yr return pe	2732.50	4.74	15.27		15.28	0.000062	0.73	8699.46	1438.81	0.09
Chalakudy river	18000	10 yr return per	1173.20	-5.71	13.24		13.24	0.000003	0.27	9806.40	1332.51	0.02
Chalakudy river	18000	20 yr return per	1415.60	-5.71	13.66		13.66	0.000004	0.31	10364.94	1354.11	0.03
Chalakudy river	18000	50 yr return per	1742.80	-5.71	14.12		14.13	0.000005	0.35	10999.66	1379.06	0.03
Chalakudy river	18000	100 yr return pe	1985.30	-5.71	14.45		14.45	0.000006	0.38	11445.97	1385.02	0.03
Chalakudy river	18000	200 yr return pe	2335.90	-5.71	14.83		14.84	0.000007	0.42	11985.98	1392.31	0.03

Reach	River Station	Profile	Q Total	Min Ch El	W.S. Elev	Crit W.S.	E.G. Elev	E.G. Slope	Vel Chnl	Flow Area	Top Width	Froude # Chl
			(m^3/s)	(m)	(m)	(m)	(m)	(m/m)	(m/s)	(m^2)	(m)	
Chalakudy river	18000	500 yr return pe	2732.50	-5.71	15.26		15.27	0.000008	0.46	12579.34	1399.65	0.04
Chalakudy river	17400	10 yr return per	1173.20	5.99	13.24		13.24	0.000007	0.17	4704.21	1036.69	0.03
Chalakudy river	17400	20 yr return per	1415.60	5.99	13.65		13.66	0.000008	0.20	5137.72	1054.39	0.03
Chalakudy river	17400	50 yr return per	1742.80	5.99	14.11		14.12	0.000009	0.23	5630.32	1074.43	0.03
Chalakudy river	17400	100 yr return pe	1985.30	5.99	14.44		14.44	0.000010	0.25	5978.04	1086.90	0.03
Chalakudy river	17400	200 yr return pe	2335.90	5.99	14.82		14.83	0.000012	0.28	6402.60	1108.50	0.04
Chalakudy river	17400	500 yr return pe	2732.50	5.99	15.25		15.26	0.000014	0.31	6877.91	1139.57	0.04
Chalakudy river	16800	10 yr return per	1173.20	3.84	13.20		13.23	0.000104	0.92	2362.95	543.09	0.11
Chalakudy river	16800	20 yr return per	1415.60	3.84	13.60		13.64	0.000119	1.02	2595.86	596.92	0.12
Chalakudy river	16800	50 yr return per	1742.80	3.84	14.06		14.10	0.000139	1.15	2879.45	666.67	0.13
Chalakudy river	16800	100 yr return pe	1985.30	3.84	14.37		14.43	0.000147	1.21	3093.35	682.28	0.14
Chalakudy river	16800	200 yr return pe	2335.90	3.84	14.75		14.81	0.000159	1.30	3355.33	698.07	0.14
Chalakudy river	16800	500 yr return pe	2732.50	3.84	15.17		15.23	0.000168	1.38	3649.56	716.56	0.15
Chalakudy river	15600	10 yr return per	1173.20	5.89	13.14		13.16	0.000109	0.64	2304.07	852.21	0.10
Chalakudy river	15600	20 yr return per	1415.60	5.89	13.55		13.57	0.000110	0.69	2657.03	886.47	0.11
Chalakudy river	15600	50 yr return per	1742.80	5.89	13.99		14.02	0.000115	0.75	3084.82	1027.57	0.11
Chalakudy river	15600	100 yr return pe	1985.30	5.89	14.31		14.34	0.000117	0.80	3418.57	1078.87	0.11
Chalakudy river	15600	200 yr return pe	2335.90	5.89	14.69		14.72	0.000122	0.85	3834.53	1125.26	0.12
Chalakudy river	15600	500 yr return pe	2732.50	5.89	15.10		15.14	0.000133	0.93	4328.06	1261.01	0.12
Chalakudy river	15000	10 yr return per	1173.20	7.46	12.75		12.97	0.001710	2.37	1078.15	652.50	0.41
Chalakudy river	15000	20 yr return per	1415.60	7.46	13.16		13.38	0.001588	2.46	1380.64	814.61	0.40
Chalakudy river	15000	50 yr return per	1742.80	7.46	13.61		13.83	0.001440	2.52	1797.14	1002.79	0.39
Chalakudy river	15000	100 yr return pe	1985.30	7.46	13.97		14.16	0.001197	2.42	2181.22	1154.99	0.36
Chalakudy river	15000	200 yr return pe	2335.90	7.46	14.39		14.55	0.000976	2.32	2695.05	1366.59	0.33
Chalakudy river	15000	500 yr return pe	2732.50	7.46	14.85		14.97	0.000711	2.09	3343.76	1440.56	0.28
Chalakudy river	14400	10 yr return per	1173.20	-1.57	12.87		12.88	0.000015	0.49	4410.79	1228.73	0.05
Chalakudy river	14400	20 yr return per	1415.60	-1.57	13.27		13.28	0.000018	0.55	4926.66	1309.09	0.05
Chalakudy river	14400	50 yr return per	1742.80	-1.57	13.71		13.73	0.000022	0.62	5522.79	1371.48	0.06
Chalakudy river	14400	100 yr return pe	1985.30	-1.57	14.05		14.06	0.000024	0.67	5985.80	1422.80	0.06
Chalakudy river	14400	200 yr return pe	2335.90	-1.57	14.44		14.46	0.000028	0.73	6548.01	1452.08	0.06
Chalakudy river	14400	500 yr return pe	2732.50	-1.57	14.87		14.89	0.000031	0.79	7192.30	1501.27	0.07
Chalakudy river	13800	10 yr return per	1173.20	5.11	12.87		12.87	0.000003	0.12	8471.20	1404.06	0.02
Chalakudy river	13800	20 yr return per	1415.60	5.11	13.27		13.27	0.000003	0.14	9041.89	1422.01	0.02
Chalakudy river	13800	50 yr return per	1742.80	5.11	13.72		13.72	0.000004	0.16	9678.77	1436.52	0.02
Chalakudy river	13800	100 yr return pe	1985.30	5.11	14.05		14.05	0.000004	0.18	10157.50	1446.90	0.02

Reach	River Station	Profile	Q Total	Min Ch El	W.S. Elev	Crit W.S.	E.G. Elev	E.G. Slope	Vel Chnl	Flow Area	Top Width	Froude # Chl
			(m^3/s)	(m)	(m)	(m)	(m)	(m/m)	(m/s)	(m^2)	(m)	
Chalakudy river	13800	200 yr return pe	2335.90	5.11	14.44		14.45	0.000005	0.20	10726.06	1459.35	0.02
Chalakudy river	13800	500 yr return pe	2732.50	5.11	14.87		14.88	0.000006	0.22	11360.92	1476.18	0.03
Chalakudy river	13200	10 yr return per	1173.20	-6.04	12.87		12.87	0.000002	0.21	6580.20	990.96	0.02
Chalakudy river	13200	20 yr return per	1415.60	-6.04	13.27		13.27	0.000003	0.24	6985.48	1019.09	0.02
Chalakudy river	13200	50 yr return per	1742.80	-6.04	13.72		13.72	0.000004	0.28	7448.94	1082.74	0.02
Chalakudy river	13200	100 yr return pe	1985.30	-6.04	14.05		14.05	0.000004	0.32	7819.06	1141.52	0.03
Chalakudy river	13200	200 yr return pe	2335.90	-6.04	14.44		14.44	0.000005	0.36	8275.98	1202.33	0.03
Chalakudy river	13200	500 yr return pe	2732.50	-6.04	14.87		14.88	0.000006	0.39	8817.90	1275.84	0.03
Chalakudy river	12600	10 yr return per	1173.20	0.13	12.86		12.87	0.000004	0.18	6778.53	1070.68	0.02
Chalakudy river	12600	20 yr return per	1415.60	0.13	13.27		13.27	0.000005	0.21	7220.46	1119.20	0.02
Chalakudy river	12600	50 yr return per	1742.80	0.13	13.71		13.72	0.000006	0.25	7729.51	1197.62	0.03
Chalakudy river	12600	100 yr return pe	1985.30	0.13	14.04		14.05	0.000007	0.27	8132.74	1243.75	0.03
Chalakudy river	12600	200 yr return pe	2335.90	0.13	14.43		14.44	0.000009	0.31	8631.61	1341.54	0.03
Chalakudy river	12600	500 yr return pe	2732.50	0.13	14.86		14.87	0.000010	0.34	9221.65	1394.73	0.04
Chalakudy river	12000	10 yr return per	1173.20	-0.87	12.86		12.86	0.000018	0.40	4026.82	1139.60	0.05
Chalakudy river	12000	20 yr return per	1415.60	-0.87	13.26		13.26	0.000019	0.43	4492.68	1179.64	0.05
Chalakudy river	12000	50 yr return per	1742.80	-0.87	13.70		13.71	0.000021	0.46	5023.75	1223.24	0.05
Chalakudy river	12000	100 yr return pe	1985.30	-0.87	14.03		14.04	0.000021	0.48	5433.52	1260.74	0.05
Chalakudy river	12000	200 yr return pe	2335.90	-0.87	14.42		14.43	0.000023	0.52	5933.00	1320.35	0.05
Chalakudy river	12000	500 yr return pe	2732.50	-0.87	14.85		14.86	0.000024	0.55	6509.72	1355.07	0.06
Chalakudy river	11400	10 yr return per	1173.20	0.26	12.85		12.85	0.000012	0.33	3450.65	850.59	0.04
Chalakudy river	11400	20 yr return per	1415.60	0.26	13.25		13.25	0.000014	0.36	3807.57	952.03	0.04
Chalakudy river	11400	50 yr return per	1742.80	0.26	13.69		13.70	0.000017	0.40	4260.38	1102.82	0.05
Chalakudy river	11400	100 yr return pe	1985.30	0.26	14.02		14.03	0.000018	0.42	4640.89	1227.49	0.05
Chalakudy river	11400	200 yr return pe	2335.90	0.26	14.40		14.42	0.000021	0.47	5143.20	1351.62	0.05
Chalakudy river	11400	500 yr return pe	2732.50	0.26	14.83		14.85	0.000023	0.51	5747.13	1448.63	0.05
Chalakudy river	10800	10 yr return per	1173.20	11.59	12.85		12.85	0.000000	0.01	9737.43	1131.94	0.01
Chalakudy river	10800	20 yr return per	1415.60	11.59	13.25		13.25	0.000001	0.02	10208.83	1215.45	0.01
Chalakudy river	10800	50 yr return per	1742.80	11.59	13.69		13.69	0.000001	0.03	10759.71	1276.80	0.01
Chalakudy river	10800	100 yr return pe	1985.30	11.59	14.02		14.02	0.000001	0.03	11184.41	1301.44	0.01
Chalakudy river	10800	200 yr return pe	2335.90	11.59	14.41		14.41	0.000001	0.04	11700.58	1392.19	0.01
Chalakudy river	10800	500 yr return pe	2732.50	11.59	14.84		14.84	0.000001	0.05	12313.81	1451.31	0.01
Chalakudy river	10200	10 yr return per	1173.20	1.48	12.84		12.85	0.000017	0.48	4574.48	872.03	0.05
Chalakudy river	10200	20 yr return per	1415.60	1.48	13.24		13.25	0.000020	0.54	4926.60	898.52	0.05
Chalakudy river	10200	50 yr return per	1742.80	1.48	13.68		13.69	0.000025	0.61	5329.19	939.87	0.06

Reach	River Station	Profile	Q Total	Min Ch El	W.S. Elev	Crit W.S.	E.G. Elev	E.G. Slope	Vel Chnl	Flow Area	Top Width	Froude # Chl
			(m^3/s)	(m)	(m)	(m)	(m)	(m/m)	(m/s)	(m^2)	(m)	
Chalakudy river	10200	100 yr return pe	1985.30	1.48	14.00		14.02	0.000028	0.66	5639.56	960.29	0.06
Chalakudy river	10200	200 yr return pe	2335.90	1.48	14.38		14.41	0.000033	0.73	6011.94	985.21	0.07
Chalakudy river	10200	500 yr return pe	2732.50	1.48	14.81		14.84	0.000038	0.81	6436.39	1014.78	0.07
Chalakudy river	9600	10 yr return per	1173.20	10.61	12.84		12.84	0.000004	0.07	3635.47	728.95	0.02
Chalakudy river	9600	20 yr return per	1415.60	10.61	13.23		13.24	0.000006	0.09	3945.54	851.04	0.02
Chalakudy river	9600	50 yr return per	1742.80	10.61	13.67		13.68	0.000008	0.11	4352.85	1000.98	0.02
Chalakudy river	9600	100 yr return pe	1985.30	10.61	14.00		14.01	0.000009	0.13	4691.59	1081.06	0.03
Chalakudy river	9600	200 yr return pe	2335.90	10.61	14.38		14.39	0.000011	0.16	5124.74	1190.22	0.03
Chalakudy river	9600	500 yr return pe	2732.50	10.61	14.80		14.82	0.000014	0.19	5652.93	1293.24	0.04
Chalakudy river	9000	10 yr return per	1173.20	13.58	12.84		12.84	0.000004		4010.93	535.16	0.00
Chalakudy river	9000	20 yr return per	1415.60	13.58	13.23		13.24	0.000005		4224.38	539.40	0.00
Chalakudy river	9000	50 yr return per	1742.80	13.58	13.67		13.68	0.000006	0.01	4461.13	568.82	0.01
Chalakudy river	9000	100 yr return pe	1985.30	13.58	13.99		14.00	0.000007	0.02	4661.19	660.38	0.02
Chalakudy river	9000	200 yr return pe	2335.90	13.58	14.38		14.39	0.000008	0.03	4937.71	782.69	0.02
Chalakudy river	9000	500 yr return pe	2732.50	13.58	14.80		14.81	0.000010	0.06	5286.66	889.09	0.02
Chalakudy river	8400	10 yr return per	1173.20	3.25	12.82		12.83	0.000043	0.53	2343.92	814.22	0.07
Chalakudy river	8400	20 yr return per	1415.60	3.25	13.22		13.23	0.000043	0.55	2673.15	851.93	0.07
Chalakudy river	8400	50 yr return per	1742.80	3.25	13.65		13.67	0.000046	0.60	3050.74	892.65	0.07
Chalakudy river	8400	100 yr return pe	1985.30	3.25	13.97		13.99	0.000046	0.62	3348.70	946.17	0.07
Chalakudy river	8400	200 yr return pe	2335.90	3.25	14.35		14.37	0.000049	0.66	3709.03	959.57	0.08
Chalakudy river	8400	500 yr return pe	2732.50	3.25	14.77		14.80	0.000051	0.70	4116.51	995.66	0.08
Chalakudy river	7800	10 yr return per	1173.20	8.76	12.76		12.80	0.000087	0.49	2093.71	941.96	0.09
Chalakudy river	7800	20 yr return per	1415.60	8.76	13.15		13.19	0.000127	0.63	2490.63	1067.75	0.11
Chalakudy river	7800	50 yr return per	1742.80	8.76	13.58		13.62	0.000125	0.66	2959.52	1115.75	0.11
Chalakudy river	7800	100 yr return pe	1985.30	8.76	13.90		13.95	0.000125	0.65	3329.81	1174.11	0.11
Chalakudy river	7800	200 yr return pe	2335.90	8.76	14.28		14.33	0.000127	0.65	3782.29	1241.83	0.11
Chalakudy river	7800	500 yr return pe	2732.50	8.76	14.70		14.75	0.000123	0.65	4310.67	1282.20	0.11
Chalakudy river	7200	10 yr return per	1173.20	8.00	12.59		12.67	0.000865	1.41	1421.52	651.74	0.28
Chalakudy river	7200	20 yr return per	1415.60	8.00	12.93		13.03	0.000798	1.47	1662.71	747.98	0.27
Chalakudy river	7200	50 yr return per	1742.80	8.00	13.36		13.47	0.000733	1.54	2000.05	815.31	0.27
Chalakudy river	7200	100 yr return pe	1985.30	8.00	13.69		13.80	0.000677	1.57	2271.50	850.99	0.26
Chalakudy river	7200	200 yr return pe	2335.90	8.00	14.06		14.17	0.000655	1.64	2590.66	875.07	0.26
Chalakudy river	7200	500 yr return pe	2732.50	8.00	14.48		14.60	0.000621	1.71	2968.41	963.43	0.26
Chalakudy river	6600	10 yr return per	1173.20	7.36	10.39	10.39	11.47	0.009389	4.31	257.73	124.45	0.89
Chalakudy river	6600	20 yr return per	1415.60	7.36	10.70	10.70	11.90	0.008930	4.46	296.37	129.07	0.88

Reach	River Station	Profile	Q Total	Min Ch El	W.S. Elev	Crit W.S.	E.G. Elev	E.G. Slope	Vel Chnl	Flow Area	Top Width	Froude # Chl
			(m^3/s)	(m)	(m)	(m)	(m)	(m/m)	(m/s)	(m^2)	(m)	
Chalakudy river	6600	50 yr return per	1742.80	7.36	11.11	11.11	12.42	0.008106	4.56	360.27	178.52	0.86
Chalakudy river	6600	100 yr return pe	1985.30	7.36	11.31	11.31	12.78	0.008525	4.76	398.26	217.63	0.88
Chalakudy river	6600	200 yr return pe	2335.90	7.36	11.81	11.81	13.23	0.007010	4.56	521.32	268.92	0.81
Chalakudy river	6600	500 yr return pe	2732.50	7.36	12.19	12.19	13.70	0.006710	4.58	642.44	371.97	0.80
Chalakudy river	4800	10 yr return per	1173.20	6.94	9.23		9.31	0.000169	0.47	1132.73	496.95	0.11
Chalakudy river	4800	20 yr return per	1415.60	6.94	9.69		9.77	0.000169	0.54	1375.57	584.24	0.12
Chalakudy river	4800	50 yr return per	1742.80	6.94	10.25		10.34	0.000169	0.61	1725.80	649.40	0.12
Chalakudy river	4800	100 yr return pe	1985.30	6.94	10.60		10.69	0.000171	0.66	1960.51	687.66	0.12
Chalakudy river	4800	200 yr return pe	2335.90	6.94	11.01		11.11	0.000179	0.73	2248.05	741.76	0.13
Chalakudy river	4800	500 yr return pe	2732.50	6.94	11.40		11.51	0.000191	0.80	2552.91	816.50	0.14
Chalakudy river	4200	10 yr return per	1173.20	6.94	9.22		9.24	0.000046	0.20	2544.99	776.69	0.06
Chalakudy river	4200	20 yr return per	1415.60	6.94	9.67		9.70	0.000048	0.23	2914.90	893.69	0.06
Chalakudy river	4200	50 yr return per	1742.80	6.94	10.24		10.27	0.000050	0.27	3463.03	1043.71	0.06
Chalakudy river	4200	100 yr return pe	1985.30	6.94	10.59		10.62	0.000052	0.30	3842.58	1124.63	0.07
Chalakudy river	4200	200 yr return pe	2335.90	6.94	11.00		11.03	0.000056	0.35	4310.80	1183.68	0.07
Chalakudy river	4200	500 yr return pe	2732.50	6.94	11.39		11.43	0.000060	0.40	4784.74	1244.94	0.07
Chalakudy river	3600	10 yr return per	1173.20	0.45	9.08		9.17	0.000363	1.48	1362.87	468.86	0.20
Chalakudy river	3600	20 yr return per	1415.60	0.45	9.51		9.63	0.000398	1.63	1603.31	643.15	0.21
Chalakudy river	3600	50 yr return per	1742.80	0.45	10.07		10.19	0.000401	1.73	1994.65	789.08	0.22
Chalakudy river	3600	100 yr return pe	1985.30	0.45	10.42		10.54	0.000396	1.78	2280.41	849.78	0.22
Chalakudy river	3600	200 yr return pe	2335.90	0.45	10.81		10.95	0.000412	1.89	2644.09	981.04	0.22
Chalakudy river	3600	500 yr return pe	2732.50	0.45	11.20		11.34	0.000416	1.97	3044.63	1136.07	0.23
Chalakudy river	3000	10 yr return per	1173.20	5.52	8.96		8.98	0.000235	0.67	3242.41	749.85	0.14
Chalakudy river	3000	20 yr return per	1415.60	5.52	9.40		9.42	0.000246	0.74	3576.12	788.26	0.15
Chalakudy river	3000	50 yr return per	1742.80	5.52	9.96		9.98	0.000248	0.80	4029.81	835.46	0.15
Chalakudy river	3000	100 yr return pe	1985.30	5.52	10.30		10.33	0.000254	0.85	4324.24	867.17	0.15
Chalakudy river	3000	200 yr return pe	2335.90	5.52	10.69		10.72	0.000273	0.92	4665.63	904.04	0.16
Chalakudy river	3000	500 yr return pe	2732.50	5.52	11.06		11.09	0.000317	1.03	5019.59	998.10	0.17
Chalakudy river	2400	10 yr return per	1173.20	8.15	8.93		8.95	0.000021	0.06	2863.68	818.80	0.03
Chalakudy river	2400	20 yr return per	1415.60	8.15	9.36		9.38	0.000024	0.09	3233.24	900.30	0.04
Chalakudy river	2400	50 yr return per	1742.80	8.15	9.91		9.93	0.000038	0.16	3790.49	1168.71	0.05
Chalakudy river	2400	100 yr return pe	1985.30	8.15	10.25		10.28	0.000039	0.19	4202.93	1214.69	0.05
Chalakudy river	2400	200 yr return pe	2335.90	8.15	10.63		10.66	0.000043	0.23	4678.12	1287.15	0.06
Chalakudy river	2400	500 yr return pe	2732.50	8.15	10.99		11.03	0.000048	0.26	5145.82	1318.00	0.06
Chalakudy river	1800	10 yr return per	1173.20	8.30	8.91		8.93	0.000074	0.10	3532.32	1055.45	0.06

Reach	River Station	Profile	Q Total	Min Ch El	W.S. Elev	Crit W.S.	E.G. Elev	E.G. Slope	Vel Chnl	Flow Area	Top Width	Froude # Chl
			(m^3/s)	(m)	(m)	(m)	(m)	(m/m)	(m/s)	(m^2)	(m)	
Chalakudy river	1800	20 yr return per	1415.60	8.30	9.33		9.36	0.000072	0.15	4003.80	1134.62	0.06
Chalakudy river	1800	50 yr return per	1742.80	8.30	9.87		9.90	0.000069	0.22	4634.07	1198.23	0.07
Chalakudy river	1800	100 yr return pe	1985.30	8.30	10.22		10.25	0.000069	0.25	5055.47	1238.68	0.07
Chalakudy river	1800	200 yr return pe	2335.90	8.30	10.60		10.63	0.000073	0.30	5536.58	1291.45	0.07
Chalakudy river	1800	500 yr return pe	2732.50	8.30	10.96		10.99	0.000080	0.36	6016.14	1393.66	0.08
Chalakudy river	1200	10 yr return per	1173.20	10.96	8.58		8.78	0.001820		1004.49	546.51	0.00
Chalakudy river	1200	20 yr return per	1415.60	10.96	9.04		9.23	0.001244		1266.12	589.14	0.00
Chalakudy river	1200	50 yr return per	1742.80	10.96	9.61		9.78	0.000891		1622.33	660.20	0.00
Chalakudy river	1200	100 yr return pe	1985.30	10.96	9.97		10.13	0.000782		1866.60	713.75	0.00
Chalakudy river	1200	200 yr return pe	2335.90	10.96	10.35		10.51	0.000734		2167.77	861.48	0.00
Chalakudy river	1200	500 yr return pe	2732.50	10.96	10.70		10.87	0.000701		2488.03	968.21	0.00
Chalakudy river	600	10 yr return per	1173.20	7.90	7.56	2.89	7.59	0.002002		1453.33	289.67	0.00
Chalakudy river	600	20 yr return per	1415.60	7.90	8.21	3.12	8.25	0.002004	0.37	1654.28	339.15	0.27
Chalakudy river	600	50 yr return per	1742.80	7.90	8.93	3.37	8.98	0.002003	0.82	1924.18	448.45	0.33
Chalakudy river	600	100 yr return pe	1985.30	7.90	9.34	3.56	9.39	0.002003	0.88	2137.69	613.09	0.34
Chalakudy river	600	200 yr return pe	2335.90	7.90	9.74	3.81	9.79	0.002004	1.16	2401.32	698.05	0.36
Chalakudy river	600	500 yr return pe	2732.50	7.90	10.11	4.07	10.17	0.002004	1.37	2678.31	841.78	0.38

SPATIAL MAPPING OF FLOOD PRONE AREAS AND RISK ASSESSMENT OF CHALAKUDY RIVER BASIN USING HEC-HMS AND HEC-RAS MODELS

By

GUDIDHA GOPI

(2018-28-002)

ABSTRACT OF THESIS

Submitted in partial fulfilment of the requirements for the degree of

DOCTOR OF PHILOSOPHY

IN

AGRICULTURAL ENGINEERING

(Soil and Water Engineering)

Faculty of Agricultural Engineering &Technology

Kerala Agricultural University

Department of Irrigation and Drainage Engineering

KELAPPAJI COLLEGE OF AGRICULTURAL ENGINEERING AND TECHNOLOGY

TAVANUR, MALAPPURAM-679573

KERALA, INDIA

2021

ABSTRACT

Floods are one among the most devastating natural disasters that affects life on the globe. For the planning and design of water resources projects in the preferred area, planners and engineers usually require reliable estimates of flood magnitude and frequency. Kerala state in the Indian sub continent received a catastrophic flood in the year 2018. The present study attempts to model the flood flows and map the flood prone areas of a river basin in Kerala. The Chalakudy river basin, one of the worst-affected river basins due to heavy rains and floods was selected for the present study. This is the fifth largest river in Kerala. The basin is predominant with agricultural land and falls under the humid tropical zone, where water resources planning and management is necessary for irrigation scheduling, flood control and design of various engineering structures.

In order to address the above issues, an attempt was made to calibrate and validate HEC-HMS model for simulating the flood hydrograph for the Chalakudy river basin. Flood frequency analysis was carried out to estimate the flood peak values using frequency distributions in HEC-SSP software. The results were compared with the estimated flood peak values for different return periods obtained from the HEC-HMS model. Hydraulic routing was done in HEC-RAS model and the flood inundation maps were prepared. The cadastral level risk areas were identified based on water surface profiles of velocity and depth of flood extent and its characteristics. Food vulnerability maps based on land use patterns were developed in order to identify the severely affected land uses.

The HEC-HMS model for the basin was developed using SCS-UH, SCS-CN, Recession and Muskingum methods to find out the loss rate, runoff transformation and routing of flood respectively. Statistical performance indices of the model, Nash-Sutcliffe efficiency (NSE) and Coefficient of correlation (R^2) values were obtained above 0.7, Error in Peak Flow (%) and Error in Volume (%) were figured below 20% and Root Mean Square Error-Standard Deviation Ratio (RSR) was acquired as 0.5 and below. These values indicated that HEC-HMS model simulation performed well in both calibration and validation. The

frequency discharge values calculated using Log Pearson type-III distribution indicated a high degree of similarity to the HEC-HMS generated values with an R^2 value of 0.862. The results of the Log Normal and Gumbel distributions are significantly lower than those of the HEC-HMS model values.

The assessment of the vulnerability due to the flooding was made with regard to the land use pattern and cadastral level risk map of Chalakudy river basin was developed for different return periods. Kadukutty Panchayat located in the downstream of Chalakudy river basin was found to be the maximum flood inundated area for 10 year return period (557 ha) and for 200 year return period (681 ha). Manjapra Panchayat located in upstream was found to be the least flood inundated area for 10 year return period (6 ha) and for 200 year return period (9 ha). Annamanada, Kadukutty, Melur and Pariyaram panchayats were under high risk areas, with depths greater than 20 m. Ayyampuzha, Chalakudy, Mala, Kuzhur, Parakkadavu and Puthenvelikara panchayats were under medium risk areas with depths varying from 10 to 20 m. Athirappilly, Manjapra and Karukutty panchayats were under low risk areas with depths less than 10 m. The flood vulnerability maps were generated by intersecting the flood plain land use map with the flooded area polygons. Paddy land near to the river banks was found to be the highest inundated by different return period floods, followed by forest and other vegetation, barren land and other land use classes.